Analysis of the relationship between ribosomal protein and SSU processome assembly in *Saccharomyces cerevisiae*

Dissertation

zur Erlangung des Doktorgrades der Naturwissenschaften (Dr. rer. nat.)
der naturwissenschaftlichen Fakultät III – Biologie und vorklinische Medizin -
der Universität Regensburg

vorgelegt von

Steffen Jakob

aus Wolfen

Januar 2010

Promotionsgesuch eingereicht am: 13. Januar 2010

Die Arbeit wurde angeleitet von: Prof. Dr. Herbert Tschochner

Prüfungsausschuss:

Vorsitzender:	Prof. Dr. Armin Kurtz
1. Prüfer:	Prof. Dr. Herbert Tschochner
2. Prüfer:	Prof. Dr. Rainer Deutzmann
3. Prüfer:	Prof. Dr. Wolfgang Seufert

Tag der mündlichen Prüfung: 24. März 2010

Die vorliegende Arbeit wurde in der Zeit von April 2006 bis Januar 2010 am Lehrstuhl Biochemie III des Institutes für Biochemie, Genetik und Mikrobiologie der Naturwissenschaftlichen Fakultät III der Universität zu Regensburg unter Anleitung von Dr. Philipp Milkereit im Labor von Prof. Dr. Herbert Tschochner angefertigt.

Ich erkläre hiermit, dass ich diese Arbeit selbst verfasst und keine anderen als die angegebenen Quellen und Hilfsmittel verwendet habe.
Diese Arbeit war bisher noch nicht Bestandteil eines Prüfungsverfahrens.
Andere Promotionsversuche wurden nicht unternommen.

Regensburg, den 13. Januar 2010

Steffen Jakob

Table of Contents

1 SUMMARY

The eukaryotic ribosome consists of two subunits, comprised in total of 79 ribosomal proteins (r-proteins) and four different ribosomal RNA (rRNA) species. Bringing these components together is a very complicated process *in vivo* involving more than 70 small nucleolar RNAs (snoRNAs) and around 150 accessory proteins. Nevertheless, the cell fulfils this challenge in a highly efficient manner. Although homologies with known protein motifs exist for some of these biogenesis factors, the exact function of these as well as for the majority of the remaining factors remains elusive.

One early aspect of eukaryotic ribosome biogenesis is the co-transcriptional assembly of the small subunit (SSU) processome. This ribonucleoprotein (RNP) particle is required for early pre-rRNA processing events, separating the maturation of the SSU from the one of the large subunit (LSU). This process involves about 40 proteins, which are all required for SSU maturation and can be classified into five subgroups. Members of four of these subgroups have been shown to exist as entities in the cell independent of their interaction with pre-ribosomes.

The goal of this work was to investigate the relationship between SSU r-protein and SSU processome assembly. To this end, representative r-proteins of all three major structural domains of the SSU rRNA were conditionally depleted in different *Saccharomyces* cerevisiae strains. Subsequently, the association of representatives of each subgroup of the SSU processome to early pre-ribosomes was analysed by complementary techniques. Among them, a mass spectrometry based method allowing the semiquantitative comparison of the protein composition of affinity purified pre-ribosomal particles was established and successfully applied. In comparison to earlier reports, more than twice the amount of proteins could be identified in these proteomic analyses of early pre-ribosomes, emphasizing the sensitivity of the established assay. Additionally, the obtained proteomic data provide evidence that factors required for maturation of the LSU are associated with these early pre-ribosomes, although in general less stable than their counterparts required for SSU maturation.

Apart from this, the results obtained by this combined approach indicate that assembly of the SSU processome UTP-A, UTP-B and Mpp10p submodules with pre-rRNA can proceed independent of r-protein assembly events. This suggests that proteins, belonging to these subclasses, assist in proper primary rRNA folding events, potentially by preventing erroneous folding and thus providing binding sites for subsequent r-protein binding. In this regard, these proteins might be envisioned to function in a “chaperone like” way, dedicated to early pre-rRNAs.

In contrast, efficient association of other SSU processome components, e.g. Noc4p or the SSU processome UTP-C submodule, with pre-ribosomes requires specific r-protein assembly events in the SSU rRNA central and 3’ domain. Moreover, the results point towards a function of Noc4p in the coordination of SSU rRNA central and 3’ domain assembly. Accordingly, establishment of a defined

central domain assembly state is required for efficient Noc4p association with early pre-ribosomes and subsequently Noc4p is required to trigger assembly events in the SSU rRNA 3′ domain leading to a mature SSU head structure.

Altogether, the data obtained in this work give a first comprehensive picture of the interplay between early steps in r-protein and SSU processome assembly with pre-rRNA in yeast cells.

2 INTRODUCTION

2.1 The ribosome

The ribosome is a ribonucleoprotein (RNP) particle consisting of two subunits, which themselves are composed of ribosomal proteins (r-proteins) and ribosomal RNA (rRNA). In the 1950s they were designated to be the place of protein synthesis, by translating the genetically stored information into poly amino acid chains (proteins) (Siekevitz, 1952; Zamecnik, 1969).
The synthesis of ribosomes in eukaryotic cells is a very energy consuming process, taking up to 60% of the whole transcriptional activity in growing yeast cells (Warner, 1999). Thus, it is a very challenging task to understand how this very complex process (involving more than 150 proteins and over 70 different RNAs) is achieved by the cell in such a high efficiency, yielding 2000 new ribosomes every minute. In the following the core components as well as transient factor requirements will be introduced in more detail, focussing mainly on early small ribosomal subunit (SSU) biogenesis and r-protein assembly.

2.1.1 Components of the ribosome

The ribosome consists of both RNA and protein components. The size of the ribosome is defined by the sedimentation coefficient, given in Svedberg (S) units. The eubacterial 70S ribosome consists of a small 30S subunit (SSU) and a large 50S subunit (LSU). The 30S subunit is formed by the 16S rRNA and 21 r-proteins. The 50S subunit is composed of the 23S and 5S rRNAs and 34 r-proteins.
The more complex eukaryotic 80S ribosome consists of a 40S SSU and a 60S LSU. The 40S subunit is formed by the 18S rRNA and in total 33 r-proteins (32 rpS and Asc1p) (rpS, ribosomal protein small subunit). The 60S subunit is composed of the 25S, 5.8S, and 5S rRNAs and 46 r-proteins (rpL, ribosomal protein large subunit) (Planta and Mager, 1998; Gerbasi et al., 2004).

2.1.2 Ribosome Structure

Structural features of the ribosome, like shape, localisation of r-proteins and orientation of the subunits to each other have been described using electron microscopy (Lake, 1976; Stöffler and Stöffler-Meilicke, 1984; Stark et al., 1995; Frank et al., 1995). However, the atomic structure was only recently solved for the prokaryotic ribosomal subunits and the entire ribosome using X-ray crystallography (Ban et al., 2000; Wimberly et al., 2000; Schluenzen et al., 2000; Yusupov et al., 2001). These atomic structures gave insight into how these huge assemblies are organised in a three dimensional space and several architectural features became visible. First of all, the region, where the two subunits join each other, also called the subunit interface, is almost devoid of r-proteins. Second, many of the r-proteins consist of a globular domain, which is found on the surface of the ribosomal subunits, and long loops or extensions which penetrate into rRNA regions. Third, both the 16S rRNA and the 23S pre-rRNA are conglomerates of helical elements, which are connected by loops.

Additionally, the comparison of the secondary and tertiary structures of the rRNA species of both subunits emphasises a striking difference between the three dimensional organisation of their rRNAs. Each of the three major secondary structural domains of the 16S rRNA forms distinct morphological features of the SSU, the 5′ domain forms the shoulder and the foot, the central domain forms the platform and the 3′ major domain forms the head. The 3′ minor domain sits on top of the body (formed by shoulder, foot and platform) at the interface site (Figure 1**a**).

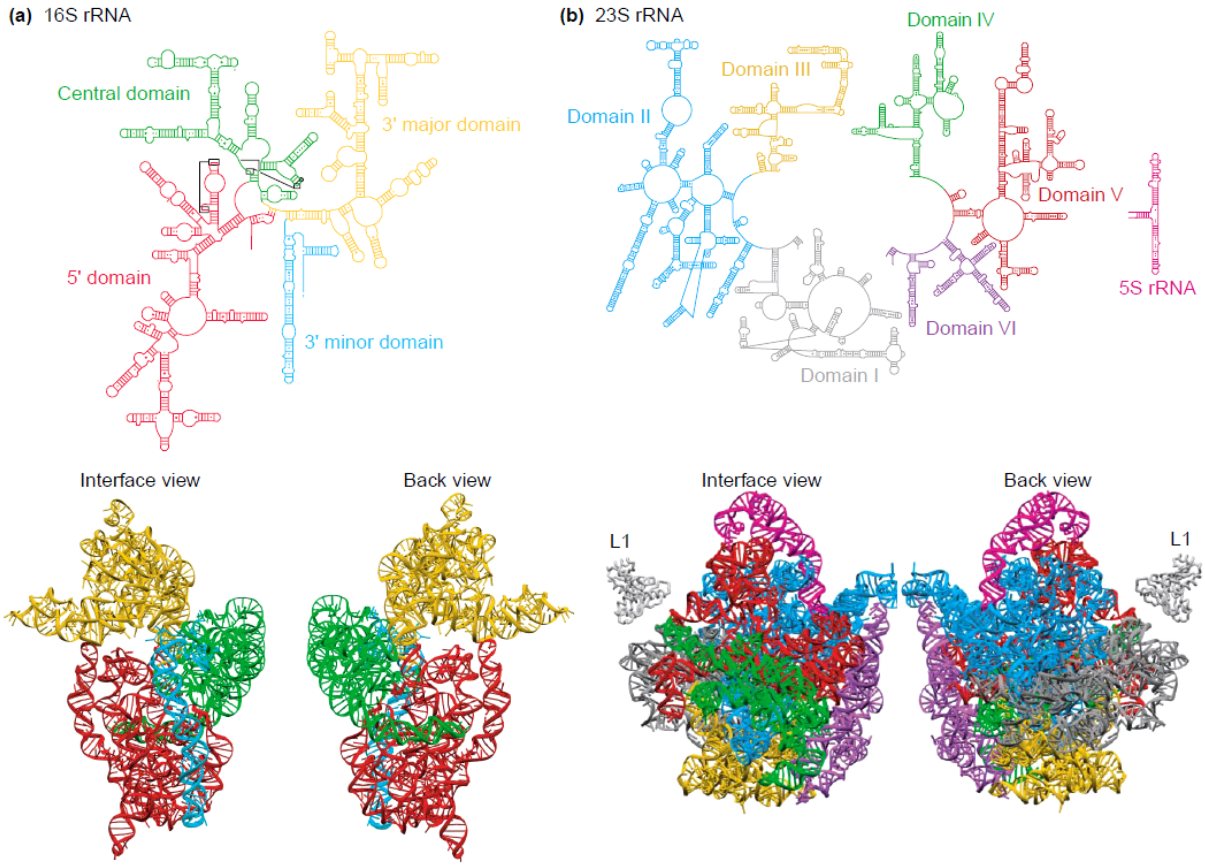

Figure 1. Comparison of the secondary and tertiary structure of the rRNAs from the 30S and 50S subunits shows differences in the three dimensional organisation.
(**a**) The secondary structure of the 16S rRNA from *Thermus thermophilus* is depicted with the classification into the three major domains and one minor domain. The SSU rRNA 5′ domain is depicted in red, the central domain in green, the 3′ major domain in yellow and the 3′ minor domain in blue. The tertiary structure is depicted below, from the intersubunit joining site (interface view) and from the solvent side (back view). Each major domain of the 16S rRNA forms one morphological feature of the 30S subunit. The SSU rRNA 5′ domain forms the shoulder and foot (red), the central domain forms the platform (green) and the 3′ major domain forms the head (yellow). The 3′ minor domain sits on top of the body (formed by shoulder, foot and platform) at the interface site (blue).
(**b**) The secondary structure of the 23S pre-rRNA from *Haloarcula marismortui* is depicted with the classification into six domains. The domain I is depicted in grey, domain II is depicted in blue, domain III is depicted in yellow, domain IV is depicted in green, domain V is depicted in red, domain VI is depicted in purple, and the 5S RNA is depicted in pink. The tertiary structure is depicted below, from the intersubunit joining site (interface view) and from the solvent side (back view). The helices of the single domains are interwoven with each other and cannot solely be attributed to morphological features. Reproduced from Ramakrishnan and Moore, 2001.

In contrast, the six major secondary structural domains of the 23S pre-rRNA are interconnected with each other and do not show this clear organisation into structural domains on the three dimensional level (Figure 1**b**).

From a functional point of view, the atomic structure revealed that the peptidyl transferase center in the 50S subunit is exclusively made of rRNA (Ban et al., 2000). In addition, the A and P site in the decoding center of the 30S subunit is mainly consisting of rRNA with some contributions of the r-proteins S9 and S13, making contact to the P-site bound tRNA (Wimberly et al., 2000; Carter et al., 2000). Thus, the enzymatic activity of peptide bond formation is catalysed by RNA and the ribosome is therefore a ribozyme (Cech, 2000). However, to perform the task of translation, the ribosome needs the structural support of r-proteins, as completely deproteinised 50S subunits are functionally inactive (Noller et al., 1992). Furthermore, r-proteins are involved in the correct codon-anticodon interaction of the second and third base of a codon (Funatsu and Wittmann, 1972; Ogle et al., 2001, 2002).

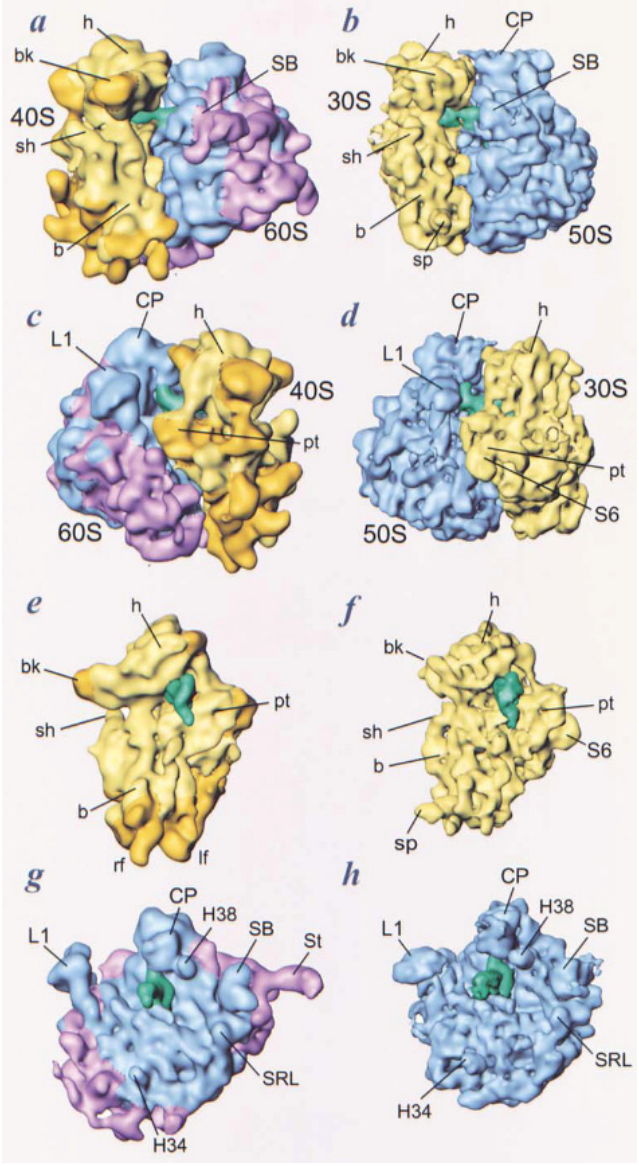

Figure 2. Comparison of the eukaryotic and prokaryotic ribosome structure
The cryo-EM map of the 80S ribosome (**a+c**) from *S. cerevisiae* consisting of the 40S (**e**) and 60S (**g**) ribosomal subunits is shown at approximately 15Å resolution. For direct comparison the cryo-EM map of the 70S ribosome (**b+d**) from *E.coli* consisting of the 30S (**f**) and 50S (**h**) ribosomal subunits is shown at approximately 11.5Å resolution (Gabashvili et al., 2000). Homologous regions are shown in blue and yellow, while additional eukaryotic specific morphological features (arising from non-homologous r-proteins and additional rRNA stretches) are shown in dark yellow and purple. The P site bound tRNA is shown in green. Structural landmarks of the SSU are labelled as following: b, body; bk, beak; h, head; lf, left foot; rf, right foot; pt, platform; sh, shoulder; sp, spur. Structural landmarks of the LSU are labelled as following: CP, central protuberance; L1, L1 protuberance; SB, stalk base; St, L7/L12 stalk; H34, helix 34; H38, helix 38; SRL, sarcin-ricin loop. Reproduced from Spahn et al., 2001.

The interaction of the ribosome with translation factors is also mediated by r-proteins (Stark et al., 2002; Wilson and Nierhaus, 2005). Additionally, several r-proteins of the LSU build a ring structure at the peptide exit tunnel. Of these proteins, L23 and L29 make contact with the signal recognition particle, which is required for secretion of newly synthesised proteins (Pool et al., 2002; Gu et al., 2003; Halic et al., 2004). Furthermore, L23 interacts with the trigger factor (TF), which is the earliest chaperone to encounter the nascent polypeptide chain (Lecker et al., 1989; Kramer et al., 2002).
To date, no atomic resolution structure is available for eukaryotic ribosomes. This is probably due to the higher complexity, which makes it more difficult to obtain crystals suitable for X-ray crystallography. The current state of art in determining the eukaryotic ribosome structure are cryo-electron microscopy (cryo-EM) studies yielding a resolution between 6Å and 9Å (Chandramouli et al., 2008; Becker et al., 2009). All eukaryotic r-proteins with prokaryotic counterparts could be modelled into the cryo-EM structure of the yeast ribosome (Spahn et al., 2001) by using the atomic resolution structure of the prokaryotic ribosome as a basis. Furthermore, additional densities in the cryo-EM structure are visible and can be attributed to eukaryotic specific rRNA regions and additional r-proteins. The overall morphology is quite similar to the prokaryotic counterpart with some additional features (see regions marked in dark yellow and purple in Figure 2).

2.2 Ribosome Biogenesis in *S. cerevisiae*

The synthesis of eukaryotic ribosomes requires RNA products made by all three DNA dependent RNA Polymerases (Pol). In the model organism *S. cerevisiae* the rRNA genes are clustered together in an operon like structure, which exists in around 150 repeats on Chromosome XII. The RNA Polymerase I (Pol I) transcribes the genes for the 25S, 18S and 5.8S rRNAs yielding in the polycistronic 35S rRNA precursor transcript. This initial precursor is processed by several endo-and exonucleases to finally result in the mature rRNAs (Figure 4). The 5S rRNA genes are transcribed by RNA Polymerase III (Pol III). Furthermore, the r-protein genes are transcribed by RNA Polymerase II (Pol II). All these different processes are coordinated by the cell to ensure that stoichiometric amounts of all components are made.
The main site of ribosome biogenesis is the nucleolus, which is a dense substructure of the nucleus (Figure 3); although some later maturation steps take place in the nucleoplasm and cytoplasm (Figure 5).
Pioneer work in the 1970s defined the size of pre-ribosomal particles, with the earliest one being the 90S pre-ribosome (Udem and Warner, 1972; Trapman et al., 1975). This pre-ribosomal particle is then separated into the 66S and 43S pre-ribosomes, which constitute precursors to the 40S and 60S subunit, respectively. The higher protein / RNA ratio in pre-ribosomes in comparison to mature ribosomes suggested the existence of several accessory factors. Recently, the improvements in the purification of protein complexes allowed defining the protein composition of several pre-ribosomal particles (Rigaut et al., 1999). In total approximately 150 accessory factors (also called ribosome biogenesis factors) were identified as part of several different pre-ribosomes, which could be sequentially ordered due to their rRNA content and subcellular localisation (Bassler et al.,

2001; Harnpicharnchai et al., 2001; Saveanu et al., 2001; Grandi et al., 2002; Fatica et al., 2002; Dragon et al., 2002; Nissan et al., 2002; Schäfer et al., 2003). The depletion phenotype in regard to rRNA processing and export was analysed for the majority of these ribosome biogenesis factors. This allowed a crude definition of the step of ribosome biogenesis in which they individually might be involved, but the exact function remains mysterious for most of the factors. Some were designated to be DExD/H-box RNA helicases, endo- or exonucleases, methyltransferases, pseudouridine synthases, AAA-type ATPases, GTPases or kinases (for review see Fromont-Racine et al., 2003).

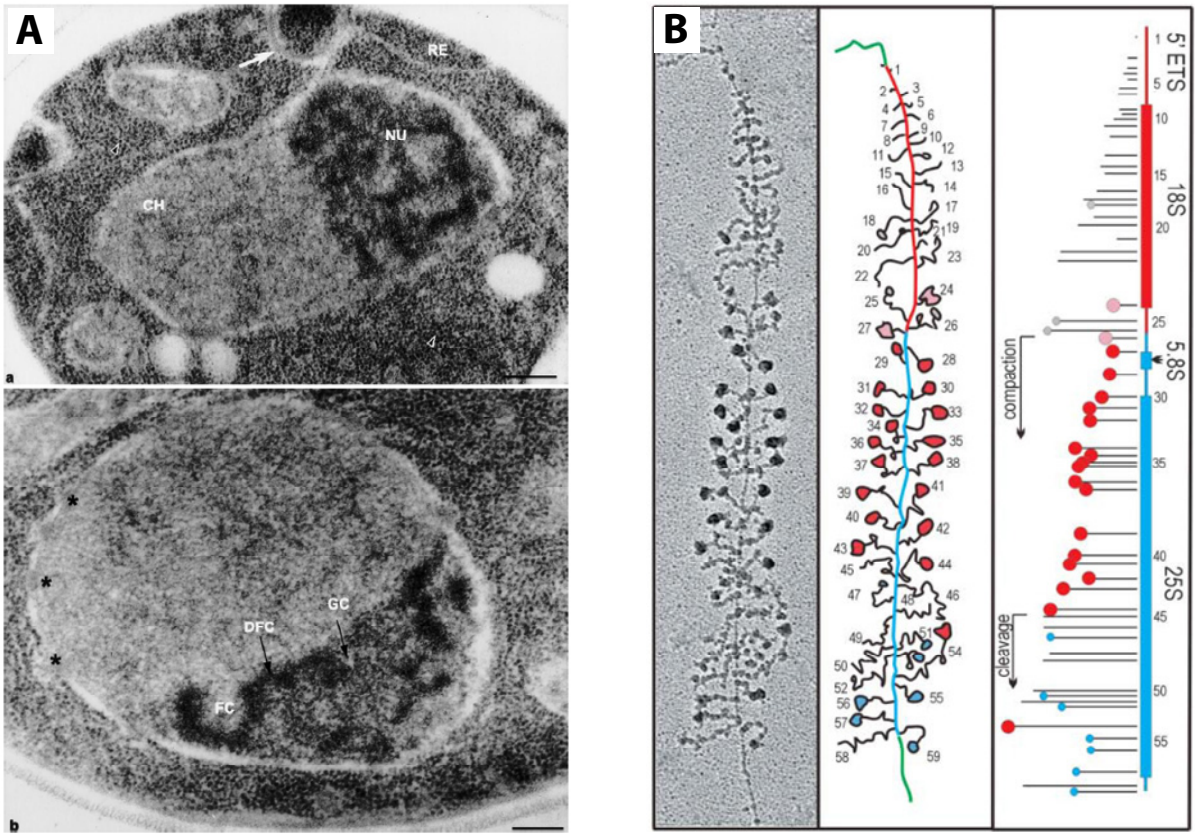

Figure 3. The nucleolus is the site of ribosome biogenesis and nucleolar genes can be visualised by Miller chromatin spreading.

(**A**) The top picture shows the overall morphology of a *S. cerevisiae* cell after cryofixation and freeze-substitution using electron microscopy. The nucleus can be divided in a low electron density region (CH) or a high electron density region (referred to as nucleolus (NU)). RE is the endoplasmatic reticulum and the white arrow points toward an invagination from the plasma membrane. The lower picture shows the morphology of the nucleolus, which can be devided into three distinct morphological compartments. The fibrillar center (FC) contains the rDNA repeats. The dense fibrillar component (DFC) is the site of Pol I transcription and early assembly events like the formation of the 90S pre-ribosome. The granular component (GC) contains maturing pre-ribosomes. Reproduced from Léger-Silvestre et al., 1999.

(**B**) One transcription unit of the rDNA locus is shown. The central string represents the DNA, while the extending strings (some with terminal balls) represent the rRNA. The transcription start site is at the top of the picture with transcript 1 being the newest, and therefore shortest, transcript. The early terminal balls (depicted in pink and red) represent the SSU processome consisting of the U3 snoRNA and about 40 factors needed for maturation of the SSU. The late terminal balls (depicted in blue) represent probably pre-LSU knobs that form after co-transcriptional cleavage of the rRNA precursor (probably at site A_2), separating the pre-40S from the pre-60S subunit. Reproduced from Osheim et al., 2004.

During the maturation pathway the rRNA is rearranged and refolded as well as modified by three different types of modifications, base methylation, methylation of the 2′ hydroxyl group of the ribose, and conversion of uridine into pseudouridine by base rotation. The later two modifications are the major ones and the site of modification is selected by formation of a heteroduplex between the pre-rRNA and small nucleolar RNAs (snoRNAs). The snoRNAs are embedded in protein complexes (snoRNPs) including the modification enzymes (methyltransferase or pseudouridine synthase) (for review see Gerbi et al., 2001). Some helicases have been suggested to play a crucial role in the release of snoRNPs from rRNA precursors (Kos and Tollervey, 2005; Liang and Fournier, 2006; Bohnsack et al., 2008, 2009). Each single modification guided by snoRNAs is not essential. However, blockage of these modifications at a global level by inhibiting the putative modification enzymes has a strong negative effect on cell growth (Tollervey et al., 1993; Zebarjadian et al., 1999), thus showing that the sum of all modifications is beneficial for the cell, while single modifications are dispensable.

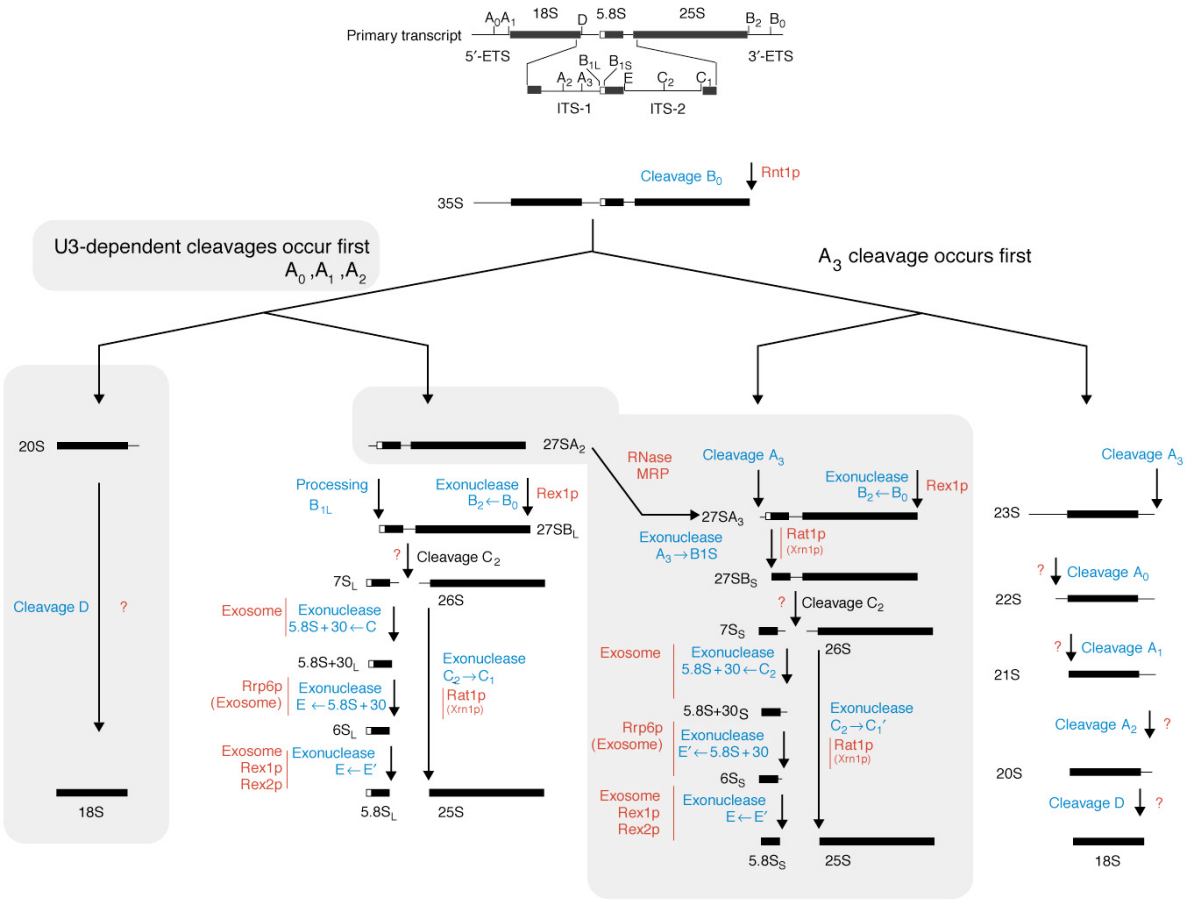

Figure 4. Schematic view of pre-rRNA processing pathways in *Saccharomyces cerevisiae*
The upper panel shows a schematic drawing of the primary transcript including the 18S, 5.8S, and 25S rRNA genes, the external transcribed spacers (5′ ETS and 3′ ETS), and the internal transcribed sequences (ITS-1 and ITS-2). In addition, the known processing sites are depicted. Processing starts at site B_0 yielding the first detectable rRNA transcript, the 35S pre-rRNA. The grey marked processing steps indicate the major processing pathways. Cleavage at sites A_0 and A_1 generates the 33S and 32S rRNA, respectively (not shown) and cleavage at site A_2 separates the precursor of the SSU (20S pre-rRNA) from the precursor of the LSU ($27SA_2$ pre-rRNA). Known processing enzymes are indicated in red. Unidentified enzymes are indicated by question marks. Reproduced from Ferreira-Cerca, 2008, originally adapted from Fatica and Tollervey, 2002.

Ribosome biogenesis starts with the transcription of the rDNA locus to yield the 35S rRNA precursor. Already during transcription several factors needed for maturation of the small subunit assemble into a huge pre-ribosomal particle with a sedimentation coefficient of around 90S (for review see Fromont-Racine et al., 2003). This particle was termed SSU processome and will be discussed in more detail in section 2.5. Besides the SSU processome components some early binding rpS were suggested to be part of this complex, as well as the U3 snoRNA, the 35S pre-rRNA and later precursors to the 18S rRNA (21S, 22S and 23S pre-rRNAs).
In contrast, almost no r-proteins of the LSU (rpL) and no biogenesis factors needed for LSU maturation were detected in the recent proteomic analyses of these early particles (Dragon et al., 2002; Grandi et al., 2002; Pérez-Fernández et al., 2007). However, other reports suggest that r-proteins and maturation factors of the LSU are part of early pre-ribosomes. For instance, some ribosome biogenesis factors of the LSU precipitate 35S pre-rRNA and some rpL were found to be part of early nucleolar pre-ribosomal particles (Merl and Jakob et al., 2010; Auger-Buendia and Longuet, 1978, among others). Furthermore, the Pol III transcribed 5S rRNA, which is packed into a particle containing Rpf2p, Rrs1p and the r-proteins rpL5 and rpL11, is incorporated into early pre-ribosomal particles containing 35S pre-rRNA (Zhang et al., 2007).

Subsequently, the rRNA is processed by different endo- and exonucleases to yield the mature 25S, 18S, and 5.8S rRNAs. Processing usually starts at the 5' end of the 35S pre-rRNA with U3 snoRNA dependent processing at sites A_0 and A_1 (Figure 4). The cut at site A_2 generates the 20S and $27SA_2$ pre-RNAs, separating the precursor particles of the SSU from the one of the LSU. This separation is accompanied by a loss of almost all constituents of the SSU processome, while other factors associate to these pre-40S and pre-60S particles. This separation also goes along with a strong stabilisation of rpS association with the 20S pre-rRNA (Ferreira-Cerca et al., 2007). Whether this stabilisation is the cause or consequence of the processing at site A_2 is not yet clear.

Around ten biogenesis factors as well as all rpS were found to be associated to the direct precursor of the 18S rRNA, the 20S pre-rRNA (Fromont-Racine et al., 2003; Schäfer et al., 2003). This 20S pre-rRNA containing particle is then exported to the cytoplasm, a process which is poorly understood, but involves interaction with the exportin Crm1p in a RanGTP dependent manner (Moy and Silver, 1999, 2002). The final maturation steps, including the processing at site D, which generates the mature 18S rRNA, occurs in the cytoplasm.

The maturation of the pre-60S subunit after separation from the pre-40S maturation pathway is more dynamic and involves much more proteins. Several precursor particles were identified, which showed besides some overlaps, differences in their protein and rRNA content and were sequentially ordered and classified as early, middle and late pre-60S particles (for summary see Figure 5). The late pre-60S particle containing the mature 25S, 5.8S, and 5S rRNAs and roughly ten biogenesis factors is exported to the cytoplasm. The export is mediated in a Ran-GTP dependent manner by an interaction of the adaptor protein Nmd3p with the exportin Crm1p. Recycling of

Nmd3p is suggested to be triggered by the incorporation of rpL10 (Hedges et al., 2005; West et al., 2005). Additionally, two other factors were suggested to be involved in LSU export, namely Arx1p and Mex67p/Mtr2p (Bradatsch et al., 2007; Yao et al., 2007; Lo and Johnson, 2009).

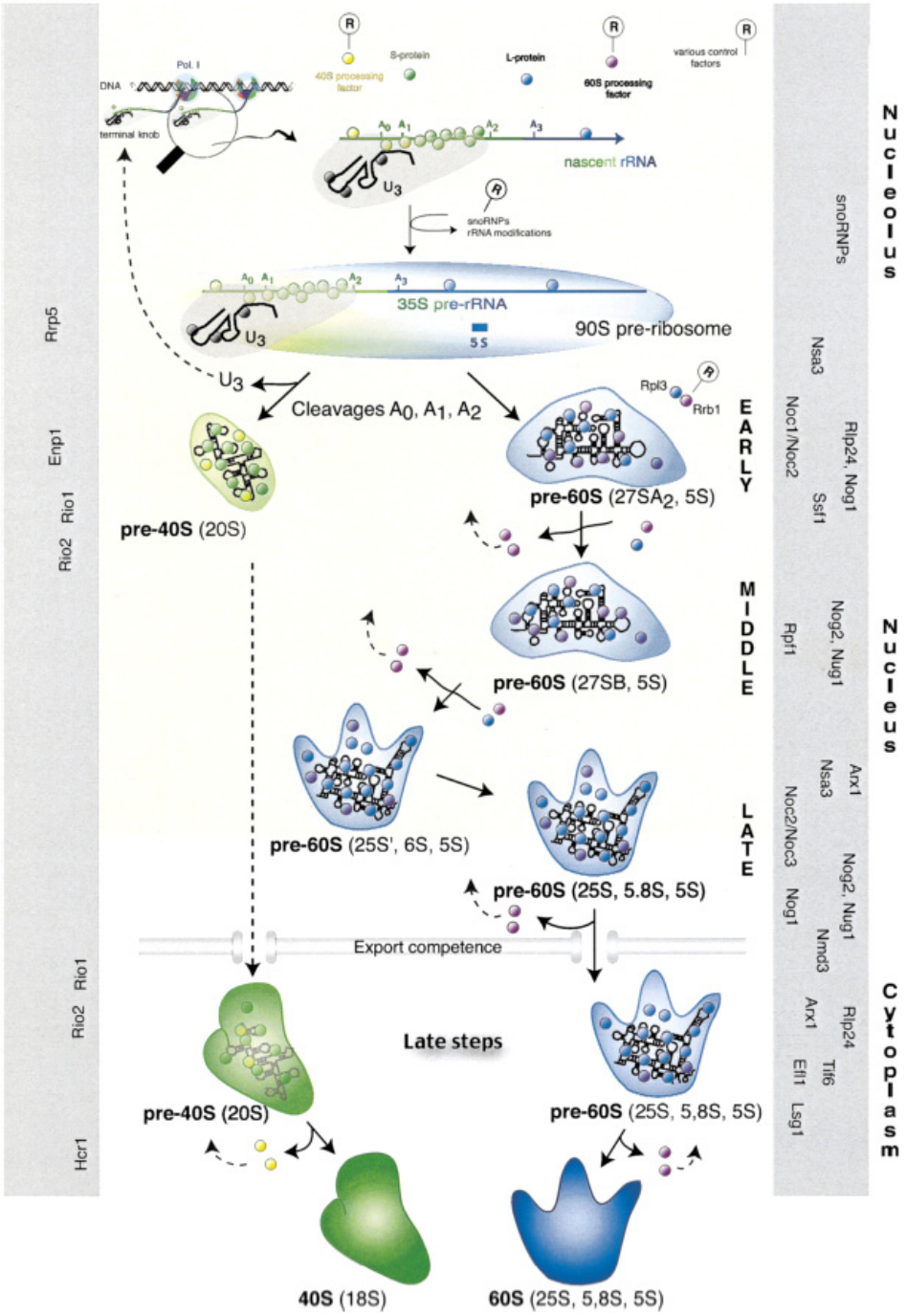

Figure 5. Ribosome biogenesis in *S. cerevisiae*
An overview of ribosome biognesis in *S. cerevisiae* is shown. The early steps, including transcription of the rDNA, as well as the formation of the 90S pre-ribosome (also termed SSU processome) occur in the nucleolus. Later maturation steps take place in the nucleoplasm and cytoplasm. Note that 60S biogenesis proceeds via multiple intermediates, while major 40S maturation steps take place inside the 90S pre-ribosome and do not involve major rearrangement steps after separation from the pre-60S subunit pathway. Ribosome biogenesis factors are shown at the left and right side, which are involved in specific steps of 40S and 60S biogenesis, respectively. Reproduced from Fromont-Racine et al., 2003.

The separation of early pre-ribosomes into pre-40S and pre-60S subunits can also initiate at site A_3. This processing step occurs independent of U3 snoRNA and generates on the hand the 23S pre-rRNA and on the other hand the $27SA_3$ pre-rRNA (Figure 4). Both precursors are further processed into the mature rRNA species of the SSU (18S rRNA) and LSU (25S and 5.8S rRNA). This processing route is suggested to be a minor alternative processing pathway.

2.3 R-protein assembly in prokaryotes

The ribosomal subunits are very huge RNP complexes and taking in account the principles of RNA folding, it is interesting to know how such a large RNA copes with all the difficulties of secondary and tertiary structure establishment, including kinetic traps of misfolded intermediates, and how this folding is achieved in conjunction with r-protein assembly. Most of our knowledge about ribosome assembly comes from *in vitro* studies in *E. coli*. The total reconstitution of functionally active prokaryotic 30S and 50S subunits from isolated rRNAs and r-proteins of *E. coli* was achieved by the groups of Nomura and Nierhaus, respectively (Traub and Nomura, 1968, 1969; Nierhaus and Dohme, 1974). Both reconstitutions require defined conditions, with moderate ionic strength, a relatively high Mg^{2+} concentration and one (30S) or two (50S) temperature steps (for review see Nierhaus and Wilson, 2004). The well balanced ionic strength is necessary, because interactions between r-proteins and rRNA would be suppressed if the ionic strength is too high, while non specific interactions would be increased if it is too low. The high Mg^{2+} concentration stabilises certain rRNA structures providing a scaffold for r-proteins and thus stabilizing r-protein / rRNA contacts. The reconstitution of both subunits is characterised by the appearance of one (30S) or two (50S) intermediates, which require an increased temperature to undergo structural rearrangements from a loose to a more compact conformation.

The achievement of the *in vitro* assembly of ribosomal subunits allowed to omit certain r-proteins from ribosome reconstitution experiments and to analyse the effect on translation fidelity using *in vitro* assays (for review see Spirin, 1999). Additionally, it paved the way for further analyses of the assembly requirements of r-proteins, which finally led to the *in vitro* assembly maps (see below). Noteworthy, the conditions of this *in vitro* reconstitutions are clearly non-physiological, suggesting that cells must have evolved a different strategy to overcome kinetic traps in the process of rRNA folding and r-protein assembly *in vivo*.

2.3.1 *In vitro* assembly

With the help of the established reconstitution of ribosomal subunits, the groups of Nomura and Nierhaus further evaluated the assembly of r-proteins by using purified individual proteins. In an enormous series of experiments, r-proteins were added in different order and combinations to the rRNA and their binding was analysed. This allowed to reveal assembly dependencies for almost all r-proteins and the results have been ordered in a so called “assembly map” (Mizushima and Nomura, 1970; Held et al., 1974; Herold and Nierhaus, 1987). The r-proteins were grouped into three different categories in accordance to their behaviour in these reconstitution experiments.

The first group are the primary binding proteins, which are capable to initiate pioneering interactions with the rRNA independent of other proteins. The secondary binders require one or more primary binding proteins for their association with rRNA, while tertiary binding proteins require both primary and secondary binders for their incorporation into ribosomal subunits.

Aiming to the nature of the interwoven tertiary structure of the 23S pre-rRNA (Figure 1), the 50S assembly map shows much more interconnections between single r-proteins and a very complex binding hierarchy. Furthermore, the reconstitution is very slow and inefficient and this is most likely also the reason why 30S assembly has been studied more extensively than 50S assembly.

Besides reconstitution of the entire 30S subunit, the three major domains of the SSU rRNA can be assembled independently of each other using fragments of 16S rRNA (Weitzmann et al., 1993; Samaha et al., 1994; Agalarov et al., 1998). Although the assembled domains exhibit a similar conformation as in the 30S structure, the tertiary binding proteins of the SSU rRNA 5′ (S5 and S12) and central domain (S21) were not able to bind stably to the isolated domains, suggesting that interactions between the single domains are needed to facilitate assembly of these tertiary binders.

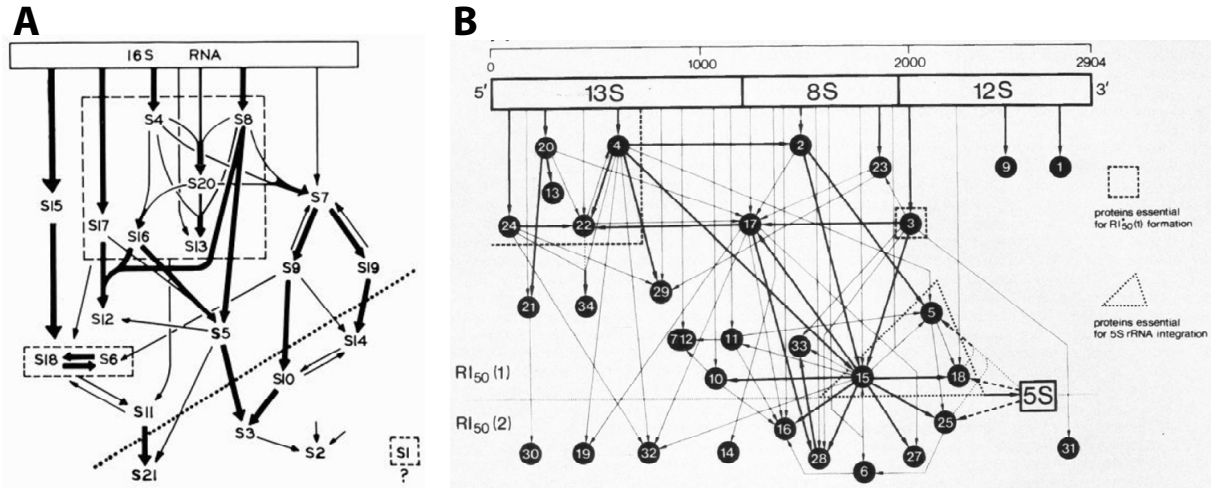

Figure 6. Assembly maps of the 30S and 50S ribosomal subunits from *E. coli*
Depicted are the original assembly maps. (**A**) The assembly map of the 30S subunit, note that the 16S rRNA is not depicted from the 5′ to 3′ end. Reproduced from Held et al., 1974. (**B**) The assembly map of the 50S subunit, with the 23S pre-rRNA depicted from the 5′ to 3′ end. Reproduced from Herold et al., 1987.

The assembly of the SSU rRNA central domain has been studied extensively, giving insights into the steps happening during assembly and pointing towards a general scheme for r-protein assembly (Orr et al., 1998; Agalarov et al., 2000; Wimberly et al., 2000). The primary binding protein S15 is capable of initiating rRNA contact and inducing a conformational change, which reorganises the central domain and makes it susceptible for assembly of downstream binding r-proteins. Interestingly, S15 shows no direct protein-protein contact to the downstream binding r-proteins,

suggesting that a change in the RNA tertiary structure facilitates assembly of the downstream r-proteins.

Studies on isolated domains also demonstrated that the SSU rRNA 5′ domain is able to acquire a native like conformation in the absence of r-proteins, but is certainly unstable without them (Adilakshmi et al., 2005). Thus, at least the 5′ domain is capable of self folding; however, stabilisation of the tertiary structure is achieved by r-protein assembly.

A generalised view of ribosome assembly could be as following; the binding site for primary binding proteins is created by transient RNA folding (which is unstable without r-proteins), this binding leads to a conformational change and stabilisation of the interaction, which creates the binding site for a secondary binder. The establishment of new favourable intermolecular interactions between the rRNA and r-protein probably drives the reorganisation of partially misfolded free RNAs or proteins (Williamson, 2000). Thus, a series of conformational changes of the rRNA, initiated and stabilised by r-proteins, leads to sequential formation of the mature and functional tertiary structure of the 16S rRNA.

Two independent studies suggest that ribosome assembly can initiate via multiple parallel folding pathways and provide evidence for a mechanism of ribosome assembly (Talkington et al., 2005; Adilakshmi et al., 2008).

With the help of isotope pulse chase experiments and subsequent quantitative mass spectrometric (PC/QMS) analysis it was possible to determine the kinetics of r-protein binding. The reconstitution reaction was initiated with 16S rRNA and ^{15}N-labeled r-proteins (pulse) for varying length of time and then chased with an excess of cold ^{14}N-labelled r-proteins. Mature 30S subunits were isolated and the ^{15}N/^{14}N ratio of each r-protein was determined using MALDI mass spectrometry. The time course of the pulse chase experiment allowed determination of the binding rates for 17 of the 21 r-proteins of the SSU. By the comparison of the binding rates two general tendencies could be observed; first, primary binding proteins bind in general faster than secondary and tertiary binding proteins, which is in accordance with the hierarchical order of assembly. Second, r-proteins of the SSU rRNA 5′ domain bind in general faster than proteins of the central or 3′ domains, consistent with a 5′ to 3′ directionality of assembly.

In addition, the theory of an assembly landscape for the 30S subunit was proposed, which is in agreement with earlier studies, suggesting several nucleation sites of ribosome assembly (Dodd et al., 1991; Nierhaus, 1991). The theory states that r-protein assembly can initiate and proceed via different routes and that there is no certain order of assembly with a global rate-limiting step that has to be passed. There are definitely some routes of assembly that are faster than others, but the advantage is that the slower ones will only slow down ribosome assembly but not completely block it, as this would be the case for a kinetic trap in a system with only one route for assembly.

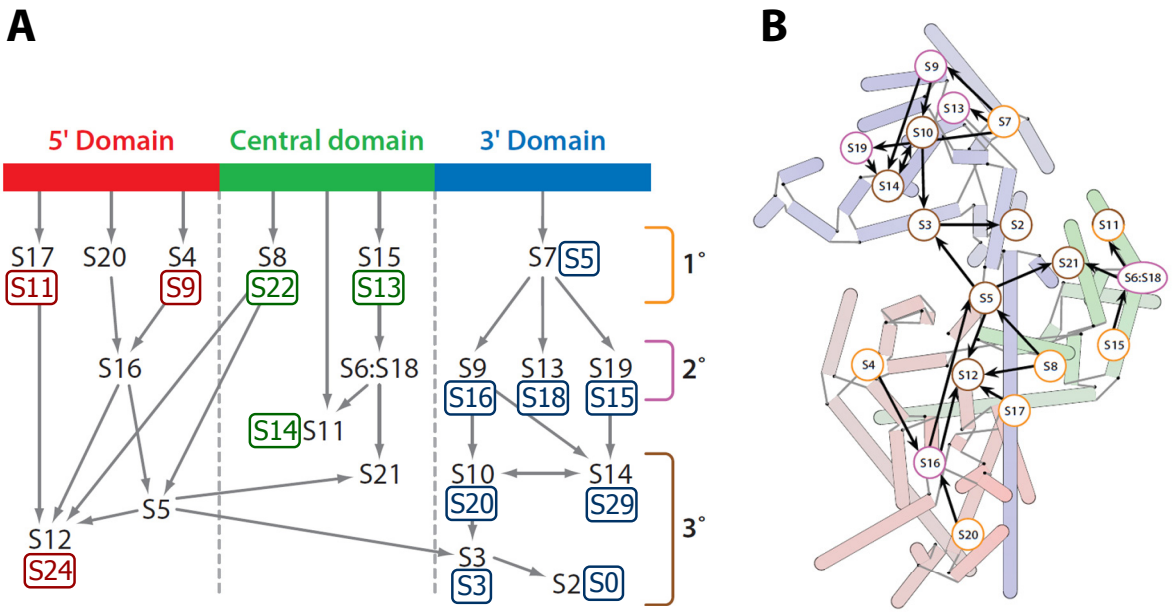

Figure 7. 30S assembly map ordered in accordance to the domain organisation of the 16S rRNA
(**A**) The different assembly trees of r-protein assembly of the prokaryotic 30S subunit are ordered in 5′ to 3′ direction of the 16S rRNA and attributed to 16S rRNA domain organisation (5′, central and 3′ domain). As described in section 2.1.2 (see also Figure 1) each of the three major domains of the secondary structure of 16S rRNA forms distinct morphological features of the 30S subunit. If existing, homologous r-proteins in *S. cerevisiae* are depicted inside boxes next to their prokaryotic counterparts. (**B**) A hybrid presentation of the secondary and tertiary structure of the 16S rRNA is depicted, showing the position of each helix, represented by a bar, in regard to its localisation in the tertiary structure. Reproduced and adapted from (Sykes and Williamson, 2009).

Time-resolved hydroxyl radical footprinting allowed real time snap shots of the early stages of ribosome assembly (Adilakshmi et al., 2008). Pre-folded 16S rRNA was incubated with r-proteins for varying length of time (ranging from 0.02 to 180s) and then exposed to a synchrotron X-ray beam generating hydroxyl radicals which can cleave unprotected nucleotides of the rRNA. The protection pattern was analysed by primer extension. The analysis revealed that early assembly events can start simultaneously at different positions of the 16S rRNA, which supports the idea of parallel folding pathways also suggested by the assembly landscape hypothesis (see above).

This interaction showed a biphasic kinetic, with an initial fast, but unstable association of r-proteins all over the rRNA, followed by a second slow phase characterised by stabilised interactions between the rRNA and r-protein by an induced fit mechanism. These slow forming interactions are determining the rate of protein addition and the hierarchical order of assembly. Meaning, even secondary and tertiary binding proteins can bind to their specific binding site on the rRNA, but stable incorporation is only possible (induced) after the preceding binding protein has overcome the slow second step and acquired a stable interaction with the rRNA, and thereby stabilizing the interaction of the downstream r-protein. It is very likely that the *in vivo* link between assembly and transcription simplifies the pathway by limiting the number of possible assembly routes.

2.3.2 *In vivo* assembly

Undoubtedly, the extensive *in vitro* study of ribosome assembly in *E. coli* gave insights into the principles of this process and revealed the hierarchical and cooperative incorporation of r-proteins into the 16S rRNA and the successive stabilisation of the tertiary structure to finally yield the functional 30S subunit. Furthermore, the experiments provide general information on RNA folding and RNA-protein interplay. However, the analyses suffer from the drawback of being an artificial situation, and the assembly process might have additional features in the *in vivo* context. This is impressively exemplified by the observation, that assembly of the SSU rRNA central domain can proceed *in vivo* without the primary binding protein S15, although admittedly much slower than in wild-type cells (Bubunenko et al., 2006). This could be explained by the reciprocity of the thermodynamics of cooperativity (Sykes et al., 2009). Cooperativity can be envisioned as a reaction of two substrates leading to a final product. In the event of ribosome assembly one substrate would be a certain RNA conformation whereas the other one is the r-protein and the final product is a structurally changed and stabilised rRNA / r-protein complex. In case of a secondary binding protein the RNA conformation is achieved by preceding binding of the primary binding protein. If this rRNA can acquire that same structure in the absence of the primary binding protein, then this structure would stabilise binding of the secondary binding protein and in turn allowing formation of the stabilised rRNA / r-protein complex.
However, besides no significant change in the overall architecture, the strain lacking S15 exhibits a cold sensitive phenotype and subunit joining is somewhat impaired. This underlines that the primary binding protein accelerates the formation of the SSU rRNA central domain by probably suppressing misfolding of the rRNA and stabilising the native structure under non optimal conditions.

Furthermore, the difference of *in vitro* and *in vivo* ribosome assembly is supported by the existence of several factors with roles in ribosome biogenesis. In *E.coli* most of the identified factors are nonessential due to the fact that this process seems to be very redundant (for review see Connolly and Culver, 2009). The few essential proteins have additional functions in other cellular processes, which makes it difficult to access the role of these factors in ribosome biogenesis. The best studied examples are rRNA / r-protein modifying enzymes and factors required *in vivo* for pre-rRNA processing. Recent progress implicated GTPases and other proteins in the process of ribosome assembly, but, although the binding sites for some of them were determined, their exact functions remain unclear. From the localisation data it is obvious that most of these factors interact with regions of the 16S rRNA that change conformation late in the assembly process, including interaction of RimM with S19 (secondary binding protein of the SSU rRNA 3' (head) domain), of RbfA with the 3' minor domain, and of Era between 3' (head) and central (platform) domain (Lövgren et al., 2004; Sharma et al., 2005; Datta et al., 2007). Another example for a factor being involved in final proofreading of ribosome function might be the late acting methylase KsgA (Xu et al., 2008). To act on its substrate, KsgA must pull out helix 45 in order to access the two adenines

that are going to be methylated. In doing so, KsgA prevents immature subunits from association with 50S subunits and therefore from entering the translational cycle. Thus, it appears that these late stages in assembly are highly controlled to result in active 30S subunits that are capable of engaging in the translation process.

In summary, the *in vitro* studies established the principle of self assembly of ribosomal subunits. While some of the principles probably apply also to *in vivo* assembly, it is obvious that *in vivo* assembly is achieved with much higher rates and less mistakes than *in vitro* assembly. Thus, the cell must have evolved different mechanisms to make this process *in vivo* as efficient as it is. Co-transcriptional assembly might reduce the amount of folding mistakes, because the larger the rRNA the higher the chance of kinetic traps. With the help of co-transcriptional assembly, short stretches of rRNA will sequentially be occupied by r-proteins, thereby inhibiting possible erroneous folding. Hence, the folding process *in vivo* might be envisioned rather as assembly of several small RNA stretches, than that of a large RNA (with all its difficulties) as it is *in vitro*.

2.4 R-protein assembly in eukaryotes

2.4.1 *In vitro* assembly

Only a few reports on *in vitro* assembly of ribosomes from eukaryotes can be found in the literature. These studies are far beyond the achievements in prokaryotes and report only partial reconstitutions, owing to the increased complexity of the eukaryotic ribosome and the existence of essential biogenesis factors (Reboud et al., 1972; Vioque et al., 1982; Lavergne et al., 1988). Recently, one group reported the *in vitro* reconstitutions of both ribosomal subunits from *Dictyostelium discoideum* (Mangiarotti and Chiaberge, 1997). Efficient assembly required immature precursor rRNA and a nuclear fraction including snoRNAs, suggesting on the hand that extra sequences in these precursors have a function in ribosome assembly and underlining on the other hand the need for additional factors. These results indicate that the prokaryotic principle of *in vitro* self-assembly of ribosomal subunits does not completely apply to ribosome assembly in eukaryotes.

2.4.2 *In vivo* assembly

In vivo assembly of r-proteins in eukaryotes has been studied with the help of electron microscopy for one rpS and one rpL (Chooi and Leiby, 1981). This group combined the technique of miller chromatin spreading with immuno-labelling of proteins (Miller and Beatty, 1969). The first technique allows the visualisation of the growing transcripts on the rDNA, while the second one allows an estimation at which step, on the growing rRNA transcripts, this protein assembles. The analysis revealed that both proteins assemble co-transcriptionally to nascent rRNA precursors. However, despite a huge potential of this technique, it has never been used since for the further analysis of r-protein assembly.

Recent improvements in the analysis of *in vivo* r-protein assembly in *S. cerevisiae* demonstrated that some principles of r-protein assembly of prokaryotes also apply to their counterparts in eukaryotes (Ferreira-Cerca et al., 2007). The analysis showed that most of the r-proteins of the SSU can already assemble to early precursors, which are not yet folded as in the mature subunits. This interaction is very weak in comparison to the interaction with later precursors, like 20S pre-rRNA, which is the direct precursor to the mature 18S rRNA. However, it is probably of relevance, as some of these r-proteins, especially the ones binding to the 5′ and central domain of the SSU rRNA, are necessary for early maturation steps. Furthermore, this is in agreement with the analysis in prokaryotes showing that there is a rather unstable interaction of r-proteins all over the 16S rRNA very early in the assembly process, which is followed by structural rearrangements and stabilization of the interaction by an induced fit mechanism between rRNA and r-proteins (Adilakshmi et al., 2008).
Thus, the early weak co-transcriptional assembly of r-proteins leads to structural rearrangements, thereby allowing rRNA processing by either providing the binding platform or exposing rRNA regions for rRNA processing factors. Alternatively, the cleavage events themselves could trigger structural rearrangements and result in stabilisation of rRNA–r-protein interactions. To date, it is not clear, whether stabilisation between rRNA–r-proteins is cause or consequence of the rRNA processing events.

The analysis revealed also the hierarchical order of assembly of the SSU rRNA 3′ (head) domain in *S. cerevisiae* (Ferreira-Cerca et al., 2007). The assembly of r-proteins was analysed after rpS5 and rpS15 depletion, the primary and secondary binding proteins of the SSU rRNA 3′ domain, respectively and showed that similar principles apply as for the prokaryotic *in vitro* assembly of this domain (Held et al., 1974). Additionally, the analysis demonstrated the existence of independent assembly domains of the SSU rRNA, because r-proteins of the 5′ and central domain (both forming the body of the SSU) were able to assemble to 20S pre-rRNA after disruption of 3′ (head) domain assembly.

The assembly of r-proteins is closely linked to several aspects of ribosome biogenesis including rRNA processing and transport. The inhibited release of Nmd3p, by missing incorporation of rpL10, leads to an export block of pre-60S particles (Hedges et al., 2005; West et al., 2005). Another well studied r-protein is rpL5. The depletion of this protein inhibits the incorporation of 5S rRNA into early pre-ribosomes and therefore causes rRNA processing and export defects of pre-60S subunits (Deshmukh et al., 1993). For the SSU, specific effects on rRNA processing and export can be attributed to incomplete assembly of r-proteins to certain structural domains of the SSU rRNA. R-proteins of the SSU rRNA 5′ and central domain, both forming the body in the three dimensional structure of the SSU, are required for early processing events at sites A_0, A_1, and A_2 (Ferreira-Cerca et al., 2005). In contrast, r-proteins binding to the SSU rRNA 3′ (head) domain are required for later rRNA processing steps generating the mature 18S rRNA. The export of the precursor to the 18S rRNA, the 20S pre-rRNA, is blocked or delayed in strains depleted of SSU rRNA 3′ domain binding r-proteins, thus linking proper head assembly to pre-40S export (Tabb-Massey et al., 2003; Léger-Silvestre et al., 2004; Ferreira-Cerca et al., 2005).

2.5 SSU processome / 90S pre-ribosome

An early pre-ribosomal particle consisting of the 35S rRNA precursor and having an estimated sedimentation coefficient of approximately 90S was already described in the 1970s, but the protein composition remained elusive until recently (Udem et al., 1972; Trapman et al., 1975). In 2002, two groups independently purified a large pre-ribosomal particle consisting of the 35S pre-rRNA, U3 snoRNA, and several biogenesis factors required for maturation of the SSU (Dragon et al., 2002; Grandi et al., 2002). The Baserga group named this particle SSU processome, because the containing factors were specifically required for maturation of the SSU, while the term processome has previously been introduced for the description of an early RNP consisting of snoRNPs and processing enzymes in analogy to the splicosome (Fournier and Maxwell, 1993; Dragon et al., 2002). Furthermore, they showed some evidence that this complex might constitute the terminal balls seen in miller chromatin spreads (Figure 3B), which assemble co-transcriptionally to the nascent rRNA precursor (Dragon et al., 2002). The Hurt group estimated the sedimentation coefficient of this pre-ribosome to be around 90S and were therefore referring to this complex as the previously described 90S pre-ribosome (Udem et al., 1972; Trapman et al., 1975; Grandi et al., 2002). Both purified pre-ribosomes show a similar protein composition, suggesting that the two groups have independently identified the same early pre-ribosome. To emphasise the differences between both purifications I will refer to the complex purified by the Hurt laboratory as 90S pre-ribosome and to the complex purified by the Baserga laboratory as the SSU processome.

Besides the identification of 28 biogenesis factors, the Baserga group identified also five ribosomal proteins (rpS4, rpS6, rpS7, rpS9, and rpS14) to be part of the SSU processome (Dragon et al., 2002). As a criterion for being a *bona fide* SSU processome component, a factor needs to interact with Mpp10p and the U3 snoRNA (both of which are known SSU processome components) and being required for early processing steps at site A_0, A_1 and A_2. The SSU processome components were named U three proteins (Utp). Except of the r-proteins, all SSU processome components showed additionally a nucleolar localisation. A refined analysis identified seven additional components of the SSU processome (Bernstein et al., 2004). Thus, these analyses indicated that the SSU processome consists in total of 35 non-ribosomal proteins and five r-proteins, the U3 snoRNA, the 35S pre-rRNA and later precursors to the 18S rRNA, mainly 23S and the low abundant 21S and 22S pre-rRNAs.

The rRNA content of the SSU processome suggests a bias for precursor particles of the SSU, because at least half of its rRNA content can be attributed to precursors of the 18S rRNA. This could explain why exclusively factors required for SSU maturation have been identified in this approach and the SSU processome might therefore be considered as an SSU assembly intermediate (Bernstein et al., 2004).

The Hurt group affinity purified 13 different ribosome biogenesis factors and identified 35 co-precipitating biogenesis factors, of which 28 are the same proteins as found by the Baserga group (Grandi et al., 2002). In addition, more r-proteins were identified in these analyses compared to the

ones of the Baserga group. Most of the identified r-proteins were rpS, whereas only few rpL could be identified. Of note, due to the very small size of some r-proteins, these were already lost from the SDS polyacrylamide gel and could therefore not be analysed. In general, r-proteins are not very stably bound to 35S pre-rRNA (Ferreira-Cerca et al., 2007). Therefore most of the r-proteins might be lost from the purification of the SSU processome, due to the purification procedure, while the purification of the 90S pre-ribosome preserved these transient interactions apparently better. The co-precipitated rRNA species have been analysed by the Hurt group using primer extension, which cannot distinguish between 23S and 35S pre-rRNAs as both have the same 5′ end. Thus, the qualitative and quantitative distribution of rRNA precursors in these 90S pre-ribosome purifications is unclear.

Depletion of the U3 snoRNA or Utps results in the loss of the terminal balls in miller spreading analyses of rRNA genes; hence these conglomerates at the 5′ end of the nascent rRNA might correspond to the SSU processome (Dragon et al., 2002). This observation points towards a co-transcriptional assembly of the SSU processome. Furthermore, a detailed analysis of these terminal balls revealed, that they are compacted as the rRNA precursor is being transcribed prior to being cleaved at site A_2 (Osheim et al., 2004). Thus, it seems that the SSU processome undergoes structural rearrangements, probably accompanied by changes in the protein composition, during the course of rRNA maturation. Whether the loose structure of the very early terminal balls contains already all SSU processome components is not clear. It seems likely that this is not the case and that association of the missing proteins results in further rRNA folding, indicated by the appearance of compacted terminal balls seen on longer transcripts (Figure 3B).

Several subcomplexes or functional entities of the SSU processome have been described in the literature. Besides the sedimentation behaviour in a sucrose gradient, the Hurt laboratory analysed the size of the Pwp2p-TAP associated protein complex on a gelfiltration column, revealing the existence of two distinct complexes, one in the range of 4-6 MDa (presumably the 90S pre-ribosome) and another one with around 600 Da (consisting of six proteins) (Grandi et al., 2002). This Pwp2p subcomplex could be confirmed by the analysis of Krogan et al. (Krogan et al., 2004). In this study different SSU processome components were affinity purified from yeast cellular extracts which were depleted of fast sedimenting ribosomal assembly intermediates (including SSU processome) by high speed centrifugation. This allowed the identification of small complexes which can exist precluded from pre-ribosomes, either because they are only loosely associated with early pre-ribosomes or represent functional entities with physiological relevance. Besides the confirmation of a Pwp2p subcomplex (Grandi et al., 2002, termed UTP-B in Krogan et al., 2004) consisting of Pwp2p, Dip2p, Utp6p, Utp13, Utp18p and Utp21p, the analysis revealed two other subcomplexes, the UTP-A submodule consisting of Utp4p, Utp8p, Utp9p, Utp10p, Utp15p, Nan1p and Pol5p and the UTP-C subcomplex consisting of Utp22p, Rrp7p, Cka1p, Cka2p, Ckb1p and Ckb2p.

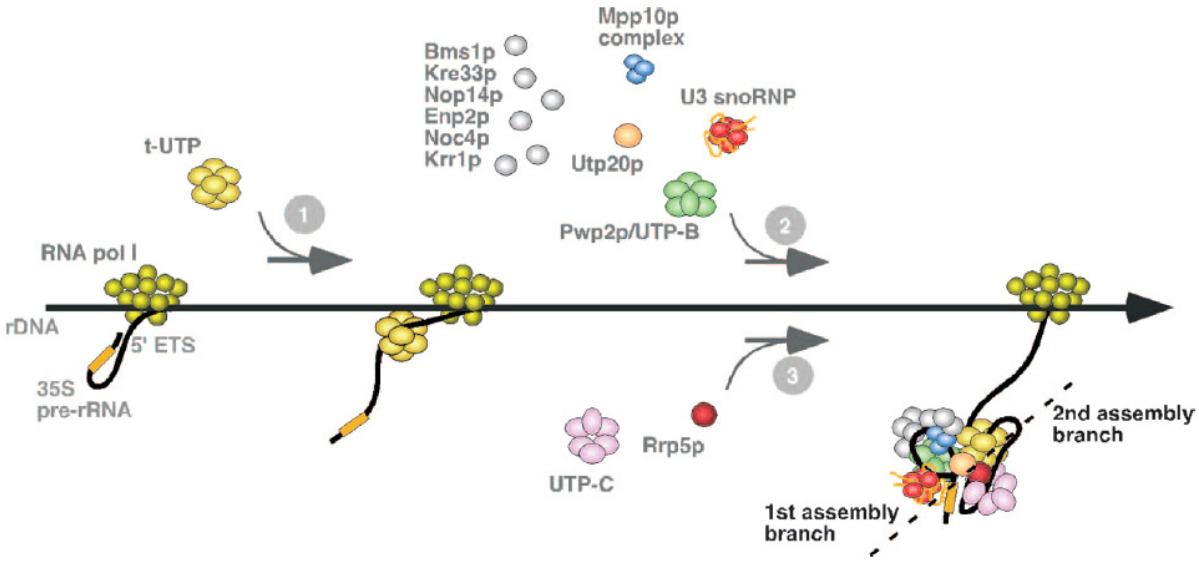

Figure 8. Hierarchical assembly of the SSU processome
A model for SSU processome subcomplex assembly has been predicted by the group of Mercedes Dosil (Pérez-Fernández et al., 2007). According to this model, the UTP-A / t-UTP (1) subcomplex is assembled co-transcriptionally to the nascent 35S rRNA precursor and is required for subsequent assembly of two independent assembly branches. One assembly branch (2) involves cooperative binding of the UTP-B subcomplex, the U3 snoRNP, and the Mpp10p complex (Dosil and Bustelo, 2004; Gérczei and Correll, 2004). This assembly is required for association of other SSU processome components of the non-defined group (Bms1p, Kre33p, Nop14p, Enp2p, Noc4p, Krr1p and Utp20p). Whether this group of proteins is also incorporated into early pre-ribosomal particles in a cooperative manner needs to be determined. The other branch requires primary binding of Rrp5p, which in turn allows association of the UTP-C subcomplex. Of note, the results of this study are also compatible with a model in which all subcomplexes are binding to early pre-RNAs as a single preassembled complex. Reproduced from Pérez-Fernández et al., 2007.

The UTP-C complex has been implicated in regulating the crosstalk between r-protein gene transcription and rRNA processing (Rudra et al., 2007). This analysis provided some evidence that Utp22p and Rrp7p are normally engaged in rRNA processing as part of the SSU processome. However, when rRNA transcription is reduced, Utp22p and Rrp7p become available to associate with casein kinase II and Ifh1p in a so called CURI complex. Ifh1p is an essential transcription factor for r-protein genes, and as part of the CURI complex it is sequestered from these genes and transcription is hence reduced.

It has been suggested that a subcomplex of the SSU processome, named t-UTP (transcription-UTP), can assemble independent of Pol I transcription with the rDNA locus and that it is required for efficient transcription by Pol I (Gallagher et al., 2004). The t-UTP subcomplex has almost the same protein composition as the UTP-A subcomplex, consisting also of seven proteins, but containing Utp5p instead of Pol5p. Thus, the UTP-A as well as the t-UTP complex probably refer to a very similar complex, with only minor differences, which could be due to the different purification methods and I will therefore refer to this subcomplex as UTP-A.
However, a recent report challenges the involvement of UTP-A members in the process of Pol I transcription (Wery et al., 2009). The authors provide evidence that proteins belonging to the UTP-

A subgroup are not required for Pol I transcription. Furthermore, they demonstrate, by the employment of chromatin immunoprecipitation experiments, that ongoing transcription and the presence of nascent transcripts are necessary for association of UTP-A, UTP-B and UTP-C within the transcription unit of the rDNA. The most significant interaction of factors of these submodules with the rDNA locus was observed in the region of the 3′ end of the 18S rRNA until the 3′ end of the 25S rRNA.

Another subcomplex named Mpp10p complex consisting of Mpp10p, Imp3p and Imp4p has been described (Lee and Baserga, 1999; Wehner et al., 2002). This complex specifically interacts with the U3 snoRNA, but not with other snoRNAs and is probably recruited to the snoRNA via Imp3p.

Furthermore, there is a fifth group including all SSU processome components that have not been grouped in one of the other four subcomplexes (UTP-A, UTP-B, UTP-C, and Mpp10p complex). This group is certainly more diverse and the members were not found to be part of one subcomplex independently of their association into pre-ribosomes. However, these proteins might associate as monomers or maybe as several smaller subcomplexes rather than one whole subcomplex, which is exemplified by the existence of a hetreodimeric complex consisting of Noc4p and Nop14p (Milkereit et al., 2003).

The 35S pre-rRNA assembly relationship between these five different subgroups has been recently investigated using a variety of methods, including RNA co-immunoprecipitation, sucrose density gradients and mass spectrometry (Pérez-Fernández et al., 2007). During this study, individual representatives of the UTP-A, UTP-B and UTP-C submodules were depleted and association of other Utps with early pre-ribosomal particles was analysed. This approach revealed a hierarchical order of assembly for the different subcomplexes (Figure 8). The UTP-A submodule is required for association of UTP-B and UTP-C, whereas UTP-B and UTP-C can assemble independent of each other. Additionally, UTP-B, which is suggested to assemble cooperatively with the U3 snoRNP and the Mpp10p complex, is necessary for association of a group of non-defined SSU processome components (Dosil et al., 2004; Gérczei et al., 2004; Pérez-Fernández et al., 2007). Furthermore, Rrp5p is required for UTP-C assembly to early pre-ribosomal particles. The results of this approach could suggest a sequential order of events, in which UTP-A might initiate contact with the pre-rRNA, followed by assembly of the UTP-B and UTP-C subcomplex (Figure 8). However, the results of this study are also compatible with a model in which all subcomplexes are binding as a single preassembled complex to early pre-rRNAs, but in which stable association of UTP-B and UTP-C certainly depends on the presence of UTP-A in this complex.

2.6 Objective

As for ribosome biogenesis factors in general, depletion phenotypes for most of the SSU processome components are known (blockage of processing at sites A_0, A_1 and A_2), but their exact molecular function is still elusive. Thus, one of the central remaining questions is: What is the molecular function of the numerous factors involved in these early steps of ribosome biogenesis?
As no endonucleases performing the cleavages at sites A_0, A_1 and A_2 have been identified, one or several of these factors might be the missing endonucleases. Other factors could assist in the assembly process by inhibiting erroneous folding of the rRNA or by active remodelling of pre-ribosomal intermediates. Some of the ribosome biogenesis factors have been designated to be NTPases, hydrolysing nucleotide triphosphates. The released energy might be used for remodelling steps requiring a major conformational change in the pre-ribosomal particle.
In this regard it has been proposed that the action of the three AAA ATPases, Rix7, Rea1 and Drg1 in the process of LSU maturation goes along with a change in the protein composition of pre-ribosomal assembly intermediates (Gadal et al., 2001; Galani et al., 2004; Pertschy et al., 2007; Kressler et al., 2008; Ulbrich et al., 2009). Thus, it can be speculated that these ATPases are involved in the disintegration of protein-protein or protein-rRNA interactions, leading to the remodelling of pre-ribosomal particles.
Two constituents of the SSU processome (Utp14p and Kre33p) show sequence homology to P-loop-type ATPases (Strunk and Karbstein, 2009). Hence, both proteins could fulfil similar functions as suggested for the three AAA ATPases required for LSU maturation.
Several ribosome biogenesis factors belong to the class of DExH/D ATPases which are also referred to as RNA helicases. These enzymes were shown to unwind RNA duplexes, dissociate proteins from RNA or to assist in RNA strand annealing (Jankowsky and Fairman, 2007). It is conceivable that all of these assigned functions can be supportive to enable the highly complex process of ribosome assembly. Some of these RNA helicases have been suggested to play a crucial role for the release of snoRNAs from pre-rRNAs (Kos et al., 2005; Liang et al., 2006; Bohnsack et al., 2008). In the case of the U3 snoRNA, this removal is required to establish the central pseudoknot structure within the SSU (Hughes, 1996, and see below). Interestingly, depletion of the majority of the SSU RNA helicases did not reveal a pronounced effect on the release of individual snoRNAs from rRNA precursors (Bohnsack et al., 2008). This observation raises the possibility that these helicases could be mainly involved in structural remodelling of pre-ribosomal particles.

However, most of the SSU processome components show no homology to known protein motifs. These proteins could, nevertheless, fulfil an RNA "chaperone like" function. The co-transcriptional binding of SSU processome components to the emerging rRNA precursor could protect specific sites in the pre-rRNA from incorrect interactions and thereby facilitate early folding events of rRNA precursors.

A similar function has been proposed for the U3 snoRNA, which is also part of the SSU processome. The U3 snoRNA might function as an "RNA chaperone" by preventing the premature formation of the universally conserved central pseudoknot structure of the SSU rRNA, forming between the loop of the 5' terminal helix and a connecting region between the central and major 3' domains (Hughes, 1996). Furthermore, r-proteins themselves exhibit an RNA chaperone activity *in vitro*, which could also support the correct folding of the rRNA *in vivo* (Semrad et al., 2004).

To shed more light on the involvement of the SSU processome in early folding and assembly events, the relationship between r-protein and SSU processome assembly has been studied during this PhD thesis. To this end, several strains have been established allowing to deplete representative r-proteins of each structural domain of the 18S rRNA (5', central and 3' domain) and to analyse the association of representatives of each subgroup of the SSU processome (UTP-A, UTP-B, UTP-C, Mpp10p complex and nondefined group) with early pre-ribosomes. One prerequisite for a successful analysis was the development of a mass spectrometry based method allowing the semiquantitative comparison of the protein composition of affinity purified pre-ribosomal particles from different mutants. As a complementary technique, direct RNA co-immunoprecipitation experiments were employed.
This comprehensive study gives insights into the interplay between r-proteins and SSU processome factors in early ribosome assembly and folding events.

3 RESULTS

3.1 Construction and analysis of yeast strains conditionally expressing rpS4, rpS21, rpS22 and rpS29

3.1.1 Strain construction

In a former systematic analysis on the function of yeast SSU r-proteins, the chromosomal copy or copies (more than two third of r-proteins are expressed in *S. cerevisiae* from two genes) of the respective genes have been deleted and rescued by a plasmid supporting the expression of the r-protein under control of a galactose inducible promoter (Ferreira-Cerca et al., 2005). This setup allowed studying the depletion phenotype of the respective protein by shifting the strain from galactose to glucose containing medium. R-proteins exhibit a very fast turnover time when not incorporated into ribosomes. Thus, it was sufficient to shift the cells for two to four hours to glucose medium in order to observe phenotypes. During this analysis, four strains failed to be constructed due to an unclear distribution of marker genes or a likely appearance of a third copy of the gene of interest. Since these strains are missing for a complete collection of galactose inducible strains of all rpS, the goal of this work was to construct these strains. The missing galactose inducible strains include the ones for rpS4, rpS21, rpS22 and rpS29, all of which are encoded by two gene copies. The strategy for the construction was as following: Haploid strains, in which one of the gene copies was replaced by a geneticine resistance marker (*KanMX4*) are commercially available and were used for crossing to yield a diploid strain harbouring both a wild-type allele and a knockout allele of both copies of the respective ribosomal protein (RP) gene. The diploid strain was then transformed with a "shuffle" vector consisting of the respective RP gene under control of its own promoter and terminator and the *URA3* marker gene as selection marker. This plasmid is necessary to complement the full knockout of both copies, which would be lethal if the r-protein is essential for yeast growth. After sporulation and meiotic division of this diploid strain, the tetrads were separated and the distribution of the knockout marker for the two copies was followed by selection medium for geneticine resistance. By taking advantage of the *URA3* gene on the shuffle plasmids, it can be tested whether the RP gene is an essential one. When 5-fluoro-orotic acid (5-FOA) is added to the medium, only *URA3* auxotrophic cells are able to grow, because cells containing the *URA3* gene convert 5-FOA to a toxic substance. Only cells which are able to survive without the plasmid harbouring *URA3* and the RP gene can grow on 5-FOA medium. Hence, cells will not be viable on 5-FOA plates, if the RP gene is essential.

In addition, this negative selection can be used to introduce the respective RP gene under control of the inducible *GAL1* promoter on a plasmid carrying a different marker gene (*LEU2*). Only cells that lose the shuffle plasmid and take up the *GAL1* plasmid with the RP gene are able to survive on galactose containing 5-FOA plates. The essential phenotype can be confirmed by the test for galactose dependent growth. For *RPS4A/B* and *RPS21A/B* this strategy proofed to be fruitful and

galactose dependent strains were obtained (Y800 and Y801), whereas no clear genotype could be established for *RPS22A/B* and *RPS29A/B* (Figure 9; Y800 and Y801).

After evaluation of the genotype of the single knockout strains of *RPS22A/B* and *RPS29A/B* it became obvious that the apparent genotype differs from the expected one. The analysis suggested a third copy (besides *RPS29A* and *RPS29B*) in the case of the *Δrps29B* strain. In a PCR using genomic DNA of this strain as a template and primers specific for the *RPS29B* gene two products were obtained. One PCR product had the size of a wild-type allele and one that of the knockout allele, which is larger in size. Interestingly, *RPS29B* seems to have duplicated in the genome, induced by the attempt of knocking out this gene in wild-type cells (data not shown). In fact, similar observations have been made before in case of *RPL4* and *RPP0*, where an additional gene copy could be detected, arising either by partial chromosome duplication or by gene translocation (Santos and Ballesta, 1994; Ohtake and Wickner, 1995). In the case of the *Δrps22A* strain no clear result for the analysis of the genotype could be obtained. Subsequently, different strategies were attempted to obtain single knockout strains for *RPS22A* and *RPS29B*. First of all, the knockout selection marker was exchanged from *KanMX4* to *HIS3MX6* for the copy of the RP gene that did not cause problems and showed a clear genotype, *RPS22B* and *RPS29A*, respectively. This allowed the direct assessment of the distribution of the knockout marker from both alleles by the selection for geneticine resistance and histidine prototrophy.

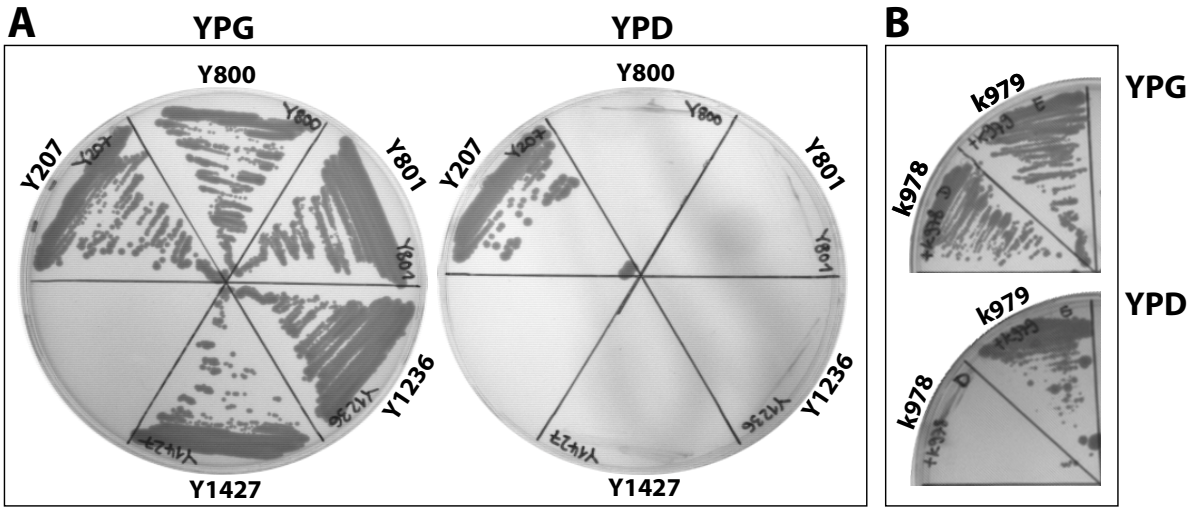

Figure 9. Growth phenotype analysis of strains conditionally expressing rpS4, rpS21, rpS22, and rpS29
(**A**) The galactose inducible strains (GAL-RPS4A (Y800), GAL-RPS21A (Y801), GAL-RPS22A (Y1427) and GAL-RPS29B (Y1236)) and a wild-type strain (Y207) were streaked out on galactose (YPG) and glucose (YPD) containing full medium plates and cultivated for three days at 30°C.
(**B**) The GAL-RPS29B (Y1236) was transformed with plasmid YCplac33-RPS29A (k978) or YCplac33-RPS29B (k979) and selected for uracil prototrophy. Positive transformants were streaked out on galactose (YPG) and glucose (YPD) containing full medium plates and cultivated for three days at 30°C.

Second, a strain with a clear genotype concerning the knockout of *RPS22A* and *RPS29B* had to be established. To obtain a GAL-RPS29 strain, a new single knockout strain for *RPS29B* was ordered and was always kept under selection pressure for geneticine resistance. Furthermore, this time transformation with the plasmid, harbouring the gene for *RPS29B* under control of the *GAL1* promoter, was performed prior to crossing with the knockout strain of the respective other copy. This plasmid is a multi copy plasmid with *RPS29B* under control of the strong *GAL1* promoter. This procedure was expected to result in a high expression level of rpS29B in these cells. Indeed, appearance of a new chromosomal copy of *RPS29B* could be prevented by this strategy, established for deleting *RPP0* by the group of Juan Ballesta (Santos et al., 1994). Crossing with the *Δrps29A* strain, sporulation and tetrad analysis yielded a haploid *Δrps29A* / *Δrps29B* strain exhibiting GAL dependent growth (Figure 9A; Y1236). Unfortunately, this approach was not successful for constructing the *Δrps22A* / *Δrps22B* strain and that is why a different strategy was needed.

A defined haploid *Δrps22A* strain could be obtained by extensive analysis of spores after tetrad dissection of a diploid strain carrying two knockout alleles of *RPS22A*, two wild-type alleles of *RPS22B* and a plasmid harbouring the wild-type copy of *RPS22A* on a shuffle plasmid (*URA3*). In addition, this analysis underlined the earlier observed inconsistency in the analysis of the genotype of *Δrps22A* single knockout strains, because most of the analysed spores showed either a PCR product corresponding to the wild-type allele or no PCR product at all. After crossing with the *Δrps22B* strain, transformation with a plasmid encoding rpS22A under the *GAL1* promoter, sporulation and tetrad analysis, a haploid *Δrps22A* / *Δrps22B* strain showing galactose dependent growth could be established (Figure 9A; Y1427).

In summary, the entire *GAL1* controlled strains of *RPS4*, *RPS21*, *RPS22* and *RPS29* exhibited galactose dependent growth, arguing that the corresponding gene products are essential for yeast cell viability (Figure 9A; compare YPD and YPG). This essential phenotype was confirmed with another plasmid (YCplac33, CEN4) bearing the wild-type gene of the respective protein under control of its own promoter / terminator and the *URA3* gene. All these shuffle strains exhibited 5-FOA sensitivity confirming the essential function of rpS4, rpS21, rpS22 and rpS29 (data not shown). Additionally, these results confirm previous reports which demonstrated the lethal phenotype of *RPS4A/B* or *RPS21A/B* knockouts (Synetos et al., 1992; Tabb-Massey et al., 2003). Interestingly, only *RPS29B* on plasmid YCplac33-RPS29B (k979), but not *RPS29A* on plasmid YCplac33-RPS29A (k978) was able to complement the full knockout of both copies and to support growth (Figure 9B; compare YPD and YPG). The identity of both plasmids was confirmed by sequencing.

3.1.2 Analysis of rRNA processing phenotypes in conditional mutants of rpS4, rpS21, rpS22 and rpS29

To study the rRNA processing after shut down of rpS4, rpS21, rpS22 and rpS29 expression, the strains were cultivated over night in galactose medium and then shifted for two and four hours to glucose containing medium. The total RNA of these cells was extracted and steady state (pre-) rRNA levels were analysed by northern blotting.

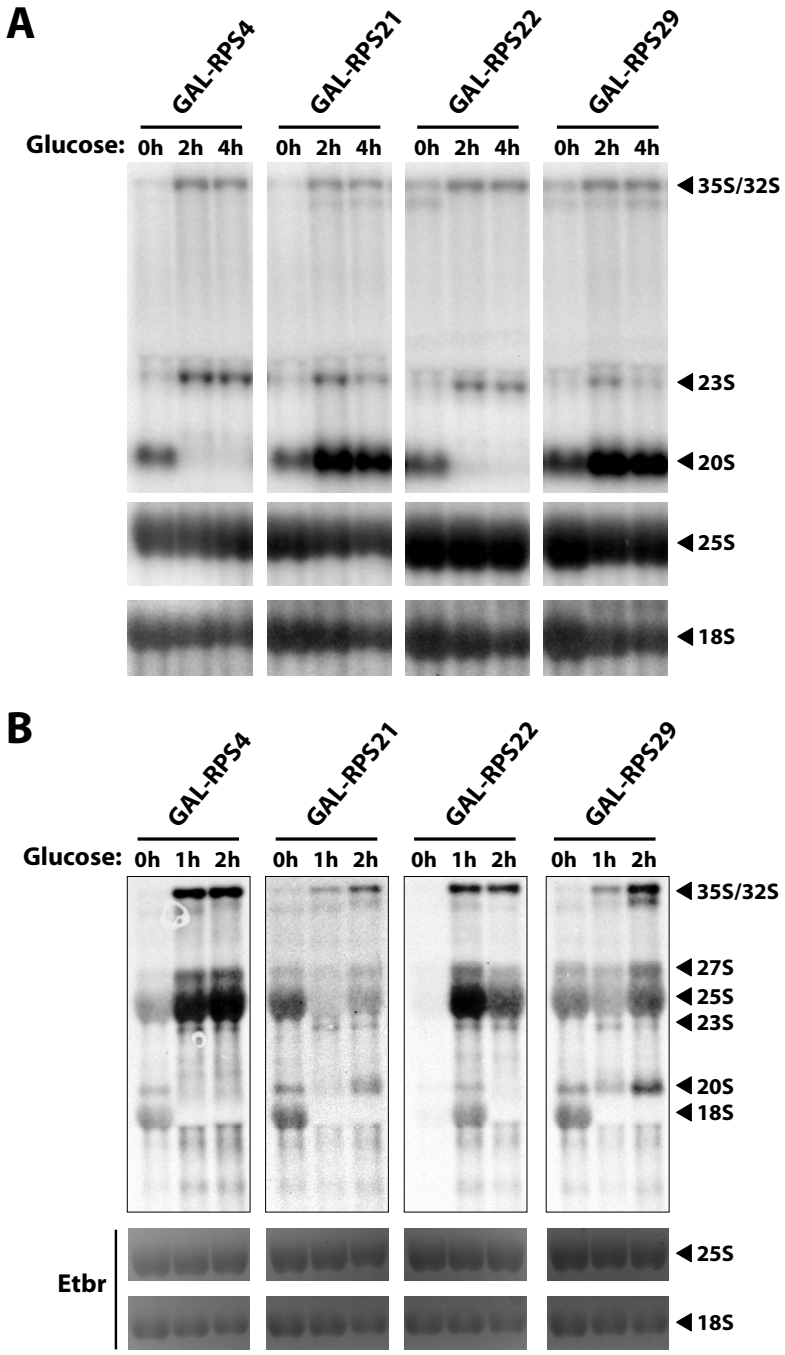

Figure 10. Analysis of steady state (A) and newly synthesised (B) (pre-) rRNA levels in strains depleted of rpS4, rpS21, rpS22, and rpS29.

(**A**) The strains Y800, Y801, Y1236 and Y1427 conditional expressing r-proteins under control of a galactose inducible promoter were grown overnight in galactose containing full medium (YPG). One part of the logarithmically growing culture was harvested (0h) and the other part was shifted to glucose containing medium (YPD) for 2 and 4 hours. The RNA from the equivalent to 5 OD_{600} cells was phenol/chloroform extracted. The equivalent to 0.5 OD_{600} cells was loaded on an agarose gel. The separated RNA was blotted onto a membrane and probed for different rRNA species, indicated at the right side (oligo 1819 hybridises within the ITS1 region (upper panel), oligo 212 hybridises within the 25S region (middle panel), and oligo 205 hybridises within the 18S region (lower panel).

(**B**) The strains Y800, Y801, Y1236 and Y1427 were cultivated in galactose medium (YPG) or for 1 and 2 hours in glucose medium (YPD). An equivalent to 1 OD_{600} cells was incubated with 20µCi of 5', 6' [^{3}H]-uracil for 20 minutes at 30°C. The RNA was phenol/chloroform extracted. The equivalent to 0.5 OD_{600} cells was loaded on an agarose gel. The separated RNA was blotted onto a membrane and the labelled rRNA was visualised with a BAS-TR 2040 screen. A Picture of the ethidium bromide stained gel is shown as a loading control, showing the level of unlabelled 18S and 25S rRNAs.

The results are shown in Figure 10A (compare lanes 0h (RP genes are expressed) with lanes 2h and 4h (RP gene expression is shut down)). The depletion of rpS4 and rpS22 led to an early rRNA processing phenotype, meaning an accumulation of 23S and 35S pre-rRNA and undetectable amounts of 20S pre-rRNA (see yeast rRNA processing scheme in Figure 4). In contrast, the depletion of rpS21 and rpS29 resulted in a later pre-rRNA processing phenotype, illustrated by the accumulation of 20S pre-rRNA, which is the direct precursor to the mature 18S rRNA, and a slight accumulation of 23S and 35S pre-rRNAs. All strains exhibited reduced amounts of mature 18S rRNA compared to 25S rRNA of the large subunit (Figure 10A; compare ratio 25S / 18S at 0h and 4h).

The phenotypes were further studied by [^{3}H]-uracil pulse experiments. In such an experiment, only newly synthesised (pre-) rRNAs are labelled by the incorporation of [^{3}H]-uracil. Figure 10B shows that in all strains production of mature 18S rRNA was largely reduced; whereas 25S rRNA production was not affected (compare lanes 0h with lanes 1h and 2h). In addition, after shut down of rpS4 and rpS22, 20S pre-rRNA production was not detectable. The early rRNA precursors, 23S and 35S, accumulate in all strains, although to a different extent.

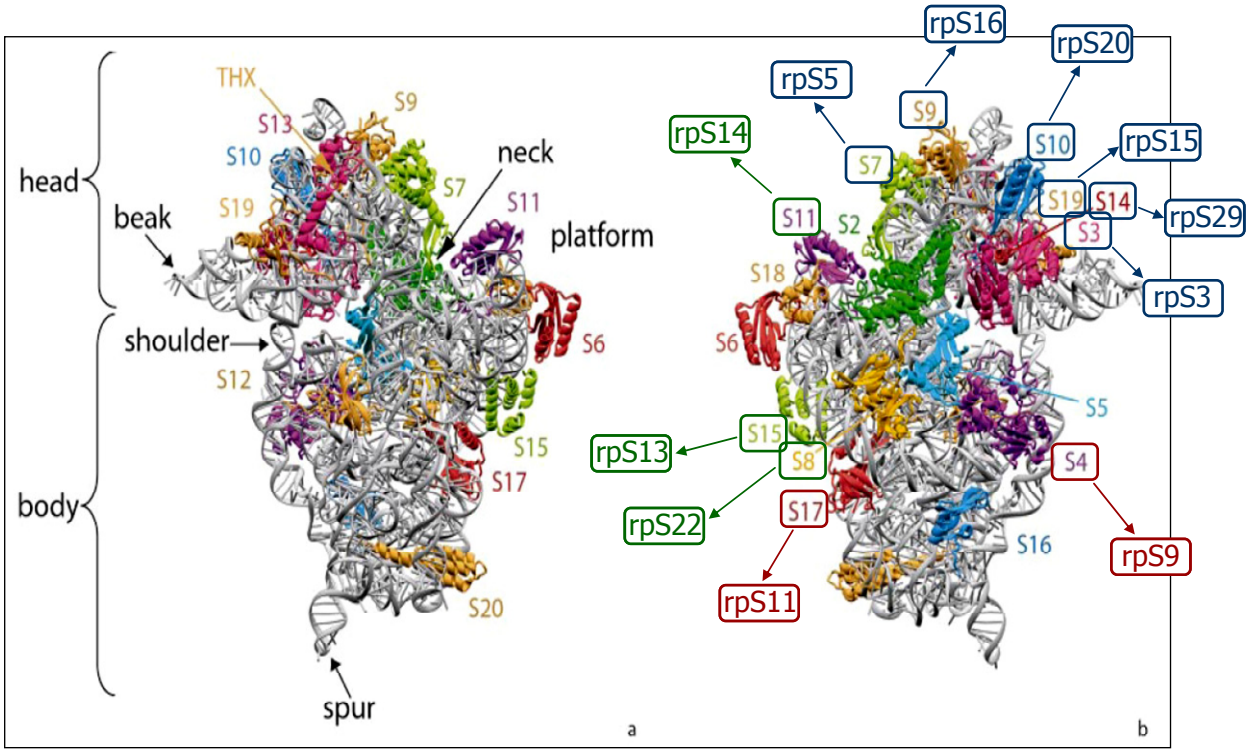

Figure 11. X-ray structure of the 30S subunit from *Thermus thermophilus*
Morphological features of the 30S subunit structure are depicted and homologous r-proteins in *S. cerevisiae* are labelled. R-proteins binding to the 5′ domain of the 16S rRNA (mature rRNA of the prokaryotic SSU) are depicted in red, the ones binding to the central domain are depicted in green and the ones binding to the 3′ major domain are depicted in blue. The 5′ domain forms the shoulder and the foot, the central domain forms the platform and both together form the body of the SSU structure. The 3′ major domain forms the head of the SSU structure. Compare also to Figure 1 and Figure 7. Reproduced and adopted from Brodersen et al., 2002.

The results for rpS22 and rpS29 are consistent with the localisation of their homologs on the structure of the *E. coli* small ribosomal subunit (30S). The homolog of rpS22 (S8) is the primary binder of the most 5′ part of the central domain of the 16S rRNA, which forms the platform of the SSU (Figure 11). Therefore, the depletion of rpS22 leads to an early rRNA processing phenotype (Figure 10). In contrast, the homolog of rpS29 (S14) is a tertiary binder of the 3′ domain of the 16S rRNA, which forms the head of the SSU and depletion results in a rather late rRNA processing phenotype (Figure 10). No homologs exist for rpS4 and rpS21 in *E. coli*, but a previous study on rpS21 reported a similar rRNA processing phenotype as shown here (Tabb-Massey et al., 2003). This late phenotype suggests that rpS21 is part of the 3′ domain, while rpS4 seems to be part of the body domain (including 5′ and central domain of the SSU rRNA). In section 3.2 and 3.3 the influence of rpS22 (as a representative for SSU rRNA central domain assembly) on the assembly of SSU processome components to nascent SSUs was investigated.

3.2 Assembly of the SSU-processome component Noc4p with pre-ribosomal particles after blockage of SSU rRNA 5′, 3′ and central domain assembly

Ribosome biogenesis in eukaryotes starts with the synthesis of the 35S rRNA precursor by polymerase I, which in the course of maturation is processed into the mature 18S, 25S, and 5.8S rRNAs (Figure 4). Co-transcriptional assembly to nascent pre-rRNA has been suggested for a group of biogenesis factors as well as for some early binding r-proteins of the SSU (Chooi et al., 1981; Gallagher et al., 2004; Wery et al., 2009). At a post-transcriptional state, these proteins can be isolated *ex vivo* as part of a huge RNP, termed 90S pre-ribosome or SSU processome (subsequently used term) together with 35S pre-rRNA and the small nucleolar U3 RNA (U3 sno-RNA) (see section 2.5). Most members of the SSU processome are called Utps (U three proteins), inferred from their association with the U3 snoRNP, and are required for the maturation of the SSU (Dragon et al., 2002; Grandi et al., 2002). Additionally, most SSU processome components localise in yeast cells to the nucleolus **(**Figure 3A). Recent studies indicate that SSU processome components can be grouped into at least four architectural and eventually functional submodules (Gallagher et al., 2004; Grandi et al., 2002; Krogan et al., 2004; Pérez-Fernández et al., 2007). The relationship between individual assembly events of r-proteins and SSU processome components with nascent SSUs was not studied so far. It was suggested that the U3 snoRNA might act as an rRNA chaperone, preventing the rRNA from erroneous interactions (Hughes, 1996). This interaction is replaced later during formation of more stable r-protein / rRNA interactions. A similar RNA "chaperone like" function could be envisioned for the large number of SSU processome components. An inverse relationship between stable assembly of r-proteins and the SSU processome with rRNA was observed. SSU processome components interact stably with early precursors, like 23S and 35S pre-rRNAs, while r-proteins interact only weekly with these early rRNA species and stably with late rRNA precursors, like 20S pre-rRNA and mature 18S rRNA. Accordingly, the strong interaction of SSU processome components with early pre-rRNAs could prevent erroneous interactions within the

rRNA. The subsequent assembly of r-proteins and concomitantly stabilization of rRNA structures would lead to a displacement of SSU processome components by r-proteins. Three scenarios are imaginable for the relationship between SSU processome components and r-proteins: (I) The SSU processome component initiates rRNA contact and serves as a kind of "RNA chaperone" or placeholder for r-protein(s); in this case the assembly of the SSU processome component would be independent of r-protein assembly. (II) The SSU processome component assembles cooperatively with r-protein (s); hence an interdependent assembly of the SSU processome component and the r-protein(s) should be observed. (III) The assembly of the SSU processome component requires the preceding binding of r-protein(s); in this case the assembly of the SSU processome component would depend on r-protein assembly.

The goal of this work was to gain knowledge whether r-proteins of the SSU are required for association of SSU processome components with nascent subunits. The four submodules of the SSU processome are called UTP-A, UTP-B, UTP-C and Mpp10p complex (see section 2.5). In addition there is a non-defined group of all other proteins not grouped in the first four groups. The latter group is very diverse in regard to the depletion phenotype and hence the function of their members. Some show an earlier rRNA processing phenotype, like most SSU processome components, while some exhibit a later phenotype. The protein Noc4p is especially interesting, because depletion of this factor did not lead to a complete block of 20S pre-rRNA production (Milkereit et al., 2003). This direct precursor to the mature 18S rRNA is still produced to some extent in *NOC4* mutant strains, which is in contrast to almost all other SSU processome components of the UTP-A, UTP-B, UTP-C and Mpp10p submodules. Remarkably, the pre-rRNA processing phenotype of *NOC4* mutant strains is very similar to the one observed after depletion of rpS16 and rpS5 (Milkereit et al., 2003; Ferreira-Cerca et al., 2005). Hence, it seemed likely that these three proteins could be involved in ribosome biogenesis of the SSU at a similar step.

To test whether rpS5 or rpS16 are required for assembly of Noc4p to pre-ribosomal complexes rRNA co-immunoprecipitation experiments in yeast cells expressing or not the respective rpS have been performed as a measurement for assembly of Noc4p to pre-ribosomes. In order to do so, the sequence for the TAP-tag (Tandem Affinity Purification) has been integrated at the 3' end of the endogenous locus of *NOC4* in the Gal-RPS5, GAL-RPS16 and some other GAL-RPS strains (see Figure 12 for list of strains). The integration of the TAP-tag at the *NOC4* locus had no influence on the growth rate of these strains (data not shown).

The advantage of this approach is, that Noc4p is still expressed under control of its endogenous promoter and that it can be purified via the Protein A moiety of the TAP-tag using an IgG sepharose matrix. For the analysis, the different strains were cultivated in galactose (on) and then transferred to glucose containing medium for four hours (off) (see Figure 12 for list of strains). The depletion of rpS5 and rpS16 resulted in a clear increase of 23S and 35S pre-rRNAs, concomitantly with a reduction of 20S pre-rRNA (Figure 12; RPS5 and RPS16, compare lanes I (on) with lanes I (off)). When looking at the RNA co-precipitation, Noc4p-TAP efficiently precipitated 23S and 35S pre-rRNAs in the wild-type strain, but only low amounts of 20S pre-rRNA (Figure 12; first blot (---),

compare lane I (on) with IP (on)). In the conditional mutant strains, the absolute amount of precipitated early rRNA precursors (23S and 35S pre-rRNAs) was not changing after depletion of rpS5 or rpS16 (Figure 12; RPS5 and RPS16, compare lanes IP (on) with IP (off)).

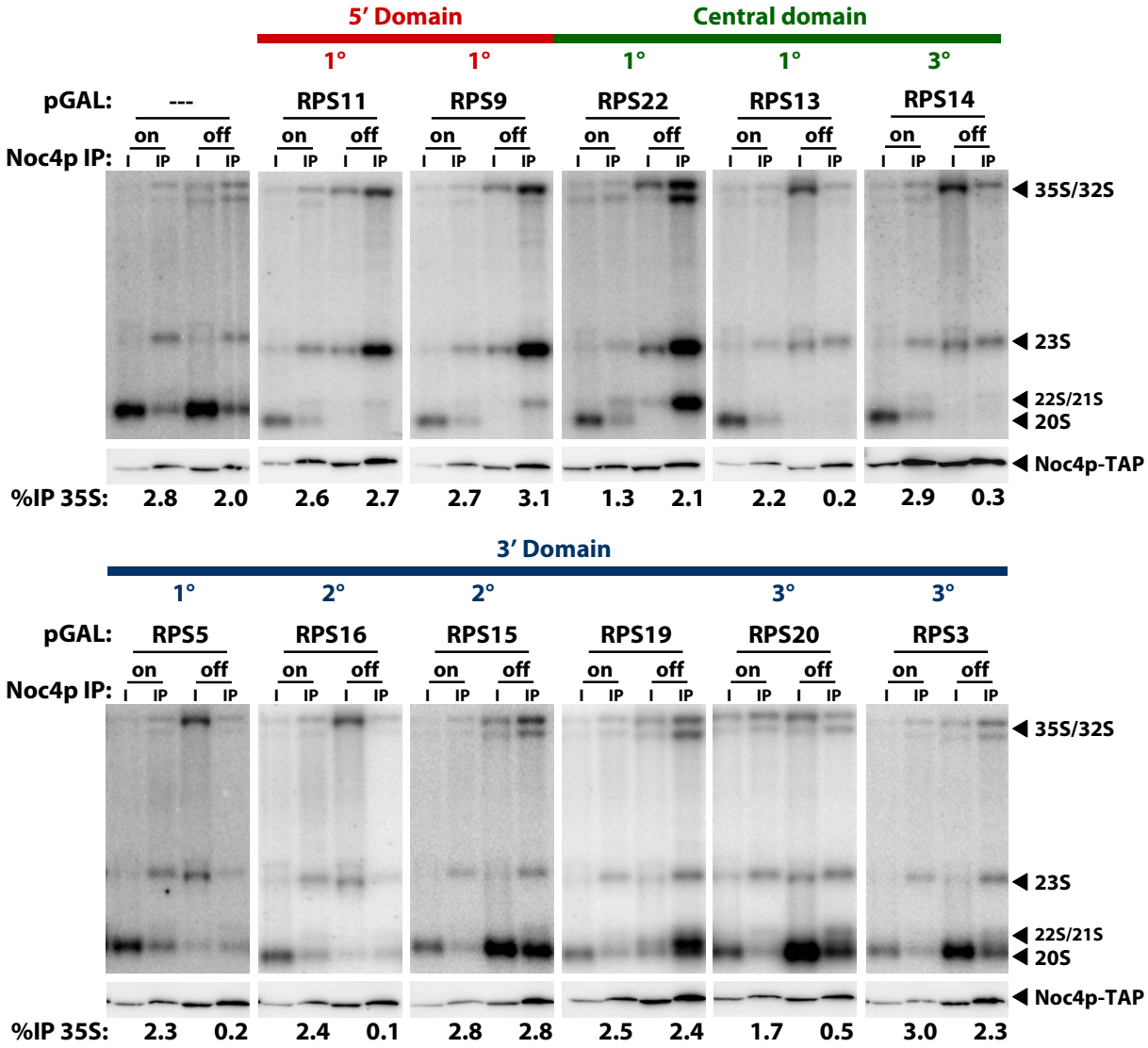

Figure 12. Co-immunoprecipitation of pre-rRNAs with Noc4p-TAP after depletion of r-proteins of the SSU

The strains Y90, Y96, Y1240, Y1241, Y1242, Y1660, Y1661, Y1887, Y1892, Y1897, Y1902, and Y2108 were cultivated in galactose (on) and glucose (off) containing full medium. Noc4-TAP was precipitated via its Protein A moiety using IgG sepharose beads. The precipitated amount of Noc4p-TAP was monitored by western blotting (PAP antibody) and the co-precipitated rRNA species were analysed by northern blotting using oligo 1819, which hybridises within the ITS1 region. The strains are ordered in regard to the localisation of the (galactose controlled) r-protein on the three major domains of the 18S rRNA (see schematic representation of the 18S rRNA primary structure in 5′ to 3′ direction above the northern blots). Below this representation, information on the binding hierarchy of the homologous r-protein in *E.coli* is depicted (primary binding protein (1°), secondary binding protein (2°) and tertiary binding protein (3°). For the northern blot equal signal intensities of input (I) and beads (IP) correspond to 1% co-precipitation of the respective rRNA. For the western blot equal signal intensities of input (I) and beads (IP) correspond to 20% precipitation of the bait protein Noc4p-TAP. The amount of precipitated 35S pre-rRNA was quantified using Multigauge and is depicted below each IP lane. For detailed description of the experimental procedure see section 5.2.6.3.

However, taking into account the strong accumulation of these early precursors in the depletion situation, this demonstrates a strong reduction of the relative precipitation of these species (Figure 12; RPS5 and RPS16, compare lanes I (on) and IP (on) with lanes I (off) and IP (off) and quantitation (%IP 35S) below each IP lane). One possible explanation would be that amounts of Noc4p are limiting in situations where early pre-rRNAs accumulate. This explanation is challenged by the observation that accumulation of early precursors in some other rpS depletion mutants, e.g. rpS9, rpS11 or rpS22, indeed led to a higher absolute precipitation of 23S and 35S pre-rRNAs by Noc4p (Figure 12; RPS9, RPS11 and RPS22, compare lanes I (on) and IP (on) with lanes I (off) and IP (off)). Therefore, the analysis revealed that rpS5 as well as rpS16 are indeed required for efficient assembly of Noc4p to early rRNA precursors.

The assembly of r-proteins has been extensively studied in *E. coli*. Nomura and colleagues demonstrated *in vitro* a hierarchical order of assembly for the r-proteins of the SSU (Held et al., 1974; Mizushima et al., 1970) (see section 2.3.1). This means a certain ribosomal protein (primary binder) has to bind first to facilitate the assembly of secondary and tertiary binding r-proteins. All r-proteins of the SSU were classified into five major assembly trees and oriented in a so called "assembly map". In this map, the homolog of rpS5 (S7) is assembling at the 3' end of the 16S rRNA (the mature rRNA species of the SSU in *E. coli*) and is the primary binder of one of the three SSU rRNA secondary structural domains, called 3' domain, which corresponds in 3D models of the SSU to the head domain (for a detailed introduction see section 2.1.2 and Figure 11). A similar hierarchy of stable incorporation of r-proteins into the head domain of nascent SSUs could be observed *in vivo* in *S. cerevisiae* (Ferreira-Cerca et al., 2007). In regard to these reports, the primary binder of the head domain, rpS5, as well as rpS16 seem to be required for assembly of Noc4p to pre-ribosomes. Next, the secondary and tertiary binders of the head domain were tested for their influence on Noc4p assembly. To this end, the galactose dependent strains of rpS3, rpS15, rpS19, and rpS20 harbouring Noc4p-TAP were analysed. The depletion of these proteins showed a later block of rRNA processing, which is demonstrated by a slight accumulation of 23S and 35S pre-rRNAs in all strains (Léger-Silvestre et al., 2004, 2005; Ferreira-Cerca et al., 2005) (Figure 12; RPS3, RPS15, RPS19 and RPS20, compare lanes I (on) with I (off)). Furthermore, a strong accumulation of 20S pre-rRNA was detected after depletion of rpS3, rpS15, and rpS20. The depletion of rpS19 led to a slight decrease in 20S pre-rRNA, concomitantly with a strong accumulation of 21S pre-rRNA.

In vivo depletion of rpS3, rpS15 and rpS19 had no impact on the precipitation efficiency of 35S pre-rRNA by Noc4p-TAP (Figure 12; RPS3, RPS15 and RPS19, compare lanes I (on) and IP (on) with lanes I (off) and IP (off)). On the contrary, the depletion of rpS20 led to a decrease of 35S pre-rRNA precipitation by Noc4p, although to a lower magnitude when compared to the one observed after rpS5 and rpS16 depletion (Figure 12; RPS20, compare lanes I (on) and IP (on) with lanes I (off) and IP (off)). It has to be pointed out, that the GAL-RPS20 strain already exhibited a slight rRNA processing defect in galactose containing medium, visible by the accumulation of 23S and 35S pre-rRNAs (Figure 12; wild-type (---) and RPS20, compare lanes I (on)).

To test, whether the effect on Noc4p-TAP assembly is specific to the SSU rRNA 3' domain binding proteins, rpS5 and rpS16, the association of Noc4p-TAP to pre-ribosomes was investigated after

depletion of several r-proteins of the body domain. The body of the SSU structure is formed by two of the three secondary structural domains of the SSU rRNA, called 5′ and central domain (for a detailed introduction see section 2.1.2 and Figure 11). The analysis of the GAL-dependent strains of rpS9, rpS11, rpS13, rpS14, and rpS22 showed an early rRNA processing defect, characterised by the accumulation of 23S and 35S pre-rRNAs (Seppl, 2005) (Figure 12; RPS9, RPS11, RPS13, RPS14 and RPS22, compare lanes I (on) with I (off)). Moreover, no 20S pre-rRNA was detectable after depletion of these r-proteins. In the case of rpS22 depletion a strong accumulation of a species larger than 20S, but smaller than 23S pre-rRNA, was observed. Considering its running behaviour in the gel this species is most probably 22S rRNA.

The depletion of rpS9, rpS11 and rpS22 had no pronounced effect on the association of Noc4p-TAP with early pre-ribosomal particles (Figure 12; RPS9, RPS11 and RPS22, compare lanes I (on) and IP (on) with lanes I (off) and IP (off)). In contrast, the depletion of rpS13 and rpS14, which could be shown *in vitro* to be part of one assembly tree of the SSU rRNA central domain in prokaryotes (Held, 1974, and see section 2.3.1), led to a decreased relative precipitation of early rRNAs by Noc4p-TAP (Figure 12; RPS13 and RPS14, compare lanes I (on) and IP (on) with lanes I (off) and IP (off)**.** This observation links efficient Noc4p recruitment to nascent SSUs to the assembly states of both the central (platform) domain and the major 3′ (head) domain.

The results of the quantitation analysis (Figure 12; %IP 35S below each IP lane) of the galactose (on) situation have to be regarded with caution as they seem to be error-prone, because of the very low signal for the 35S pre-rRNA in the input (I) lane. The quantitation results of the depletion situation (off) are much more reliable, because these early rRNA species are accumulating in most of the rpS depletion mutants.

Taken together, the analysis demonstrated that primary SSU rRNA 3′ domain (head) assembly, as well as central (platform) domain assembly are necessary for efficient association of Noc4p to early rRNA precursors, whereas secondary and tertiary assembly events of the 3′ domain as well as assembly of the 5′ domain (assembly trees of rpS9, rpS11 and rpS22) are dispensable for efficient recruitment of Noc4p to nascent SSUs.

3.3 Assembly of other SSU processome components with pre-ribosomal particles after blockage of SSU rRNA 5′, 3′ and central domain assembly

As mentioned above (see 3.2) Noc4p is part of an early pre-ribosomal particle called SSU processome and belongs to a subgroup of SSU processome components not linked to the UTP-A, UTP-B, UTP-C or Mpp10p submodules (see section 2.5). I next asked, whether other SSU processome components are also disturbed in their association to pre-ribosomes after depletion of r-proteins of the SSU. One representative of each subgroup of the SSU processome was chosen, namely Utp4p (UTP-A), Pwp2p (UTP-B), Utp22p (UTP-C) and Imp3p (Mpp10p).

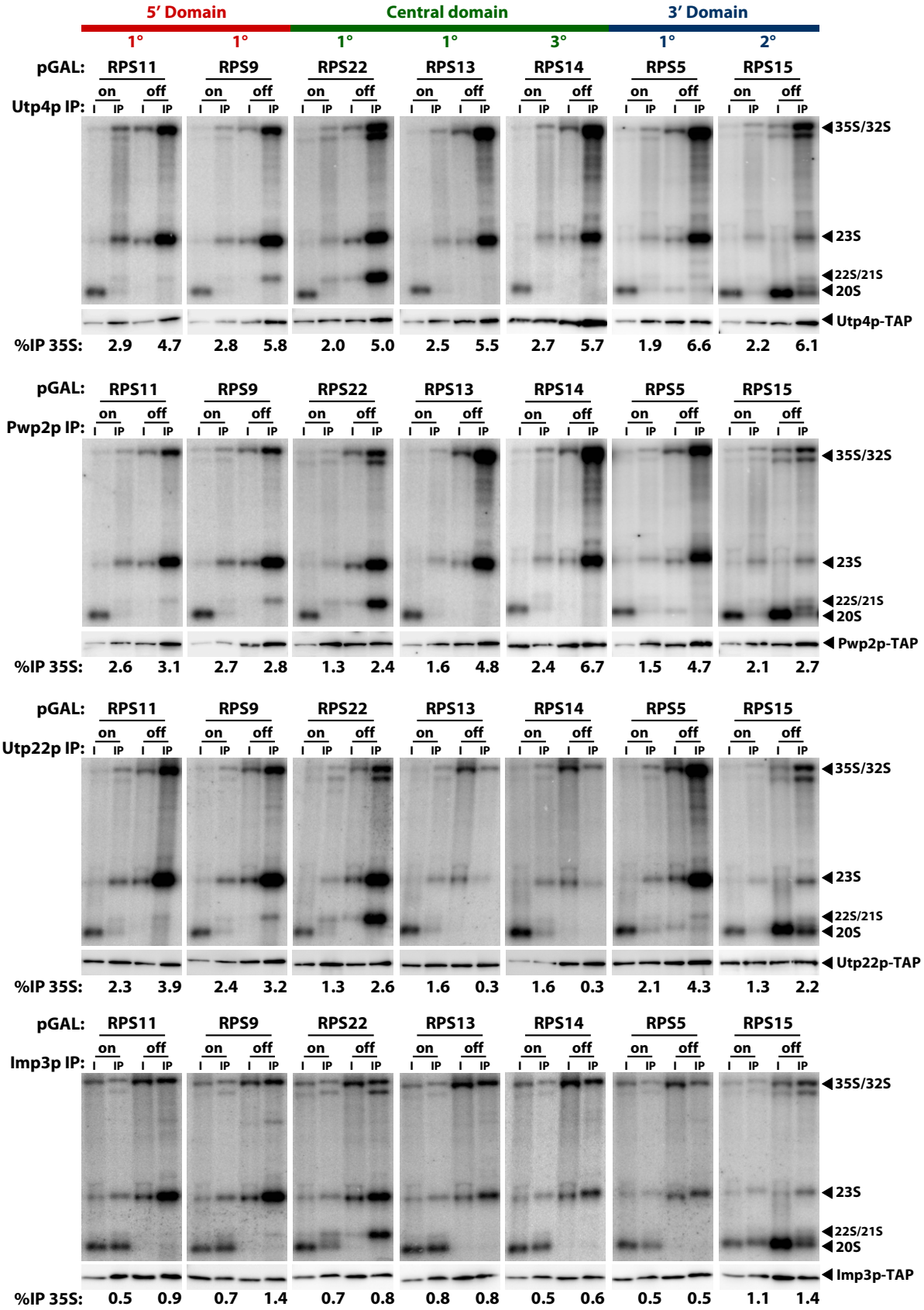

Figure 13. Co-immunoprecipitation of pre-rRNAs with Utp4p-TAP (UTP-A), Pwp2p-TAP (UTP-B), Utp22p-TAP (UTP-C) or Imp3p-TAP (Mpp10p complex) after depletion of r-proteins of the SSU

The strains carrying Utp4p-TAP (Y1524, Y1528, Y1883, Y1888, 1893, 1898, and Y2104), Pwp2p-TAP (Y1525, Y1529, Y1884, Y1889, 1894, 1899, and Y2105), Utp22p-TAP (Y1911, Y1913, Y1885, Y1890, 1895, 1900, and Y2106), and Imp3p-TAP (Y1912, Y1914, Y1886, Y1891, 1896, 1901, and Y2107) were cultivated in galactose

(on) and glucose (off) containing full medium. The respective TAP-tagged bait protein was precipitated via its Protein A moiety using IgG sepharose beads. The precipitated amount of the bait protein was monitored by western blotting (PAP antibody) and the co-precipitated rRNA species were analysed by northern blotting using oligo 1819, which hybridises within the ITS1 region. The strains are ordered in regard to the localisation of the (galactose controlled) r-protein on the three major domains of the 18S rRNA (see schematic representation of the 18S rRNA primary structure in 5' to 3' direction above the northern blots). Below this representation, information on the binding hierarchy of the homologous r-protein in *E.coli* is depicted (primary binding protein (1°), secondary binding protein (2°) and tertiary binding protein (3°). For the northern blot equal signal intensities of input (I) and beads (IP) correspond to 1% co-precipitation of the respective rRNA. For the western blot equal signal intensities of input (I) and beads (IP) correspond to 20% precipitation of the bait protein Noc4p-TAP. The amount of precipitated 35S pre-rRNA was quantified using Multigauge and is depicted below each IP lane. For detailed description of the experimental procedure see section 5.2.6.3.

The endogenous loci of these genes were manipulated by homologous recombination in several conditional RPS mutant strains as described for Noc4p-TAP in section 3.2, resulting in strains expressing the protein of interest in fusion with the TAP-tag. The expression of the correct fusion proteins was confirmed by western blot analysis (Figure 13; lanes I (on)). The following conditional RPS strains have been chosen for the analysis: GAL-RPS5, GAL-RPS9, GAL-RPS11, GAL-RPS13, GAL-RPS14, GAL-RPS15 and GAL-RPS22 (see Figure 13 for list of strains).

This selection includes representatives of all three major domains of the 18S rRNA; rpS11 and rpS9 bind to the 5'-domain, rpS22, rpS13, and rpS14 bind to the central domain, and rpS5 and rpS15 bind to the 3' domain (Figure 7). The endogenous integration of the TAP-tag had no effect on the growth rate of the constructed stains, except for Imp3p, with 22kDa the smallest of all analysed proteins (data not shown). The strains harbouring Imp3p-TAP were growing slower than the corresponding wild-type strains and an rRNA processing defect was revealed by northern blot analysis, which is demonstrated by a slight accumulation of 23S and 35S pre-rRNAs (Figure 13; Imp3p, compare lanes I (on) with lanes I (off)). The C-terminal fusion of the TAP-tag (~25 kDa) to Imp3p more than doubles the molecular weight in comparison to the wild-type protein and might thus interfere with its physiological function.

Utp4p-TAP, a member of the early binding UTP-A submodule, precipitated 23S and 35S rRNA precursors in the non depleted wild-type situation (Figure 13; Utp4p-TAP, compare lanes I (on) and IP (on)). The precipitation efficiency of these pre-rRNAs was increased after depletion of all chosen rpS, which means that Utp4p-TAP can assemble independent of the tested r-proteins to pre-ribosomal particles (Figure 13; Utp4p-TAP, compare lanes I (on) and IP (on) with lanes I (off) and IP (off)). The same is true for TAP-tagged Pwp2p, which is part of the UTP-B submodule, although showing lower levels of relative precipitation of early pre-rRNAs in most of the depletion mutants in comparison to the precipitation levels by Utp4p-TAP (Figure 13; Pwp2p-TAP, compare lanes I (on) and IP (on) with lanes I (off) and IP (off)). When looking at the immunoprecipitations of Utp22p-TAP, a member if the UTP-C module, it became obvious that the efficiency of 35S pre-rRNA precipitation was decreased after rpS13 and rpS14 depletion, two representatives of the SSU rRNA central domain (Figure 13; Utp22p-TAP / RPS13, RPS14, compare lanes I (on) and IP (on) with lanes I (off) and IP (off)). The precipitation efficiency of early precursors by Utp22p-TAP, after depletion of

all other r-proteins tested, was comparable to the ones of Utp4p-TAP and Pwp2p-TAP in the same mutants (Figure 13; Utp22p-TAP / RPS5, RPS9, RPS11, RPS15, and RPS22, compare lanes I (on) and IP (on) with lanes I (off) and IP (off)). This suggests that the assembly tree of rpS13 and rpS14 is specifically required for efficient assembly of the UTP-C submodule to pre-ribosomal particles.
The TAP-tagged version of the member of the Mpp10p complex, Imp3p, showed overall a less efficient precipitation of rRNA precursors, when compared to the precipitation efficiency of other SSU processome factors (Figure 13; compare quantitation (%IP 35S) of Imp3p-TAP with Utp4p-TAP). Besides this fact, the association of Imp3p with early pre-rRNAs was not altered after depletion of all tested r-proteins (Figure 13; Imp3p, compare lanes I (on) and IP (on) with lanes I (off) and IP (off)).
In summary, rpS assembly is dispensable for association of Utp4p (UTP-A submodule), Pwp2p (UTP-B) and Imp3p (Mpp10p). In contrast, the central domain (platform) assembly tree of the SSU, including the r-proteins rps13 and rpS14, is needed for efficient assembly of Utp22p (UTP-C submodule) (for summary see also Figure 29).

3.4 Semi Quantitative analysis of protein complexes using iTRAQ

3.4.1 Introduction

The method for relative quantitation of proteins using amine-reactive isobaric tagging reagents was introduced by Ross et al. in 2004 (Ross et al., 2004). This method allows one to compare amounts of proteins contained in different test samples. The principle of this method is that the proteins of interest are labelled with different isotopic reagents and analysed by mass spectrometry.
In detail, proteins from different samples are digested with trypsin to yield defined peptides of smaller size which are suitable for mass spectrometric analysis. These tryptic peptides are then covalently labelled with different isotopic iTRAQ reagents. These reagents consist of an amine reactive group which reacts with N-terminal amino groups and ε-amino groups of lysine residues. The differently labelled peptides are subsequently combined and subjected to a MALDI TOF (Matrix Assisted Laser Desorption Ionisation Time Of Flight) analysis. In the MS/MS (Tandem mass spectrometry) mode, reporter ions are released from peptides originating from different samples and are used for quantitation of the respective protein. A more detailed description is given in Figure 14 and Figure 15.
During my diploma thesis I was able to proof that this method is useful for relative comparison of the protein content of isolated ribosomal subunits (Jakob, 2006). In this work, the sample was fractionated into six fractions by use of a reversed phase column in a 10ul pipette tip (Zip Tip) prior to the MS/MS analysis. During these experiments, it became apparent that the sample was already too complex for this kind of fractionation, therefore only a low number of peptides for each r-protein were identified.

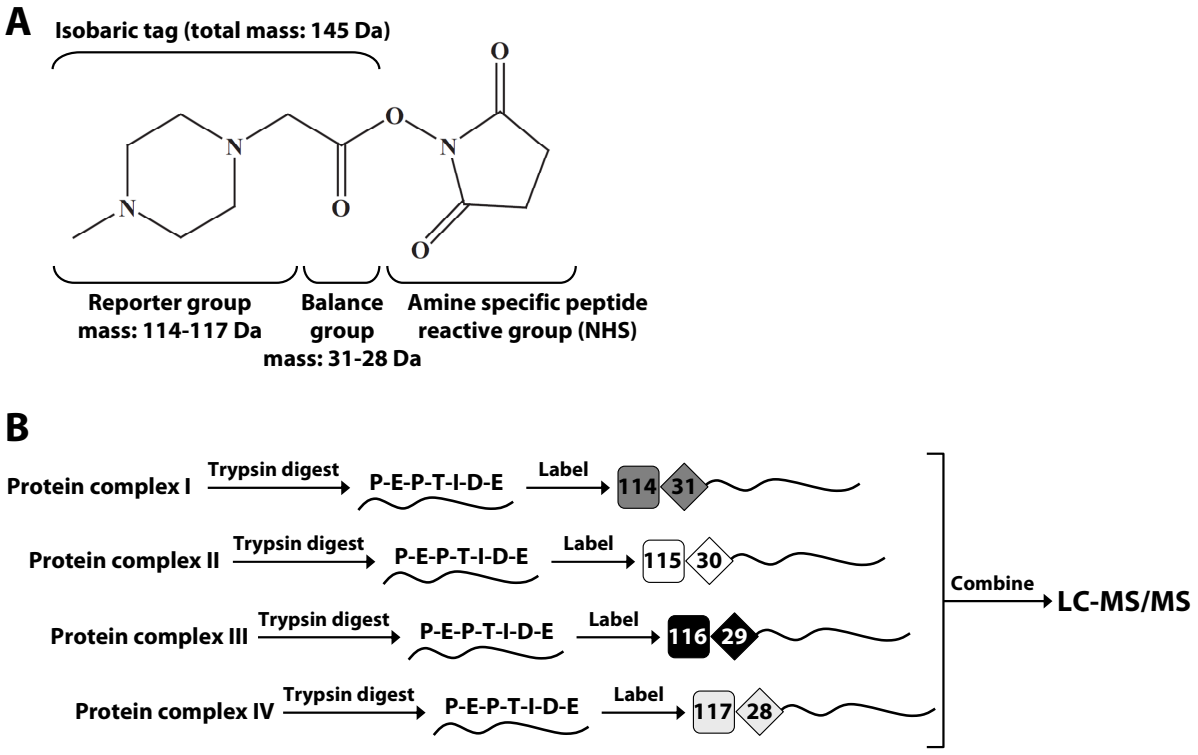

Figure 14. Structure of the iTRAQ reagent and overview of the workflow
(**A**) The structure of the iTRAQ reagents (isobaric Tag for Relative and Absolute protein Quantitation), consisting of a reporter group with a mass of 114-117 Da, a balance group with a mass of 31-28 Da and an amine reactive group (NHS ester) is depicted. Four different iTRAQ reagents are available and are designed in a manner that all have the same mass, although exhibiting different isotopes. The balance group is compensating the mass of the reporter group in a way that the total mass of this isobaric tag is always 145 Da.
(**B**) Up to four different samples can be compared to each other at the same time. Prior to the trypsin digest the cysteines of the purified proteins are reduced (TCEP) and alkylated (MMTS) to block cysteines from reaction with the iTRAQ reagents (not depicted). The proteins of the purified complexes are digested with trypsin to yield defined peptides of smaller size which are suitable for identification by MALDI MS/MS analysis. These peptides are labelled and afterwards combined. The mixed sample is separated on a reversed phase column and analysed with a MALDI TOF/TOF mass spectrometer (4800 proteomic analyzer from Applied Biosystems). Reproduced and adopted from Yan and Chen, 2005.

Since the goal of this method was to analyse even more complex samples, consisting of up to 200 proteins, the fractionation system was changed to a modern nano HPLC system from Dionex.
This machine is capable of separating a complex mixture of peptides into several hundred fractions. The nano HPLC was combined with an automatic spotting device, directly mixing each fraction with the matrix and spotting it onto a MALDI target plate. The system can be run as a two dimensional system with a cation exchange column being the first and a reversed phase column being the second dimension, thus enabling almost an infinite number of fractions. This procedure should be advantageous by reducing the complexity of fractions, because only five to eight peptides can be further fragmented in the currently used mass spectrometer. Nevertheless this setup proved to be less reliable. For this reason, a one dimensional setup including only the reversed phase column was applied in further experiments. This setup was sufficient to deal with the complexity of the samples analysed in this study and was much more reliable than the two

dimensional setup. Using this setup, the sample was separated into 384 fractions, therefore allowing up to 2400 peptides (~8 peptides per spot) to be fragmented and quantified.

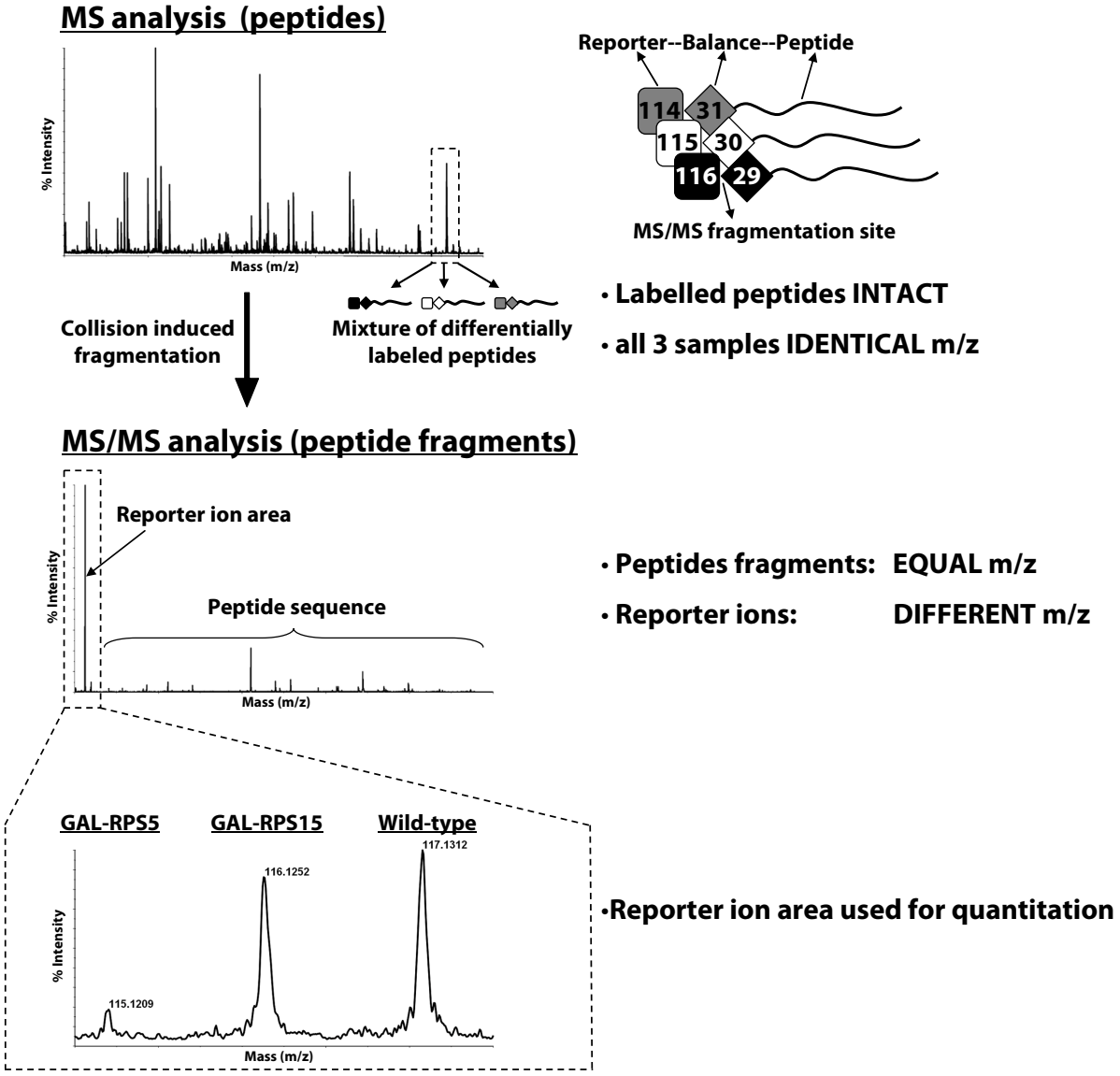

Figure 15. Schematic overview of the mass spectrometry analysis of iTRAQ samples
This schematic overview shows the analysis of three differentially labelled samples. In the MS analysis the mass to charge ratio (m/z) of the different peptides are separated by their mass differences. A representative MS spectrum is shown, which is typically conducted in a mass range between 800 Da and 4000 Da. One peak consists of the differentially labelled peptides from all three purified protein complexes. In this mode, all peptides are intact and the balancing group is compensating the mass difference of the reporter ion group. Thus, the shown peak is a mixture of the peptides originating from the three different samples and exhibiting an identical m/z. In the MS/MS mode, selected peptides can be further fragmented by collision with gas molecules (collision induced dissociation). The fragmentation results in different peptide fragments, which are used for identification of the respective peptide by MASCOT data base search. The peptide fragments from all three different samples have an equal m/z and sum up to one signal peak. However, the reporter ions are released from the peptides and exhibit different masses representing the three samples. The area of each reporter ion is used for quantitation. In the shown example, the respective protein of the sample purified after rpS15 depletion (GAL-RPS15) changes only marginally compared to the wild-type level, while a strong decrease of the reporter ion can be observed after rpS5 (GAL-RPS5) depletion.

3.4.2 Characterisation of general features of the quantitation using iTRAQ

One crucial feature of a quantitation assay is that the signals to be quantified behave proportional to the used laser intensity and to each other. Preferably, this should be even true when the dynamic range of analysed peptide quantities is very large. To test, whether iTRAQ reporter ions behave proportional to each other with different applied laser intensities, an experiment approaching this task was performed. Pre-ribosomes were purified via Enp1p-TAP (SSU biogenesis factor) from an untagged wild-type strain (background control) and two different strains (Y419 and Y439) carrying Enp1p-TAP. Co-purifying proteins were digested with trypsin and labelled with different iTRAQ reagents (detailed description in Figure 14). Several peptides were subjected to fragmentation in the MS/MS-mode and decreasing laser intensities for ionisation of these peptides were used. The laser intensity is given in arbitrary units, which usually has to be adjusted for every single experiment, due to the nature of the sample and the condition of the laser.

The results for four representative peptides originating from Enp1p-TAP co-purifying proteins are shown in Figure 16. The iTRAQ area of the respective reporter ions is plotted against the laser intensity. The absolute iTRAQ areas for these peptides differ very much from each other, ranging from 70.000 up to 1.100.000. This reflects the dynamic range observed in a typical iTRAQ experiment. Except for the 2451.213 Da peptide (Figure 16A), the data showed that the iTRAQ reagent cluster area was rising more or less linear with increasing laser intensities. A reason why this is not true for the 2451.213 Da peptide, could be that a laser intensity of 3400 induces a fragmentation which is at the edge of the detection limit. As a result the iTRAQ area at this data point is not in the linear range.

An alternative explanation is that the sample was already used up, because the acquisition was started with the highest laser intensity first. The latter explanation is supported by the observation that all peptides shown, exhibit no linear relationship at lower laser intensities. The phenomenon can be reasoned most probably by a combination of both explanations.

The peptides with the masses of 2451.213 Da, 2360.271 Da and 1241.749 Da showed a reduction of the iTRAQ area at the highest laser intensity (Figure 16A, B and C). This could be due to post source decay (PSD) of the peptides. According to this phenomenon, peptides are fragmented already during the ionisation process due to high laser intensities. Hence, the peptide fragments, which arrive earlier than the parent ion at the collision cell, are excluded from fragmentation by the time ion selector (TIS). As a consequence, this leads to a reduced amount of reporter ions of the respective peptide at the detector of the mass spectrometer.

The iTRAQ reagent cluster area of the 115 Da and 116 Da reporter ions of the 1241.749 Da peptide behaved not proportional to each other (Figure 16C). Here, the 116 Da cluster area was rising at the highest laser intensity, while the one of 115 Da was falling. However, apart from these exceptions, the different reporter ions behaved proportional to each other. As expected, the control strain expressing untagged Enp1p showed a low iTRAQ area, which is at background level (Figure 16; iTRAQ reagent 114).

In summary, the different reporter ions behave linear and proportional to each other in a wide range of poorly and well fragmenting peptides, as well as in a large range of different laser intensities. However, the laser intensity should be carefully adjusted for each experiment, considering the variation of the sample concentration and the changing laser power. In addition, several identified peptides of a protein are desirable for a better statistic of the quantitation, since the iTRAQ reagent areas sometimes behave not exactly proportional to each other.

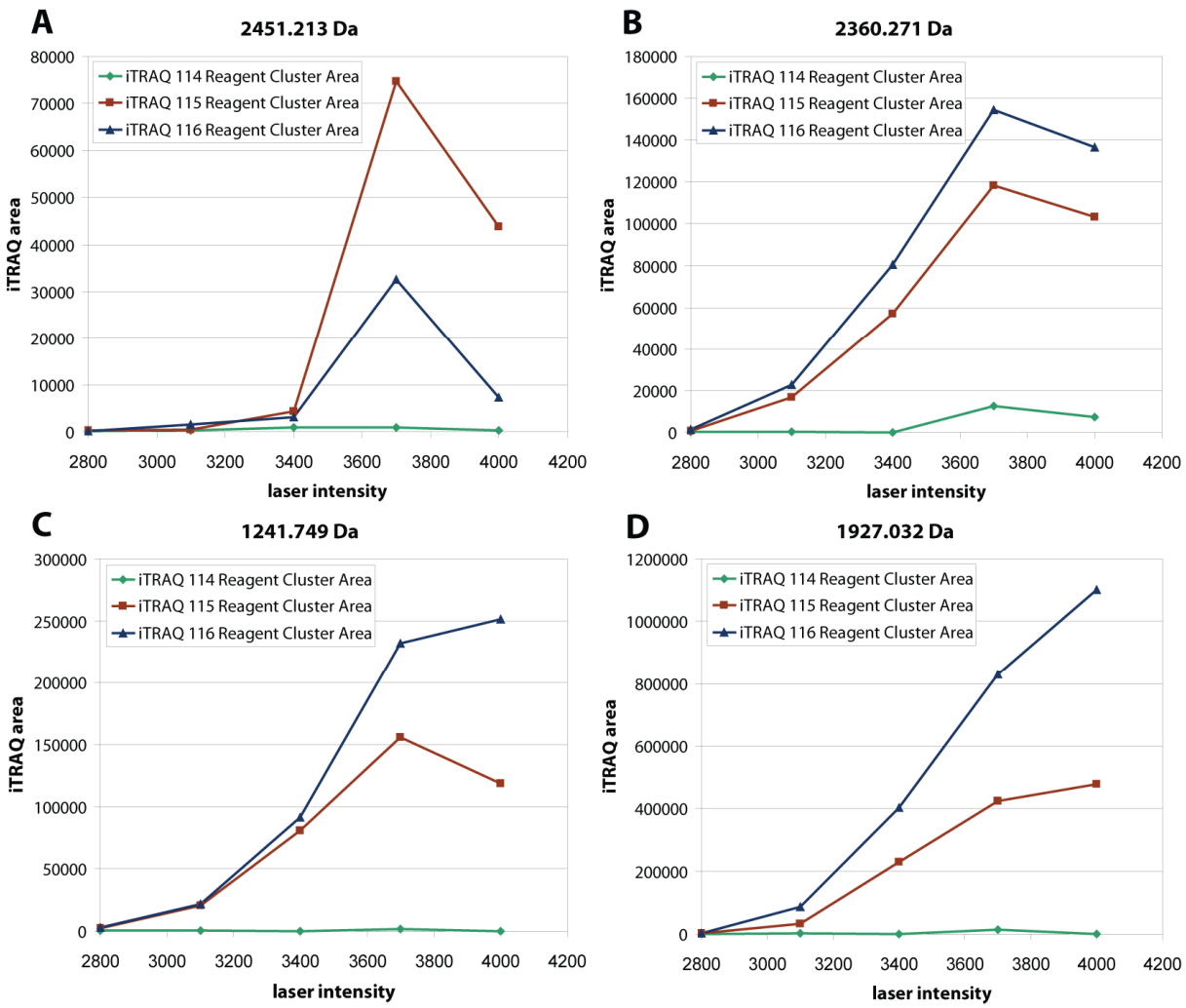

Figure 16. Influence of the laser intensity on the value of the iTRAQ reagent cluster area
Cell lysates from a wild-type strain (Y207, labelled with iTRAQ reagent 114) and two strains expressing Enp1p as a C-terminal fusion with the TAP-tag (Y419 labelled with iTRAQ reagent 115 and Y439 labelled with iTRAQ reagent 116) were prepared using glass beads. Pre-ribosomes were affinity purified via the Protein A moiety of Enp1p-TAP. Bound proteins were eluted from the IgG coupled sepharose matrix with 500mM NH_4OH. The eluted proteins were digested using trypsin and the resulting peptides from each sample were labelled with different iTRAQ reagents. The labelled peptides were separated on a nano-flow HPLC system (Dionex Ultimate 3000) and spotted online via the Probot system (Dionex) on the MALDI target. Two peptides per spot were further fragmented in the MS/MS mode, thus giving rise to peptide fragments used for identification and reporter ions used for quantitation of the respective protein (detailed description in Figure 14 and Figure 15). Different laser intensities were used starting with the highest one. Four representative peptides of this analysis are depicted, with the iTRAQ area plotted against the laser intensity. The peptide with the mass of 2451.213 Da was assigned to Mrt4p, the one with the mass of 2360.271 Da to rpL8A, the 1241.749Da peptide to rpL19 and the 1927.032 Da peptide to rpL10.

3.4.3 Establishment of an assay for quantitative analysis of protein complexes using iTRAQ

During my diploma thesis I used mature 40S subunits for setting up the assay for relative protein quantitation by isobaric peptide labelling using iTRAQ. One of the technical objectives of my PhD thesis was to combine the purification of pre-ribosomal particles with the relative protein quantitation by iTRAQ. This intention was achieved in collaboration with Juliane Merl, a PhD student in our institute. She intended to compare assemblies of ribosome biogenesis factors purified from yeast cells with or without ongoing pre-rRNA synthesis. This biological question turned out to be an optimal test case for application of the methodology described above. While she focused on the purification of these pre-ribosomal particles, I concentrated on the analysis and comparison of the purified complexes. A comprehensive description of the biological outcome of these analyses can be found in her PhD thesis (Merl, 2009) as well as in a manuscript describing the outcome of this project (Merl and Jakob et al., 2010). Here, I just want to focus on some important, general technical observations we made during these experiments.

First of all, the relative quantitation using iTRAQ does not yield an absolute ratio reflecting the actual change in protein abundance, but is rather giving a semiquantitative estimate. Meaning, that comparison of two complex protein samples with the applied iTRAQ setup will reliably detect the tendencies in relative enrichment of peptides in one or the other sample, but not the absolute magnitude of changes. During the above mentioned analyses three strains were compared to each other, a wild-type strain, a wild-type strain carrying a bait protein fused to the TAP-tag, and a mutant strain carrying the same bait protein with the TAP-tag. The comparison of affinity purified protein complexes from wild-type strains expressing or not the tagged bait protein should in theory allow the discrimination between specific and unspecific co-purifying proteins. The specific binders should be highly enriched in the wild-type bait-TAP strain, while unspecific binder should be present in both purifications to a similar extent. In reality this was not always the case, some specific proteins were highly enriched as judged by SDS-PAGE, but the quantitation revealed only 2-5 fold enrichment. This low enrichment did not reflect the actual ratio, because when the untagged wild-type control was analysed alone, these proteins were not identified. This showed that these proteins were indeed not detectable in the untagged control purification and a comparison of the unspecific to the specific purification should result in a much higher enrichment. These results demonstrated that the dynamic range of the quantitation is not linear, especially for two samples exhibiting large differences in protein content. This phenomenon was observed independently by other experts in the field using quantitative mass spectrometry (personal communication Janine Maddock (University of Michigan) and Henning Urlaub (MPI Göttingen)). Thus, the quantitation using iTRAQ is not an absolute quantitation and gives only a direction of whether certain proteins are enriched or not. This should be kept in mind when working with iTRAQ.

Second, the protein identification by MASCOT database search in the NCBI database can give several annotations for one single protein, therefore making the data evaluation problematic. For

this reason, an own yeast protein database was established for these analyses. The database is simply stored as an Excel file and therefore it can be easily updated and organised. Following the MASCOT database search, the NCBI accession numbers are checked against the new yeast database and each peptide is assigned to one single protein.

Third, the sensitivity of the mass spectrometer needs to be well controlled. Low amounts of proteins are used for these analyses, thus an optimal working mass spectrometer setup is indispensable. Therefore, the sensitivity of the mass spectrometer should be controlled by testing the fragmentation and detection performance with a highly diluted standard peptide mixture mimicking the low concentration of the actual sample.

Fourth, a manual evaluation of the dataset is recommended. Non-redundant peptides as well as outliers, if reasonable, should be excluded from the quantitation. If one protein is identified by several peptides, one or more outlier peptides can be easily detected. Obviously, this is not feasible for a protein identified by only two peptides.

Fifth, it turned out that the setup, as described up to here, can be limited in terms of sensitivity for the analysis of more complex samples. This drawback results mainly from increased non-specific binding of proteins to the IgG sepharose matrix during the affinity purification procedure. Thus, a substantial fraction of the total identified peptides in a typical experiment was derived from non-specific interactions with the affinity-matrix. As this method is intended to study the composition of very large SSU processome derived assemblies, a purification strategy increasing the ratio of specifically versus non-specifically purified proteins is preferable.

Recent work from the laboratory of Michael Rout showed that antibody (IgG) conjugated magnetic beads are suitable for the affinity purification of large RNP complexes via TAP-tagged components (Oeffinger et al., 2007). This approach was tested in collaboration with Jan Linnemann, for the purification of Enp1p-TAP from yeast extracts, a ribosome biogenesis factor needed for maturation of the SSU and part of early pre-ribosomes.

The purification using IgG conjugated magnetic beads was done in direct comparison to the purification with IgG coupled sepharose beads using cell lysates from a wild-type strain and a strain expressing Enp1p-TAP. The analysis of the purified complexes by SDS-PAGE confirmed the unspecific binding of mature ribosomes and other contaminants to the IgG sepharose matrix, as can be seen in the purification from a wild-type lysate harbouring no Enp1p-TAP (Figure 17; wild-type, lane (SB)). In vast contrast, the purification via IgG coupled magnetic beads from the same wild-type lysate showed almost no contamination by unspecific binders (Figure 17; wild-type, compare MB with SB). However, the purification from the cell lysate including Enp1p-TAP with magnetic beads yielded a distinct pattern of proteins (Figure 17; lane Enp1p-TAP (MB)). In comparison, the purification using sepharose beads showed some new appearing protein bands, but is overall not distinguishable from the untagged control purification (Figure 17; compare lane Enp1p-TAP (SB) with wild-type (SB)). The results of this experiment were very promising for the employment of this purification technique to the analysis of pre-ribosomes from different mutants. Especially, the highly specific enrichment of large pre-ribosomal particles and the low background

of unspecific binders in affinity purified fractions will most likely improve the identification of co-purifying interaction partners by mass spectrometry.

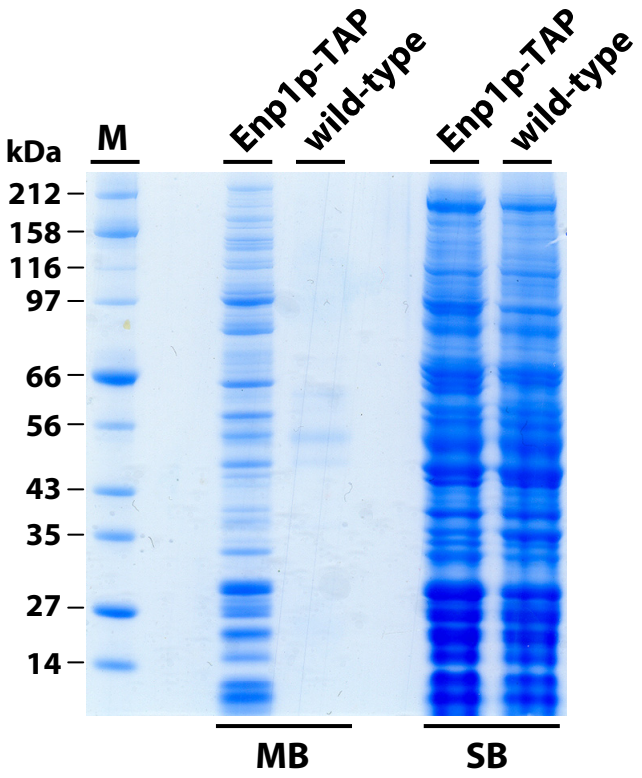

Figure 17. Comparison of the purification of pre-ribosomal particles via Enp1p-TAP using either magnetic beads (MB) or sepharose beads (SB) coupled to IgG
Cell lysates from a wild-type strain (Y207, wild-type) and a strain expressing Enp1p as a C-terminal fusion with the TAP-tag (Y419, Enp1p-TAP) were prepared using glass beads. The cell lysates were divided and one part was added to magnetic beads while the other part was added to sepharose beads. After extensive washing steps, the bound proteins were eluted by raising the pH, using 500mM NH_4OH. Equal amounts of the eluted proteins were loaded on a gradient NuPAGE gel, together with a protein marker (M) and stained with simple blue safe stain (Invitrogen). The size of the marker protein bands are depicted at the left side of the gel.

3.4.4 Comparative analysis of proteins co-purifying with Noc4p-TAP after *in vivo* depletion of primary (rpS5) or secondary (rpS15) SSU rRNA 3' domain binding proteins

In section 3.2 and 3.3, a direct approach has been applied to study the assembly of SSU processome components following r-protein depletion. The disadvantage of this approach is that only some examples of each SSU processome subgroup can be analysed, because the analysis of all possible combinations would be way to labour intensive. For this reason, the introduced quantitative analysis of affinity purified protein complexes has been used to study changes in the protein composition of purified pre-ribosomes after inactivation of certain r-proteins. To do so, pre-ribosomal components were purified using Noc4p-TAP as the bait in strains expressing rpS5 or rpS15 under control of the *GAL1* promoter. These strains, as well as a wild-type strain were cultivated four hours in glucose containing medium. The purification of Noc4p-TAP containing complexes was performed using IgG coupled sepharose beads and IgG coupled magnetic beads. In the direct comparison of both purifications 13 ribosome biogenesis factors (by a total amount of 19 peptides) could be identified using sepharose beads compared to 68 factors (306 peptides) using magnetic beads (compare Figure 18 with Figure 19). This tendency was even more pronounced when looking at the identified peptides per protein. In the case of the purification using sepharose

beads, most of the preys were identified by only one single peptide, whereas in the experiment using magnetic beads in average five peptides per protein could be identified. Besides these differences, both approaches showed a similar outcome in terms of how co-purification of classes of SSU processome components with Noc4p-TAP is affected by *in vivo* depletion of rpS5 (primary binder of the SSU rRNA 3' domain) or rpS15 (secondary binder of the 3' domain). However, due to better coverage and statistics in co-purification experiments done with magnetic beads only the results obtained with this approach will be discussed in detail.

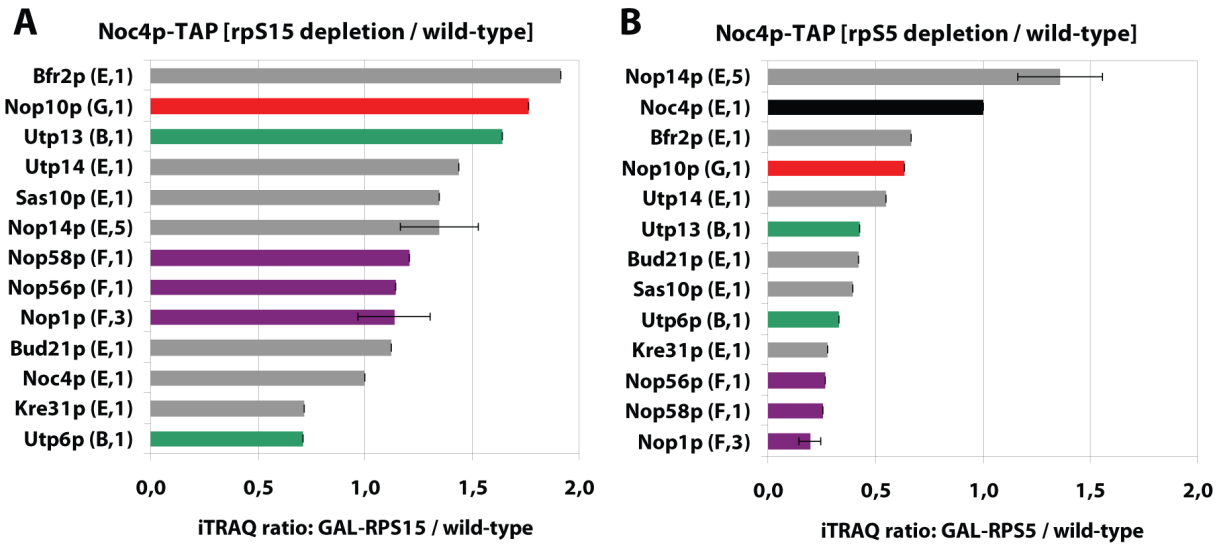

Figure 18. Quantitative analysis of the protein composition of pre-ribosomes purified via Noc4p-TAP using IgG coupled sepharose beads.
Pre-ribosomes were purified via Noc4p-TAP from cell lysates of a wild-type strain (Y96) and strains depleted either for rpS5 (GAL-RPS5, Y1241) or rpS15 (GAL-RPS15, Y90). Bound proteins were eluted from the IgG coupled sepharose matrix with 500mM NH_4OH. The eluted proteins were digested using trypsin and the resulting peptides from each sample were labelled with different iTRAQ reagents. The labelled peptides were separated on a nano HPLC system (Dionex Ultimate 3000) and spotted online via the Probot system (Dionex) on the MALDI target. Up to eight peptides per spot were further fragmented in the MS/MS mode, thus giving rise to peptide fragments used for identification and reporter ions used for quantitation of the respective protein (detailed description in Figure 14 and Figure 15). The relative amounts of proteins purified from the GAL-RPS15 (**A**) and GAL-RPS5 (**B**) strains are normalised to the purification from the wild-type strain. A mean value, with the corresponding standard deviation, of all identified peptides of a single protein is depicted. The iTRAQ ratios of the co-purifying proteins were normalised to the iTRAQ ratio of the bait protein (highlighted by a black bar). A classification of the identified proteins, as well as the number of identified peptides is depicted in parentheses. The protein classification is as following: B= UTP-B subcomplex (green), E=non-grouped SSU processome factors (grey), F= box C/D snoRNP (purple) and G= box H/ACA snoRNP (red).

Proteins co-purifying with Noc4p-TAP included a vast number of SSU processome components, covering all submodules (UTP-A, UTP-B, UTP-C, Mpp10p complex, and non-grouped factors), almost all r-proteins of both subunits, biogenesis factors needed for maturation of pre-60S subunits, factors associated with mature ribosomes and some known contaminants (see Table 1).

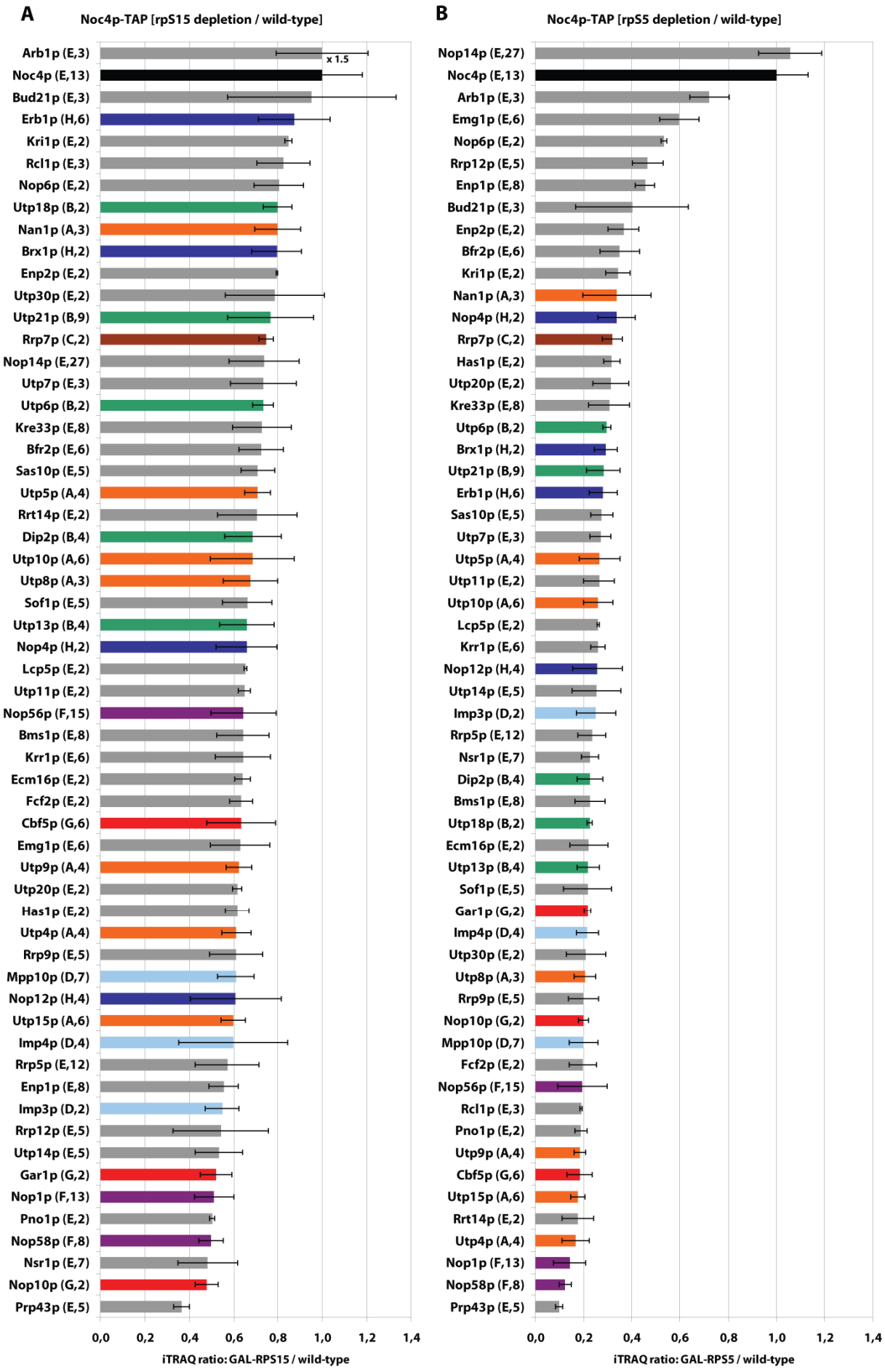
A
Noc4p-TAP [rpS15 depletion / wild-type]
x 1.5
Arb1p (E,3)
Noc4p (E,13)
Bud21p (E,3)
Erb1p (H,6)
Kri1p (E,2)
Rcl1p (E,3)
Nop6p (E,2)
Utp18p (B,2)
Nan1p (A,3)
Brx1p (H,2)
Enp2p (E,2)
Utp30p (E,2)
Utp21p (B,9)
Rrp7p (C,2)
Nop14p (E,27)
Utp7p (E,3)
Utp6p (B,2)
Kre33p (E,8)
Bfr2p (E,6)
Sas10p (E,5)
Utp5p (A,4)
Rrt14p (E,2)
Dip2p (B,4)
Utp10p (A,6)
Utp8p (A,3)
Sof1p (E,5)
Utp13p (B,4)
Nop4p (H,2)
Lcp5p (E,2)
Utp11p (E,2)
Nop56p (F,15)
Bms1p (E,8)
Krr1p (E,6)
Ecm16p (E,2)
Fcf2p (E,2)
Cbf5p (G,6)
Emg1p (E,6)
Utp9p (A,4)
Utp20p (E,2)
Has1p (E,2)
Utp4p (A,4)
Rrp9p (E,5)
Mpp10p (D,7)
Nop12p (H,4)
Utp15p (A,6)
Imp4p (D,4)
Rrp5p (E,12)
Enp1p (E,8)
Imp3p (D,2)
Rrp12p (E,5)
Utp14p (E,5)
Gar1p (G,2)
Nop1p (F,13)
Pno1p (E,2)
Nop58p (F,8)
Nsr1p (E,7)
Nop10p (G,2)
Prp43p (E,5)
0,0
0,2
0,4
0,6
0,8
1,0
1,2
1,4
iTRAQ ratio: GAL-RPS15 / wild-type
B
Noc4p-TAP [rpS5 depletion / wild-type]
Nop14p (E,27)
Noc4p (E,13)
Arb1p (E,3)
Emg1p (E,6)
Nop6p (E,2)
Rrp12p (E,5)
Enp1p (E,8)
Bud21p (E,3)
Enp2p (E,2)
Bfr2p (E,6)
Kri1p (E,2)
Nan1p (A,3)
Nop4p (H,2)
Rrp7p (C,2)
Has1p (E,2)
Utp20p (E,2)
Kre33p (E,8)
Utp6p (B,2)
Brx1p (H,2)
Utp21p (B,9)
Erb1p (H,6)
Sas10p (E,5)
Utp7p (E,3)
Utp5p (A,4)
Utp11p (E,2)
Utp10p (A,6)
Lcp5p (E,2)
Krr1p (E,6)
Nop12p (H,4)
Utp14p (E,5)
Imp3p (D,2)
Rrp5p (E,12)
Nsr1p (E,7)
Dip2p (B,4)
Bms1p (E,8)
Utp18p (B,2)
Ecm16p (E,2)
Utp13p (B,4)
Sof1p (E,5)
Gar1p (G,2)
Imp4p (D,4)
Utp30p (E,2)
Utp8p (A,3)
Rrp9p (E,5)
Nop10p (G,2)
Mpp10p (D,7)
Fcf2p (E,2)
Nop56p (F,15)
Rcl1p (E,3)
Pno1p (E,2)
Utp9p (A,4)
Cbf5p (G,6)
Utp15p (A,6)
Rrt14p (E,2)
Utp4p (A,4)
Nop1p (F,13)
Nop58p (F,8)
Prp43p (E,5)
0,0
0,2
0,4
0,6
0,8
1,0
1,2
1,4
iTRAQ ratio: GAL-RPS5 / wild-type

Figure 19. Quantitative analysis of the protein composition of pre-ribosomes purified via Noc4p-TAP using IgG coupled magnetic beads

Pre-ribosomes were purified via Noc4p-TAP from cell lysates of a wild-type strain (Y96) and strains depleted either for rpS5 (GAL-RPS5, Y1241) or rpS15 (GAL-RPS15, Y90). Bound proteins were eluted from the IgG coupled magnetic bead matrix with 500mM NH_4OH. The eluted proteins were digested using trypsin and the resulting peptides from each sample were labelled with different iTRAQ reagents. The labelled peptides were separated on a nano HPLC system (Dionex Ultimate 3000) and spotted online via the Probot system (Dionex) on the MALDI target. Up to eight peptides per spot were further fragmented in the MS/MS mode, thus giving rise to peptide fragments used for identification and reporter ions used for quantitation of the respective protein (detailed description in Figure 14 and Figure 15). The relative amounts of proteins purified from the GAL-RPS15 (**A**) and GAL-RPS5 (**B**) strains are normalised to the purification from the wild-type strain. A mean value, with the corresponding standard deviation, of all identified peptides of a single protein is depicted. Only proteins, identified by at least two non-redundant peptides were included in the quantitation analysis. The iTRAQ ratios of the co-purifying proteins were normalised to the iTRAQ ratio of the bait protein (highlighted by a black bar). A classification of the identified proteins, as well as the number of identified peptides is depicted in parentheses. The protein classification is as following: A=UTP-A subcomplex (orange), B= UTP-B subcomplex (green), C=UTP-C subcomplex (brown), D= Mpp10p complex (light blue), E=non-grouped SSU processome factors (grey), F= box C/D snoRNP (purple), G= box H/ACA snoRNP (red) and H=LSU biogenesis factor (dark blue).

The semiquantitative comparison of the purification from wild-type cells to the purification from the GAL-RPS15 cells indicated that the depletion of rpS15, a secondary binder of the SSU rRNA 3' (head) domain, led just to minor decreases in the co-purification efficiency of almost all identified ribosome biogenesis factors with Noc4p-TAP, with ratios between 0.5 and 1.0 for most of the factors (Figure 19A). This demonstrated that Noc4p is still significantly incorporated into pre-ribosomal particles containing these factors when rpS15 is *in vivo* depleted. This result is in agreement with the observations made in the corresponding (pre-) rRNA co-immunoprecipitation experiments with Noc4p-TAP in the GAL-RPS15 strain, which indicated that Noc4p efficiently precipitates rRNA precursors in this mutant and is still incorporated into pre-ribosomes (see section 3.2).

In contrast, mass spectrometric analyses indicated that the depletion of rpS5, the primary binder of the SSU rRNA 3' domain, leads to a decrease in Noc4p-TAP co-purification by a factor of 2.5 to 4.0 for most of these identified biogenesis factors (Figure 19B).

This result underlines that association of Noc4p with pre-ribosomal particles, containing these factors, is largely affected after rpS5 depletion. However, a small group of factors including Nop14p, Arb1p, Emg1p, Nop6p, Rrp12p, Enp1p and Bud21p behaved differently and showed a GAL-RPS5 / wild-type ratio between 0.4 and 1.0, indicating that these factors are still in a complex with Noc4p-TAP after depletion of rpS5. Especially, Nop14p is not impaired in its ability to associate with Noc4p-TAP after disruption of primary SSU rRNA 3' domain assembly (GAL-RPS5 / wild-type ratio of 1.06). The significance of this observation is supported by previous reports showing that Noc4p and Nop14p exist in a heterodimeric complex and that this interaction is needed for incorporation of Noc4p into early pre-ribosomes (Milkereit et al., 2003; Kühn et al., 2009).

In addition, Nop14p is required for proper localisation of Emg1p, while mutations in Nop6p can compensate for the loss of function of Emg1p (Liu and Thiele, 2001; Buchhaupt et al., 2007). Thus, Noc4p, Nop14p, Emg1p and Nop6p show a functional relationship to each other. In this regard, no

data exists for Arb1p, Rrp12p, Enp1p and Bud21p, but the herein reported co-purification behaviour with Noc4p-TAP after depletion of rpS5 suggests that these proteins are also functionally related to each other.

3.4.5 Comparative analysis of the protein composition of early pre-ribosomes purified by Utp4p-TAP after disruption of SSU 5', 3' or central domain assembly

The direct analysis of the assembly of SSU processome components in strains depleted for certain rpS revealed that SSU pre-rRNA association with the SSU processome components Utp4p (UTP-A), Pwp2p (UTP-B) and Imp3p (Mpp10p) was not affected by lack of assembly of individual r-proteins. Therefore, these factors can be used to purify pre-ribosomal complexes in absence of r-protein assembly events. This allows analysing effects on early pre-ribosomal protein composition after disruption of defined r-protein assembly events in a more general way. For these analyses, Utp4p-TAP was chosen as the bait protein. The purification was done from strains conditionally expressing the SSU rRNA 3' domain constituents rpS5 (primary binder) and rpS15 (secondary binder), the 5' domain constituent rpS9 and the central domain constituent rpS13. In addition, a wild-type strain was taken as a control. All strains express an Utp4p-TAP fusion protein. As shown above, the depletion of rpS5, rpS9 and rps13 causes comparable pre-rRNA processing phenotypes, namely an accumulation of 23S and 35S pre-rRNAs, and undetectable amounts (rps9, rpS13) or strong reduction (rpS5) of 20S pre-rRNA (Ferreira-Cerca et al., 2005) (Figure 12; RPS5, RPS9 and RPS13, compare lanes I (on) with I (off)).

Number of identified proteins (peptides total; proteins identified by one peptide)			
	Noc4p-TAP (GAL-RPS5,S15)	**Utp4-TAP** (GAL-RPS5,S9,S13)	**Utp4p-TAP** (GAL-RPS15)
biogenesis Factors	**68 (306;10)**	**88 (449;15)**	**88 (704;14)**
SSU maturation	57 (285;3)	61 (379;7)	63 (634;4)
LSU maturation	11 (21;7)	27 (70;8)	25 (70;10)
r-proteins	**67 (310;10)**	**64 (218;19)**	**65 (273;7)**
rpS	28 (117;3)	26 (78;8)	29 (116;4)
rpL	39 (193;7)	38 (140;11)	36 (157;3)
other proteins	**59 (218;26)**	**122 (390;55)**	**94 (329;34)**
heat shock proteins	7 (59;1)	8 (54;1)	8 (53;2)
ribosome associated	4 (54;1)	4 (51;0)	4 (50;0)
rest	48 (105;24)	110 (285;54)	82 (226;32)
total	**194 (834;46)**	**274 (1057;89)**	**247(1306;55)**

Table 1. Summary of the results of the semiquantitative MS analyses from section 3.4.4 and 3.4.5
The number of identified proteins in the different pre-ribosome affinity purifications is depicted. The first number in parenthesis shows the total amount of identified peptides, whereas the second number shows the amount of proteins identified by only one single peptide. Note that the proteins identified by only one single peptide were excluded from the quantitation analysis depicted in Figure 19 and Figure 20.

Therefore, the composition of early pre-ribosomes purified from cells depleted for rpS5 and rpS13 has been compared to the purification from cells depleted for rpS9. *In vivo* depletion of rpS15, a secondary binder of the SSU rRNA 3' (head) domain, caused some accumulation of 20S pre-rRNA (Ferreira-Cerca et al., 2005) (Figure 12; RPS15, compare lanes I (on) with I (off)), indicating that SSU processome dependent processing steps at A_0, A_1 and A_2 are only moderately affected (see rRNA processing scheme in Figure 4). To detect subtle changes in pre-ribosomal protein composition the SSU processome composition in wild-type and rpS15 depleted cells has been compared to each other.

By purifying Utp4p-TAP, 88 ribosome biogenesis factors could be identified, of which more than two third are required for maturation of the SSU and the rest for maturation of the LSU (Table 1). The factors of the LSU are generally identified by fewer peptides than the SSU factors, suggesting that these factors are only transiently associated with Utp4p-TAP purified pre-ribosomes. In addition, r-proteins of both subunits, ribosome associated factors and known contaminants were identified.

This direct comparison of Utp4p-TAP associated early pre-ribosomes purified from a strain lacking or not rpS15 indicated only minor changes in the respective protein compositions (Figure 20A). Apparently, association of all the analysed factors with Utp4p-TAP purifying particles is largely independent of assembly of rpS15 with nascent SSUs. This is in agreement with the direct RNA co-immunoprecipitation experiments shown in section 3.2 and 3.3. All tested factors (Noc4p, Utp4p, Pwp2p, Utp22p and Imp3p) were able to associate independent of the presence of rpS15 to pre-ribosomal particles. The analysis of Nop4p-TAP associated pre-ribosomes after rpS15 depletion (see section 3.4.4) showed a similar outcome demonstrating that the secondary SSU rRNA 3' domain binder rpS15 is not strictly needed for assembly of all identified ribosome biogenesis factors with early nuclear pre-ribosomes.

The semiquantitative comparison of pre-ribosomes purified after disruption of SSU rRNA 5' domain assembly (GAL-RPS9) to the purification from wild-type cells demonstrated an increased purification efficiency of the majority of co-purifying factors (Figure 20B). This is most pronounced for several SSU processome factors of the non-defined group (e.g. Enp1p, Utp30p, Emg1p, Rcl1p, Nop14p, Noc4p, Rok1p, Rrp12p, Bms1p, Kre33p, Bfr2p, Enp2p, Pno1p, Sof1p and Sas10p) and to a lesser extent for some LSU biogenesis factors (Nog1p, Nip7p and Dbp2p) and components of the UTP-C subcomplex (Rrp7p and Utp22p). This phenomenon could be explained by the higher enrichment of the accumulating early pre-RNAs (23S and 35S pre-rRNA) after depletion of rpS9 (Figure 13; Utp4p-TAP/ RPS9, compare lanes I (on) and IP (on) with lanes I (off) and IP (off)). In contrast, some factors behave differently than the majority of co-purifying biogenesis factors and show a slight decrease in their co-purification efficiency with Utp4p-TAP after rpS9 depletion. These proteins include components of the box C/D snoRNPs (Nop1p, Nop56p, and Nop58p), the box H/ACA snoRNPs (Nop10p, Gar1p, and Cbf5p), some SSU processome factors of the non-defined group (Prp43p, Utp20p, Nsr1p, Kri1p and Nop6p), and some LSU biogenesis factors (Brx1p, Nop12p, Noc1p, Ebp2p, Tif6p, Noc2p and Nop15p). Apparently, SSU rRNA 5' domain assembly is needed for their efficient association with early pre-ribosomes.

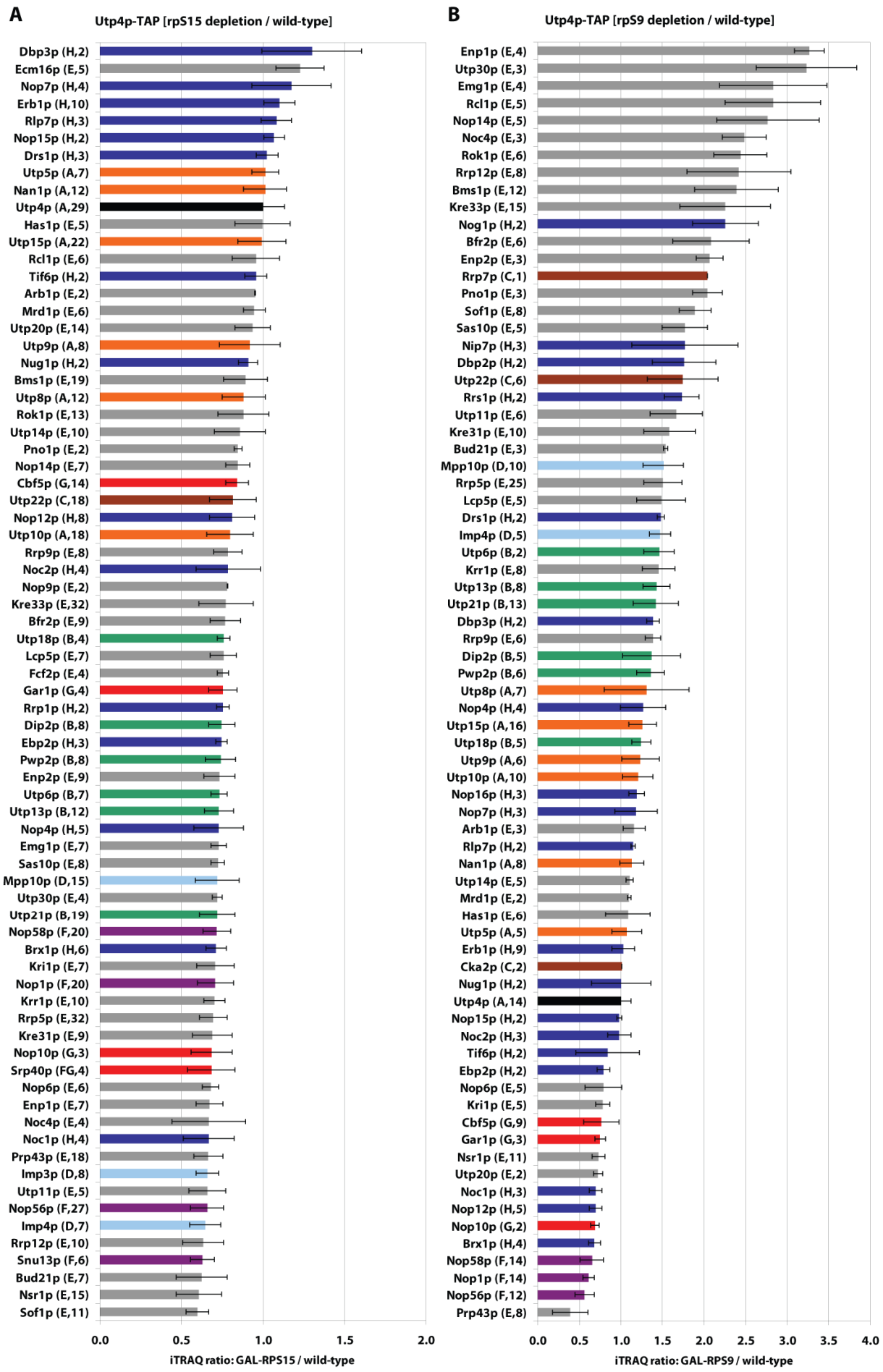
A
Utp4p-TAP [rpS15 depletion / wild-type]
Dbp3p (H,2)
Ecm16p (E,5)
Nop7p (H,4)
Erb1p (H,10)
Rlp7p (H,3)
Nop15p (H,2)
Drs1p (H,3)
Utp5p (A,7)
Nan1p (A,12)
Utp4p (A,29)
Has1p (E,5)
Utp15p (A,22)
Rcl1p (E,6)
Tif6p (H,2)
Arb1p (E,2)
Mrd1p (E,6)
Utp20p (E,14)
Utp9p (A,8)
Nug1p (H,2)
Bms1p (E,19)
Utp8p (A,12)
Rok1p (E,13)
Utp14p (E,10)
Pno1p (E,2)
Nop14p (E,7)
Cbf5p (G,14)
Utp22p (C,18)
Nop12p (H,8)
Utp10p (A,18)
Rrp9p (E,8)
Noc2p (H,4)
Nop9p (E,2)
Kre33p (E,32)
Bfr2p (E,9)
Utp18p (B,4)
Lcp5p (E,7)
Fcf2p (E,4)
Gar1p (G,4)
Rrp1p (H,2)
Dip2p (B,8)
Ebp2p (H,3)
Pwp2p (B,8)
Enp2p (E,9)
Utp6p (B,7)
Utp13p (B,12)
Nop4p (H,5)
Emg1p (E,7)
Sas10p (E,8)
Mpp10p (D,15)
Utp30p (E,4)
Utp21p (B,19)
Nop58p (F,20)
Brx1p (H,6)
Kri1p (E,7)
Nop1p (F,20)
Krr1p (E,10)
Rrp5p (E,32)
Kre31p (E,9)
Nop10p (G,3)
Srp40p (FG,4)
Nop6p (E,6)
Enp1p (E,7)
Noc4p (E,4)
Noc1p (H,4)
Prp43p (E,18)
Imp3p (D,8)
Utp11p (E,5)
Nop56p (F,27)
Imp4p (D,7)
Rrp12p (E,10)
Snu13p (F,6)
Bud21p (E,7)
Nsr1p (E,15)
Sof1p (E,11)
0.0
0.5
1.0
1.5
2.0
iTRAQ ratio: GAL-RPS15 / wild-type
B
Utp4p-TAP [rpS9 depletion / wild-type]
Enp1p (E,4)
Utp30p (E,3)
Emg1p (E,4)
Rcl1p (E,5)
Nop14p (E,5)
Noc4p (E,3)
Rok1p (E,6)
Rrp12p (E,8)
Bms1p (E,12)
Kre33p (E,15)
Nog1p (H,2)
Bfr2p (E,6)
Enp2p (E,3)
Rrp7p (C,1)
Pno1p (E,3)
Sof1p (E,8)
Sas10p (E,5)
Nip7p (H,3)
Dbp2p (H,2)
Utp22p (C,6)
Rrs1p (H,2)
Utp11p (E,6)
Kre31p (E,10)
Bud21p (E,3)
Mpp10p (D,10)
Rrp5p (E,25)
Lcp5p (E,5)
Drs1p (H,2)
Imp4p (D,5)
Utp6p (B,2)
Krr1p (E,8)
Utp13p (B,8)
Utp21p (B,13)
Dbp3p (H,2)
Rrp9p (E,6)
Dip2p (B,5)
Pwp2p (B,6)
Utp8p (A,7)
Nop4p (H,4)
Utp15p (A,16)
Utp18p (B,5)
Utp9p (A,6)
Utp10p (A,10)
Nop16p (H,3)
Nop7p (H,3)
Arb1p (E,3)
Rlp7p (H,2)
Nan1p (A,8)
Utp14p (E,5)
Mrd1p (E,2)
Has1p (E,6)
Utp5p (A,5)
Erb1p (H,9)
Cka2p (C,2)
Nug1p (H,2)
Utp4p (A,14)
Nop15p (H,2)
Noc2p (H,3)
Tif6p (H,2)
Ebp2p (H,2)
Nop6p (E,5)
Kri1p (E,5)
Cbf5p (G,9)
Gar1p (G,3)
Nsr1p (E,11)
Utp20p (E,2)
Noc1p (H,3)
Nop12p (H,5)
Nop10p (G,2)
Brx1p (H,4)
Nop58p (F,14)
Nop1p (F,14)
Nop56p (F,12)
Prp43p (E,8)
0.0
0.5
1.0
1.5
2.0
2.5
3.0
3.5
4.0
iTRAQ ratio: GAL-RPS9 / wild-type

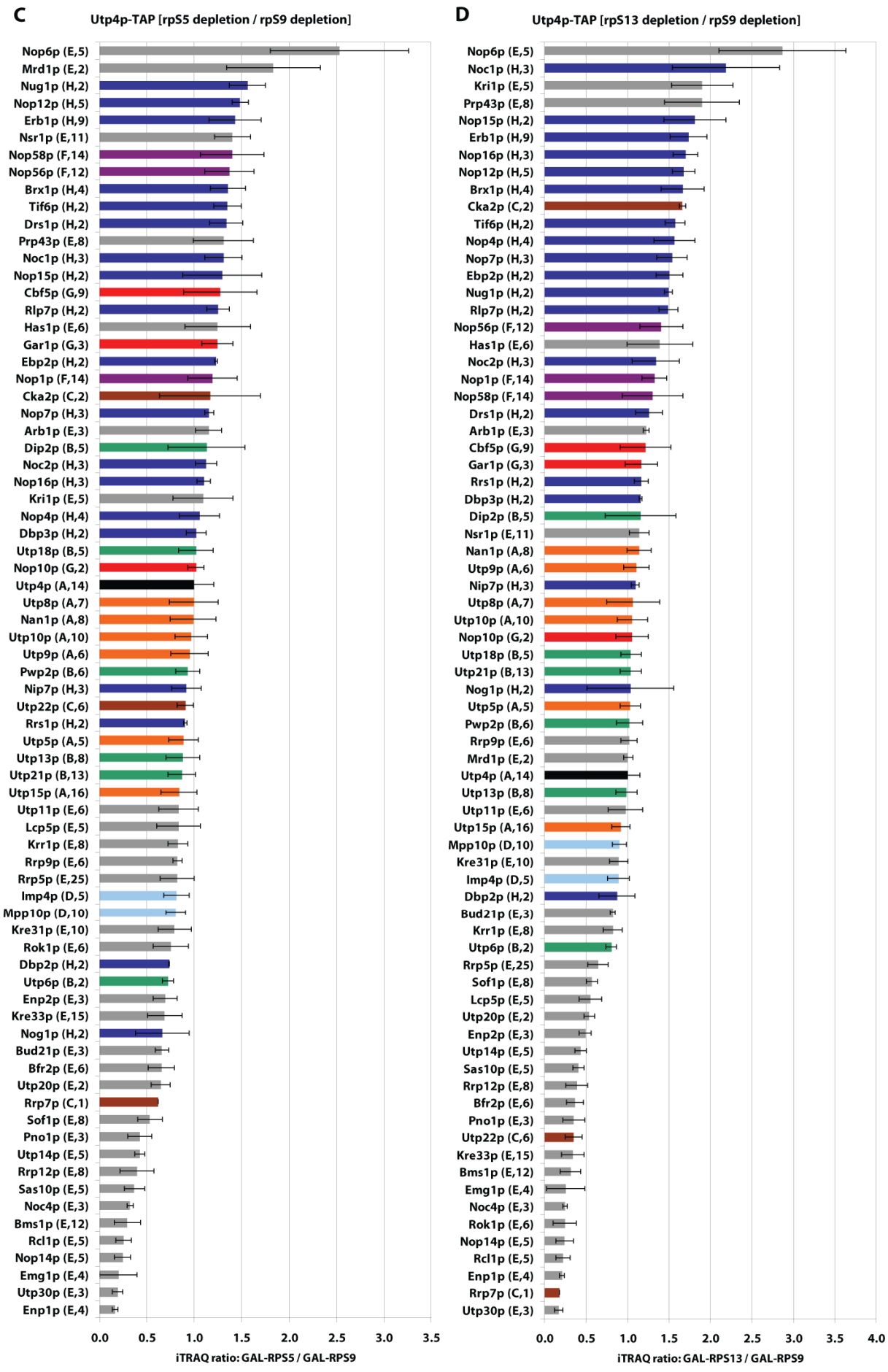
C
Utp4p-TAP [rpS5 depletion / rpS9 depletion]
Nop6p (E,5)
Mrd1p (E,2)
Nug1p (H,2)
Nop12p (H,5)
Erb1p (H,9)
Nsr1p (E,11)
Nop58p (F,14)
Nop56p (F,12)
Brx1p (H,4)
Tif6p (H,2)
Drs1p (H,2)
Prp43p (E,8)
Noc1p (H,3)
Nop15p (H,2)
Cbf5p (G,9)
Rlp7p (H,2)
Has1p (E,6)
Gar1p (G,3)
Ebp2p (H,2)
Nop1p (F,14)
Cka2p (C,2)
Nop7p (H,3)
Arb1p (E,3)
Dip2p (B,5)
Noc2p (H,3)
Nop16p (H,3)
Kri1p (E,5)
Nop4p (H,4)
Dbp3p (H,2)
Utp18p (B,5)
Nop10p (G,2)
Utp4p (A,14)
Utp8p (A,7)
Nan1p (A,8)
Utp10p (A,10)
Utp9p (A,6)
Pwp2p (B,6)
Nip7p (H,3)
Utp22p (C,6)
Rrs1p (H,2)
Utp5p (A,5)
Utp13p (B,8)
Utp21p (B,13)
Utp15p (A,16)
Utp11p (E,6)
Lcp5p (E,5)
Krr1p (E,8)
Rrp9p (E,6)
Rrp5p (E,25)
Imp4p (D,5)
Mpp10p (D,10)
Kre31p (E,10)
Rok1p (E,6)
Dbp2p (H,2)
Utp6p (B,2)
Enp2p (E,3)
Kre33p (E,15)
Nog1p (H,2)
Bud21p (E,3)
Bfr2p (E,6)
Utp20p (E,2)
Rrp7p (C,1)
Sof1p (E,8)
Pno1p (E,3)
Utp14p (E,5)
Rrp12p (E,8)
Sas10p (E,5)
Noc4p (E,3)
Bms1p (E,12)
Rcl1p (E,5)
Nop14p (E,5)
Emg1p (E,4)
Utp30p (E,3)
Enp1p (E,4)
0.0
0.5
1.0
1.5
2.0
2.5
3.0
3.5
iTRAQ ratio: GAL-RPS5 / GAL-RPS9
D
Utp4p-TAP [rpS13 depletion / rpS9 depletion]
Nop6p (E,5)
Noc1p (H,3)
Kri1p (E,5)
Prp43p (E,8)
Nop15p (H,2)
Erb1p (H,9)
Nop16p (H,3)
Nop12p (H,5)
Brx1p (H,4)
Cka2p (C,2)
Tif6p (H,2)
Nop4p (H,4)
Nop7p (H,3)
Ebp2p (H,2)
Nug1p (H,2)
Rlp7p (H,2)
Nop56p (F,12)
Has1p (E,6)
Noc2p (H,3)
Nop1p (F,14)
Nop58p (F,14)
Drs1p (H,2)
Arb1p (E,3)
Cbf5p (G,9)
Gar1p (G,3)
Rrs1p (H,2)
Dbp3p (H,2)
Dip2p (B,5)
Nsr1p (E,11)
Nan1p (A,8)
Utp9p (A,6)
Nip7p (H,3)
Utp8p (A,7)
Utp10p (A,10)
Nop10p (G,2)
Utp18p (B,5)
Utp21p (B,13)
Nog1p (H,2)
Utp5p (A,5)
Pwp2p (B,6)
Rrp9p (E,6)
Mrd1p (E,2)
Utp4p (A,14)
Utp13p (B,8)
Utp11p (E,6)
Utp15p (A,16)
Mpp10p (D,10)
Kre31p (E,10)
Imp4p (D,5)
Dbp2p (H,2)
Bud21p (E,3)
Krr1p (E,8)
Utp6p (B,2)
Rrp5p (E,25)
Sof1p (E,8)
Lcp5p (E,5)
Utp20p (E,2)
Enp2p (E,3)
Utp14p (E,5)
Sas10p (E,5)
Rrp12p (E,8)
Bfr2p (E,6)
Pno1p (E,3)
Utp22p (C,6)
Kre33p (E,15)
Bms1p (E,12)
Emg1p (E,4)
Noc4p (E,3)
Rok1p (E,6)
Nop14p (E,5)
Rcl1p (E,5)
Enp1p (E,4)
Rrp7p (C,1)
Utp30p (E,3)
0.0
0.5
1.0
1.5
2.0
2.5
3.0
3.5
4.0
iTRAQ ratio: GAL-RPS13 / GAL-RPS9

Figure 20. Quantitative analysis of the protein composition of pre-ribosomes purified via Utp4p-TAP using IgG coupled magnetic beads.
Pre-ribosomes were purified via Utp4p-TAP from cell lysates of a wild-type strain (Y1907) and strains depleted either for rpS5 (GAL-RPS5, Y1524), rpS9 (GAL-RPS9, Y1883), rpS13 (GAL-RPS13, Y1893) or rpS15 (GAL-RPS15, Y1528). Bound proteins were eluted from the IgG coupled magnetic bead matrix with 500mM NH_4OH. The eluted proteins were digested using trypsin and the resulting peptides from each sample were labelled with different iTRAQ reagents. The labelled peptides were separated on a nano HPLC system (Dionex Ultimate 3000) and spotted online via the Probot system (Dionex) on the MALDI target. Up to eight peptides per spot were further fragmented in the MS/MS mode, thus giving rise to peptide fragments used for identification and reporter ions used for quantitation of the respective protein (detailed description in Figure 14 and Figure 15). The relative amounts of proteins purified from the GAL-RPS15 (**A**) and GAL-RPS9 (**B**) strains are normalised to the purification from the wild-type strain, whereas the relative amounts of proteins purified from the GAL-RPS5 (**C**) and the GALRPS13 (**D**) strains are normalised to the purification from the GAL-RPS9 strain. A mean value, with the corresponding standard deviation, of all identified peptides of a single protein is depicted. Only proteins, identified by at least two non-redundant peptides were included in the quantitation analysis (as an exception Rrp7p was identified by only one single peptide and included in figure B, C and D). The iTRAQ ratios of the co-purifying proteins were normalised to the iTRAQ ratio of the bait protein (highlighted by a black bar). A classification of the identified proteins, as well as the number of identified peptides is depicted in parentheses. The protein classification is as following: A=UTP-A subcomplex (orange), B= UTP-B subcomplex (green), C=UTP-C subcomplex (brown), D= Mpp10p complex (light blue), E=non-grouped SSU processome factors (grey), F= box C/D snoRNP (purple), G= box H/ACA snoRNP (red) and H=LSU biogenesis factor (dark blue).

This result has to be taken into account, when interpreting pre-ribosome co-purifications after rpS5 and rpS13 depletion normalised to the purification after depletion of rpS9 (see below).

Comparison of early Utp4p-TAP associated pre-ribosomes purified from cells depleted for the primary SSU rRNA 3′ domain binder rpS5 with the ones purified from cells depleted for the 5′ domain binder rpS9 showed a different result than after depletion of secondary 3′ domain binder rpS15. Upon rpS5 depletion, a small group of proteins, including Bms1p, Emg1p, Enp1p, Noc4p, Nop14p, Rcl1p, Rrp12p, Sas10p and Utp30p seemed to be significantly disturbed in their association to Utp4p-TAP containing pre-ribosomes (Figure 20C; GAL-RPS5 / GAL-RPS9 ratio below 0.40). Furthermore, this was also true to a lesser extent for Pno1p and Utp14p (GAL-RPS5 / GAL-RPS9 ratio between 0.4 and 0.5). These factors are all SSU processome components not belonging to the four submodules (UTP-A, UTP-B, UTP-C, and MPP10p) described earlier (see section 2.5). This result is in good agreement with the reduced 23S / 35S pre-rRNA precipitation efficiency of Noc4p-TAP after rpS5 depletion (see section 3.2). Furthermore, in contrast to other SSU processome components, Nop14p, Emg1p, Rrp12p and Enp1p still co-purified with Noc4p-TAP after rpS5 depletion (see section 3.4.4). This analysis demonstrated that these proteins are still associated with the bait protein Noc4p-TAP under this condition. Thus, if the interaction of Noc4p with early pre-ribosomes is reduced after rpS5 depletion and these proteins are still associated with Noc4p, they should in turn be depleted from the accumulating pre-ribosomes purified with Utp4p-TAP.

A similar result was obtained after depletion of the SSU rRNA central domain binder rpS13. The ratio (GAL-RPS13 / GAL-RPS9) for most of the factors co-purifying with Utp4p-TAP from cells depleted for rpS13 versus rpS9 was higher than 0.5, while some proteins showed significantly lower ratios (Figure 20D). The group of proteins depleted from affinity purified Utp4p-TAP fractions after shut down of rpS13 expression contained the proteins: Bfr2p, Bms1p, Emg1p, Enp1p, Kre33p,

Noc4p, Nop14p, Pno1, Rcl1p, Rok1p, Rrp7p, Rrp12p, Utp22p and Utp30p (GAL-RPS13 / GAL-RPS9 ratio below 0.4) and to a lesser extent Enp2p, Sas10p and Utp14p (GAL-RPS13 / GAL-RPS9 ratio between 0.4 and 0.5). This group included the same proteins like after rpS5 depletion and furthermore six additional factors, namely Bfr2p, Kre33p, Enp2p, Rok1p, Rrp7p and Utp22p. In the case of Noc4p and Utp22p (UTP-C submodule) this is in agreement with the RNA co-immunoprecipitation experiments shown in Figure 12 and Figure 13, which revealed that rpS13 is necessary for efficient assembly of both proteins with nascent SSUs (see section 3.2 and 3.3). Interestingly, Rrp7p and Utp22p are both constituents of the SSU processome UTP-C submodule and behave, in contrast to another predicted UTP-C component Cka2p, in the same manner. However, although Rrp7p was unequivocally identified by one single peptide, no statistics exist for this protein regarding the quantitation data.
Several ribosome biogenesis factors seem to be specifically enriched in Utp4p-TAP associated pre-ribosomes accumulating in cells depleted for primary SSU rRNA 3′ domain binder rpS5 or central domain binder rpS13, when compared to early pre-ribosomes accumulating in cells depleted for the 5′ domain binder rpS9. This indicates that these proteins are underrepresented in the purification after rpS9 depletion and suggests that efficient assembly of these factors, including several LSU maturation factors, requires proper SSU rRNA 5′ domain assembly. Of note, the normalisation of the purification after depletion of rpS5 (GAL-RPS5) and rpS13 (GAL-RPS13) to the purification after depletion of rpS9 (GAL-RPS9) is misleading for Prp43p and Utp20p. Both proteins are impaired in their association to pre-ribosomal particles in all three depletion strains, when normalising to the wild-type purification, although to different extent (Figure 20B and data not shown).

In summary, these analyses show that after disruption of secondary SSU rRNA 3′ domain assembly (GAL-RPS15) all identified factors are still co-purifying with Utp4p-TAP. In contrast, primary 3′ domain assembly (GAL-RPS5) is needed for a group of 11 proteins to efficiently interact with pre-ribosomal particles. The same group of proteins and six additional factors depend on proper central domain assembly (GAL-RPS13) for their association with pre-ribosomal particles (for summary see also Figure 29).

3.5 Assembly of ribosomal proteins in the temperature sensitive *noc4-8* strain

The observation that rpS5, rpS13, rpS14 and rpS16 are needed for efficient assembly of Noc4p to pre-ribosomes opened the question whether this is also true *vice versa* (see section 3.2). To test this, the temperature sensitive *noc4*-8 mutant strain was transformed with a collection of vectors constitutively expressing r-proteins as a fusion protein with the Flag-epitope. In this case, the Flag-tagged r-proteins of the SSU (Flag-rpSX) are co-expressed with the endogenous copy of the respective gene and can be affinity purified using an anti-Flag resin (M2 Sigma). A pre-culture of

the *noc4-8* strain carrying the Flag-rpSX vector is cultivated under selective conditions (SDC-ura) at the permissive temperature (24°C) overnight and diluted in full medium on the next day. This culture is kept at 24°C for one generation time and then split, whereas one part is cultivated at 24°C and the other part at the restrictive temperature of 37°C. An anti-Flag immunoprecipitation was performed and the co-precipitated rRNA was analysed via northern blotting (Figure 21). It has been shown that r-proteins of the SSU are stably incorporated into pre-ribosomes at the level of 20S pre-rRNA, which is the direct precursor to the mature 18S rRNA (Ferreira-Cerca et al., 2007). In contrast the precipitation of early rRNA species, like 23S or 35S pre-rRNA, is very inefficient. In this regard, the amount of precipitated 20S pre-rRNA was taken as a measurement for incorporation of the respective rpS into pre-ribosomes.

The efficiency of individual immunoprecipitations is internally controlled through the analysis of the precipitation efficiency of mature ribosomes by the Flag-tagged rpSX. Thus, the amount of precipitated 20S pre-rRNA can be normalised to the amount of precipitated mature 18S rRNA.

As seen in Figure 22 (compare lanes 1 and 3), the inactivation of Noc4p by cultivation of the temperature sensitive *noc4-8* strain for three hours at 37°C resulted in a decrease of 20S pre-rRNA, whereas the amount of early rRNA precursors did not change significantly.

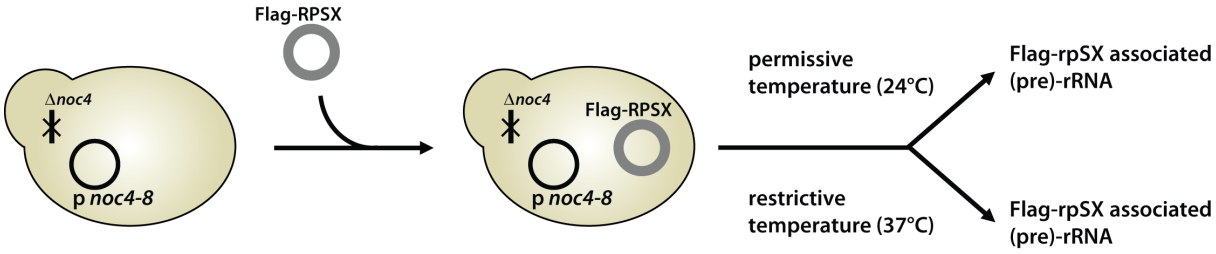

Figure 21. Schematic overview of the experimental setup used for studying *in vivo* assembly of ribosomal proteins of the SSU (rpS) in the temperature sensitive *noc4-8* strain

The strain harbouring a knockout of the endogenous *NOC4* (Δ*noc4*) is carrying the temperature sensitive *noc4-8* allele on a plasmid and therefore viable at the permissive temperature (24°C). Noc4p is expressed under the control of the *NOP1* promoter and as an N-terminal fusion with the Protein A-tag. The strain is transformed with a plasmid carrying a gene coding for an r-protein fused to the Flag-tag (Flag-RPSX). The strain is cultivated either at the permissive temperature (24°C) or at the restrictive temperature (37°C) for three hours. An RNA co-immunoprecipitation using the Flag-tagged rpSX as a bait protein is performed and the precipitated rRNA is analysed by northern blotting.

When looking at the precipitation of 20S pre-rRNA, only a slight defect in assembly of rpS13 and rpS14 (central domain) after inactivation of Noc4p is observed (Figure 22; rpS13 and rpS14, compare lanes 1 and 2 with lanes 3 and 4). In contrast, the precipitation of 20S pre-rRNA via Flag-rpS5 and Flag-rpS16 (SSU rRNA 3' domain) is more dramatically reduced after Noc4p inactivation (Figure 22; rpS5 and rpS16, compare lanes 1 and 2 with lanes 3 and 4).

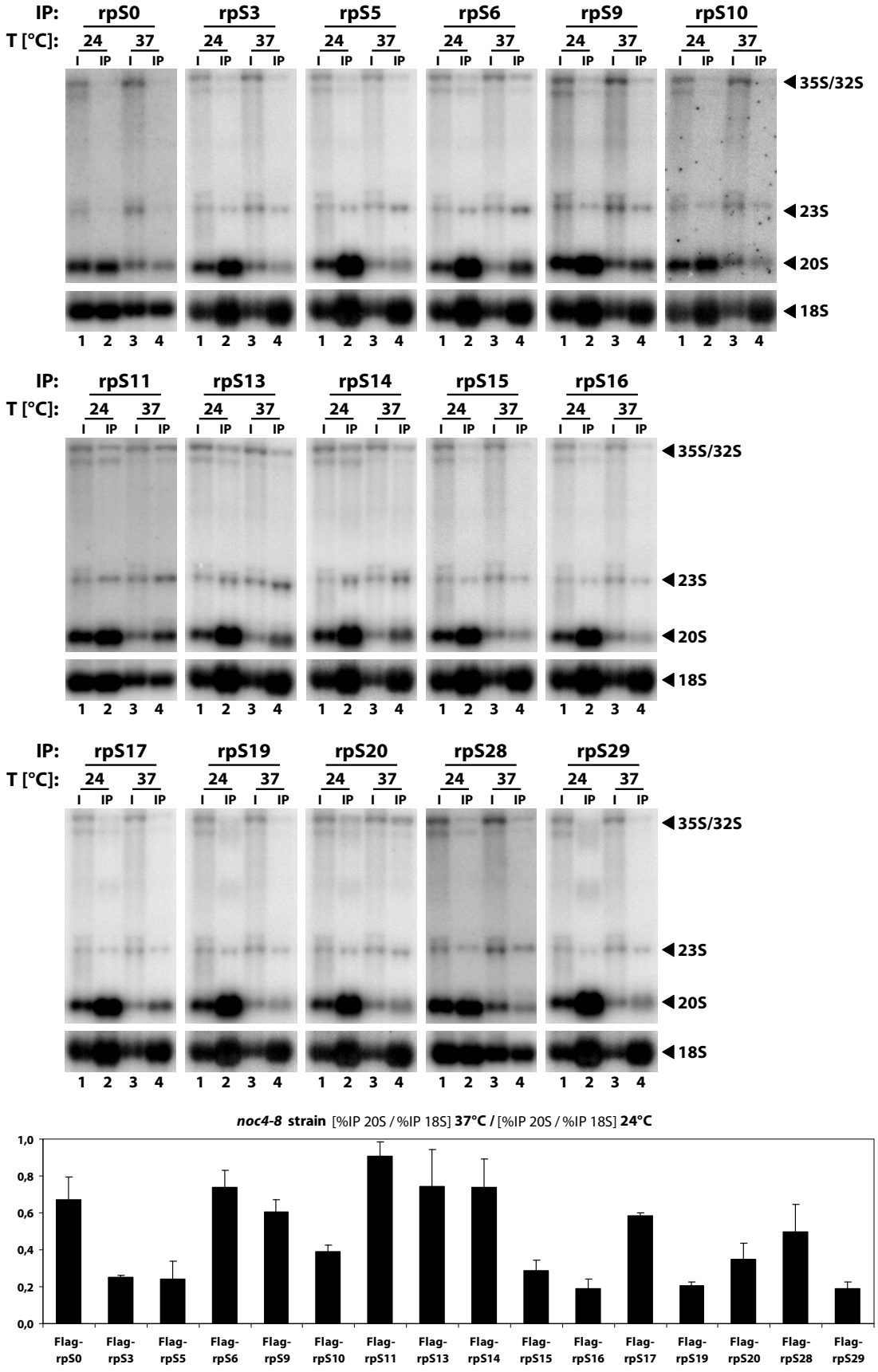

Figure 22. Co-immunoprecipitation of rRNA by Flag-tagged r-proteins of the SSU in the *noc4-8* strain
The temperature sensitive *noc4-8* strain (Y40) was transformed with plasmids carrying a gene coding for an r-protein fused to the Flag-tag (k351, k424, k427, k429, k432, k522, k622, k623, k766, k991, k999, k1000, k1001, k1006, k1015, and k1111). Positive transformants were selected and cultivated over night in selective

medium. The cells were inoculated in full medium to an OD_{600} of 0.2 and grown for one generation time at 24°C. One part of the logarithmically growing culture was grown at 24°C and the other part was shifted to 37°C for 3 hours. The respective Flag-tagged r-protein was precipitated using anti-Flag M2 beads (Invitrogen) and the co-precipitated rRNA species were analysed by northern blotting using oligo 1819, which hybridises within the ITS1 region (upper panel) and oligo 205, which hybridises within the 18S region (lower panel). The different rRNA species are indicated at the right side. Equal signal intensities of input (I) and beads (IP) correspond to 3% co-precipitation of the respective rRNA. The amount of precipitated 20S and 18S rRNA was quantified using Multigauge and a ratio was calculated with the following formula: [(IP/Input)20S / (IP/Input)18S]37°C / [(IP/Input)20S / (IP/Input)18S]24°C. Two independent experiments were performed and the result of the quantitation is depicted below.

This demonstrated that, although rpS5, rpS13, rpS14, and rpS16 are required for Noc4p assembly, *vice versa* this is only true for rpS5 and rpS16.

The assembly of r-proteins has been extensively studied in prokaryotes and the experiments established a hierarchical order of assembly for the r-proteins of the SSU in *E.coli* (Held et al., 1974; Mizushima et al., 1970) (see section 2.3.1). This means, a primary binding r-protein has to bind first to facilitate the assembly of secondary and tertiary binding r-proteins. The r-proteins of the SSU were classified into five major assembly trees and oriented in a so called "assembly map". In this map, the homolog of rpS13 (S15) is the primary binder of the central domain of the SSU rRNA. The homolog of rpS14 (S11) is a tertiary binder of the same domain and its assembly depends on rpS13. The homolog of rpS5 (S7) is the primary binder of the SSU rRNA 3′ (head) domain of the SSU rRNA. Presumably, the observed disruption of efficient primary SSU rRNA 3′ domain assembly after inactivation of the Noc4p variant in the *noc4-8* mutant should have an effect on the assembly of secondary and tertiary binding proteins of the 3′ domain.

To test this hypothesis, the association of secondary and tertiary binding proteins of the SSU rRNA 3′ domain with 20S pre-rRNA was analysed in the *noc4-8* mutant. Almost all tested homologs of eubacterial r-proteins of the SSU rRNA 3′ domain (rpS3, rpS15, rpS19, rpS20 and rpS29) were impaired in their ability to assemble to 20S pre-rRNA after inactivation of Noc4p by shifting the *noc4-8* strain to the restrictive temperature (Figure 22; rpS3, rpS15, rpS19, rpS20 and rpS29, compare lanes 1 and 2 with lanes 3 and 4).

The only exception is rpS0 (Figure 22; rpS0, compare lanes 1 and 2 with lanes 3 and 4), which is not affected by the inactivation of Noc4p. This is in agreement with the *in vivo* assembly analysis of the SSU rRNA 3′ (head) domain, showing that rpS0 can assemble independent of rpS5 in eukaryotes due to a reduced contact of rpS0 with the SSU head structure (Ferreira-Cerca et al., 2007). Two r-proteins, showing a late head like rRNA processing defect upon depletion (Ferreira-Cerca et al., 2005), but having no counterparts in *E. coli*, rpS10 and rpS28, showed an intermediate assembly defect (Figure 22; rpS10and rpS28, compare lanes 1 and 2 with lanes 3 and 4). The *in vivo* assembly of these r-proteins depends on the presence of rpS5, as shown in eukaryotes (Ferreira-Cerca et al., 2007). However, in this analysis the observed effects on the assembly of secondary and tertiary binding r-proteins were in general much more pronounced, probably due to a direct depletion of rpS5, the primary binder of the head domain.

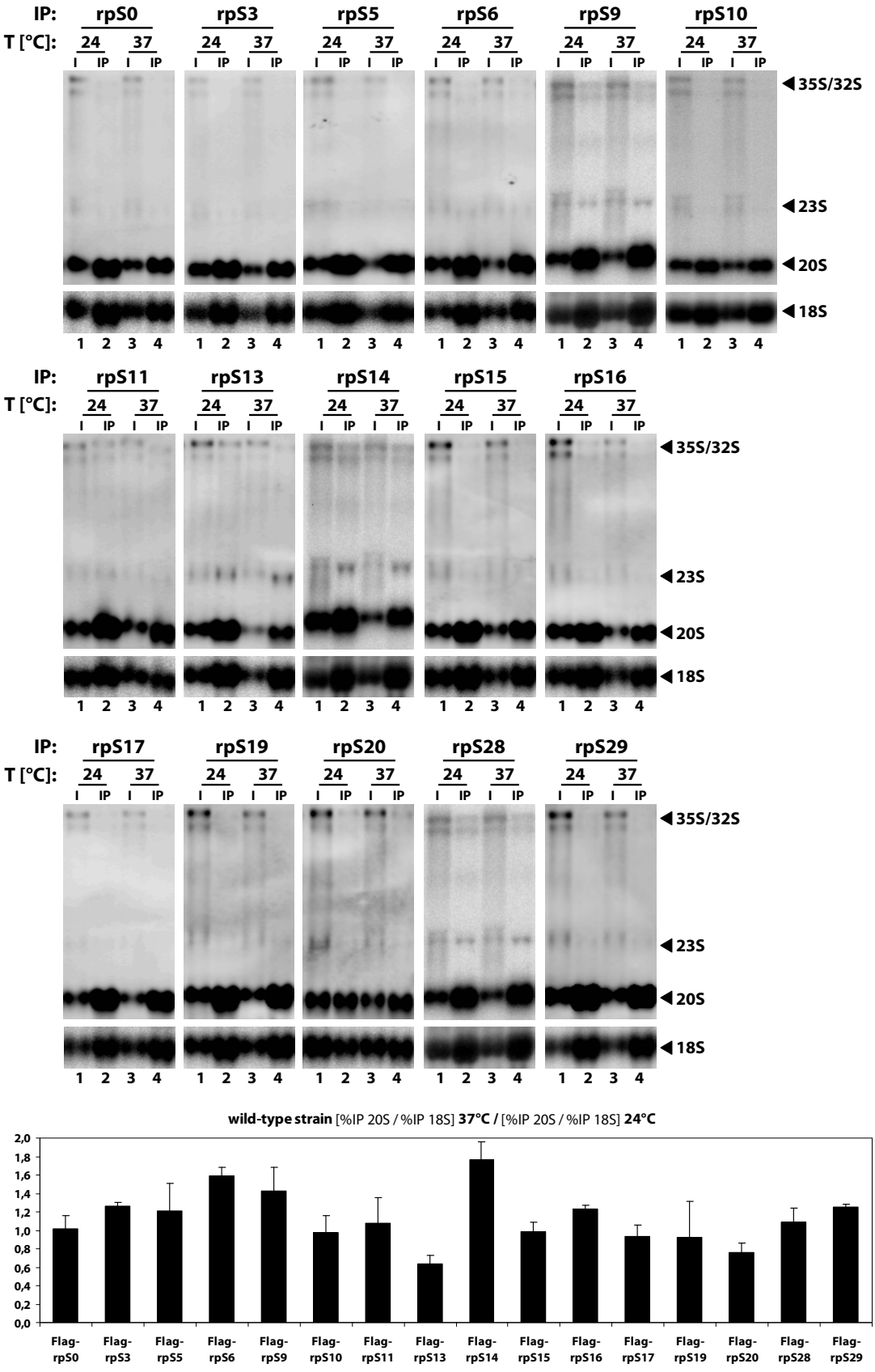

Figure 23. Co-immunoprecipitation of rRNA by Flag-tagged r-proteins of the SSU in the wild-type strain BY4741

The wild-type strain BY4741 (Y206) was transformed with plasmids carrying a gene coding for an r-protein fused to the Flag-tag (k351, k424, k427, k429, k432, k522, k622, k623, k766, k991, k999, k1000, k1001, k1006, k1015, and k1111). Positive transformants were selected and cultivated over night in selective medium. The

cells were inoculated in full medium to an OD_{600} of 0.2 and grown for one generation time at 24°C. One part of the logarithmically growing culture was grown at 24°C and the other part was shifted to 37°C for 3 hours. The respective Flag-tagged r-protein was precipitated using anti-Flag M2 beads (Invitrogen) and the co-precipitated rRNA species were analysed by northern blotting using oligo 1819, which hybridises within the ITS1 region (upper panel) and oligo 205, which hybridises within the 18S region (lower panel). The different rRNA species are indicated at the right side. Equal signal intensities of input (I) and beads (IP) correspond to 3% co-precipitation of the respective rRNA. The amount of precipitated 20S and 18S rRNA was quantified using Multigauge and a ratio was calculated with the following formula: [(IP/Input)20S / (IP/Input)18S]37°C / [(IP/Input)20S / (IP/Input)18S]24°C. Two independent experiments were performed and the result of the quantitation is depicted below.

Hence, the intermediate assembly defect of rpS10 and rpS28 in the *noc4-8* mutant could be a result of the partially, but not complete, disruption of rpS5 association with 20S pre-rRNA after inactivation of Noc4p.

R-proteins of the SSU rRNA 5′ domain (Figure 22; rpS6, rpS9, rpS11, rpS13, rpS14 and rpS17, compare lanes 1 and 2 with lanes 3 and 4) showed just a slight assembly defect and were able to assemble 2 to 4 times more efficient to 20S pre-rRNA in comparison to r-proteins of the 3′ domain.

Interestingly, some r-proteins precipitated more efficiently 35S pre-rRNA. This is true for rpS6, rpS11, rpS13, rpS14 and rpS20 (Figure 22; rpS6, rpS11, rpS13, rpS14 and rpS20, compare 35S pre-rRNA in lanes 1 and 2 with lanes 3 and 4). These r-proteins seem to be incorporated more stably at the level of this early rRNA precursor than other r-proteins. Except for rpS20, these are all early binding r-proteins of the body domain and this is in agreement with their early function in ribosome maturation. However, it is unclear why this phenomenon is also observed for rpS20.

The observed assembly defects could still be explained simply by a temperature effect on the assembly of the head domain. To rule this out, the same rRNA-IP experiments were performed in a wild-type strain (BY4742). This analysis showed that most r-proteins were able to associate to 20S pre-rRNA even more efficient when the wild-type strain was grown at 37°C in comparison to cultivation at 24°C (Figure 23, compare lanes 1 and 2 with lanes 3 and 4). The only exceptions are rpS13 and rpS20, which assemble a little bit less efficient at 37°C in comparison to 24°C. Hence, it seems unlikely that the assembly defect of r-proteins of the SSU rRNA 3′ domain after Noc4p inactivation is just due to the raise of temperature.

In summary, Noc4p is specifically required for efficient assembly of the SSU rRNA 3′ (head) domain, but has only a minor impact on the assembly of r-proteins of the 5′ or central domain (for summary see also Figure 29).

3.6 Assembly of ribosomal proteins in other temperature sensitive mutants of *NOC4*

During the course of the first characterisation of Noc4p, a total of nine temperature sensitive *NOC4* mutants were isolated (Milkereit et al., 2003). *Noc4-8* was the best characterised one and was therefore chosen for the analysis of r-protein assembly after inactivation of Noc4p (see section 3.5). The remaining eight ts-mutants were now used to study the influence of Noc4p on the assembly of

rpS5, the primary binder of the SSU rRNA 3′ (head) domain. The analysis revealed that association of rpS5 with 20S pre-rRNA was reduced after inactivation of the respective Noc4p variant in all *noc4* ts-mutants at the restrictive temperature of 37°C, although to a different extent **(**Figure 24; compare lanes 1 and 2 with lanes 3 and 4). The assembly of rpS5 with 20S pre-rRNA appeared to be less affected in four strains including *noc4-2*, *noc4-3*, and *noc4-10* and was least affected in the *noc4-1* strain (Figure 24; compare lanes 1 and 2 with lanes 3 and 4 and see quantitation below). When looking at the growth phenotype at different temperatures, *noc4-1* together with *noc4-4* exhibited a very strong growth defect at 37°C (Table 2). In contrast to the same growth impairment at 37°C, the *noc4-4* strain exhibited a very strong assembly defect of rpS5 at 37°C, while the *noc4-1* strain was only minor affected. The *noc4-1* strain could exhibit an assembly defect at later steps of SSU rRNA 3′ domain assembly, thus explaining the similar growth impairment as the *noc4-4* strain. Meaning, the primary binder rpS5 could be able to assemble in this mutant, but secondary or tertiary binder could be more affected in their assembly to the 3′ domain.

To test this hypothesis, the assembly of rpS15 and rpS3 (secondary and tertiary binder of the SSU rRNA 3′ domain) was investigated in this strain. In addition, rpS11, which is part of the SSU rRNA 5′ domain, was taken as a negative control, because assembly of this r-protein should proceed independently of Noc4p (see section 3.5). The results demonstrated an impairment of efficient assembly of rpS3 and rpS15, but not of rpS11, to 20S pre-rRNA in the *noc4-1* mutant (Figure 25; rpS3, rpS11 and rpS15, compare lanes 1 and 2 with lanes 3 and 4).

Strain	*NOC4* allele	Growth defect at 37°C	Assembly defect of rpS5 at 37°C
Y34	*noc4-1*	++++	+
Y35	*noc4-2*	+	++
Y36	*noc4-3*	++	++
Y37	*noc4-4*	++++	++++
Y38	*noc4-5*	+++	+++
Y39	*noc4-7*	+	+++
Y40	*noc4-8*	++	+++
Y41	*noc4-9*	++	++++
Y42	*noc4-10*	++	++

Table 2. Summary of the growth and rpS5 assembly phenotypes in different temperature sensitive *noc4* strains

The table is a summary of the results from the RNA co-immunoprecipitations from section 3.6 (Figure 24) and from a growth phenotype analysis of the different temperature sensitive noc4 strains. The growth phenotype analysis has been performed by spotting different dilutions of cells on full medium agar plates (YPD) and incubation at different temperatures. The results obtained for the different growth behaviour at 37°C is summarised in arbitrary units.

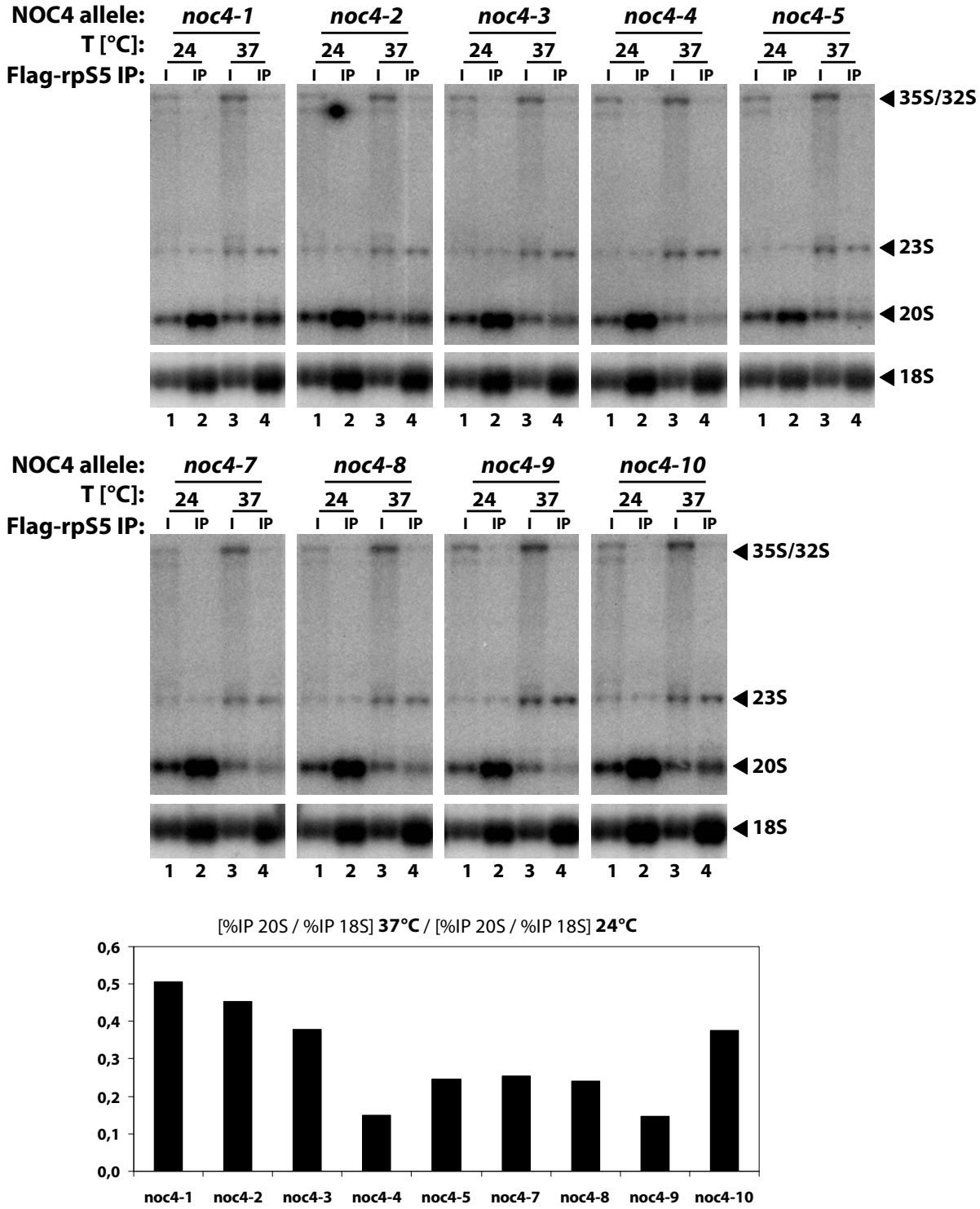

Figure 24. Co-immunoprecipitation of rRNA by Flag-rpS5 in different temperature sensitive *noc4* strains

The temperature sensitive *noc4* strains (Y34, Y35, Y36, Y37, Y38, Y139, Y40, Y41 and Y42) were transformed with a plasmid carrying the gene coding for rpS5 fused to the Flag-tag (k351). Positive transformants were selected and cultivated over night in selective medium. The cells were inoculated in full medium to an OD_{600} of 0.2 and grown for one generation time at 24°C. One part of the logarithmically growing culture was grown at 24°C and the other part was shifted to 37°C for 3 hours. Flag-rpS5 was precipitated using anti-Flag M2 beads (Invitrogen) and the co-precipitated rRNA species were analysed by northern blotting using oligo 1819, which hybridises within the ITS1 region (upper panel) and oligo 205, which hybridises within the 18S region (lower panel). The different rRNA species are indicated at the right side. Equal signal intensities of input (I) and beads (IP) correspond to 3% co-precipitation of the respective rRNA. Twice the amount of the

24°C samples were loaded for the 37°C samples (I and IP) for better quantitation results. This has to be taken in account, when judging the depletion phenotype at 37°C (comparison of I at 24°C vs. I at 37°C), while the relative amount of co-precipitated rRNAs can be directly compared to each other. The amount of precipitated 20S and 18S rRNA was quantified using Multigauge and a ratio was calculated with the following formula: [(IP/Input)20S / (IP/Input)18S]37°C / [(IP/Input)20S / (IP/Input)18S]24°C. The result of the quantitation is depicted below.

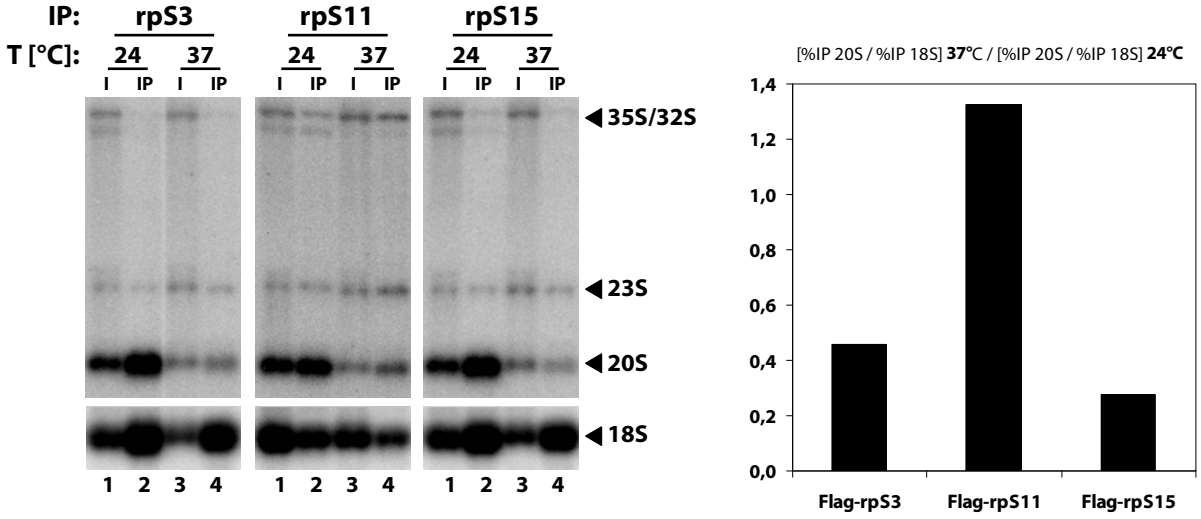

Figure 25. Co-immunoprecipitation of rRNA by Flag-tagged r-proteins of the SSU in the *noc4-1* strain
The temperature sensitive *noc4-1* strain (Y34) was transformed with plasmids carrying a gene coding for an r-protein fused to the Flag-tag (k424, k1001, k429). Positive transformants were selected and cultivated over night in selective medium. The cells were inoculated in full medium to an OD_{600} of 0.2 and grown for one generation time at 24°C. One part of the logarithmically growing culture was grown at 24°C and the other part was shifted to 37°C for 3 hours. The respective Flag-tagged r-protein was precipitated using anti-Flag M2 beads (Invitrogen) and the co-precipitated rRNA species were analysed by northern blotting using oligo 1819, which hybridises within the ITS1 region (upper panel) and oligo 205, which hybridises within the 18S region (lower panel). The different rRNA species are indicated at the right side. Equal signal intensities of input (I) and beads (IP) correspond to 3% co-precipitation of the respective rRNA. The amount of precipitated 20S and 18S rRNA was quantified using Multigauge and a ratio was calculated with the following formula: [(IP/Input)20S / (IP/Input)18S]37°C / [(IP/Input)20S / (IP/Input)18S]24°C. The result of the quantitation is depicted on the right side.

In summary, different temperature sensitive alleles *of NOC4* affect SSU rRNA 3' (head) assembly in specific ways: in most mutants, assembly of primary binder rpS5 is affected, in others, as *noc4-1* effects on SSU head domain assembly start to be obvious on the level of secondary / tertiary binders, like rpS15 or rpS3, respectively.

3.7 Assembly of ribosomal proteins in the temperature sensitive *nop14-2* strain

Previous work indicated a direct interaction of Noc4p with Nop14p (Milkereit et al., 2003). Furthermore, Nop14p was shown to be required for the recruitment of Noc4p to pre-ribosomal

particles (Kühn et al., 2009). Because of this strong relationship of both proteins, the involvement of Nop14p in the assembly process of r-proteins of the SSU was investigated.

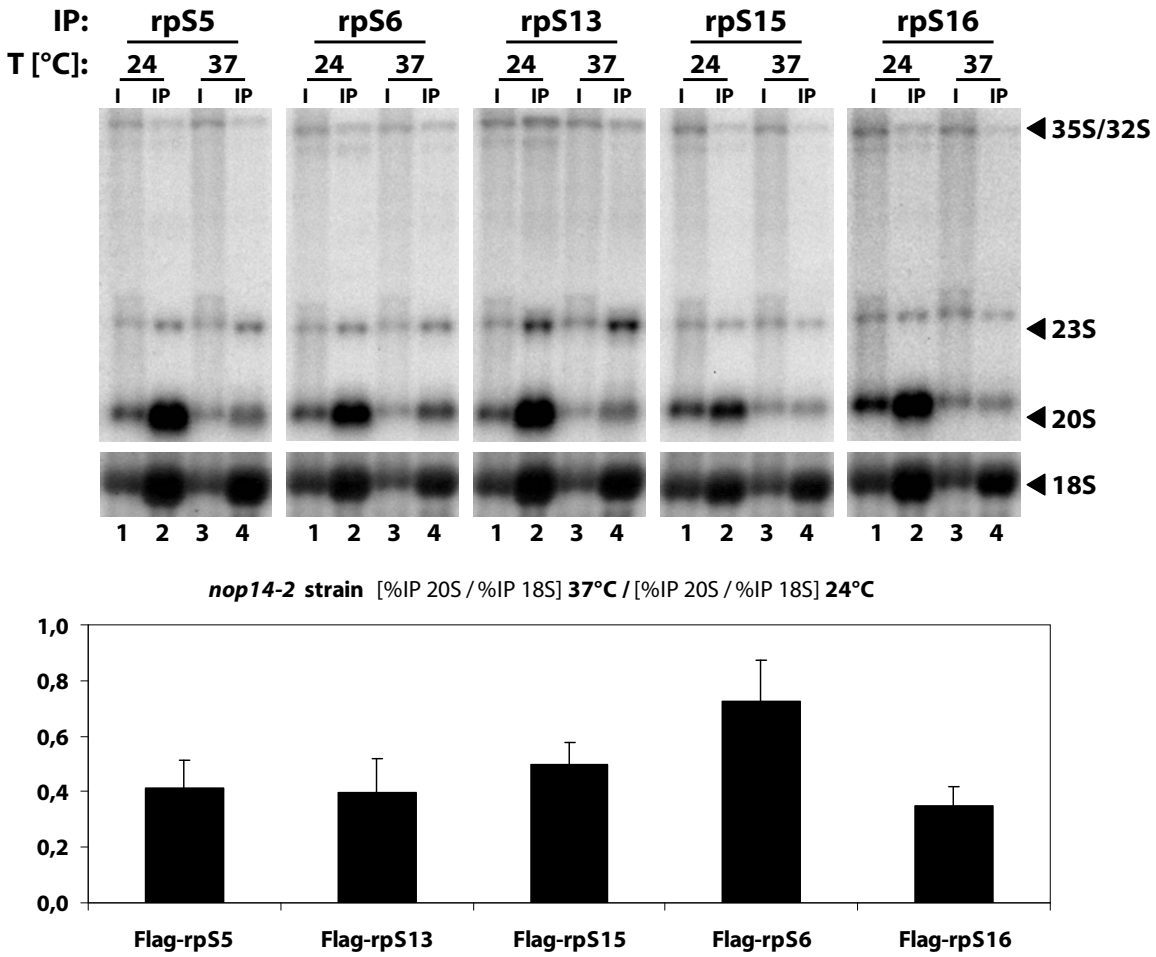

Figure 26. Co-immunoprecipitation of rRNA by Flag-tagged r-proteins of the SSU in the *nop14-2* strain
The temperature sensitive *nop14-2* strain (Y175) was transformed with plasmids carrying a gene coding for an r-protein fused to the Flag-tag. Positive transformants were selected and cultivated over night in selective medium. The cells were inoculated in full medium to an OD_{600} of 0.2 and grown for one generation time at 24°C. One part of the logarithmically growing culture was grown at 24°C and the other part was shifted to 37°C for 3 hours. The respective Flag-tagged r-protein was precipitated using anti-Flag M2 beads (Invitrogen) and the co-precipitated rRNA species were analysed by northern blotting using oligo 1819, which hybridises within the ITS1 region (upper panel) and oligo 205, which hybridises within the 18S region (lower panel). The different rRNA species are indicated at the right side. Equal signal intensities of input (I) and beads (IP) correspond to 3% co-precipitation of the respective rRNA. The amount of precipitated 20S and 18S rRNA was quantified using Multigauge and a ratio was calculated with the following formula: [(IP/Input)20S / (IP/Input)18S]37°C / [(IP/Input)20S / (IP/Input)18S]24°C. The result of the quantitation is depicted on the right side.

The association of a subset of r-proteins with 20S pre-rRNA, including representatives of the SSU body (rpS6 and rpS13) and head domain (rpS5, rpS15 and rpS16), was tested after inactivation of the corresponding Nop14p variant in the temperature sensitive *nop14-2* mutant. The phenotype after Nop14p inactivation is similar to the depletion phenotype of Noc4p, rpS5 and rpS16, namely

an accumulation of 23S and 35S pre-rRNAs and a decrease of 20S pre-rRNA (Figure 26; compare lanes 1 and 3). The tested r-proteins of the SSU 3' (head) domain, rpS5, rpS15 and rpS16 showed a decreased 20S RNA precipitation after inactivation of the Nop14p variant at 37°C, although the effect was weaker compared to the *noc4-8* strain (Figure 26; rpS5, rpS15 and rpS16, compare lanes 1 and 2 with lanes 3 and 4). In contrast rpS6, an r-protein of the SSU body (5' and central domain), showed only a slight reduction of 20S pre-rRNA precipitation at 37°C in comparison to 24°C (Figure 26; rpS6, compare lanes 1 and 2 with lanes 3 and 4). This reduction is similar to the one observed in the *noc4-8* mutant. Interestingly, rpS13 showed also a decreased precipitation efficiency of 20S pre-rRNA, comparable to the effect observed for the tested SSU head proteins (Figure 26; rpS13, compare lanes 1 and 2 with lanes 3 and 4**)**. RpS13 is part of the SSU rRNA central domain and was originally intended to act as a negative control; however, surprisingly it behaved different than in the *noc4-8* strain.

In summary, the assembly defect observed in the *nop14-2* strain differed from that observed in the *noc4-8* mutant. First of all, the extent of the assembly defect is not as severe as in the *noc4-8* mutant. This could simply be explained by a leaky ts phenotype. Accordingly, the Nop14p variant could still be partially active and therefore allow better assembly of the analysed r-proteins. Alternatively, the effect of Nop14p on SSU rRNA 3' domain assembly could be alleviated, because Nop14p is not directly involved in assembly of these proteins, but rather indirect by facilitating Noc4p assembly (Kühn et al., 2009). The inhibition of Noc4p assembly by inactivation of Nop14p would therefore inhibit r-protein assembly of the SSU rRNA 3' (head domain).

Second, the SSU rRNA central domain protein, rpS13, is impaired in its association to pre-ribosomes after inactivation of Nop14p, which suggests a direct involvement of Nop14p in the assembly of this protein.

3.8 Characterisation of the temperature sensitive *noc4-8* strain

To further characterise the *noc4-8* mutant, the association of the corresponding Noc4p variant with pre-ribosomes was analysed. In the *noc4-8* mutant, the temperature sensitive allele of *NOC4* is expressed in fusion with the Protein A-tag. The immunoprecipitation was therefore performed using an IgG-sepharose matrix. The strain was either cultivated at 24°C or 37°C and co-purified rRNA was analysed. ProtA-Noc4p efficiently precipitated early rRNA precursors, like 23S and 35S pre-rRNAs, at the permissive temperature of 24°C (Figure 27A; *noc4-8*, compare lane I (24) and IP (24)). However, this precipitation is reduced by a factor of four after inactivation of ProtA-Noc4p at the restrictive temperature of 37°C (Figure 27A; *noc4-8*, compare lane I (24) and IP (24) with lane I (37) and IP (37)). The amount of precipitated ProtA-Noc4p was controlled by western blotting and revealed a reduced level of ProtA-Noc4p at 37°C and concomitantly a reduction of the absolute precipitated amount of ProtA-Noc4p. Taken this into account, the precipitation of 35S pre-rRNA was normalised to the actual amount of the precipitated bait protein. This normalised quantitation suggests that the precipitation efficiency of 35S pre-rRNA precursors by ProtA-Noc4p was not altered at 37°C (Figure 27A; see normalised quantitation). The same experiment was performed in a

wild-type strain, which exhibited a slightly reduced precipitation of 35S pre-rRNA at 37°C (Figure 27A; *NOC4*, compare lane I (24) and IP (24) with lane I (37) and IP (37)).

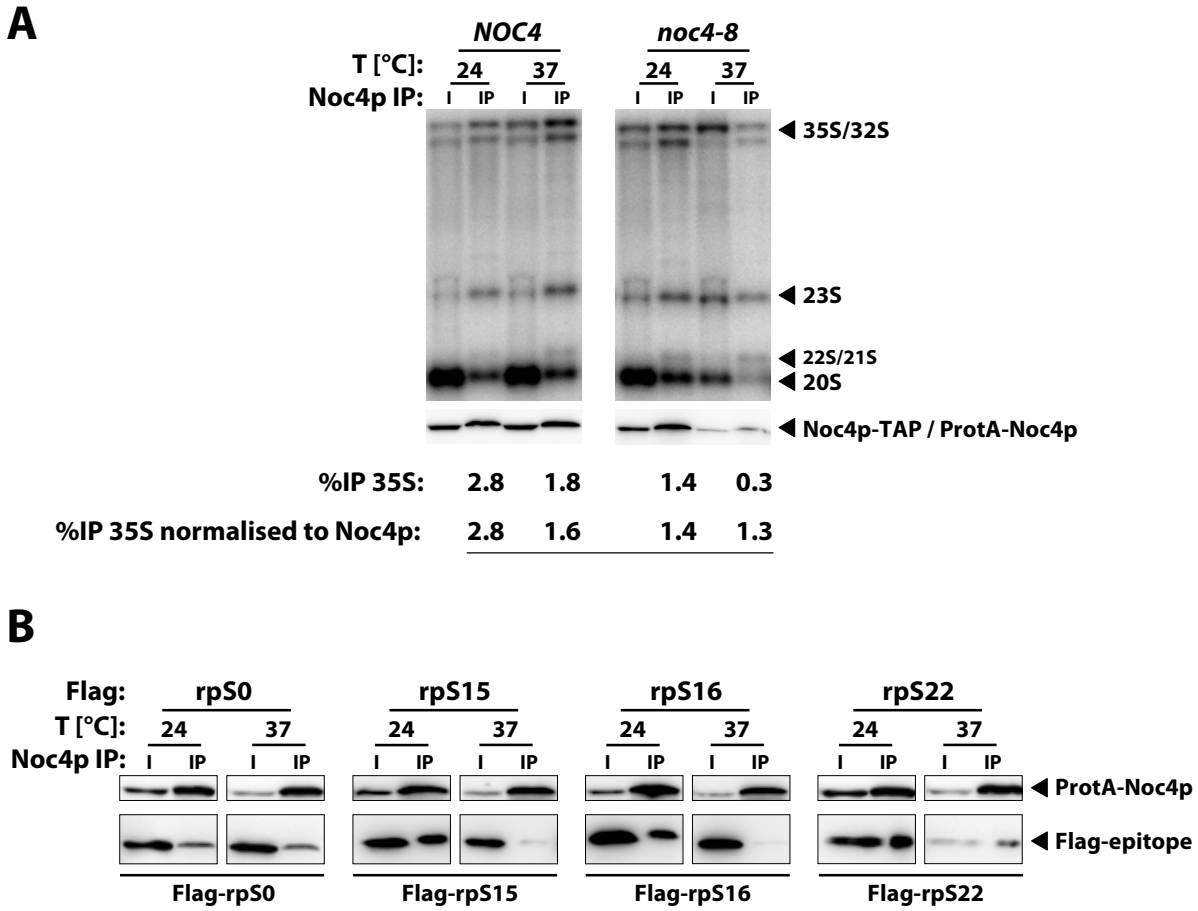

Figure 27. Co-immunoprecipitation of pre-RNAs (A) or Flag-tagged rpS (B) by ProtA-Noc4p in the temperatures sensitive *noc4-8* strain

(**A**) The wild-type strain (Y96) carrying Noc4p-TAP and the temperature sensitive *noc4*-8 (Y40) strain, expressing Noc4p in fusion with the Protein A-tag (ProtA-Noc4p) were cultivated in galactose (on) and glucose (4 hours, off) containing full medium. Noc4p-TAP/ProtA-Noc4pwas precipitated via its Protein A moiety using IgG sepharose beads. The precipitated amount of Noc4p-TAP/ProtA-Noc4pwas monitored by western blotting (PAP antibody) and the co-precipitated rRNA was analysed by northern blotting using oligo 1819, which hybridises within the ITS1 region. For the northern blot equal signal intensities of input (I) and beads (IP) correspond to 1% co-precipitation of the respective rRNA. For the western blot equal signal intensities of input (I) and beads (IP) correspond to 20% precipitation of the bait protein Noc4p-TAP/Noc4p-ProA. The amount of precipitated 35S pre-rRNA as well as the amount of Noc4p-TAP/ProtA-Noc4pwas quantified using Multigauge and is depicted below each IP lane. The second row shows a quantitation of the amount of precipitated 35S pre-rRNA normalised to the amount of precipitated Noc4p-TAP/Noc4p-ProA.

(**B**) The temperature sensitive *noc4-8* strain (Y40) was transformed with plasmids carrying a gene coding for an r-protein fused to the Flag-tag (Flag-RPS0 (k991), Flag-RPS15 (k429), Flag-RPS16 (k622) and Flag-RPS22 (k764). Positive transformants were selected and cultivated over night in selective medium. The cells were inoculated in full medium to an OD_{600} of 0.2 and grown for one generation time at 24°C. One part of the logarithmically growing culture was grown at 24°C and the other part was shifted to 37°C for 3 hours. The *noc4-8* encoded ProtA-Noc4pvariant was precipitated via its Protein A moiety using IgG sepharose beads and the precipitated proteins were analysed by western blotting. The Protein A-tag was detected with the PAP antibody and the Flag-epitope with a primary anti-Flag M2 antibody and a secondary anti-mouse antibody. Equal signal intensities of input (I) and beads (IP) correspond to 20% precipitation of the respective protein.

This analysis demonstrated that the *noc4-8* encoded Noc4p variant is able to associate with early precursors after inactivation at 37°C and opened the question whether Noc4p associated pre-ribosomes are comprised of the full set of r-proteins in the *noc4-8* mutant. When Noc4p is able to assemble in the *noc4-8* mutant to pre-ribosomes at 37°C, but at the same time the assembly of SSU head r-proteins is disturbed (see section 3.5), Noc4p should consequently precipitate reduced amounts of the affected r-proteins. To test this assumption, the following strategy was applied; the *noc4-8* strain was transiently transformed with plasmids expressing individual r-proteins as a fusion protein with the Flag-tag. The strains were kept in selection medium over night and transferred to full medium for one generation time at the next day. Afterwards, the culture was split and cultivated for three hours either at 24°C or at 37°C. Following precipitation of ProtA-Noc4p using IgG sepharose beads, the amount of precipitated ProtA-Noc4p and of co-purifying r-proteins was analysed by western blotting. The experiment demonstrated a reduced precipitation of Flag-rpS15 and Flag-rpS16 (r-proteins of the SSU head) with ProtA-Noc4p at the restrictive temperature (Figure 27B; rpS15 and rpS16, compare lanes I (24) and IP (24) with lanes I (37) and IP (37)). In contrast, the relative amounts of precipitated Flag-rpS0 and Flag-rpS22 (r-proteins of the SSU body) with ProtA-Noc4p did not change after inactivation of the *noc4-8* encoded ProtA-Noc4p variant at 37°C (Figure 27B; rpS0 and rpS22, compare lanes I (24) and IP (24) with lanes I (37) and IP (37)).

In summary, the analysis showed that the Noc4p variant in the *noc4-8* mutant is still associated with pre-ribosomes containing r-proteins of the SSU body domain, but not of the head domain, at the restrictive temperature of 37°C. This suggests that the Noc4p variant is able to assemble to pre-ribosomes, but the recruitment of r-proteins of the SSU head domain is specifically impaired in this mutant at the restrictive temperature.

3.9 Assembly of SSU processome components in the absence of Noc4p

Recently, the assembly of SSU processome components with nascent SSUs has been studied after depletion of representatives of three SSU processome subcomplexes (UTP-A, UTP-B and UTP-C) (Pérez-Fernández et al., 2007) (see section 2.5). Almost no data exists about the assembly relationships between the four SSU processome subcomplexes and the very diverse class of non-defined SSU processome components. Thus, it was investigated whether the association of other SSU processome components with early pre-ribosomes are dependent on Noc4p.

To this end, a galactose inducible strain of Noc4p was used, which allows the efficient depletion of Noc4p to undetectable amounts after cultivation for 16 hours in glucose containing medium. A representative member of the four subcomplexes and of the non-defined group of the SSU processome has been chosen and the sequence for the TAP-tag has been integrated at the 3' end of the endogenous loci of *UTP4* (UTP-A), *PWP2* (UTP-B), *UTP22* (UTP-C), *IMP3* (Mpp10p) and *ENP1* (non-defined group) in the GAL-NOC4 strain. The depletion of Noc4p led to a slight reduction of 20S pre-rRNA and a strong accumulation of 23S and 35S pre-rRNAs (Figure 28; compare lanes I (on) with I (off)). The 23S and 35S pre-rRNAs are efficiently precipitated by Utp4p-TAP (UTP-A), Pwp2p-

TAP (UTP-B) and Utp22p-TAP (UTP-C) and this precipitation is even enhanced after depletion of Noc4p (Figure 28; Utp4p, Pwp2p and Utp22p, compare lanes I (on) and IP (on) with lanes I (off) and IP (off)).

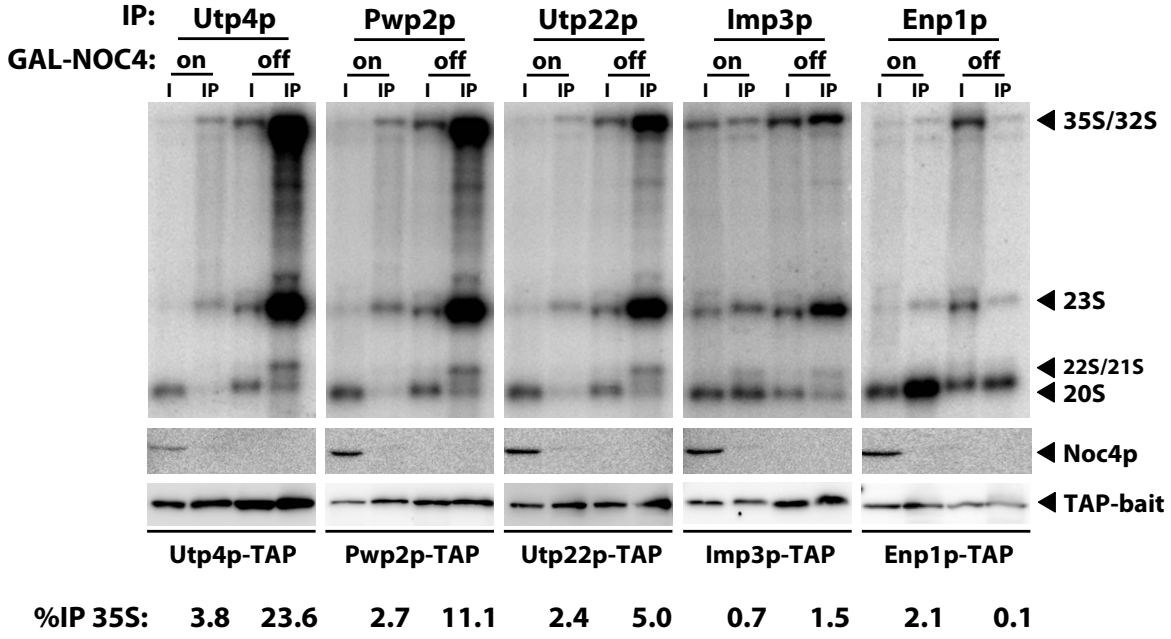

Figure 28. Co-immunoprecipitation of rRNA via Utp4p-TAP, Pwp2p-TAP, Utp22p-TAP, Imp3p-TAP or Enp1p-TAP after depletion of Noc4p
Strains carrying *NOC4* under control of a galactose inducible promoter and the respective bait as a TAP-fusion were cultivated either in galactose (on) or for 16 hours in glucose (off) containing full medium (Utp4p-TAP (Y1903), Pwp2p-TAP (Y1904), Utp22p-TAP (Y1905), Imp3p-TAP (Y1906) and Enp1p-TAP (Y2112)). The respective TAP-tagged bait protein was precipitated via its Protein A moiety using IgG sepharose beads and the co-precipitated rRNA was analysed by northern blotting using oligo 1819, which hybridises within the ITS1 region. In addition, the protein levels were analysed by western blotting. The Protein A moiety of the bait was detected with the PAP antibody and Noc4p with an anti-Noc4p antibody and a secondary anti-rat antibody. For the northern blot equal signal intensities of input (I) and beads (IP) correspond to 1% co-precipitation of the respective rRNA. For the western blot equal signal intensities of input (I) and beads (IP) correspond to 20% precipitation of the respective protein. The amount of precipitated 35S pre-rRNA was quantified using Multigauge and is depicted below each IP lane.

This effect is most pronounced for Utp4p, which showed a six fold increase in precipitation efficiency of early rRNA precursors after depletion of Noc4p. The GAL-NOC4-strain harbouring Imp3-TAP (Mpp10p complex) showed a slow growth phenotype and a slight rRNA processing defect, demonstrated by the accumulation of early precursors in galactose containing medium (Figure 28; Imp3p, see lane I (on)). Nevertheless, the precipitation of 35S pre-rRNA by Imp3p-TAP is also increased to some extent after depletion of Noc4p (Figure 28; Imp3p, compare lane I (on) and IP (on) with lane I (off) and IP (off)). Enp1p, a non-defined SSU processome component, was also tested in regard to its rRNA co-immunoprecipitation behaviour. Enp1p associates already with early pre-ribosomes and therefore precipitated early rRNA precursors, like 23S and 35S pre-RNAs (Figure 28; Enp1p, compare lane I (on) and IP (on)). During the course of maturation of the SSU, Enp1p

stays associated even with late 40S pre-ribosomal particles (Chen et al., 2003; Schäfer et al., 2003). This fact is supported by the efficient precipitation of 20S pre-rRNA, the direct precursor to the mature 18S rRNA. Interestingly, the precipitation of early precursors is largely reduced after shut down of Noc4p, while 20S pre-rRNA precipitation is only slightly reduced (Figure 28; Enp1p, compare lane I (on) and IP (on) with lane I (off) and IP (off).

Taken together, this analysis showed that Utp4p, Pwp2p, Utp22p and Imp3p are able to assemble to early pre-ribosomal particles in the absence of Noc4p. In contrast, the non-defined SSU processome component Enp1p needs Noc4p for efficient assembly to early pre-ribosomal particles, while association with late particles is only slightly affected.

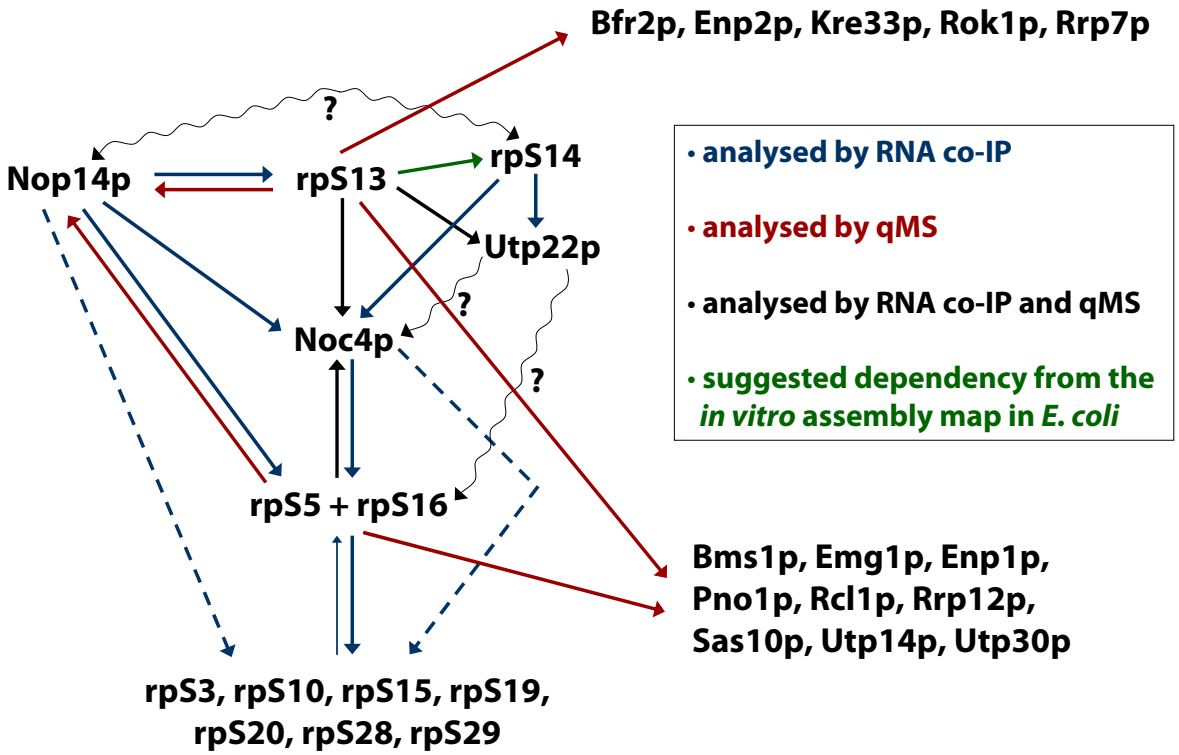

Figure 29. Summary of the assembly network of components of SSU pre-ribosomal particles
The members of the UTP-A, UTP-B and Mpp10p subcomplex can associate to early pre-ribosomes independent of all rpS tested and are not shown. Noc4p, Nop14p and the UTP-C subcomplex (Utp22p, Rrp7p) can associate to early pre-ribosomes independent of SSU rRNA 5′ domain assembly and this relationship is therefore omitted. SSU rRNA 5′ domain assembly takes place independently of Noc4p and Nop14p and is also not shown. An arrow pointing towards a protein means that this protein depends for its association to pre-ribosomes on the function/presence of the protein from which the arrow is originating. The blue dashed lines from Noc4p and Nop14p to the secondary and tertiary binder of the SSU 3′ (head) domain (rpS3, rpS10, rpS15, rpS19, rpS20, rpS28 and rpS29) account for the hierarchical order of SSU head assembly (Held et al., 1974). Accordingly, Noc4p and Nop14p might just have an indirect influence on the assembly of the secondary and tertiary binder of the head domain, because they are directly needed to facilitate the assembly of the primary binder rpS5 and rpS16. Some dependencies illustrated were not established in this PhD thesis: The association of Noc4p to pre-ribosomes depends on the interaction of its C-terminus with Nop14p (Kühn et al., 2009), blue arrow from Nop14p to Noc4p). Additionally, *In vitro* studies in *E. coli* established that rpS14 is a tertiary binder of the same assembly tree as the primary binder rpS13, which binds to the SSU rRNA central domain (Held et al., 1974). Therefore, rpS14 depends for its association to pre-ribosomes on the presence of rpS13 (green arrow from rpS13 to rpS14). Interesting relationships that were not studied during this work are shown by wavy lines and question marks.

4 DISCUSSION

4.1 rRNA processing phenotypes of ribosomal proteins S4, S21, S22, and S29 and correlation with their localisation in the SSU

During this work four strains, carrying the gene coding for an r-protein under control of the galactose inducible promoter (*GAL1*) were constructed, following analysis of the requirement of the respective r-protein for cell growth and rRNA processing. The detailed analysis of rpS4, rpS21, rpS22 and rpS29 showed that all proteins are essential for cell growth (see section 3.1.1and 3.1.2). For rpS4 (Synetos et al., 1992) and rpS21 (Tabb-Massey et al., 2003) this is in agreement with earlier reports. Furthermore, the described rRNA processing defect of cells depleted for rpS21 reported by Tabb-Massey correlates with the herein described phenotype (Tabb-Massey et al., 2003) (see 3.1.2). The rRNA processing defects after depletion of rpS4, rpS22 and rpS29 were described for the first time. The depletion of rpS4 and rpS22 resulted in an early rRNA processing defect, with accumulation of 23S and 35S pre-rRNAs and no 20S pre-rRNA production (see 3.1.2). This phenotype correlates for many other ribosomal proteins with a localisation of the respective proteins in the body domain (consisting of the SSU rRNA 5′ and central domain) of the SSU (Brodersen et al., 2002; Ferreira-Cerca et al., 2005). For rpS22 this is confirmed by structural information from the homologous protein (S8) in *E. coli*, which localises to the SSU rRNA central domain (Figure 11and Brodersen et al., 2002). Depletion of rpS21 and rpS29 resulted in later rRNA processing defects, with 20S pre-rRNA accumulation but no conversion into 18S rRNA (see 3.1.2). Whether this accumulating 20S pre-rRNA is exported, needs to be determined. This rather late phenotype correlates for many other r-proteins with their respective localisation around the SSU head/neck domain (Brodersen et al., 2002; Ferreira-Cerca et al., 2005).

The SSU head domain consists of the 3′ part of the 18S rRNA and the r-proteins that associate in this region. The systematic analysis of the r-proteins of the SSU demonstrated that complete depletion of r-proteins of the head domain never caused a complete block of 20S pre-rRNA production, although it was made to varying extent in the different mutants (Ferreira-Cerca et al., 2005). The depletion phenotype of rpS29 is consistent with the localisation of its homolog (S14) in *E. coli* at the head domain, while no homolog and therefore no structural information exist for rpS4 and rpS21 (Figure 11 and Brodersen et al., 2002). Furthermore, the assembly of rpS29 depends on the primary (rpS5) and secondary binder (rpS15) of the SSU rRNA 3′ (head) domain (Ferreira-Cerca et al., 2007). Some r-proteins, like rpS0 and rpS2, show a late rRNA processing defect, like rpS21 and rpS29, but no dependency on the primary binder of head domain (Ferreira-Cerca et al., 2005, 2007). Whether rpS21 also depends on the presence of the primary binder of the head domain will be subject of future research.

Interestingly, only *RPS29B*, but not *RPS29A* (both under control of their endogenous promoters), could support cell growth in the *Δrps29A* / *Δrps29B* strain. Both gene products show 91% sequence

identity (51/56 amino acids are identical). Thus, either *RPS29A* is not expressed under these conditions or *RPS29B* might have an essential function, which cannot be compensated by *RPS29A*. A global analysis of protein expression levels in yeast suggests that both proteins are expressed (Ghaemmaghami et al., 2003). Nevertheless, the expression levels of rpS29A/B in this report (5000-7000 molecules / cell) appear very low compared to other r-proteins (50000-100000 molecules / cell).

Due to the slight difference in amino acid sequence of rpS29A and rpS29B, both proteins can be distinguished in mass spectrometric analyses. However, in the presented analyses only peptides which can be attributed either to both rpS29 copies or which were specific for rpS29B were identified. Thus, to date, it is unclear whether rpS29A is expressed in yeast cells. To get an answer to this question, both proteins could be tagged in wild-type cells and the expression level could be monitored using western blot.

4.2 Establishment of an assay for semiquantitative analysis of pre-ribosomal particles

4.2.1 Affinity purification of pre-ribosomes: technical considerations

During this work, an assay for the semiquantitative comparison of the protein composition of pre-ribosomal particles has been developed (Merl and Jakob et al., 2010). The employment of a combination of pre-ribosome purification via a TAP-tagged biogenesis factor and subsequent quantitation of the co-purifying proteins using mass spectrometry proved to be suitable for the analysis of large RNPs.

In addition, this assay has been used as a general approach for studying effects of r-protein depletion on SSU processome assembly. While this assay confirmed the results of RNA co-immunoprecipitation experiments, it was also suitable for the identification of new relationships between other factors not studied directly.

The ribosome biogenesis factors of interest were purified via the protein A moiety of the TAP-tag using two different affinity matrices. Interestingly, the direct comparison of the purification of pre-ribosomes via Noc4p-TAP using either IgG coupled sepharose or magnetic beads revealed vast quality differences between these two purifications (see 3.4.3). The background of unspecific bound proteins was very high when using sepharose beads, whereas almost no background was detected when using magnetic beads. This could be due to the fact that the magnetic beads are solid and have only an outer surface, while sepharose beads exhibit pores and have therefore an inner surface as well. These inner pores have on the one hand an exclusion volume, thus preferentially allowing binding of protein complexes up to a certain size. In addition, the exclusion volume could hamper contaminants from being washed away. As there was a high background of unspecific proteins with sepharose beads each HPLC fraction showed a high protein complexity.

Consequently, the MS/MS analysis resulted in fewer assignments to ribosome biogenesis factors. Hence, the IgG coupled magnetic beads were used for purifications of pre-ribosomal particles.

4.2.2 Characterisation of the protein composition of affinity-purified early pre-ribosomal particles: identification of LSU biogenesis factors in early pre-ribosomes

Using the combined experimental setup of tryptic in-solution digest, peptide separation on nano-flow HPLC and MALDI-MS/MS, 68 and 88 preys could be identified from pre-ribosomal fractions affinity-purified from yeast extracts via TAP tagged Noc4p and Utp4p, respectively. This approach with its remarkable sensitivity is superior to standard affinity purifications as previously only up to 35 co-purifying proteins could be identified in affinity-purified yeast SSU processome fractions (Dragon et al., 2002; Grandi et al., 2002; Pérez-Fernández et al., 2007). Therefore, this experimental setup is an excellent tool for the analysis of huge RNPs.
In addition, these earlier analyses reported that the SSU processome consists mainly of biogenesis factors required for maturation of the SSU, because no factors required for LSU maturation (except some rpL) were identified in these studies.

In the herein presented data, some ribosome biogenesis factors of the large subunit could be identified as part of early pre-ribosomes, although these were represented in average by fewer peptides than SSU biogenesis factors (see 3.4. and Table 1). The amount of peptide gives an idea of the abundance of the protein in the purification. Thus, a low number of assigned peptides point towards a low abundance of the respective protein and hence towards a transient interaction of this factor with the bait protein. It has to be added, that the amount of peptides from a single protein that can be identified depends also on the size of the protein, the distribution of lysine and arginine residues and the general properties of the peptide sequence. A large protein will in average give rise to more peptides. In contrast, an uneven distribution or low frequency of lysine and arginine residues will result in very small or large peptides which are not suitable for identification by MALDI mass spectrometry. Furthermore, the properties of the peptide sequence influence the ionisation behaviour. Nevertheless, the amount of identified peptides can be used as an estimate for the abundance of the respective protein in the purified pre-ribosomes.
Some of the identified ribosome biogenesis factors of the LSU were identified by a high number of peptides in former purifications of different LSU biogenesis factors (Merl and Jakob et al., 2010). At least for these proteins this argues against a general unsuitability of the peptides for MALDI-MS/MS analyses. As there is a tendency for low coverage of almost all LSU factors in the described purifications, this argues for a low abundance or transient interaction of these factors with the purified pre-ribosomes. This transient interaction could explain why these factors were not previously identified as part of early pre-ribosomal complexes. In purifications of pre-ribosomes with other biogenesis factors (e.g. Rio2p-TAP, a factor associated with late pre-40S particles) using

the same protocol no factors required for LSU maturation could be identified (data not shown). This shows that the herein identified LSU factors are not unspecific binding proteins.

The original SSU processome / 90S pre-ribosome affinity purifications contained large amounts of pre-ribosomes in which the separation of LSU and SSU precursor rRNAs through cleavage in the internal transcribed spacer 1 (ITS-1) had already happened, resulting in the loss of LSU precursor components (Dragon et al., 2002; Grandi et al., 2002; Granneman and Baserga, 2004).

This observation explains well the observed bias for SSU biogenesis factors in the analysed complexes and argues that these early pre-ribosomal particles, referred to in the literature as SSU processome / 90S pre-ribosome might therefore to a significant amount represent SSU assembly intermediates (Dragon et al., 2002; Grandi et al., 2002; Bernstein et al., 2004).

However, it seems that pre-rRNA species cleaved (21S, 22S, and 23S pre-rRNAs) or not cleaved (35S pre-rRNA) in the ITS-1 region, are precipitated in approximately equal amounts, suggesting only a certain bias towards SSU precursor containing particles (Bernstein et al., 2004; Gallagher et al., 2004). Furthermore, it has been suggested by the Baserga group that the earliest 90S pre-ribosome might also contain 60S factors (Granneman et al., 2004).

The pre-ribosome purification of the present work showed a similar distribution of 23S and 35S pre-rRNA co-precipitation, with almost similar amounts of both species present (see 3.2 and 3.3). This suggests that the pre-rRNA content is similar to the former described purifications of early pre-ribosomes. However, much more biogenesis factors including LSU factors have been identified in the herein described purifications. It is unreasonable, that the 23S pre-rRNA containing particle is responsible for the association with biogenesis factors of the LSU. The interaction with these factors is probably more due to an interaction within a particle containing the 35S pre-rRNA. The half-life time of this pre-rRNA is prolonged and accumulates in all r-protein mutants analysed in this study. This prolonged half-life time might give LSU maturation factors more time to associate with early pre-ribosomes, providing a possible explanation why these factors have been identified in the presented analyses but not in previous studies (Dragon et al., 2002; Grandi et al., 2002; Pérez-Fernández et al., 2007).

Other reports strengthen the idea that biogenesis factors and r-proteins of the LSU are indeed involved in early ribosome assembly events. First, some LSU factors efficiently precipitate 35S pre-rRNA (Merl and Jakob et al., 2010). Second, one r-protein of the LSU has been found to assemble co-transcriptionally with nascent pre-RNA chains in *Drosophila melanogaster* (Chooi et al., 1981). Third, several r-proteins of the LSU have been isolated as part of nucleolar pre-ribosomal fractions (Kumar and Warner, 1972; Prestayko et al., 1974; Kuter and Rodgers, 1976; Auger-Buendia et al., 1978; Auger-Buendia et al., 1979).

4.2.3 Semiquantitative comparison of the protein composition of affinity purified pre-ribosomes by iTRAQ and MALDI-MS/MS: general considerations

One general aspect that has to be kept in mind when analysing affinity purified pre-ribosomes is that the population of isolated complexes is heterogeneous. There is not just one defined pre-ribosome purified by Noc4p-TAP or Utp4p-TAP, but rather a range of dynamic pre-ribosomal complexes. Therefore, the quantitative analysis can only give an average of all the different complexes.
Furthermore, the stoichiometry between the purified factors cannot be accessed using this approach. Only changes in the protein composition of the purified pre-ribosomes in relation to the reference sample can be measured. Absolute quantitation could provide information about the abundance of single preys in certain purifications. For this approach two or more standard peptides of each co-purified factor would have to be mixed in equimolar ratios, labelled with an iTRAQ reagent and added to the differentially labelled peptides derived from the purified pre-ribosomes. As there are more than 100 biogenesis factors, this approach would have been too expensive and labour intensive and thus was not further considered.

After depletion of several r-proteins a reduced co-purification of some ribosome biogenesis factors with pre-ribosomes was observed (see below). In general, there are two main explanations why a protein could be absent from the purified pre-ribosomal particles. Either its association depends indeed on the presence of the depleted r-protein, or this protein is not part of the accumulating pre-ribosome and associates at a later step of ribosome assembly. In the latter case the underrepresentation of the factor in the purified pre-ribosome would not be a direct effect of the depletion of the respective r-protein, but rather an indirect effect.

In summary, the method of comparative analysis of early pre-ribosomes using quantitative mass spectrometry proved to be a valuable tool for the identification of a high number of co-purifying ribosome biogenesis factors and for the detection of changes in their abundance in different ribosome biogenesis mutants. Gentle purification conditions preserved less stable interactions, while the MALDI MS/MS setup was sensitive enough to identify low abundant proteins in the purification.

4.3 SSU rRNA 3’ domain assembly events and recruitment of SSU processome components

The SSU processome can be subdivided into five major subgroups. Representative proteins of each subgroup, namely Utp4p (UTP-C), Pwp2p (UTP-B), Utp22p (UTP-C), Imp3p (Mpp10p complex) and Noc4p (non-defined), were tested for their association with early rRNA precursors after depletion of

certain r-proteins using RNA co-immunoprecipitations. With respect to the r-proteins, representatives of all three structural domains of the SSU rRNA have been chosen. RpS11 and rpS13 bind to the SSU rRNA 5′ domain, rpS22, rpS13 and rpS14 bind to the central domain and rpS5 and rpS15 bind to the 3′ domain (see 3.2 and 3.3).

The analysis revealed that r-protein assembly to the SSU rRNA 3′ domain is dispensable for association of the UTP-A, UTP-B, UTP-C and Mpp10p subcomplex to early pre-ribosomes (see 3.3). In contrast, the presence of the primary binder of the 3′ domain, rpS5, is required for the assembly of Noc4p (non-defined) (see 3.2). A refined analysis revealed that rpS16 is also needed for efficient Noc4p assembly, while the secondary binder of the 3′ domain, rpS15, and all tested tertiary binder of the 3′ domain are dispensable (see 3.2). The results of the direct rRNA co-IP have been confirmed by the semiquantitative analysis of the protein composition of pre-ribosomes after depletion of certain r-proteins. The purification of pre-ribosomes with Noc4p-TAP or Utp4p-TAP after depletion of rpS15 showed only a slight overall reduction of the co-purification efficiency with all factors (see 3.4.4 and 3.4.5). In contrast, the purification of Utp4-TAP after depletion of rpS5 showed a consistent reduction in the co-purification of 11 proteins. This group of 11 proteins requires, in contrast to all other identified SSU processome components, primary SSU rRNA 3′ (head) domain assembly events for their association with early pre-ribosomes.

Noc4p, which is one of the 11 proteins depleted from Utp4p-TAP associated pre-ribosomes, was also analysed for the co-purification of SSU processome components after rpS5 depletion. In this mutant Noc4p-TAP co-purified with seven proteins, whereas interaction with all other ribosome biogenesis factors was drastically disturbed, consistent with an inefficient interaction of Noc4p-TAP with early pre-RNAs (see 3.2 and 3.4.4). Noc4p-TAP was still associated with Nop14p and to a lesser extent with Arb1p, Bud21p, Emg1p/Nep1p, Rrp12p, Enp1p and Nop6p. Five of these eight proteins showed consistently a reduced co-purification with pre-ribosomes purified with Utp4p-TAP after rpS5 depletion. The result for the remaining three proteins might appear contradictory on the first view, because the interaction of Noc4p-TAP with early pre-ribosomes is strongly reduced, while the interaction of Utp4p-TAP with these particles is even enhanced. Thus, if some factors are still interacting with Noc4p after rpS5 depletion, they should in turn be absent from the pre-ribosomes purified with Utp4p-TAP.

Bud21p showed an intermediate effect in both purifications, which can explain its behaviour. It could partly be associated to pre-ribosomes (purified with Utp4p-TAP) and partly interact with Noc4p-TAP after dissociation from pre-ribosomes. The situation is different for Nop6p and Arb1p, which are both significantly enriched in the Noc4p-TAP and Utp4p-TAP purifications (see 3.4.4 and 3.4.5). However, free Nop6p and Arb1p could associate with Noc4p-TAP after its dissociation from pre-ribosomes, whereas the pre-ribosome associated proportion of both proteins stays associated with these particles.

Conditional mutants of *NOP14*, *ENP1* and *EMG1/NEP1* show a similar phenotype with accumulation of 23S pre-rRNA and reduction of 20S pre-rRNA (Liu et al., 2001; Chen et al., 2003). Enp1p depletion leads in addition to accumulation of 21S pre-rRNA (Chen et al., 2003). Nop6p and Bud21p are non-

essential, but *bud21* knockout cells exhibit a cold-sensitive phenotype and accumulation of 22S rRNA and reduction of 20S pre-rRNA at room temperature (Gallagher et al., 2004). Rrp12p is required for synthesis and export of both ribosomal subunits and mutants of *RRP12* show a rather late rRNA processing phenotype with 21S and 20S pre-rRNA accumulation (Oeffinger et al., 2004). Arb1p is also required for maturation of the SSU and LSU and mutants of *ARB1* show strong accumulation of early precursors (23S and 35S pre-rRNAs) and a minor accumulation of 20S pre-rRNA (Dong et al., 2005).
Taken together, all proteins can be found in early 90S pre-ribosomal particles and show an intermediate phenotype with accumulation of early precursors and production of 20S pre-rRNA, to varying extent. Importantly, all the mentioned factors differ in respect to their mutant phenotypes from other SSU processome components. The similar behaviour in the presented proteomic analyses and the described functional relationship strengthen the notion, that they might be involved in similar steps of ribosome biogenesis.

Other observations further support the notion of functional links between several members of this group of SSU-processome components and SSU rRNA 3' (head) domain assembly: Enp1p was shown to exist in a salt stable complex with rpS3, a tertiary binder of the head domain, suggesting that Enp1p also binds to the same region as rpS3, namely the beak region of the head domain (Schäfer et al., 2006). Furthermore, Enp1p requires Noc4p for its incorporation into early pre-ribosomes (see 3.9). Emg1 was suggested to be involved in assembly of rpS19, which is a binder of the SSU rRNA 3' domain. This hypothesis was based on genetic screens, demonstrating that overexpression of rpS19 can partially suppress the Emg1p depletion phenotype (Buchhaupt et al., 2006). Furthermore, Nop14p is needed for nuclear localisation of Emg1p and mutations in Nop6p can suppress the malfunction of Emg1p (Liu et al., 2001; Buchhaupt et al., 2007). Probably the best established physical interaction between members of this group of SSU processome components is the one between Noc4p and Nop14p. It has been shown that both proteins exist in a heterodimeric complex and that Noc4p is probably recruited to pre-ribosomes via an interaction with Nop14p (Milkereit et al., 2003; Kühn et al., 2009). Taken together, the proteins Noc4p, Nop14p, Emg1p**,** Enp1p and Nop6p are showing a functional relationship to one another.
These proteins are candidates for a Noc4p subcomplex, existing as an entity outside of pre-ribosomes. Alternatively, these proteins could constitute several different subcomplexes. Similar subcomplexes consisting of two to eight proteins have been shown to exist in yeast cells after shutdown of rRNA synthesis (Merl and Jakob et al., 2010). The *in vivo* role of these subcomplexes is yet unknown. They might leave the ribosome as an entity and are then recycled for the next association round, or they might represent a functional subcomplex which is recruited as a whole to the pre-ribosome.

Co-immunoprecipitation of pre-rRNAs with Noc4p-TAP demonstrated that the relative amount of precipitated 35S pre-rRNA is reduced after depletion of rpS5 and rpS16, although the absolute amount was more or less constant (see 3.2). Two scenarios can be envisioned; either Noc4p is

associated only to a subpopulation of these early pre-ribosomes or the overall interaction is less stable. Both scenarios would lead to a reduced relative precipitation of early precursors by Noc4p-TAP. An explanation for this observation could be that the amount of Noc4p-TAP present in the cell might be limiting. Accordingly, Noc4p-TAP would not be able to precipitate higher amounts of the accumulating early precursor. However, this explanation is challenged by the observation that the accumulating 35S pre-rRNA after depletion of other r-proteins is indeed precipitated with the same efficiency. This showed that the amount of Noc4p-TAP is not limiting and that a free pool of this protein exists in the cell, which can associate to accumulating early rRNA precursors.

An important question is, whether ribosome assembly proceeds *in vivo* in a 5′ to 3′ direction of the SSU rRNA. For example, it is unclear whether the SSU rRNA 3′ domain can assemble without prior 5′ domain assembly. Interestingly, the inhibition of (primary) SSU rRNA 5′ domain assembly events (rpS11 and rpS9) had no effect on the assembly of Noc4p-TAP to pre-ribosomes (see 3.2). Consequently, SSU rRNA 3′ domain assembly events seem to proceed to some extent when 5′ domain assembly is inhibited. Otherwise the disruption of SSU rRNA 5′ domain assembly would also lead to assembly defects of Noc4p, as its efficient recruitment to pre-ribosomes requires primary 3′ domain assembly events.
On the one hand, it seems that certain assembly states of SSU rRNA domains can be established independent of a strict 5′ to 3′ directionality in this mutant situation. On the other hand, it needs to be determined, whether a mature SSU rRNA 3′ (head) domain assembly state can be established in the absence of 5′ domain assembly.

In summary, primary SSU rRNA 3′ domain assembly is required for efficient Noc4p association with early pre-ribosomes and a group of 10 other proteins. In contrast, secondary and tertiary binding events of the SSU rRNA 3′ domain are dispensable for recruitment of all identified ribosome biogenesis factors to pre-ribosomes. Additionally, members of the UTP-A, UTP-B, UTP-C and Mpp10p subcomplexes were not impaired in their association with early pre-ribosomes after depletion of r-proteins of the SSU rRNA 3′ domain.

4.4 SSU rRNA central domain assembly and recruitment of SSU processome components

The co-immunoprecipitation analyses of SSU processome components after depletion of certain r-proteins revealed that SSU rRNA central domain assembly (rpS13 and rpS14) is dispensable for association of the UTP-A, UTP-B and Mpp10p subcomplexes to early pre-ribosomes (see 3.3). In contrast, the presence of rpS13 and rpS14 is required for assembly of Utp22p (UTP-C) and Noc4p (non-defined) to early pre-ribosomes (see 3.2 and 3.3). The results of the direct rRNA co-IP have been confirmed by the semiquantitative analysis of the protein composition of pre-ribosomes. 17 proteins, including Utp22p and Noc4p, are impaired in their association to pre-ribosomes after

depletion of rpS13 (see 3.4.5). 11 of these proteins are the same as the ones impaired in their recruitment to pre-ribosomes after rpS5 depletion (see 3.4.5 and 4.3).

These analyses demonstrated that in addition to the requirement of proper primary SSU rRNA 3′ domain assembly (rpS5 and rpS16), Noc4p requires central domain assembly (rpS13 and rpS14) for efficient incorporation into pre-ribosomal particles. RpS14 is located at the platform (central domain) in close proximity to rpS5. Noc4p provides therefore a link between SSU rRNA 3′ domain and central domain assembly. The homolog of rpS14, S11, is categorised in regard to its assembly in a species-specific manner in eubacteria. It is classified as a primary binder in the thermophilic *Aquifex aeolicus* (Recht and Williamson, 2004), whereas in *E. coli*, its association requires the homolog of rpS13 (S15) and a heterodimer of *E. coli* S6 and S8 and is therefore designated as a tertiary binder (Held et al., 1974 and Figure 7). In contrast, rpS13 is located further away from rpS5 in proximity to rpS11 (Brodersen et al., 2002 and Figure 11). This might suggest that rpS13 does not directly interact with Noc4p, but is indirectly needed for assembly of Noc4p, because it is needed for assembly of rpS14. In turn, rpS14 is located in proximity to rpS5 and rpS16 - the two head binding r-proteins herein shown to be required for efficient Noc4 recruitment to pre-ribosomes.
In summary, the data indicate that SSU rRNA central domain assembly events (assembly of rpS13 and rpS14) are necessary to facilitate recruitment of Noc4p, which in turn is required for efficient head domain assembly, as discussed below (see 3.5 and 4.5). This Noc4p mediated dependency between SSU rRNA 3′ (head) domain and central (platform) domain assembly could serve as a checkpoint that head assembly events do not proceed until a crucial assembly state of the SSU platform is reached. Interestingly, it was suggested before, that *in vivo* coupling of rRNA transcription and r-protein assembly would define a 5′ to 3′ direction of ribosome assembly (Nierhaus, 1980) and that this directionality could be crucial to avoid non-productive folding / assembly states *in vivo*.

The six additional proteins, which are impaired in their association with pre-ribosomes after rpS13 depletion, not after rpS5 depletion, include Utp22p as well as another protein of the UTP-C submodule, namely Rrp7p (see 3.4.5). In contrast, another UTP-C (Cka2p) component is still associated with pre-ribosomes in the strain depleted of rpS13. This indicates that Cka2p is either indeed part of the UTP-C sub module, as suggested by earlier data (Krogan et al., 2004), but behaves differently compared to other UTP-C members in certain aspects, or it is not part of the UTP-C submodule. The assignment of the four subunits of casein kinase II (Cka1p, Cka2p, Ckb1p and Ckb2p) as a part of the SSU processome and in detail as an UTP-C component was deduced from data obtained by Krogan et al. (Krogan et al., 2004). In this approach, high molecular weight pre-ribosomal particles were removed by high speed centrifugation and subsequently co-immunoprecipitations of different proteins from the supernatant were performed. As a result small complexes which exist independently of their association with pre-ribosomes could be identified. However, the *in vivo* relevance and biological function of these small complexes remain elusive, as the dissociation of these entities from pre-ribosomes could be an artefact of the centrifugation

step. A closer look at the original MS data revealed that the claimed six UTP-C components (Utp22p, Rrp7p, Cka1p, Cka2p, Ckb1p and Ckb2p) have never been found together in a complex obtained by one single purification (Krogan et al., 2004). In fact, in purifications where these proteins were used as bait, just a subgroup of the others co-purified. Most controversially, as judged by SDS-PAGE analyses, the purification of Utp22p yielded stoichiometric amounts of co-purified Rrp7p, but only sub-stoichiometric amounts of the casein kinase II subunits. Furthermore, a direct implication of casein kinase II in ribosome assembly has never been reported so far. Of note, it has been suggested that Utp22p and Rrp7p might form a complex with Ifh1p (a factor needed for efficient RP gene transcription) and casein kinase II in certain physiological situations where Pol I dependent synthesis of pre-rRNA is reduced, therefore providing an interface between r-protein synthesis and ribosome biogenesis (Rudra et al., 2007).
Taken together, the data suggest that the four subunits of casein kinase II might not be directly involved in ribosome biogenesis providing a possible explanation for the different behaviour of Cka2p in comparison to the UTP-C members, Utp22p and Rrp7p. Alternatively, the interaction of Utp22p (and Rrp7p) with casein kinase II could be stabilised and mediated by the interaction within the pre-ribosome, whereas interaction outside the pre-ribosome could be unstable. However, this explanation would still argue against the UTP-C subcomplex existing as an entity consisting of Utp22p, Rrp7p, and casein kinase II.

The requirements for Utp22p assembly are different to the ones for Noc4p assembly, as the latter requires both SSU rRNA central domain (rpS13 and rpS14) and primary 3' domain (rpS5 and rpS16) assembly events for its association to pre-ribosomes. In contrast, Utp22p requires only SSU rRNA central domain (rpS13 and rpS14) assembly events for its association to early pre-ribosomes. Whether Utp22p facilitates efficient assembly of rpS13 and/or rpS14, as observed for rpS5 and rpS16 in case of Noc4p (see 3.5 and discussion below), needs to be determined.

4.5 Noc4p is required for efficient assembly of the SSU 3' (head) domain, but not for assembly of UTP-A, UTP-B, UTP-C and Mpp10 SSU processome modules to early pre-ribosomes

The temperature sensitive *noc4-8* mutant is a well-characterised mutant in regard to its phenotypes in rRNA processing, transport, and the consequent imbalanced accumulation of ribosomal subunits (Milkereit et al., 2003). Furthermore, additional studies revealed that Noc4p exists as a heterodimer with Nop14p and that this interaction is needed for the efficient recruitment of Noc4p to pre-ribosomes (Milkereit et al., 2003; Kühn et al., 2009). In order to reveal the specific function of Noc4p in ribosome biogenesis, the assembly of r-proteins of the SSU after inactivation of Noc4p, using the temperature sensitive *noc4-8* mutant, was analysed.

The analysis revealed that Noc4p is specifically required for efficient assembly of the 3' (head) domain of the SSU rRNA, which includes the proteins rpS3, rpS5, rpS15, rpS16, rpS19, rpS20, and rpS29 (see 3.5).

Together with the analyses discussed in section 4.3, the data indicate an interdependent relationship of pre-ribosome association between rpS5, rpS16, and Noc4p (see 3.2 and 3.5). All other r-proteins of the SSU rRNA 3' domain are dispensable for Noc4p recruitment to pre-ribosomes. A reasonable explanation for the observed assembly defects of rpS3, rpS15, rpS19, rpS20 and rpS29 after Noc4p inactivation comes from the *in vitro* and *in vivo* hierarchy of SSU head domain assembly events (Held et al., 1974; Ferreira-Cerca et al., 2007). If assembly of the primary binder of the head domain rpS5 (and/or rpS16) is affected, consequences on binding of the secondary and tertiary binders can be expected. Thus, the effect on the latter would rather be an indirect effect mediated by the perturbed assembly of rpS5 and rpS16. However, it cannot be ruled out that Noc4p has a direct influence on the assembly of secondary and tertiary SSU head binding proteins.

Further analysis of the temperature sensitive *noc4-8* mutant demonstrated that the Noc4p variant encoded by *noc4-8* is still associated with 35S pre-rRNA at the restrictive temperature, although the absolute amount of Noc4p and concomitantly the absolute amount of precipitated 35S pre-rRNA is reduced. Moreover, the Noc4p variant encoded by *noc4-8* still co-purified r-proteins of the body domain, but not the head domain. Thus, it seems that the inactivated *noc4-8* protein is still capable of associating with early SSU precursors containing r-proteins of the body domain, whereas it is unable to facilitate assembly of the SSU head domain.

In the publication of Pérez-Fernández et al., a hierarchical order of assembly for some of the SSU processome components, including components of the UTP-A, UTP-B, UTP-C, and Mpp10p subcomplexes and Rrp5, was established (Pérez-Fernández et al., 2007 and see 2.5).
To test whether other SSU processome components play a role in the Noc4p mediated SSU head assembly events, the requirement of Noc4p for the recruitment of these components was tested.
The results demonstrated that Noc4p is not necessary for the assembly of Utp4p (UTP-A), Pwp2p (UTP-B), Utp22p (UTP-C) and Imp3p (Mpp10p complex) to pre-ribosomes (see 3.9). In contrast, Noc4p is required for efficient recruitment of Enp1p, a putative binder of the beak structure of the SSU head domain (Schäfer et al., 2006), to pre-ribosomes. The results described above (see 3.4.4 and 4.3) have already shown that Enp1p, together with Noc4p, is a member of a specific group of SSU processome components whose association with pre-ribosomes is destabilised in the absence of primary head binder rpS5. Additionally, the inactivation of Noc4p leads to inefficient assembly of rpS5. Altogether, these results indicate that pre-ribosomes with an incomplete head assembly state seen in mutants of *NOC4* are not due to a reduced incorporation of SSU processome UTP-A, UTP-B, UTP-C or Mpp10p submodules.

4.6 Ribosome biogenesis factors function in r-protein assembly – A common theme?

Around 150 accessory factors have been implicated in the process of ribosome biogenesis. Almost all factors are only defined by the rRNA processing phenotype exhibited after depletion of the respective protein, but the exact function is unknown. The analyses of this PhD thesis provide evidence that SSU processome components as Noc4p facilitate r-protein assembly of specific SSU subdomains. Such a function of ribosome biogenesis factors in r-protein assembly has been suggested for several factors, and evidence for such a function has been shown recently for Rpf2p and Rrs1p in assembly of a particle consisting of 5S rRNA, rpL5, and rpL11 with pre-60S subunits (Zhang et al., 2007). Another example is the kinase Hrr25p which is involved in stable assembly of rpS3 to the SSU head domain (Schäfer et al., 2006). This incorporation correlated with major changes in pre-ribosome structure. Some indirect genetic evidence supports the idea that a few other factors act as assembly factors *in vivo* in eukaryotes. The main argument is that overexpression of several r-proteins led to (partial) suppression of the depletion phenotype of some biogenesis factors (Baudin-Baillieu et al., 1997; Tabb et al., 2001; Loar et al., 2004; Buchhaupt et al., 2006). Thus, it can be speculated that specific ribosome biogenesis factors are involved in distinct steps of r-protein assembly. How this assembly is facilitated, remains unclear, but three major scenarios can be imagined:

First, certain assembly steps could require *in vivo* major conformational changes or release of erroneous pre-rRNA secondary structures, which could be promoted in an energy consuming way by NTPase activities. Interestingly, around 20% of all ribosome biogenesis factors are NTP hydrolysing enzymes, including GTPases, ATPases, Kinases or RNA helicases (Karbstein, 2007; Strunk et al., 2009). Additionally, some NTPases have been identified during the presented analyses as part of early pre-ribosomes, including eight helicases (Ecm16p/Dhr1p, Rok1p, Dbp2p, Dbp3p, Drs1p, Spb4p, Has1p and Prp43p), three GTPases (Bms1p, Nog1p and Nug1p) and four putative ATPases (Utp14p, Kre33p, Rix1p and Arb1p).

A good example for a GTPase involved in ribosome assembly is the prokaryotic GTPase Era (Inoue et al., 2003, 2006; Sharma et al., 2005).The binding of Era in the cleft between head and platform keeps the SSU in an extended conformation, inhibiting the formation of a translation competent SSU. After completion of proper SSU assembly, it has been suggested that replacement of Era by the r-protein S1 transitions the premature SSU to a mature SSU (Sharma et al., 2005).

Second, certain factors could recruit r-proteins through direct physical interactions, as indicated for Rpf2p and Rrs1p during 5S RNP assembly (Morita et al., 2002; Zhang et al., 2007). A similar function could be envisaged for Noc4p, rpS5 and rpS16 because all three proteins show an interdependent assembly to early pre-ribosomes. However, further work needs to be done to support this hypothesis.

Third, factors could associate with pre-ribosomal RNA elements prior to stable assembly of r-proteins (at sites later occupied by r-proteins), minimising establishment of non-productive RNA-RNA or RNA-protein interactions in the *in vivo* context and thereby fulfilling a "chaperone like" function.

The binding characteristic of UTP-A, UTP-B and Mpp10p subcomplexes is in agreement with the proposed function as a kind of "RNA chaperone" in early assembly / folding events. All three subcomplexes were able to associate independent of r-protein assembly to early pre-ribosomes. Furthermore, these factors are recruited co-transcriptionally to nascent pre-rRNAs (Dragon et al., 2002; Osheim et al., 2004; Wery et al., 2009). Hence, the involvement of theses proteins in early aspects of ribosome maturation could generate certain structural features of the rRNA providing binding sites for subsequent r-protein association. None of the factors of the UTP-A, UTP-B or Mpp10p subcomplex show homology to known NTPase motifs. However, these proteins might fulfil their "chaperone like" function without an ATP cycle, as shown for some protein chaperones (Bukau, 1999). In this regard, one well-studied example is Hsp47, which is an ATP independent chaperone acting in the maturation process of collagen (Hendershot and Bulleid, 2000).

SSU processome components and r-proteins show a difference in their binding characteristics to rRNA precursors. Whereas SSU processome components interact strong with early and weak with late precursors, it is the other way around for r-proteins. This inverse relationship between binding characteristics of r-proteins and SSU processome components, during the course of rRNA processing / ribosome maturation, points towards an optimised function of these factors in different aspects of ribosome assembly. Accordingly, early co-transcriptional and stable binding of SSU processome components could inhibit contacts in the rRNA which might lead to erroneous rRNA folding or kinetic traps in the folding process. Subsequent folding of the rRNA into certain conformations could facilitate transient r-protein binding. These folding events go along with a compaction of the SSU processome, which can be seen when looking at the change of the terminal ball morphology in miller chromatin spreading experiments (Osheim et al., 2004 and Figure 3). Eventually, the stabilisation and compaction of rRNA structures will result in a stable binding of r-proteins with late rRNA precursors and mature rRNAs, while SSU processome components show only very weak or no interactions with these rRNA species.
Hence, the SSU processome components and r-proteins might have two distinct RNA "chaperone like" functions. The SSU processome might have evolved to support early folding events and thus show strong binding to early rRNA precursors, while r-proteins support later folding events which closely resemble the mature tertiary structure of the rRNA. Ultimately, the r-proteins stabilise the mature ribosome structure. The division into early and late "RNA chaperones" might have evolved to achieve efficient ribosome maturation. The specialised function results in a less error-prone folding, because SSU processome factors are optimised for these steps. Concomitantly, this separation leads to a more stable ribosome structure, because r-proteins are optimised to stabilise

the mature ribosome structure. The observation that r-proteins exhibit an RNA chaperone function *in vitro* supports the idea that they might exhibit a similar function *in vivo* (Semrad et al., 2004).

In vitro assembly of the prokaryotic SSU does not require assembly factors, but a temperature dependent step, which leads to a major structural change and thereby facilitates stable interaction of all r-proteins (Traub et al., 1968, 1969). However, *in vitro* assembly is achieved with less efficiency and is significantly slower than *in vivo* assembly of the SSU. Additionally, *in vivo* assembly must get along without the temperature step. Thus, ribosome biogenesis factors might assist in assembly events *in vivo* to ensure a fast rate of ribosome synthesis.
It has been demonstrated that r-protein association with rRNA *in vitro* shows a biphasic nature. The first contacts occur very fast, but are not very stable. In a slower second phase the interaction of r-proteins with rRNA is stabilised by an induced fit mechanism (Adilakshmi et al., 2008). The presented data indicate that SSU processome components might play a crucial role for the establishment of stable interactions between r-proteins and rRNA *in vivo* in eukaryotes. After inactivation of Noc4p, the r-proteins of the head domain were still able to interact to a certain extent with pre-ribosomes (see 3.5). However, a stable Interaction, perhaps by an induced fit mechanism, between r-proteins and rRNA requires the presence of functional Noc4p.

One well studied example of an "RNA chaperone" is not a protein but a snoRNA, which is also part of the SSU processome. The U3 snoRNA base pairs with the 5′ terminal helix and a connecting region between the central and major 3′ domains, thereby preventing the premature formation of the universally conserved central pseudoknot structure forming between these two parts of the rRNA (Hughes, 1996). Thus, the U3 snoRNA might inhibit erroneous rRNA folding and assist in the folding process to form the central pseudoknot structure. Interestingly, a similar mechanism has been proposed for prokaryotes, which might supply the same function exhibited by the U3 snoRNA through a cis element present in the 5′ ETS of rRNA precursors (Dennis et al., 1997). The herein presented data is in accordance with a function of the U3 snoRNA in early RNA folding. The results demonstrate that the Mpp10p complex, which is part of the U3 snoRNP, can assemble independent of r-protein assembly. Thus, this complex might assist the "RNA chaperone" activity of the U3 snoRNA.

The relationship between SSU rRNA central domain (rpS13 and rpS14) and 3′ domain assembly might suggest a coordinated sequential order of assembly events. Accordingly, the presence of rpS13 and rpS14 is required for association of Noc4p with early pre-ribosomes. Noc4p association would in turn facilitate establishment of the SSU rRNA 3′ (head) domain, which is most likely initiated by a cooperative binding of Noc4p, rpS5 and rpS16 to this region. This fact is underscored by the observation that these factors show an interdependent assembly relationship (see 3.2 and 3.5). The cooperative binding of these three proteins indicate that Noc4p binds in vicinity to rpS5 and rpS16 and probably rpS14 which is closely located to rpS5, therefore providing a physical link between SSU rRNA central and 3′ domain assembly.

Furthermore, the dependency of Rrp7p and Utp22p association on SSU rRNA central domain assembly events suggests that these proteins might be located in vicinity to rpS13 and rpS14. Further experiments could reveal the exact binding site of these proteins on the rRNA. The proteins could be cross-linked to the bound rRNA region and the position of the cross-link subsequently identified by CRAC (cross-linking and analysis of cDNAs) or by a combination of primer extension and mass spectrometry analyses (Urlaub et al., 2000; Granneman et al., 2009). In addition, a rough localization on the three dimensional structure of pre-ribosomes could be obtained by immuno electron microscopy (Nissan et al., 2004; Ulbrich et al., 2009).

5 MATERIALS AND METHODS

5.1 Materials

5.1.1 Chemicals

Chemicals were purchased at the highest available purity from Sigma-Aldrich, Merck, Fluka, Roth or J.T.Baker, except 5-FOA (Toronto Research Chemicals), agarose, electrophoresis grade (Invitrogen), bromine phenol blue (Serva), G418/Geneticin (Gibco), milk powder (Sukofin), Nonidet P-40 substitute (NP40) (USB Corporation), Tris ultrapure (USB Corporation) and Tween 20 (Serva).
Ingredients for growth media were purchased from BD Biosciences (Bacto Agar, Bacto Peptone, Bacto Tryptone and Bacto Yeast Extract), Q-Biogene, Bio101, Inc. or Sunrise Science Products (Complete supplement mixtures (CSM), Yeast nitrogen base (YNB), amino acids and adenine) and Sigma-Aldrich (D(+)-glucose, D(+)-galactose, amino acids and uracil). Water was always purified with an Elga Purelab Ultra device prior to use.

5.1.2 Buffers and media

If not indicated otherwise, the solvent is H_2O. The pH values were measured at room temperature. Percentage is mass per volume (m/v), if not indicated otherwise. The pH was adjusted with HCl or NaOH if not indicated otherwise.

Buffer	Ingredients	Concentration
LB medium	Tryptone Yeast extract NaCl 1M NaOH Agar (plates) Autoclave	10g/l 5g/l 5g/l 1ml/l 20g/l
LB/Amp	Ampicillin in LB medium, add when temperature of medium ≤ 50°C	50µg/ml
YPD	Yeast extract Peptone Glucose Agar (plates) Autoclave	10g/l 20g/l 20g/l 20g/l
YPG	Yeast extract Peptone Galactose Agar (plates) Autoclave	10g/l 20g/l 20g/l 20g/l
YPD/YPG with Geneticin	Geneticin (Gibco) in YPD	400mg/l

Synthetic medium (SDC/SGC)	YNB	6.7g/l
	CSM	see product sheet
	Glucose/Galactose	20g/l
	Agar (plates)	20g/l
	Autoclave	
Sporulation plates	Yeast extract	2.5g/l
	KaOAc	15g/l
	Glucose/Galactose	0.5g/l
	CSM complete	see product sheet
	Agar	20g/l
	Autoclave	
SOB	Bacto-Trypton	2%
	Bacto-Yeast extract	0.5%
	NaCl	8.55mM
	KCl,	2.5mM
	$MgCl_2$	10mM
	pH 7	
5x TBE-buffer	Tris	445mM
	Boric acid	445mM
	EDTA	10mM
10x DNA loading buffer	Bromophenol blue	0,25%
	Xylen cyanol	0,25%
	Glycerine	40%
10xMOPS buffer	Sodium acetate trihydrate	20mM
	MOPS (Fluka)	0.2M
	EDTA pH 8	10mM
	pH7 with NaOH	
RNA hybridisation buffer	Formamide deionised	50%
	SSC	5x
	SDS	0.5%
	H_2O	10%
	Denhards	5x
50xDenhards	Ficoll (Typ 400)	10mg/ml
	Polyvinylpyrrolidone	10mg/ml
	BSA (Fraction V)	10mg/ml
	store at -20°C	
RNA solubilisation buffer	Formamide	50%
	Fromaldehyde	8%
	MOPS buffer	1x
	H_2O	18%
Buffer R_D	Glucose	2%
	Peptone	1%
	Malt extract	0.6%
	Yeast extract	0.01%
	Mannitol	12%
	Magnesium acetate	17.8mM

Buffer R_G	Galactose	2%
	Peptone	1%
	Malt extract	0.6%
	Yeast extract	0.01%
	Mannitol	12%
	Magnesium acetate	17.8mM
20x SSC	NaCl	3M
	Tri-sodium citrate dehydrate	0,3M
	pH 7 with HCl	
Protease inhibitors 100x	Benzamidine	33mg/ml
	PMSF	17mg/ml
10x electrophoresis buffer	Tris	250mM
	Glycine	1,92M
	SDS	1,0%
Transfer buffer (Western Blot)	Tris	25mM
	Glycine	192mM
	Methanol	20%
4x Upper Tris	Tris	0,5M
	SDS	0,4%
	Bromophenol blue	
	pH 6,8 with HCl	
4x Lower Tris	Tris	1,5M
	SDS	0,4%
	pH 8,8 with HCl	
HU buffer	SDS	5%
	Tris-HCl pH 6.8	200mM
	EDTA	1mM
	β-mercapto-ethanol	1.5%
	Urea	8M
	Bromophenolblue; store at -20°C	
TELit	LiOAc	100mM
	Tris-HCl pH 8	10mM
	EDTA pH 8	1mM
	pH 8 with HOAc	
LitSorb	Sorbitol	1M
	dissolved in TELit	
	sterile filtration, store at 4°C	
LitPEG	Polyethylene glycol (PEG3350 (Sigma))	40%
	dissolved in TELit	
	sterile filtration, store at 4°C	
Buffer A200	Tris–HCl pH 8	20mM
	KCl	200mM
	MgAc	5mM
	Triton X-100	0.2%
	DTT	1mM
	Protease inhibitors	1x

Buffer MB	Tris–HCl pH 8	20mM
	KCl	200mM
	MgAc	5mM
	Protease inhibitors	1x
AE buffer	NaOAc pH 5.3	50mM
	EDTA pH 8	10mM
	Xylene cyanol FF (Sigma)	0.025%
	Bromophenol blue (Serva)	0.025%
5x MaBS	Maleic acid	0.5M
	NaCl	0.75M
	pH 7.5	
5x DIG reaction buffer	Tris-HCl pH 9.5	0.5M
	NaCl	0.5M
	$MgCl_2$	25mM

5.1.3 *Saccharomyces cerevisiae* strains

No	Name	Genotype	Origin
30	NOC4-Shuffle	*his3-1 leu2-0 lys2-0 MET15 ura3-0 YPR144c::kanMX4 YCplac33-144c (URA3)*	Draken, Esther
34	noc4-1	*his3-1 leu2-0 lys2-0/LYS2? MET15/met15-0? ura3-0 YPR144c::kanMX4 pNOPPA1-noc4-1 (LEU2)*	Draken, Esther
35	noc4-2	*his3-1 leu2-0 lys2-0/LYS2? MET15/met15-0? ura3-0 YPR144c::kanMX4 pNOPPA1-noc4-2 (LEU2)*	Draken, Esther
36	noc4-3	*his3-1 leu2-0 lys2-0/LYS2? MET15/met15-0? ura3-0 YPR144c::kanMX4 pNOPPA1-noc4-3 (LEU2)*	Draken, Esther
37	noc4-4	*his3-1 leu2-0 lys2-0/LYS2? MET15/met15-0? ura3-0 YPR144c::kanMX4 pNOPPA1-noc4-4 (LEU2)*	Draken, Esther
38	noc4-5	*his3-1 leu2-0 lys2-0/LYS2? MET15/met15-0? ura3-0 YPR144c::kanMX4 pNOPPA1-noc4-5 (LEU2)*	Draken, Esther
39	noc4-7	*his3-1 leu2-0 lys2-0/LYS2? MET15/met15-0? ura3-0 YPR144c::kanMX4 pNOPPA1-noc4-7 (LEU2)*	Draken, Esther
40	noc4-8	*his3-1 leu2-0 lys2-0/LYS2? MET15/met15-0? ura3-0 YPR144c::kanMX4 pNOPPA1-noc4-8 (LEU2)*	Draken, Esther
41	noc4-9	*his3-1 leu2-0 lys2-0/LYS2? MET15/met15-0? ura3-0 YPR144c::kanMX4 pNOPPA1-noc4-9 (LEU2)*	Draken, Esther
42	noc4-10	*his3-1 leu2-0 lys2-0/LYS2? MET15/met15-0? ura3-0 YPR144c::kanMX4 pNOPPA1-noc4-10 (LEU2)*	Draken, Esther
89	pGAL-RPS15	*his3-1 leu2-0 ura3-0 lys2-0? met15-0? YOL040c::kanMX4 pFL36-pGalRPS15 (LEU2)*	Milkereit, Philipp
90	pGAL-RPS15 NOC4-TAP	*his3-1 leu2-0 ura3-0 lys2-0? met15-0? YOL040c::kanMX4 NOC4::NOC4-TAP-URA3 pFL36-pGalRPS15 (LEU2)*	Milkereit, Philipp
96	BY4742 NOC4-TAP	*his3-1 leu2-0 ura3-0 lys2-0 NOC4::NOC4-TAP-URA3*	Milkereit, Philipp
175	nop14-2	*ura3-52 leu2-1 ydl148c::kanMX pNOPPA1-noc5-2 (LEU2)*	Kühn, Holger
206	BY4741	*his3-1 leu2-0 met15-0 ura3-0*	Euroscarf

207	BY4742	*his3-1 leu2-0 lys2-0 ura3-0*	Euroscarf
259	pGAL-RPS9	*his3-1 leu2-0 lys2-0 met15-0 ura3-0 YBR189w::kanMX4 YPL081w::HIS3 YCplac111-pGAL-RPS9A (LEU2)*	Ferreira-Cerca, Sébastien
318	pGAL-RPS16A	*his3-1 leu2-0 met15-0 LYS ura3-0 YDL083c::kanMX4 YMR143w::HIS3 YCplac111-pGAL-RPS16A (LEU2)*	Ferreira-Cerca, Sébastien
323	pGAL-RPS5	*his3-1 leu2-0 ura3-0 lys2-0 YJR123w::kanMX4 YCplac111-pGAL-RPS5 (LEU2)*	Ferreira-Cerca, Sébastien
325	pGAL-RPS11A	*his3-1 leu2-0 lys2-0 met15-0 ura3-0 YBR048w::kanMX4 YDR025w::HIS3 YCplac111-pGAL-RPS11A (LEU2)*	Ferreira-Cerca, Sébastien
327	pGAL-RPS3	*his3-1 leu2-0 ura3-0 met15-0? lys2-0? YNL178w::kanMX4 YCplac111-pGAL-RPS3*	Ferreira-Cerca, Sébastien
399	pGAL-RPS14	*his3-1 leu2-0 met15-0 lys2-0 ura3-0 YCR031c::HIS3Mx6 YJL191w::kanMX4 Ycplac111-pGAL-RPS14 (LEU2)*	Pöll, Gisela
403	YCC95 NOC4-TAP	*ade5 his7-2 leu2-112 trp1-289 ura3-52 rrn3-8 NOC4::NOC4-TAP-TRP1*	Ridinger, Katrin
405	pGAL-FLAG-NOC4	*his3-1 leu2-0 lys2-0 MET15 ura3-0 YPR144c::kanMX4 YCplac111-pGAL-FLAG-NOC4 (LEU2)*	Milkereit, Philipp
543	CG379	*ade5-1 his7-2 leu2-3,-112 trp1-289 ura3-52*	(Cadwell et al., 1997)
567	pGAL-RPS19	*his3-1 leu2-0 ura3-0 yol121c::kanMX4 ynl302c::kanMX4? YCplac111-pGAL-RPS19 (LEU2)*	Neueder, Andreas
579	CG 379 NOC4-TAP	*ade5 his7-2 leu2-112 trp1-289 ura3-52 NOC4::NOC4-TAP-TRP1*	Merl, Juliane
698	pGAL-RPS3-SE	*his3-1 leu2-0 ura3-0 met15-0 lys2-0 YNL178w::kanMX4 YCplac111-pGAL-RPS3-SE (LEU2)*	Pöll, Gisela
701	pGAL-RPS13-SE	*his3-1 leu2-0 ura3-0 MET15 LYS2 YDR064w::kanMX4 YCplac111-pGAL-RPS13-SE (LEU2)*	Pöll, Gisela
795	dRPS22A	*his3-1/his3-1 leu2-0/leu2-0 lys2-0/LYS2 MET15/met15-0 ura3-0/ura3-0 YJL190c::kanMX4/YJL190c*	This study
796	dRPS22A - dRPS22A	*his3-1/his3-1 leu2-0/leu2-0 lys2-0/LYS2 MET15/met15-0 ura3-0/ura3-0 YJL190c::kanMX4 YJL190c::kanMX4*	This study
797	dRPS29B	*his3-1/his3-1 leu2-0/leu2-0 lys2-0/LYS2 MET15/met15-0 ura3-0/ura3-0 YDL061c::kanMX4/YDL061c*	This study
798	RPS4-Shuffle	*his3-1 leu2-0 lys2-0? met15-0? ura3-0 YJR145C::kanMX4 YHR203C::kanMX4 YCplac33-RPS4A (URA3)*	This study
799	RPS21-Shuffle	*his3-1 leu2-0 lys2-0? met15-0? ura3-0 YKR057W::kanMX4 YJL136C::kanMX4 YCplac33-RPS21A (URA3)*	This study
800	pGAL-RPS4A	*his3-1 leu2-0 lys2-0? met15-0? ura3-0 YJR145C::kanMX4 YHR203C::kanMX4 YCplac111pGAL-RPS4A (LEU2)*	This study
801	pGAL-RPS21A	*his3-1 leu2-0 lys2-0? met15-0? ura3-0 YKR057W::kanMX4 YJL136C::kanMX4 YCplac111pGAL-RPS21A (LEU2)*	This study
802	pGAL-FLAG-RPS4	*his3-1 leu2-0 lys2-0? met15-0? ura3-0 YJR145C::kanMX4 YHR203C::kanMX4 YCplac111pGAL-Flag-RPS4A (LEU2)*	This study
803	pGAL-FLAG-RPS21	*his3-1 leu2-0 lys2-0? met15-0? ura3-0 YKR057W::kanMX4 YJL136C::kanMX4 YCplac111pGAL-Flag-RPS21A (LEU2)*	This study
842	dRPS4A	*his3-1 leu2-0 met15-0 ura3-0 YJR145C::kanMX4*	This study

843	dRPS4B	*his3-1 leu2-0 lys2-0 ura3-0 YHR203C::kanMX4*	This study
979	HRR25-wt	*HRR25-HIS3::hrr25::KanMX4 ho::LYS2 ura3 leu2::hisG trp1::hisG his3::hisG*	This study
980	hrr25-as	*hrr25-as1-HIS3::hrr25::KanMX4 ho::LYS2 ura3 leu2::hisG trp1::hisG his3::hisG*	This study
1198	pGAL-RPS20	*his3-1 leu2-0 ura3-0 met15-0 LYS2 YHL015w::kanMX4 YCplac111-pGAL-RPS20_new (LEU2)*	Neueder, Andreas
1231	dRPS29A (HIS3MX6)	*leu2-0 lys2-0 ura3-0 YLR388w::HIS3MX6 BY4742*	This study
1232	dRPS22B (HIS3MX6)	*his3-1 leu2-0 lys2-0 ura3-0 YLR367w::HIS3MX6 BY4742*	This study
1234	dRPS22A	*his3-1 leu2-0 met15-0 ura3-0 YJL190c::kanMX4 BY4741*	This study
1236	pGAL-RPS29B	*his3-1 leu2-0 ura3-0 MET? LYS? YDL061c::kanMX4 YLR388w::HIS3MX6 YCplac111-pGAL- RPS29B (LEU2)*	This study
1238	dRPS22B	*his3-1 leu2-0 met15-0 ura3-0 YLR367w::kanMX4 BY4741*	This study
1239	dRPS22B (HIS3MX6)	*his3-1 leu2-0 met15-0 ura3-0 YLR367w::HIS3MX6 BY4741*	This study
1240	pGAL-RPS16A Noc4-TAP	*his3-1 leu2-0 met15-0 LYS ura3-0 YDL083c::kanMX4 YMR143w::HIS3 NOC4::NOC4-TAP-URA3 YCplac111-pGAL-RPS16A (LEU2)*	This study
1241	pGAL-RPS5 Noc4-TAP	*his3-1 leu2-0 ura3-0 lys2-0 YJR123w::kanMX4 NOC4::NOC4-TAP-URA3 YCplac111-pGAL-RPS5 (LEU2)*	This study
1242	pGAL-RPS19 Noc4-TAP	*his3-1 leu2-0 ura3-0 yol121c::kanMX4 ynl302c::kanMX4? NOC4::NOC4::NOC4-TAP-URA3 YCplac111-pGAL-RPS19 (LEU2)*	This study
1243	rio2-1	*trp1 leu2 his3 ura3 rio2::kanMX4 pRS315-rio2-1 (leu)*	(Schäfer et al., 2003)
1244	BMS1 wt	*leu2 ura3-52 trp1 ade2 ade3 his3d200*	(Gelperin et al., 2001)
1245	bms1-1	*leu2 ura3-52 trp1 ade2 ade3 lys2 bms1-1*	(Gelperin et al., 2001)
1246	KRR1 wt (W303)	*krr1::HIS3 ade2-1 ura3-1 trp1-1 leu2-3, 112 his3-11, 15 can1-100 ssd1-d2 pTS1010 (Ycp-KRR1-TRP1)*	(Sasaki et al., 2000)
1247	krr1-17	*krr1::HIS3 ade2-1 ura3-1 trp1-1 leu2-3, 112his3-11, 15 can1-100 ssd1-d2 pTS1010-17 (Ycp-krr1-17)*	(Sasaki et al., 2000)
1248	krr1-18	*krr1::HIS3 ade2-1 ura3-1 trp1-1 leu2-3, 112his3-11, 15 can1-100 ssd1-d2 pTS1010-18 (Ycp-krr1-18)*	(Sasaki et al., 2000)
1249	enp1-1 (W303)	*Δenp1::his5+ ade2-1 ura3-1 TRP1::enp1-1 leu2-3, 112 his3-11, 15 can1-100*	(Chen et al., 2003)
1423	RPS29B-Shuffle	*his3-1 leu2-0 ura3-0 MET? LYS? YDL061c::kanMX4 YLR388w::HIS3MX6 YCplac33-RPS29B (URA3)*	This study
1425	RPS22A-Shuffle	*his3-1 leu2-0 ura3-0 MET? LYS? YJL190c::kanMX4 YLR367w::HIS3MX6 YCplac33-RPS22A (URA3)*	This study
1427	pGal-RPS22A	*his3-1 leu2-0 ura3-0 MET? LYS? YJL190c::kanMX4 YLR367w::HIS3MX6 YCplac111-pGAL-RPS22A (LEU2)*	This study
1429	dRPS22A	*his3-1 leu2-0 ura3-0 MET? LYS? YJL190c::kanMX4*	This study
1524	pGAL-RPS5 UTP4-TAP	*his3-1 leu2-0 ura3-0 lys2-0 YJR123w::kanMX4 UTP4::UTP4-TAP-URA3 YCplac111-pGAL-RPS5 (LEU2)*	This study

1525	pGAL-RPS5 PWP2-TAP	*his3-1 leu2-0 ura3-0 lys2-0 YJR123w::kanMX4 PWP2::PWP2-TAP-URA3 YCplac111-pGAL-RPS5 (LEU2)*	This study
1527	pGAL-RPS5 MPP10-TAP	*his3-1 leu2-0 ura3-0 lys2-0 YJR123w::kanMX4 MPP10::MPP10-TAP-URA3 YCplac111-pGAL-RPS5 (LEU2)*	This study
1528	pGAL-RPS15 UTP4-TAP	*his3-1 leu2-0 ura3-0 lys2-0? met15-0? YOL040c::kanMX4 UTP4::UTP4-TAP-URA3 pFL36-pGalRPS15 (LEU2)*	This study
1529	pGAL-RPS15 PWP2-TAP	*his3-1 leu2-0 ura3-0 lys2-0? met15-0? YOL040c::kanMX4 PWP2::PWP2-TAP-URA3 pFL36-pGalRPS15 (LEU2)*	This study
1531	pGAL-RPS15 MPP10-TAP	*his3-1 leu2-0 ura3-0 lys2-0? met15-0? YOL040c::kanMX4 MPP10::MPP10-TAP-URA3 pFL36-pGalRPS15 (LEU2)*	This study
1532	pGAL-RPS16A UTP4-TAP	*his3-1 leu2-0 met15-0 LYS ura3-0 YDL083c::kanMX4 YMR143w::HIS3 UTP4::UTP4-TAP-URA3 YCplac111-pGAL-RPS16A (LEU2)*	This study
1533	pGAL-RPS16A PWP2-TAP	*his3-1 leu2-0 met15-0 LYS ura3-0 YDL083c::kanMX4 YMR143w::HIS3 PWP2::PWP2-TAP-URA3 YCplac111-pGAL-RPS16A (LEU2)*	This study
1536	pGAL-RPS19 UTP4-TAP	*his3-1 leu2-0 ura3-0 yol121c::kanMX4 ynl302c::kanMX4 UTP4::UTP4-TAP-URA3 YCplac111-pGAL-RPS19 (LEU2)*	This study
1537	pGAL-RPS19 PWP2-TAP	*his3-1 leu2-0 ura3-0 yol121c::kanMX4 ynl302c::kanMX4 PWP2::PWP2-TAP-URA3 YCplac111-pGAL-RPS19 (LEU2)*	This study
1538	pGAL-RPS19 RRP7-TAP	*his3-1 leu2-0 ura3-0 yol121c::kanMX4 ynl302c::kanMX4 RRP7-TAP-URA3 YCplac111-pGAL-RPS19 (LEU2)*	This study
1540	CG379 UTP4-TAP	*ade5-1 his7-2 leu2-3,-112 trp1-289 ura3-52 UTP4::UTP4-TAP-URA3*	This study
1541	CG379 PWP2-TAP	*ade5-1 his7-2 leu2-3,-112 trp1-289 ura3-52 PWP2::PWP2-TAP-URA3*	This study
1542	CG379 RRP7-TAP	*ade5-1 his7-2 leu2-3,-112 trp1-289 ura3-52 RRP7::RRP7-TAP-URA3*	This study
1544	YCC95 UTP4-TAP	*ade5 his7-2 leu2-112 trp1-289 ura3-52 rrn3-8 UTP4::UTP4-TAP-URA3*	This study
1545	YCC95 PWP2-TAP	*ade5 his7-2 leu2-112 trp1-289 ura3-52 rrn3-8 PWP2::PWP2-TAP-URA3*	This study
1660	pGAL-RPS3 NOC4-TAP	*his3-1 leu2-0 ura3-0 met15-0? lys2-0? YNL178w::kanMX4 NOC4::NOC4-TAP-URA3 YCplac111-pGAL-RPS3*	This study
1661	pGAL-RPS20 NOC4-TAP	*his3-1 leu2-0 ura3-0 met15-0 LYS2 YHL015w::kanMX4 NOC4::NOC4-TAP-URA3 YCplac111-pGAL-RPS20_new (LEU2)*	This study
1883	pGAL-RPS9 UTP4-TAP	*his3-1 leu2-0 lys2-0 met15-0 ura3-0 YBR189w::kanMX4 YPL081w::HIS3 UTP4::UTP4-TAP-URA3 YCplac111-pGAL-RPS9A (LEU2)*	This study
1884	pGAL-RPS9 PWP2-TAP	*his3-1 leu2-0 lys2-0 met15-0 ura3-0 YBR189w::kanMX4 YPL081w::HIS3 PWP2::PWP2-TAP-URA3 YCplac111-pGAL-RPS9A (LEU2)*	This study
1885	pGAL-RPS9 UTP22-TAP	*his3-1 leu2-0 lys2-0 met15-0 ura3-0 YBR189w::kanMX4 YPL081w::HIS3 UTP22::UTP22-TAP-URA3 YCplac111-pGAL-RPS9A (LEU2)*	This study
1886	pGAL-RPS9 IMP3-TAP	*his3-1 leu2-0 lys2-0 met15-0 ura3-0 YBR189w::kanMX4 YPL081w::HIS3 IMP3::IMP3-TAP-URA3 YCplac111-pGAL-RPS9A (LEU2)*	This study
1887	pGAL-RPS9 NOC4-TAP	*his3-1 leu2-0 lys2-0 met15-0 ura3-0 YBR189w::kanMX4 YPL081w::HIS3 NOC4::NOC4-TAP-URA3 YCplac111-pGAL-RPS9A (LEU2)*	This study

1888	pGAL-RPS11A UTP4-TAP	*his3-1 leu2-0 lys2-0 met15-0 ura3-0 YBR048w::kanMX4 YDR025w::HIS3 UTP4::UTP4-TAP-URA3 YCplac111-pGAL-RPS11A (LEU2)*	This study
1889	pGAL-RPS11A PWP2-TAP	*his3-1 leu2-0 lys2-0 met15-0 ura3-0 YBR048w::kanMX4 YDR025w::HIS3 PWP2::PWP2-TAP-URA3 YCplac111-pGAL-RPS11A (LEU2)*	This study
1890	pGAL-RPS11A UTP22-TAP	*his3-1 leu2-0 lys2-0 met15-0 ura3-0 YBR048w::kanMX4 YDR025w::HIS3 UTP22::UTP22-TAP-URA3 YCplac111-pGAL-RPS11A (LEU2)*	This study
1891	pGAL-RPS11A IMP3-TAP	*his3-1 leu2-0 lys2-0 met15-0 ura3-0 YBR048w::kanMX4 YDR025w::HIS3 IMP3::IMP3-TAP-URA3 YCplac111-pGAL-RPS11A (LEU2)*	This study
1892	pGAL-RPS11A NOC4-TAP	*his3-1 leu2-0 lys2-0 met15-0 ura3-0 YBR048w::kanMX4 YDR025w::HIS3 NOC4::NOC4-TAP-URA3 YCplac111-pGAL-RPS11A (LEU2)*	This study
1893	pGAL-RPS13 UTP4-TAP	*his3-1 leu2-0 ura3-0 MET15 LYS2 YDR064w::kanMX4 UTP4::UTP4-TAP-URA3 YCplac111-pGAL-RPS13-SE (LEU2)*	This study
1894	pGAL-RPS13 PWP2-TAP	*his3-1 leu2-0 ura3-0 MET15 LYS2 YDR064w::kanMX4 PWP2::PWP2-TAP-URA3 YCplac111-pGAL-RPS13-SE (LEU2)*	This study
1895	pGAL-RPS13 UTP22-TAP	*his3-1 leu2-0 ura3-0 MET15 LYS2 YDR064w::kanMX4 UTP22::UTP22-TAP-URA3 YCplac111-pGAL-RPS13-SE (LEU2)*	This study
1896	pGAL-RPS13 IMP3-TAP	*his3-1 leu2-0 ura3-0 MET15 LYS2 YDR064w::kanMX4 IMP3::IMP3-TAP-URA3 YCplac111-pGAL-RPS13-SE (LEU2)*	This study
1897	pGAL-RPS13 NOC4-TAP	*his3-1 leu2-0 ura3-0 MET15 LYS2 YDR064w::kanMX4 NOC4::NOC4-TAP-URA3 YCplac111-pGAL-RPS13-SE (LEU2)*	This study
1898	pGAL-RPS22 UTP4-TAP	*his3-1 leu2-0 ura3-0 MET? LYS? YJL190c::kanMX4 YLR367w::HIS3MX6 UTP4::UTP4-TAP-URA3 YCplac111-pGAL-RPS22A (LEU2)*	This study
1899	pGAL-RPS22 PWP2-TAP	*his3-1 leu2-0 ura3-0 MET? LYS? YJL190c::kanMX4 YLR367w::HIS3MX6 PWP2::PWP2-TAP-URA3 YCplac111-pGAL-RPS22A (LEU2)*	This study
1900	pGAL-RPS22 UTP22-TAP	*his3-1 leu2-0 ura3-0 MET? LYS? YJL190c::kanMX4 YLR367w::HIS3MX6 UTP22::UTP22-TAP-URA3 YCplac111-pGAL-RPS22A (LEU2)*	This study
1901	pGAL-RPS22 IMP3-TAP	*his3-1 leu2-0 ura3-0 MET? LYS? YJL190c::kanMX4 YLR367w::HIS3MX6 IMP3::IMP3-TAP-URA3 YCplac111-pGAL-RPS22A (LEU2)*	This study
1902	pGAL-RPS22 NOC4-TAP	*his3-1 leu2-0 ura3-0 MET? LYS? YJL190c::kanMX4 YLR367w::HIS3MX6 NOC4::NOC4-TAP-URA3 YCplac111-pGAL-RPS22A (LEU2)*	This study
1903	pGAL-FLAG-NOC4 UTP4-TAP	*his3-1 leu2-0 lys2-0 MET15 ura3-0 YPR144c::kanMX4 UTP4::UTP4-TAP-URA3 YCplac111-pGAL-FLAG-NOC4 (LEU2)*	This study
1904	pGAL-FLAG-NOC4 PWP2-TAP	*his3-1 leu2-0 lys2-0 MET15 ura3-0 YPR144c::kanMX4 PWP2::PWP2-TAP-URA3 YCplac111-pGAL-FLAG-NOC4 (LEU2)*	This study
1905	pGAL-FLAG-NOC4 UTP22-TAP	*his3-1 leu2-0 lys2-0 MET15 ura3-0 YPR144c::kanMX4 UTP22::UTP22-TAP-URA3 YCplac111-pGAL-FLAG-NOC4 (LEU2)*	This study
1906	pGAL-FLAG-NOC4 IMP3-TAP	*his3-1 leu2-0 lys2-0 MET15 ura3-0 YPR144c::kanMX4 IMP3::IMP3-TAP-URA3 YCplac111-pGAL-FLAG-NOC4 (LEU2)*	This study
1907	BY4742 UTP4-TAP	*his3-1 leu2-0 lys2-0 ura3-0 UTP4::UTP4-TAP-URA3*	This study

1908	BY4742 PWP2-TAP	*his3-1 leu2-0 lys2-0 ura3-0 PWP2::PWP2-TAP-URA3*	This study
1909	BY4742 UTP22-TAP	*his3-1 leu2-0 lys2-0 ura3-0 UTP22::UTP22-TAP-URA3*	This study
1910	BY4742 IMP3-TAP	*his3-1 leu2-0 lys2-0 ura3-0 IMP3::IMP3-TAP-URA3*	This study
1911	pGAL-RPS5 UTP22-TAP	*his3-1 leu2-0 ura3-0 lys2-0 YJR123w::kanMX4 UTP22::UTP22-TAP-URA3 YCplac111-pGAL-RPS5 (LEU2)*	This study
1912	pGAL-RPS5 IMP3-TAP	*his3-1 leu2-0 ura3-0 lys2-0 YJR123w::kanMX4 IMP3::IMP3-TAP-URA3 YCplac111-pGAL-RPS5 (LEU2)*	This study
1913	pGAL-RPS15 UTP22-TAP	*his3-1 leu2-0 ura3-0 lys2-0? met15-0? YOL040c::kanMX4 UTP22::UTP22-TAP-URA3 pFL36-pGalRPS15 (LEU2)*	This study
1914	pGAL-RPS15 IMP3-TAP	*his3-1 leu2-0 ura3-0 lys2-0? met15-0? YOL040c::kanMX4 IMP3::IMP3-TAP-URA3 pFL36-pGalRPS15 (LEU2)*	This study
1915	pGAL-RPS16A UTP22-TAP	*his3-1 leu2-0 met15-0 LYS ura3-0 YDL083c::kanMX4 YMR143w::HIS3 UTP22::UTP22-TAP-URA3 YCplac111-pGAL-RPS16A (LEU2)*	This study
1916	pGAL-RPS16A IMP3-TAP	*his3-1 leu2-0 met15-0 LYS ura3-0 YDL083c::kanMX4 YMR143w::HIS3 IMP3::IMP3-TAP-URA3 YCplac111-pGAL-RPS16A (LEU2)*	This study
2104	pGAL-RPS14 UTP4-TAP	*his3-1 leu2-0 met15-0 lys2-0 ura3-0 YCR031c::HIS3Mx6 YJL191w::kanMX4 UTP4::UTP4-TAP-URA3 Ycplac111-pGAL-RPS14 (LEU2)*	This study
2105	pGAL-RPS14 PWP2-TAP	*his3-1 leu2-0 met15-0 lys2-0 ura3-0 YCR031c::HIS3Mx6 YJL191w::kanMX4 PWP2::PWP2-TAP-URA3 Ycplac111-pGAL-RPS14 (LEU2)*	This study
2106	pGAL-RPS14 UTP22-TAP	*his3-1 leu2-0 met15-0 lys2-0 ura3-0 YCR031c::HIS3Mx6 YJL191w::kanMX4 UTP22::UTP22-TAP-URA3 Ycplac111-pGAL-RPS14 (LEU2)*	This study
2107	pGAL-RPS14 IMP3-TAP	*his3-1 leu2-0 met15-0 lys2-0 ura3-0 YCR031c::HIS3Mx6 YJL191w::kanMX4 IMP3::IMP3-TAP-URA3 Ycplac111-pGAL-RPS14 (LEU2)*	This study
2108	pGAL-RPS14 NOC4-TAP	*his3-1 leu2-0 met15-0 lys2-0 ura3-0 YCR031c::HIS3Mx6 YJL191w::kanMX4 NOC4::NOC4-TAP-URA3 Ycplac111-pGAL-RPS14 (LEU2)*	This study
2109	pGAL-RPS21 ENP1-TAP	*his3-1 leu2-0 lys2-0? met15-0? ura3-0 YKR057W::kanMX4 YJL136C::kanMX4 ENP1::ENP1-TAP-URA3 YCplac111pGAL-RPS21A (LEU2)*	This study
2110	pGAL-RPS29B ENP1-TAP	*his3-1 leu2-0 ura3-0 MET? LYS? YDL061c::kanMX4 YLR388w::HIS3MX6 ENP1::ENP1-TAP-URA3 YCplac111-pGAL- RPS29B (LEU2)*	This study
2111	pGAL-RPS3-SE HRR25-TAP	*his3-1 leu2-0 ura3-0 met15-0 lys2-0 YNL178w::kanMX4 HRR25::HRR25-TAP-URA YCplac111-pGAL-RPS3-SE (LEU2)*	This study
2112	pGAL-FLAG-NOC4 ENP1-TAP	*his3-1 leu2-0 lys2-0 MET15 ura3-0 YPR144c::kanMX4 ENP1::ENP1-TAP-URA3 YCplac111-pGAL-FLAG-NOC4 (LEU2)*	This study
	YCC95	*ade5 his7-2 leu2-112 trp1-289 ura3-52 rrn3-8 Allel*	(Cadwell et al., 1997)

5.1.4 Plasmids

No	Name	Features	Cloning strategy	Origin
351	pRPS28-short-FLAG-RPS5	RPS5 ORI (E.coli) 2µ URA3	subclone BamHI/PstI K259 in K349	Pöll, Gisela & Milkereit, Philipp
424	pRPS28-FLAG-RPS3	RPS3 ORI (E.coli) 2µ URA3	subclone BamHI/PstI K257 in K349	Pöll, Gisela & Milkereit, Philipp
427	pRPS28-FLAG-RPS13	RPS13 ORI (E.coli) 2µ URA3	subclone BamHI/PstI K270 in K349	Pöll, Gisela & Milkereit, Philipp
429	pRPS28-FLAG-RPS15	RPS15 ORI (E.coli) 2µ URA3	subclone BamHI/PstI K236 in K349	Pöll, Gisela & Milkereit, Philipp
432	pRPS28-FLAG-RPS19A	RPS19A ORI (E.coli) 2µ URA3	subclone BamHI/PstI K341 in K349	Pöll, Gisela & Milkereit, Philipp
522	pRPS28-RPS6A-FLAG	RPS6A ORI (E.coli) 2µ URA3	subclone BamHI/PstI K414 in K487	Ferreira-Cerca, Sébastien
622	pRPS28-FLAG-RPS16A-SE	RPS16A ORI (E.coli) 2µ URA3	PCR BamHI/PstI in K349	Neueder, Andreas
623	pRPS28-FLAG-RPS20-VI	RPS20 ORI (E.coli) 2µ URA3	PCR BamHI/PstI in K349	Neueder, Andreas
748	YCplac111-pGAL-RPS4A	RPS4A ORI (E.coli) ARS1 CEN4 LEU2	Oligos 497+1103 BamHI+PstI in K230	This study
749	YCplac111-pGAL-RPS21A	RPS21A ORI (E.coli) ARS1 CEN4 LEU2	Oligos 480+1104 BamHI+PstI in K230	This study
750	YCplac111-pGAL-RPS22A	RPS22A ORI (E.coli) ARS1 CEN4 LEU2	Oligos 473+1105 BamHI+PstI in K230	This study
751	YCplac111-pGAL-RPS29A	RPS29A ORI (E.coli) ARS1 CEN4 LEU2	Oligos 477+1106 BamHI+PstI in K230	This study
766	pRPS28-FLAG-RPS29A	RPS29A ORI (E.coli) 2µ URA3	subclone BamHI/PstI K751 in K349	Pöll, Gisela
781	pGEMT-P_S22A-HIS3MX6-T_S22A	HIS3MX6	Oligos 1142+1143 HindIII+EcoRI, Oligos 1206+1141 SacII+XhoI in K235	This study
782	pGEMT-P_S29B-HIS3MX6-T_S29B	HIS3MX6	Oligos 1146+1147 HindIII+EcoRI, Oligos 1207+1145 SacII+XhoI in K235	This study
783	YCplac33-RPS4A	RPS4A ORI (E.coli) ARS1 CEN4 URA3	Oligos 408+409 PstI+KpnI in V49	This study
784	YCplac33-RPS21A	RPS21A ORI (E.coli) ARS1 CEN4 URA3	Oligos 404+405 SacI+KpnI in V49	This study
785	YCplac33-RPS22A	RPS22A ORI (E.coli) ARS1 CEN4 URA3	Oligos 398+399 SacI+KpnI in V49	This study
786	YCplac33-RPS29A	RPS29A ORI (E.coli) ARS1 CEN4 URA3	Oligos 396+397 SacI+KpnI in V49	This study

974	YCplac111-pGAL-RPS29B	RPS29B ORI (E.coli) ARS1 CEN4 LEU2	Oligos 1315+1316 BamHI+PstI in K230	This study
975	YCplac111-pGAL-RPS22A-Term	RPS22A ORI (E.coli) ARS1 CEN4 LEU2	Oligos 473+1317 BamHI+PstI in K230	This study
976	YCplac111-pGAL-RPS29B-Term	RPS29B ORI (E.coli) ARS1 CEN4 LEU2	Oligos 1315+1318 BamHI+PstI in K230	This study
977	YCplac33-RPS22A	RPS22A ORI (E.coli) ARS1 CEN4 URA3	Oligos 398+399 SacI+KpnI in V49	This study
978	YCplac33-RPS29A	RPS29A ORI (E.coli) ARS1 CEN4 URA3	Oligos 396+397 SacI+KpnI in V49	This study
979	YCplac33-RPS29B	RPS29B ORI (E.coli) ARS1 CEN4 URA3	Oligos 1661+1662 SacI+KpnI in V49	This study
991	pRPS28-FLAG-RPS0B	RPS0B ORI (E.coli) 2µ URA3	subclone BamHI/PstI K251 in K349	Pöll, Gisela & Milkereit, Philipp
999	pRPS28-RPS9A-FLAG	RPS9A ORI (E.coli) 2µ URA3	subclone BamHI/PstI K415 in K487	Ferreira-Cerca, Sébastien
1000	pRPS28-RPS10A-FLAG	RPS10A ORI (E.coli) 2µ URA3	subclone BamHI/PstI K390 in K487	Ferreira-Cerca, Sébastien
1001	pRPS28-FLAG-RPS11A	RPS11A ORI (E.coli) 2µ URA3	subclone BamHI/PstI K268 in K349	Pöll, Gisela & Milkereit, Philipp
1006	pRPS28-FLAG-RPS17A	RPS17A ORI (E.coli) 2µ URA3	subclone BamHI/PstI K340 in K349	Pöll, Gisela & Milkereit, Philipp
1015	pRPS28-FLAG-RPS28B	RPS28B ORI (E.coli) 2µ URA3	subclone BamHI/PstI K282 in K349	Pöll, Gisela & Milkereit, Philipp
1111	pRPS28-FLAG-RPS14A-SE	RPS14A ORI (E.coli) 2µ URA3	PCR BamHI/PstI in K792	Neueder, Andreas
1263	YCplac111GAL-Flag-RPS29B	RPS29B ORI (E.coli) ARS1 CEN4 LEU2	BamHI/PstI fragment of K974 in K231	This study
1264	YEplac195-pRPS28-short-FLAG-RPS29B	RPS29B ORI (E.coli) 2µ URA3	BamHI/PstI fragment of K974 in K349	This study
1265	YCplac111GAL-RPS4-Flag	RPS4A ORI (E.coli) ARS1 CEN4 LEU2	Oligos 497+2045 BamHI+PstI in k390	This study
1266	YCplac111GAL-RPS22-Flag	RPS21A ORI (E.coli) ARS1 CEN4 LEU2	Oligos 473+2046 BamHI+PstI in k390	This study
1267	YCplac22-pNop1-ProA-noc4-8	noc4-8 ORI (E.coli) ARS1 CEN4 TRP1	KpnI/SacI fragment of K106 in K26	This study
1268	YCplac22-pNop1-ProA-noc4-8-Nat1	noc4-8 ORI (E.coli) ARS1 CEN4 TRP1	Oligos 2179+2180 (K1060) SalI in K1267	This study
1269	YCplac22-pNop1-ProA-noc4-8-Nat1_Rev	noc4-8 ORI (E.coli) ARS1 CEN4 TRP1	Oligos 2179+2180 (K1060) SalI in K1267	This study
1270	YEplac195-pRPS28-short-S4-Flag	RPS4A ORI (E.coli) 2µ URA3	BamHI/PstI fragment of K1265 in K487	This study

1271	YEplac195-pRPS28-short-S22-Flag	RPS21A ORI (E.coli) 2µ URA3	BamHI/PstI fragment of K1266 in K487	This study
1272	YCplac22-pGal-Noc4	NOC4 ORI (E.coli) ARS1 CEN4 TRP1	SphI/PstI fragment of K23 in V48	This study
1273	YCplac22-pGal-Noc4 Nat1	NOC4 ORI (E.coli) ARS1 CEN4 TRP1	Oligos 2181+2182 (K1060) SalI in K1272	This study
1274	YCplac22-pGal-Noc4 Nat1-Rev	NOC4 ORI (E.coli) ARS1 CEN4 TRP1	Oligos 2181+2182 (K1060) SalI in K1272	This study

5.1.5 Oligonucleotides

No	Name	Sequence
92	o-noc_do	GCAGTGAGCGCAACGCAATTAATGTGAG
92	o-noc-do	GCAGTGAGCGCAACGCAATTAATGTGAG
93	o-noc_up	CAATAACTCCGATCAAATTAACTCAAATCA AC
93	o-noc-up	CAATAACTCCGATCAAATTAACTCAAATCAAC
106	ypr144c R2 (144c2R -Xho 1)	TTTTTTCTCGAGTAATAACGCGGGGATCAGCGGT
108	ypr144c F2 (144c2F- HindIII)	TTTTTTAAGCTTATGGTATTGCTTATATCAGAAATTAAAG
154	148c R1	TTTTTTGTCGACGGCAGACTGTGTCGTGTACATC
154	148cR1-SalI	TTTTTTGTCGACGGCAGACTGTGTCGTGTACATC
155	148c F1	TTTTTTCTGCAGATGGCCGGTTCACAACTTAAGAAT
155	148cF1-PstI	TTTTTTCTGCAGATGGCCGGTTCACAACTTAAGAAT
189	Noc4-revTAB	TAAATGTATATATACACACTTTTAAAACTTCGTTGTTCATCTTCGCTTtacgactcactataggg
190	Noc4-1TAB	AGCGAAGCGTCATCCCAAGGTAACGTCTACTTGCCTGGGGTAGCATGGtccatggaaaagagaag
282	kanC_F	TGATTTTGATGACGAGCGTAAT
416	YCplac-Flag-5′	GATCATGGATTACAAGGATGACGACGATAAGGGTACCG
417	YCplac-Flag-3′	GATCCGGTACCCTTATCGTCGTCATCCTTGTAATCCAT
473	S22A_Gal_F	CGCCGCGGATCCATGACCAGATCTTCCGTT
477	S29A_GAL_F	CGCCGCGGATCCATGGCTCACGAAAACGTC
480	S21A_E_GAL_F	CGCCGCGGATCCATGGAAAACGATAAGGGCCAATTAGTCGAACTTTACGTTCCAAGA
497	S4A_F_Bam	CGCCGCGGATCCATGGCTAGAGGACCAAAGAAGCATCTAAAAAGA
505	kanB_R	CTGCAGCGAGGAGCCGTAAT
512	Dim1-nach-S2	CTTAGGTAAATAGTATACAAGCACTTACATAATTGATAAGAGAGCATCGATGAATTCGAGCTCG
513	Dim1-vor-S3	CTAAGGCTATTATATGCTTTTCACCAGGTTGGTATCCATTTTTCACGTACGCTGCAGGTCGAC
616	RPS10-CT-Ps_FLAG-HindIII_R	TTTTTTAAGCTTTTACTTATCGTCGTCATCCTTGTAATCCATCTGCAGATATCTTCTTTGTGGTCTTTG

1103	S4A_R_PstI	CGCCGCCTGCAGCCAATACAATCACACACACAC
1104	S21A_R_PstI	CGCCGCCTGCAGAATATTTACGGGGTTTTG
1105	S22A_R_PstI	CGCCGCCTGCAGTTTACTCTATTAACGCAT
1106	S29A_R_PstI	CGCCGCCTGCAGGACTTCCTATCCTGTCCA
1118	S22A_d_his3_F	TAGTATTTTTTATAAAACAAGACCAACATACATATCCAAGAGATCTGTTTAGCTTGCCTCG
1119	S22A_d_his3_R	AGTATATAAAGCTACCGAAAAGGTTGTTGTAACAAGTAGCGTTTAAACTGGATGGCGGCGT
1120	S29B_d_his3_F	TTCAATTTTGAAAACTTATTGGTTATAGAATATATACAAAAGATCTGTTTAGCTTGCCTCG
1121	S29B_d_his3_R	AAAAAAGGTTAATGATTACGATGTTACAATCGCTCTTGACGTTTAAACTGGATGGCGGCGT
1122	S21B_R267	GCGCGGTGACGAATCAATGCG
1123	S21B_d_his3_F	AAAGTTTTATAAACATTGTTAACGAATTTGACTTTAAAGGAGATCTGTTTAGCTTGCCTCG
1124	S21B_d_his3_R	AAACGACTTCCCCTCTTCTTTTTATTCAATATTTATCTTTGTTTAAACTGGATGGCGGCGT
1125	HIS3MX6_R634	GCCAACGCATGGATCATATG
1140	P_S22A_F_SacI	CGCCGCGAGCTCTACTGTTTGCCTCGGCCTGCC
1141	P_S22A_R_XhoI	CGAGGCAAGCTAAACAGATCTCTCGAGCTTGGATATGTATGTTGGTCT
1142	T_S22A_F_HindIII	ACGCCGCCATCCAGTTTAAACAAGCTTGCTACTTGTTACAACAACCTT
1143	T_S22A_R_EcoRI	CGCCGCGAATTCTTGAGGATTGGCCGTATCGAA
1144	P_S29B_F_SacI	CGCCGCGAGCTCGACGTGTATGCAGAATGAAGG
1145	P_S29B_R_XhoI	CGAGGCAAGCTAAACAGATCTCTCGAGTTTGTATATATTCTATAACCA
1146	T_S29B_F_HindIII	ACGCCGCCATCCAGTTTAAACAAGCTTGTCAAGAGCGATTGTAACATC
1147	T_S29B_R_EcoRI	CGCCGCGAATTCGGCGTTGCTACGAAGATTTAA
1206	P_S22A_F_SacII	CGCCGCCCGCGGTACTGTTTGCCTCGGCCTGCC
1207	P_S229B_F_SacII	CGCCGCCCGCGGGACGTGTATGCAGAATGAAGG
1315	S29B_Gal_F_BamHI	CGCCGCGGATCCATGGCTCACGAAAACGTTTGG
1316	S29B_R_PstI	CGCCGCCTGCAGTCTGAATAAGAGAACTACTCG
1317	S22A_R_PstI-Term	CGCCGCCTGCAGTTAGTAAACGAAACCCAAAAT
1318	S29B_R_PstI-Term	CGCCGCCTGCAGTTATCTGTACTTGTGGAAACC
1319	HIS3MX6_R	CTCTTGAGTAAAGTCGTAAGC
1320	HIS3MX6_F	GATTTGGACATGCTTATTGTC
1415	S22A_Tet_F	CAAATATTGAGGACGCGCGATTACCAGCGGCATGTTTACTcagctgaagcttcgtacgc
1416	S22A_Tet_R	TGGCATTCAAAGCATCAGCTAAAACGGAAGATCTGGTCATataggccactagtggatctg
1417	S29B_Tet_F	TTCAATTTTGAAAACTTATTGGTTATAGAATATATACAAAcagctgaagcttcgtacgc
1418	S29B_Tet_R	ATCTTCTTGGGTGGGAGAACCAAACGTTTTCGTGAGCCATataggccactagtggatctg
1659	Pno1-TAP-F	GAACTTACGTACCGTTGCATCTAGATTAAAAGAACGCTACtccatggaaaagagaag
1660	Pno1-TAP-R	TATAAATATTATACAGATGATGAAAGCCCACAAATTATGTtacgactcactataggg
1661	RPS29B_F_SacI	CGCCGCGAGCTCAACCGTCAGTACAAGAAGTGG

1662	RPS29B_R_KpnI	CGCCGCGGTACCTCTGAATAAGAGAACTACTCG
1809	Pwp2-TAP-F	AATGAAAATGATTCCAGTGATGAAGAAGAAAATGAGAAAGAGCTTCCTtccatggaaaagagaag
1810	Pwp2-TAP-R	GGGAATACATGATGTGAATGTGCATAAATAGAGGACAGTGAATATTTTtacgactcactataggg
1811	Rrp7-TAP-F	GAAAGAATCAAGGTAATGAAAGCTAAGAGAAAATTCAATCCATACACTtccatggaaaagagaag
1812	Rrp7-TAP-R	TTTATAGATATATTGAGATATGTTGAATATGATGACGAGGATGGTGGTtacgactcactataggg
1813	Utp4-TAP-F	ACTTTTCACTCCAAACAAAAGGCGTTTATTCAACCAAAGTTAGTGTTTtccatggaaaagagaag
1814	Utp4-TAP-R	GCCTTTTAATAGCATCTCTCTATTCTTCGGTATGTTGACTTAAATTAAtacgactcactatagggg
1815	Mpp10-TAP-F	AAAACGAAGAAGAGCAGATCAGGGCCAGATAGCACAAATATAAAACTTtccatggaaaagagaag
1816	Mpp10-TAP-R	AAGAAATAATTTTTTACCTAAATACAAACTAAGTCTTCTTCGGCGTGTtacgactcactataggg
1817	TRP_URA_KL_F	GATATCGAATTCCTGCAGCC
1948	Mpp10_F_+1521	CGCTTGAAGAATGGTGTTGC
1949	Mpp10_R_+2051	CTATCTTCCAATACCTCTTG
1950	Rrp7_F_+626	GGATGGATTCACATTAGTTG
1951	Rrp7_R_+1172	CATTATGTTAAGAAGAAGAG
2041	Noc5_+600	GATGCTGAGCTACAGCAA
2042	Noc5_+1250	ACCAAAATTGGCTGAAGG
2043	Noc5_+1900	CGGTTGATCAATGTGTCT
2044	Noc2_seq_fw_II	TGCGCAACACGATGAAGCC
2045	RPS4_R_PstI-Stop	CGCCGCCTGCAGTAAACCTTGTTGAGCTCTTC
2046	RPS22_R_PstI-Stop	CGCCGCCTGCAGGTAAACGAAACCCAAAATCTT
2176	Noc4_Int_F	CTATTGCCATGAAGAGAGATCTATTAAAAAGAAACGTCAAAGAATATGGTGGACAACAAATTCAAC
2177	Noc4_Int_R	TAAATGTATATATACACACTTTTAAAACTTCGTTGTTCATCTTCGCTTGCAGTGAGCGCAACGCA
2178	pNOP_F	CTATTGCCATGAAGAGAGATCTATTAAAAAGAAACGTCAAAGAATATGATTGAGTCATCAGCCTC
2179	Nat1_F_SalI	CGCCGCGTCGACTTAATTAAGGCGCGCCAGATC
2180	Nat1_R_SalI	CGCGCGGTCGACATTACAACAGGTGTTGTCCTC
2181	Nat1_F_ApaI	GCGTATGGGCCCTTAATTAAGGCGCGCCAGATC
2182	Nat1_R_ApaI	GCGTATGGGCCCATTACAACAGGTGTTGTCCTC
2183	Pno1-1_F1_SalI	CGCCGCGTCGACATGGTTGCGCCTACTGCTTTGA
2184	Pno1-1_R1	CGGCAATACGATCGATGGCTCT
2185	Pno1-1_F2	AGAGCCATCGATCGTATTGCCG
2186	Pno1-1_R2_EcoRI	CGCCGCGAATTCTTAGTAGCGTTCTTTTAATCTAGA
2187	Nob1-4_F1_SalI	CGCCGCGTCGACATGACCGAAAACCAAACCGCAC

2188	Nob1-4_R1	AGATTTAGATTCCCCCCCCGCGCTACATT
2189	Nob1-4_F2	AATGTAGCGCGGGGGGGGAATCTAAATCT
2190	Nob1-4_R2_EcoRI	CGCCGCGAATTCCTAACTTCTCCTTTTGGAACTGT
2261	Utp22-TAP-F	GAGATTGCTGCATTCGGGAATGACATGGTTATAAATTTTGAGACAGATtccatggaaaagagaag
2262	Utp22-TAP-R	TTTAATATTATACAGATACTTCTAAAAGTTATGATTTTGTTGTTTATTtacgactcactatagggg
2263	Utp22_F_201	GTGAATGGTGGAGAGAAAGGA
2264	Utp22_R_205	CGTTTACCTAGCTTTATTCTGA
2265	Mpp10_F_202	CAGATTGCGCAGGGCTTTGA
2266	Mpp10_R_202	CAGCACATTCTTCTGGTATTTA
2267	Imp3-TAP-F	AAAACCTTGTTGAGATACAGAAACCAAATCGACGATTTTGATTTTTCAtccatggaaaagagaag
2268	Imp3-TAP-R	AGATGATAAATCGAGTATTGATACAGAAAACGTAAGTTTGTAGTCAATtacgactcactataggg
2269	Imp4-TAP-F	TGGCAGTTGAGAAGATTCATAAGGACTGCCAATAAAAAAGACTATTTGtccatggaaaagagaag
2270	Imp4-TAP-R	AGGCCTCATCGGCCTTCTATTTTAACCTTTACAAATCTATAAAAAAATtacgactcactataggg
2271	Hrr25-TAP-F	CCACAACAGCCGCCTCAAGATAAACCAGCTGGCCAGTCAATTTGGTTGtccatggaaaagagaag
2272	Hrr25-TAP-R	TATATATACATATGTTTATTTTTGTGCGTTTTGAGCAATATATGTTGCtacgactcactatagggg
2273	Imp3_F_190	GGCGGAAACTATACAAGATGC
2274	Imp3_R_215	CGATGAGAAATTGTTTTGCGG

Grey sequence = restriction site

Lower case letter = priming site in the plasmid used as template for amplification

5.1.6 Probes

No	Target region	Detected rRNA species	Sequence
205	18S	35S, 32S, 23S, 22S, 21S, 20S and 18S	CATGGCTTAATCTTTGAGAC
212	25S	35S, 32S, 27S (all) and 25S	CTCCGCTTATTGATATGC
1819	D-A2 (ITS1)	35S, 32S, 23S, 22S, 21S and 20S	GTAAAAGCTCTCATGCTCTTGCC

5.1.7 Enzymes

Enzyme	Origin
Antarctic Phosphatase	New England Biolabs
iProof high-fidelity DNA polymerase	Bio-Rad
Restriction Endonucleases	New England Biolabs
T4 DNA ligase	New England Biolabs
Taq DNA polymerase	New England Biolabs
Trypsin, modified, sequencing grade, from bovine pancreas	Roche

5.1.8 Kits

Kit	Origin
PCR purification kit	Invitrogen
Plasmid Mini-kit	Invitrogen
QIAEX II gel extraction kit	Qiagen

5.1.9 Size-Standards (NEB)

Standard type	Size of the standard bands
2log DNA ladder	10000, 8000, 6000, 5000, 4000, 3000, 2000, 1500, 1200, 1000, 900, 800, 700, 600, 500/517, 400, 300, 200, 100 [Bp]
Protein Marker, Broad Range (2–212 kDa)	212, 158, 116, 97.2, 66.4, 55.6, 42.7, 34.6, 27, 20, 14.3, 6.5 [kDa]
ColorPlus Prestained Protein Marker, Broad Range (7–175 kDa)	175, 80, 58, 46, 30, 23, 17, 7 [kDa]

5.1.10 Antibodies

Antibody	Species	Dilution	Origin
α-HA (3F10)	rat	1:5000	Roche
α-Noc4 (Dom 3C2.1.1), monoclonal	rat	1:10	Dr. Kremmer, GSF München
PAP (Peroxidase Anti-Peroxidase)	rabbit	1:6000	Dako Cytomation, Z 0113
anti-Flag M2	mouse	1:5000	Sigma
anti-rat (peroxidase-conjugated)	goat	1:5000	Jackson Immuno Research
anti-mouse (peroxidase-conjugated)	goat	1:5000	Jackson Immuno Research

5.1.11 Equipment

Device	Manufacturer
4700 Proteomics Analyzer MALDI-TOF/TOF	Applied Biosystems
Alpha 2-4 lyophilizer	Christ
Biofuge Fresco refrigerated tabletop centrifuge	Hereaus
Biofuge Pico tabletop centrifuge	Hereaus
C412 centrifuge	Jouan
Centrikon T-1170 ultracentrifuge	Kontron Instruments
Centrikon T-324 centrifuge	Kontron Instruments
CT422 refrigerated centrifuge	Jouan
Electrophoresis system model 45-2010-i	Peqlab Biotechnologie GmBH
FPLC-System (Pumps P-500; Controller LCC-501+; Fraction collector FRAC-100)	Pharmacia Biotech
Gel Max UV transilluminator	Intas
IKA-Vibrax VXR	IKA

Incubators	Memmert
LAS-3000 chemiluminescence imager	Fujifilm
MicroPulser electroporation apparatus	Bio-Rad
NanoDrop ND-1000 spectrophotometer	Peqlab Biotechnologie GmBH
Optima L-80 X ultracentrifuge	Beckman Coulter
PCR Sprint thermocycler	Hybaid
Power Pac 3000 power supplies	Bio-Rad
Pulverisette 6 planetary mono mill	Fritsch
Roto-Shake Genie	Scientific Industries
Shake incubators Multitron / Minitron	Infors
Speed Vac Concentrator	Savant
Thermomixer compact	Eppendorf
Trans-Blot SD Semi-dry transfer cell	Bio-Rad
UltiMate 3000 NanoHPLC	Dionex
Ultrospec 3100pro spectrophotometer	Amersham
XCell SureLock Mini-Cell electrophoresis system	Invitrogen

5.1.12 Software

Software	Manufacturer
4000 Series Explorer v.3.6	Applied Biosystems
Acrobat 7.0 Professional v.7.0.9	Adobe
Chromeleon v.6.70	Dionex
Data Explorer v.4.5 C	Applied Biosystems
GPS Explorer v.3.5	Applied Biosystems
Illustrator CS v.11.0.0	Adobe
Image Reader LAS-3000 v.1.12	Fujifilm
Mascot	Matrix Science
Microsoft Office 2003	Microsoft
ND-1000 v.3.5.2	Peqlab Biotechnologie GmBH
Photoshop CS v.8.0.1	Adobe

5.2 Methods

5.2.1 Work with *Escherichia coli*

5.2.1.1 Preparation of competent cells for electroporation

The XL1-blue strain was used as a host for amplification of plasmid DNA. In order to increase the efficiency of plasmid DNA uptake, *E. coli* competent cells for electroporation were prepared. The

exposure to an electrical charge of *E. coli* cells induces the formation of transient membrane pores through which DNA molecules can pass (Neumann and Rosenheck, 1972).
Cells were grown in SOB at 37°C to mid-log phase (OD_{600}=0.35-0.6), chilled on ice for 15min and centrifuged. Cells were washed 3 times with ice-cold sterile water to reduce the ionic strength of the cell suspension. The cells were resuspended in 10% sterile glycerol (on average 1-3x10^{10} cells per ml), aliquoted (50µl) and stored at –80°C.

5.2.1.2 Transformation by electroporation

The cell aliquot was thawed on ice and pipetted into a chilled 0.2cm electroporation cuvette. About 1ng of a plasmid miniprep or up to 3µl of a ligation sample was pipetted into the cell drop. Pulsing was performed with programme EC2 in a micropulser. Immediately after the pulse, 1ml 37°C LB medium was added and the sample was transferred to a microreaction tube following an incubation step for 30-60min at 37°C. The cells were spun down for one minute at 5000rpm in a microcentrifuge. About 900µl were discarded and the pellet was resuspended in the remaining supernatant, plated onto LB-Amp and incubated overnight at 37°C.

5.2.1.3 Liquid culture for plasmid isolation

A single colony was picked from a plate and transferred into a sterile tube containing 5ml of LB-Amp medium. The culture was incubated over night at 37°C.

5.2.2 Work with *Saccharomyces cerevisiae*

5.2.2.1 Preparation of competent yeast cells

50ml of an logarithmically growing yeast culture (OD_{600}=0.5-0.7) was pelleted (500g, 5min at room temperature). The pellet was washed at room temperature with 25ml autoclaved H_2O, then with 5ml LitSorb. The pellet was resuspended in 360µl LitSorb and 40µl of salmon sperm DNA (10 mg/ml-Invitrogen) was boiled at 95°C for 5 minutes and added to the cell suspension. After mixing, 50µl aliquots were transferred to fresh reaction tubes and placed at -80°C for storage.

5.2.2.2 Transformation of competent yeast cells

Treatment of yeast cells with alkali cations (e.g. Li^+, Cs^+, K^+ see (Ito et al., 1983) is effective to induce competence of yeast cells to take up linear and circular DNA molecules.
The cell aliquot was thawed on ice, DNA (~20ng for plasmid transformation and ~10µg for DNA integration) was added to the cells and the sample was mixed. 6 volumes of LitPEG were added; samples were mixed thoroughly and incubated at room temperature for about 30 minutes. 1/9 of total volume (cells plus DNA plus LitPEG) of pure, sterile DMSO was added, samples were mixed and heat-shocked at 42°C for about 15 minutes. Cells were pelleted (2000rpm, 3 minutes at room temperature in a table-top centrifuge), the supernatant was completely removed and the cells were resuspended in sterile water and plated on the selective medium.

When cells were selected for antibiotic resistance (e.g. geniticin and nourseothricin) they were resuspended after the heat-shock in 1ml appropriate rich medium (without antibiotics). Cells were grown at appropriate temperature (30°C for wild-type cells, 24°C for temperature sensitive strains) for about 1-2 generation times. After that, cells were pelleted, 9/10 of the supernatant were discarded. The cell pellet was resuspended in the remaining supernatant and plated on selective medium. When cells were selected for resistance to geneticin, they should be replica-plated to identify positive clones.
Noteworthy, temperature-sensitive strains in this study were also exposed to the heat-shock at 42°C, since these cells were still viable after this treatment and the transformation rate was increased in comparison to a heat-shock at 30°C.

5.2.2.3 Mating of yeast haploid strains

Haploid yeast strains of opposing mating type (Mat a and α) and each carrying a specific selection marker, were grown independently overnight. Cells were mixed, and incubated from 10-24h to allow mating. Diploid cells were isolated using a double selection medium specific for each initial haploid strain. Thus, only diploid cells carrying both selection markers were able to survive.

5.2.2.4 Sporulation of yeast cells

Starvation of nitrogen and carbon source induces sporulation of diploid strains. In this condition diploid strains undergo meiosis division resulting in the formation of 4 spores (tetrad) contained in an ascospore. Cells were incubated minimum 7 days on sporulation media.

5.2.2.5 Tetrad analysis

Sporulated cells were resuspended in sterile water containing zymolyase (10mg/ml) and incubated 5min in order to open the cell wall of the ascospore. The spores were isolated by micromanipulation using a MSM Singer micromanipulator. Isolated offspring were genetically characterised by selection on the appropriate media.

5.2.2.6 Long-term storage

All yeast strains were stored in duplicate at –80°C in culture media supplemented with 16.5% (w/v) glycerol.

5.2.2.7 Auxotrophic secletion

Complete synthetic media is composed of 6.7g of yeast nitrogen base containing the required salts, vitamins, and a nitrogen source (Sunrise Science) supplemented with the appropriate amino acids and nucleotides mixture (Sunrise Science) and a carbon source (glucose or galactose) to allow cell growth and/ or selection. For culture on solid media 2% Bacto-agar was added.
Amino acids and nucleotides used in synthetic media (final concentration): Adenine 10mg/L; L-Arginine HCl 50mg/L; L-Aspartic acid 80mg/L; L-Histidine HCl 20mg/L; L-Leucine 100mg/L; L-Lysine 50mg/L; L-Methionine 20mg/L; L-Phenylalanine 50mg/L; L Threonine 100mg/L; L-Tryptophan

50mg/L; L-Tyrosine 50mg/L; Uracil 20mg/L; L-Valine 140mg/L (single components were all purchased from Sigma). Pre-made drop out mixtures of amino acids and nucleotides were all purchased from Sunrise Science and used as indicated by the manufacturer.

5.2.2.8 5-fluoro-orotic acid (5-FOA) selection

The 5-FOA is converted by the orotidine-5'-phosphate decarboxylase encoded by the *URA3* gene (in *S. cerevisiae*) into a toxic substance, the 5' fluorouridine monophosphate, which severely limits cell growth (Boeke et al., 1984). Therefore this molecule is useful to characterise loss (of function) of the *URA3* gene in a yeast population in different assays.
5-FOA containing medium was made with synthetic media containing the required drop out mix and carbon source supplemented with 1g/L of 5-fluoroorotic acid, monohydrate (Toronto Research Chemicals).

5.2.2.9 Geneticin selection

Geneticin or G418 is an aminoglycoside antibiotic that irreversibly binds the 80S ribosome and inhibits protein synthesis in eukaryotic and prokaryotic cells. The geneticin effect can be inactivated in pro- or eukaryotes by the expression of the aminoglycoside 3'–phosphotransferase encoded by the *KanMX* gene that inactivates the aminoglycoside inhibitory effect through phosphorylation of the geneticin molecule (Eustice and Wilhelm, 1984).
Selection was commonly made on full medium (materials & methods 1.2.1.1.) supplemented with 200 mg/ml of G418 sulfate (Difco). The geneticin resistance selection can also be made on a modified synthetic medium using proline 1g/L (Sigma) as nitrogen source instead of ammonium sulfate (Cheng et al., 2000).

5.2.3 Work with DNA

5.2.3.1 Native agarose gel electrophoresis

Agarose gel electrophoresis was used to separate DNA fragments of different lengths. In this work, electrophoresis was performed routinely with 1.0-1.2% (w/v) agarose, 0.5xTBE gels containing 0.2mg/ml ethidium bromide, and 0.5xTBE as electrophoresis buffer. To determine the lengths of the fragments, 1µg of DNA standard (2log ladder) was used in a concentration of 500µg/ml in 1xDNA loading buffer.

5.2.3.2 Polymerase Chain Reaction (PCR)

For amplification of DNA fragments for integration in the yeast genome, PCR was performed with yeast genomic DNA (200-500ng) or plasmid DNA (20-40ng) as templates in a 100µl reaction [20mM Tris-HCl, 10mM $(NH_4)_2SO_4$, 10mM KCl, 2mM $MgSO_4$, 0.1% Triton X-100, 25mM of reverse and forward primers, 25mM dNTP, and 2-5U Taq Polymerase (NEB)]. The main PCR program used in this

work was 1 cycle 95°C for 5min; 45°C for 2min; 72°C for 2min followed by 35 cycles 95°C for 1min; 45°C for 2min; 72°C for 2min, and 1 cycle 95°C for 1min; 45°C for 2min; 72°C for 10min.
For amplification of DNA fragments used for cloning, proofreading PCR was performed with yeast genomic DNA (200-500ng) or plasmid DNA (20-40ng) as templates in a 100µl reaction [20mM Tris-HCl, 10mM $(NH_4)_2SO_4$, 10mM KCl, 2mM $MgSO_4$, 0.1% Triton X-100, 25mM of reverse and forward primers, 25mM dNTP, and iProof high-fidelity DNA polymerase.
Samples (1/10th) were analysed by agarose gel electrophoresis and subsequently purified with PCR purification kit according to the manufacturer or precipitated with Ethanol (see below) for cloning or integration, respectively.

5.2.3.3 Digestion of DNA with restriction endonucleases

A variety of prokaryotic restriction endonucleases (NEB) were used to digest DNA in order to prepare defined DNA fragments for cloning or to check for presence and correct orientation of inserted DNA fragments. Restriction endonucleases were essentially used as suggested by the manufacturer.

5.2.3.4 Purification of DNA by Ethanol precipitation

DNA was precipitated from aqueous solution by addition of 2.5 volumes of absolute ethanol and 1/10th volume of 3M NaOAc pH 5.8 for minimum 20min at -20°C. Ethanol depletes the hydration shell from nucleic acids and expose negatively charged phosphate groups. Counter cations (here Na^+) bind the charged groups and reduce the repulsive forces between the polynucleotide chains, allowing the formation of a precipitate. Samples were centrifuged 10min, 14000rpm at 4°C. To eliminate salt, the pellet was washed with ice-cold 70% ethanol. After removal of the supernatant, the nucleic acid pellet was dried at room temperature, and solubilised in 10mM Tris-HCl pH 8.

5.2.3.5 Purification of PCR products

The PCR purification Kit by Invitrogen is a fast and easy method to purify enzymatically treated DNA samples (e.g. PCR products, ligation reactions). DNA above an exclusion size (depending on experimental conditions) is bound to a silicate gel column while smaller DNA molecules (primers), salts, nucleotides, enzymes and glycerol are removed. DNA was eluted with 10mM Tris-HCl, pH 8.

5.2.3.6 Purification of DNA fragments from agarose gel

DNA fragments of interest were cut out from agarose gels and eluted using a commercial kit following the indications provided by the manufacturer (QIAEX II gel extraction kit).

5.2.3.7 DNA ligation

In order to clone DNA sequences into yeast/ bacterial vectors, quantity of purified DNA fragments digested with restriction endonuclease(s) was measured by UV spectroscopy (see 5.2.3.8). A three-time excess of insert DNA compared to the vector DNA fragment was incubated in a 20µl ligase reaction (400U T4 DNA ligase NEB, 50mM Tris-HCl, 10mM $MgCl_2$, 1mM ATP, 10mM Dithiothreitol,

25mg/ml BSA) 2h at room temperature or over-night at 16°C. Two µl of the ligation reaction was used for *E. coli* transformation (see 5.2.1.2).

5.2.3.8 DNA quantitation using UV spectroscopy

Concentration of pure DNA samples was measured by nanodrop UV spectroscopy at 260nm wavelength (1 OD_{260}=50µg/ml). To determine contamination with proteins and RNA, absorbance was concomitantly measured at 280nm. The ratio of OD_{260}/OD_{280} of pure DNA is between 1.8 and 2.0.

5.2.3.9 DNA sequencing and oligonucleotides synthesis

All DNA sequencing and primer synthesis were performed by MWG. Oligonucleotides used in this work are listed in section 5.1.5.

5.2.3.10 Purification of plasmid DNA from *E.coli* (mini-preparation)

Isolation of plasmid DNA from bacteria was performed according to the manufacturer using the Plasmid Mini-kit from Invitrogen. Briefly, cells were lysed, and plasmid DNA was isolated from the lysate by DNA trapping on a matrix. The plasmid DNA was further washed with alcohol-based solution, and eluted from the matrix with 10mM Tris-HCl pH 8.

5.2.4 Work with RNA

5.2.4.1 Hot-phenol RNA extraction

RNA extractions were essentially performed as described previously (Schmitt et al., 1990). This protocol is suited for extraction of total RNA from low amount of samples. Cell pellets or cell extracts were resuspended in 500µl AE buffer and mixed with 500µl phenol (Roth) equilibrated in AE buffer and 50µl of 10% SDS. The samples were incubated on a thermomixer (Eppendorf) 5min at 65°C full mix speed (14000rpm) and chilled on ice for 2min. The aqueous phase containing the RNAs was collected, followed by one phenol extraction (500µl phenol) and one chloroform extraction (500µl chloroform). RNAs were precipitated from the aqueous phase at -20°C for 10min after addition of 2.5 volume of absolute ethanol and 1/10th volume of 3M NaOAc pH 5.3. Precipitated RNA, when used for denaturing agarose gel electrophoresis, were solubilised in RNA solubilisation buffer, denatured for 15 min at 65°C and stored at -20°C.

5.2.4.2 Denaturing agarose gel electrophoresis of high molecular weight RNA

RNA species over 1000 bases were resolved on denaturating agarose gels (1.3% agarose (Invitrogen), 2% formaldehyde; 0.1mg/ml ethidium bromide; 1xMOPS buffer). Gels were run for 14–16h at 40V in 1xMOPS and 2% formaldehyde electrophoresis buffer.

5.2.4.3 Northern Blotting (Vacuum transfer)

Resolved RNAs were transferred and immobilised on positively charged membranes (Positive™ MP-Biomedicals) using different methods (described below). In every case, the RNAs were cross-linked to the membranes by 1min exposition to UV light (254/312nm).

Vacuum transfer was used for nonradioactive RNA samples. Prior to transfer, the agarose gels were washed once 5min in milli-Q water, once 20min in 0.05M NaOH to hydrolyse the RNAs and facilitate the transfer of larger RNAs, and were further equilibrated 20min in 10xSSC. The RNAs were transferred from the gel onto the positively charged membrane (Positive™ MP-Biomedicals) applying a vacuum of 5bar for 90min using a vacuum blotter (Biorad).

5.2.4.4 Northern Blotting (Passive capillary transfer)

Passive capillary transfer was used for tritium labelled RNA samples. Prior to transfer, agarose gels were treated as described in 5.2.4.3, except that gels were incubated twice 20min in 10xSSC. Transfer of the RNAs from the agarose gel to the membrane was then achieved over-night by drawing the transfer buffer (10xSSC) from the reservoir upward through the gel into a stack of pumping paper. The RNAs were eluted from the gel and deposited onto the positively charged membrane with the help of the buffer stream.

5.2.4.5 Radioactive probe labelling and detection

Different RNA species immobilised on solid supports can be detected using specific DNA probes under conditions allowing the formation of specific RNA of interest/ probe hybrids. Probes used in this work are listed in 5.1.6.

5' ends of all oligo-probes were labelled with ^{32}P. Ten pmol of oligo-probe were incubated with 50mCi of $\gamma^{32}P$-ATP (Amersham), in 1xPNK buffer (70mM Tris-HCl, 10mM $MgCl_2$, 5mM DTT) and 10U of T4 polynucleotide kinase (NEB) for 30-45min at 37°C. Reactions were stopped by addition of 1ml of 0.5M EDTA pH 8. Labelled probes were purified from the non-incorporated nucleotides by gel exclusion column (Spin6-Biorad). Incorporated radioactivity was estimated by counting 1µl of purified-labelled probes using a scintillation counter (1600TR-Packard). Membranes were pre-hybridised at least 1h at 37°C in RNA hybridisation buffer. Membranes were then incubated at 37°C over-night after addition of 1-2x10^6cpm of radiolabelled oligo-probe per blot. The membranes were washed twice 15min in 2xSSC at 30°C. Signals were acquired exposing the membrane to a Phosphoimager screen and/ or BioMax MS/MR film (Fujifilm).

5.2.4.6 Non-radioactive probe labelling and detection

Digoxigenin-labelled RNA probes were synthesised using the DIG-Northern starter kit (Roche) as recommended by the manufacturer.

In brief, PCR products containing the T7 promoter followed by the region of interest were used as template for *in vitro* transcription in presence of digoxigenin modified NTP. The resulting probe was stored in aliquot in 50% formamide at –20°C.

Membranes were pre-hybridised for minimum 1h at 65°C in RNA hybridisation buffer. Membranes were then incubated at 65°C over-night after addition of 1-2µl of DIG-labelled probe per blot. The membranes were washed twice for 10min in RNA hybridisation buffer and twice 15min in 0.1xSSC, 0.1% SDS at 65°C. Blots were washed 3min at room temperature in washing buffer (1xMaBS with 0.3% N-lauroylsarcosine). Membranes were incubated 1h at room temperature in blocking buffer (1xMaBS with 1xblocking reagent (Roche)), followed by 30min incubation with 0.75U/ml of anti-DIG antibody conjugated to alkaline phosphatase (Roche) in blocking buffer. Membranes were washed three times 10min at RT in washing buffer and 5min in DIG reaction buffer. Chemi-luminescent substrate (1% CDP-Star-Roche) was added to the membrane. The signals were acquired using a Fuji LAS Reader 3000 (30 sec increment steps high binning).

5.2.4.7 Signal quantiation

DIG-labelled and radioactive signals were quantified using MultiGauge (Fuji).

5.2.4.8 Analysis of neo-synthesised rRNA

Cells were grown overnight in YPG medium. The culture was split and one part was grown in YPG whereas the other part was grown in YPD for 1 to 2h in order to shut down expression of the *GAL1*-dependent *RPSX*. For each sample $1OD_{600}$ of cells was centrifuged and resuspended either in 100µl buffer R_G (cells grown in YPG) or buffer R_D (cells grown in YPD). 20µCi of 5',6'-[^{3}H] uracil (GE Healthcare or Perkin Elmer) was added and the cells were incubated at 30°C for 22min. Total RNA was extracted as described in 5.2.4.1 and same amounts of samples were loaded onto a denaturing agarose gel, transferred onto a membrane (Positive TM, MP-Biomedicals), sprayed with a liquid enhancer (EN3HANCE spray surface, Perkin Elmer) and subjected to fluorography (BioMax MS film, FUJI).

5.2.5 Work with proteins

5.2.5.1 Denaturing protein extraction of yeast cells

About 1ml of an over night yeast liquid culture was spun down. Cells were resuspended in 1ml ice-cold water. Samples were chilled on ice and supplemented with 150µl of pre-treatment solution (1.85M NaOH, 1M β-mercapto-ethanol) for 15min on ice. Proteins were precipitated with 150µl 55% trichloro acetic acid for 10min on ice and pelleted (13000rpm, 10min at 4°C in table-top centrifuge). The supernatant was discarded and the pellet resuspended in 30-50µl HU-buffer. If colour turned yellow, the pH of the suspension was too acidic and was neutralised with ammonia gas until the colour turned blue again. Proteins were denatured for 10min at 65°C while shaking. Insoluble cell particles were pelleted (13000rpm, 1min). An adequate volume of the supernatant, dependent on the abundance of the examined protein, was analysed by Western blot.

5.2.5.2 SDS-polyacrylamide gel electrophoresis (SDS-PAGE)

Proteins were separated according to molecular weight by vertical, discontinuous SDS-PAGE according to Laemmli (Laemmli, 1970). The discontinuous system consists of a lower separating gel (10-13% acrylamide, 375mM Tris-HCl pH 8.8, 0.1% SDS) and an upper stacking gel (4% acrylamide, 125 mM Tris-HCl pH 6.8, 0.1% SDS). Gels were run for 1h at 150V in 1xelectrophoresis buffer. The proteins were visualised by staining with Coomassie® Brilliant Blue G-250. Molecular weights of the different proteins were estimated using protein markers of known molecular weight (NEB).

5.2.5.3 Western Blotting

Separated proteins by SDS-PAGE were transferred from the gel to a solid support and immobilised. The membrane can be probed with a specific antibody against the protein of interest, allowing the identification and quantitation of a specific protein in complex mixtures.
In this work, SDS-PAGE resolved proteins were transferred on PVDF membrane in transfer buffer using a semi-dry blot apparatus (Biorad) for 1.5h at 24V. Immobilised proteins were stained with Ponceau S (0.5% Ponceau, 1% acetic acid).

5.2.5.4 Detection of proteins by chemiluminescence

The membrane was blocked with blocking solution (5% milk powder in 1xTBS) to prevent unspecific binding of the antibody. Blocking was performed in a tray for 1h at room temperature or over night at 4°C while shaking. The membrane was wrapped into a 50ml falcon tube containing the first antibody dilution (appropriate dilution in 1xTBS with 5% milk powder, 3ml for large membrane) and rotated at room temperature for 1h. After two 5min washes with 1x TBS in a tray, the membrane was wrapped into a 50ml falcon tube with the second antibody (appropriate dilution in 1xTBS with 5% milk powder, 3ml for large membrane) and rotated at room temperature for 30min. The membrane was washed three times for 5min with 1xTBS. The secondary antibody is coupled to horseradish peroxidase (POD) which catalyses the oxidation of diacylhydrazides via an activated intermediate that decays to the ground state by emission of light in the visible range. The membrane was put between the two sheets of a thin plastic bag (ROTH) and covered with a liquid film of reaction substrates (BM chemiluminescence blotting substrate (POD), ROCHE). The positions of the PSM bands were marked with a fluorescent pen. Detection follows immediately after addition of the substrate in a LAS-3000 fluorescence reader (FUJIFILM).

5.2.6 Additional biochemical methods

5.2.6.1 Affinity purification using IgG coupled magnetic beads

The cell pellet corresponding to 2.5l yeast culture with OD_{600}=0.8-1.0 was resuspended in 1.5ml of cold buffer MB with 1mM DTT and 0.04U/µl RNasin per 1g cell pellet. 800µl of this cell suspension was added to 1.4ml glass beads (Ø 0.75 – 1mm) and divided into 2ml reaction tubes. A cell lysate was prepared by vigorous shaking of the cell suspension in a Vibrax shaker for 20min, followed by

2min on ice. This procedure was repeated twice. The cell lysate was cleared from cell debris by two centrifugation steps, 1x 5min at 14000rpm and 1x 10min at 14000rpm. The protein concentration of the cleared lysate was determined using the Bradford assay. Triton X-100 (0.5%) and Tween 20 (0.1%) was added to the cell lysate. The whole amount of cell lysate (typically 2.0-2.4ml with 120-180mg of total protein) was incubated with 250µl of equilibrated (3x washing with buffer A200 with 1x protease inhibitors) IgG coupled magnetic beads slurry and rotated for 1h at 4°C. The beads were washed 7 times (1x 1ml, 5x 2ml and 1x 10ml) with cold buffer MB with 0.5% Triton X-100 and 0.1% Tween 20 in a BioRad 10ml column. Bound proteins were eluted 2x with 500µl of freshly prepared 500mM NH_4OH solution and rotation for 20min at RT. Both supernatants were pooled in an original Eppendorf 1.5ml reaction tube and lyophilised over night.

5.2.6.2 Affinity purification using IgG coupled sepharose beads

Affinity purification experiments using 400ul of IgG coupled sepharose beads slurry (Amersham) were performed essentially the same as with IgG coupled magnetic beads.

5.2.6.3 Co-immunoprecipitation of rRNA using IgG coupled sepharose beads

The cell pellet corresponding to 100ml yeast culture with OD_{600}=0.8-1.0 was resuspended in 500ul cold buffer A200 with 0.04U/µl RNasin. A cell lysate was prepared by vigorous shaking of the cell suspension with 1.4ml glass beads (Ø 0.75 – 1mm) in a Vibrax shaker for 20min, followed by 2min on ice and another 20min shaking in the Vibrax. The cell lysate was cleared from cell debris by two centrifugation steps, 1x 5min at 14000rpm and 1x 10min at 14000rpm. The protein concentration of the cleared lysate was determined using the Bradford assay. 6mg of whole protein extract was incubated with 120µl of equilibrated (3x washing with buffer A200) IgG coupled sepharose beads slurry (Amersham) and rotated for 1.5h at 4°C. The beads were washed 7 times (1x 1ml, 5x 2ml and 1x 10ml) with cold buffer A200 in a BioRad 10ml column. For the precipitation of TAP tagged biogenesis factors the washed beads were split and 1/6 was used for protein analysis by western blotting, whereas 5/6 was used for RNA analysis by northern blotting.

5.2.6.4 Co-immunoprecipitation of rRNA using anti-Flag M2 beads

Co-immunoprecipitation of rRNA using 90ul of anti-Flag M2 beads slurry (Sigma) were performed essentially the same as with IgG coupled sepharose beads. For the precipitation of Flag tagged r-proteins the whole washed beads were used for RNA analysis by northern blotting.

5.2.7 Quantitative MALDI mass spectrometry

5.2.7.1 Trypsin digest and iTRAQ labelling

The lyophilised protein samples were resuspended in 20µl dissolution buffer (iTRAQ™ labelling kit, Invitrogen) and reduced with 5mM Tris-(2-carboxyethyl)phosphine at 60°C for 1h. Cysteins were blocked with 10mM methyl-methanethiosulfonate (MMTS) at room temperature for 10min. After

trypsin digest for 20h at 37°C, tryptic peptides of the purifications of interest were labelled with different combinations of the four iTRAQ™ reagents according to the manufacturer (Invitrogen). The differentially labelled peptides were combined and lyophilised (Ross et al., 2004).

5.2.7.2 Peptide separation and automated spotting of the peptide fractions

The combined differently labelled peptides were dissolved for 2h in 0.1%TFA and loaded on a nano-flow HPLC-system (Dionex) harbouring a C18-Pep-Mep column (LC-Packings). The peptides were separated by a gradient of 5% to 95% of buffer B (80% acetonitrile/0.05% TFA) and fractions were mixed with 5 volumes of CHCA (alpha-cyano-4-hydroxy cinnamic acid; Sigma) matrix (2mg/ml in 70% acetonitrile/0.1%TFA) and spotted online via the Probot system (Dionex) on a MALDI-target.

5.2.7.3 MALDI TOF/TOF analysis

MS/MS analyses were performed on an Applied Biosystems 4700 or 4800 Proteomics Analyzer MALDI-TOF/TOF mass spectrometer operated in positive ion reflector mode and evaluated by searching the NCBInr protein sequence database with the Mascot search engine (Matrix Science) implemented in the GPS Explorer software (Applied Biosystems). Laser intensity was adjusted due to laser condition and sample concentration. The eight most intense peptide peaks per spot detected in the MS mode were further fragmented yielding the respective MS/MS spectra.

5.2.7.4 iTRAQ data evaluation

Only proteins identified by at least two nonredundant peptides with a Confidence Interval > 95% were included in the analysis. The peak area for iTRAQ™ reporter ions were interpreted and corrected by the GPS-Explorer software (Applied Biosystems) and Excel (Microsoft). An iTRAQ ratio average of all peptides of a given protein was calculated and outliers were deleted by manual evaluation. The iTRAQ ratios of the co-purifying proteins were normalised to the ratio of the bait protein.

6 REFERENCES

Adilakshmi, T., Bellur, D. L., and Woodson, S. A. (2008). Concurrent nucleation of 16S folding and induced fit in 30S ribosome assembly. Nature *455*, 1268-1272.

Adilakshmi, T., Ramaswamy, P., and Woodson, S. A. (2005). Protein-independent folding pathway of the 16S rRNA 5' domain. J. Mol. Biol *351*, 508-519.

Agalarov, S. C., Sridhar Prasad, G., Funke, P. M., Stout, C. D., and Williamson, J. R. (2000). Structure of the S15,S6,S18-rRNA complex: assembly of the 30S ribosome central domain. Science *288*, 107-113.

Agalarov, S. C., Zheleznyakova, E. N., Selivanova, O. M., Zheleznaya, L. A., Matvienko, N. I., Vasiliev, V. D., and Spirin, A. S. (1998). In vitro assembly of a ribonucleoprotein particle corresponding to the platform domain of the 30S ribosomal subunit. Proc. Natl. Acad. Sci. U.S.A *95*, 999-1003.

Auger-Buendia, M. A., and Longuet, M. (1978). Characterization of proteins from nucleolar preribosomes of mouse leukemia cells by two-dimensional polyacrylamide gel electrophoresis. Eur. J. Biochem *85*, 105-114.

Auger-Buendia, M. A., Longuet, M., and Tavitian, A. (1979). Kinetic studies on ribosomal proteins assembly in preribosomal particles and ribosomal subunits of mammalian cells. Biochim. Biophys. Acta *563*, 113-128.

Ban, N., Nissen, P., Hansen, J., Moore, P. B., and Steitz, T. A. (2000). The complete atomic structure of the large ribosomal subunit at 2.4 A resolution. Science *289*, 905-920.

Bassler, J., Grandi, P., Gadal, O., Lessmann, T., Petfalski, E., Tollervey, D., Lechner, J., and Hurt, E. (2001). Identification of a 60S preribosomal particle that is closely linked to nuclear export. Mol. Cell *8*, 517-529.

Baudin-Baillieu, A., Tollervey, D., Cullin, C., and Lacroute, F. (1997). Functional analysis of Rrp7p, an essential yeast protein involved in pre-rRNA processing and ribosome assembly. Mol. Cell. Biol *17*, 5023-5032.

Becker, T., Bhushan, S., Jarasch, A., Armache, J., Funes, S., Jossinet, F., Gumbart, J., Mielke, T., Berninghausen, O., Schulten, K., et al. (2009). Structure of monomeric yeast and mammalian Sec61 complexes interacting with the translating ribosome. Science *326*, 1369-1373.

Bernstein, K. A., Gallagher, J. E. G., Mitchell, B. M., Granneman, S., and Baserga, S. J. (2004). The small-subunit processome is a ribosome assembly intermediate. Eukaryotic Cell *3*, 1619-1626.

Boeke, J. D., LaCroute, F., and Fink, G. R. (1984). A positive selection for mutants lacking orotidine-5'-phosphate decarboxylase activity in yeast: 5-fluoro-orotic acid resistance. Mol. Gen. Genet *197*, 345-346.

Bohnsack, M. T., Kos, M., and Tollervey, D. (2008). Quantitative analysis of snoRNA association with pre-ribosomes and release of snR30 by Rok1 helicase. EMBO Rep *9*, 1230-1236.

Bohnsack, M. T., Martin, R., Granneman, S., Ruprecht, M., Schleiff, E., and Tollervey, D. (2009). Prp43 bound at different sites on the pre-rRNA performs distinct functions in ribosome synthesis. Mol. Cell *36*, 583-592.

Bradatsch, B., Katahira, J., Kowalinski, E., Bange, G., Yao, W., Sekimoto, T., Baumgärtel, V., Boese, G., Bassler, J., Wild, K., et al. (2007). Arx1 functions as an unorthodox nuclear export receptor for the 60S preribosomal subunit. Mol. Cell *27*, 767-779.

Brodersen, D. E., Clemons, W. M., Carter, A. P., Wimberly, B. T., and Ramakrishnan, V. (2002). Crystal structure of the 30 S ribosomal subunit from Thermus thermophilus: structure of the proteins and their interactions with 16 S RNA. J. Mol. Biol *316*, 725-768.

Bubunenko, M., Korepanov, A., Court, D. L., Jagannathan, I., Dickinson, D., Chaudhuri, B. R., Garber, M. B., and Culver, G. M. (2006). 30S ribosomal subunits can be assembled in vivo without primary binding ribosomal protein S15. RNA *12*, 1229-1239.

Buchhaupt, M., Kötter, P., and Entian, K. (2007). Mutations in the nucleolar proteins Tma23 and Nop6 suppress the malfunction of the Nep1 protein. FEMS Yeast Res *7*, 771-781.

Buchhaupt, M., Meyer, B., Kötter, P., and Entian, K. (2006). Genetic evidence for 18S rRNA binding and an Rps19p assembly function of yeast nucleolar protein Nep1p. Mol. Genet. Genomics *276*, 273-284.

Bukau, B. (1999). Molecular Chaperones and Folding Catalysts: Regulation, Cellular Function and Mechanisms illustrated edition. (Taylor & Francis Ltd).

Cadwell, C., Yoon, H. J., Zebarjadian, Y., and Carbon, J. (1997). The yeast nucleolar protein Cbf5p is involved in rRNA biosynthesis and interacts genetically with the RNA polymerase I transcription factor RRN3. Mol. Cell. Biol *17*, 6175-6183.

Carter, A. P., Clemons, W. M., Brodersen, D. E., Morgan-Warren, R. J., Wimberly, B. T., and Ramakrishnan, V. (2000). Functional insights from the structure of the 30S ribosomal subunit and its interactions with antibiotics. Nature *407*, 340-348.

Cech, T. R. (2000). Structural biology. The ribosome is a ribozyme. Science *289*, 878-879.

Chandramouli, P., Topf, M., Ménétret, J., Eswar, N., Cannone, J. J., Gutell, R. R., Sali, A., and Akey, C. W. (2008). Structure of the mammalian 80S ribosome at 8.7 A resolution. Structure *16*, 535-548.

Chen, W., Bucaria, J., Band, D. A., Sutton, A., and Sternglanz, R. (2003). Enp1, a yeast protein associated with U3 and U14 snoRNAs, is required for pre-rRNA processing and 40S subunit synthesis. Nucleic Acids Res *31*, 690-699.

Cheng, T. H., Chang, C. R., Joy, P., Yablok, S., and Gartenberg, M. R. (2000). Controlling gene expression in yeast by inducible site-specific recombination. Nucleic Acids Res *28*, E108.

Chooi, W. Y., and Leiby, K. R. (1981). An electron microscopic method for localization of ribosomal proteins during transcription of ribosomal DNA: a method for studying protein assembly. Proc. Natl. Acad. Sci. U.S.A *78*, 4823-4827.

Connolly, K., and Culver, G. (2009). Deconstructing ribosome construction. Trends Biochem. Sci *34*, 256-263.

Datta, P. P., Wilson, D. N., Kawazoe, M., Swami, N. K., Kaminishi, T., Sharma, M. R., Booth, T. M., Takemoto, C., Fucini, P., Yokoyama, S., et al. (2007). Structural aspects of RbfA action during small ribosomal subunit assembly. Mol. Cell *28*, 434-445.

Dennis, P. P., Russell, A. G., and Moniz De Sá, M. (1997). Formation of the 5' end pseudoknot in small subunit ribosomal RNA: involvement of U3-like sequences. RNA *3*, 337-343.

Deshmukh, M., Tsay, Y. F., Paulovich, A. G., and Woolford, J. L. (1993). Yeast ribosomal protein L1 is required for the stability of newly synthesized 5S rRNA and the assembly of 60S ribosomal subunits. Mol. Cell. Biol *13*, 2835-2845.

Dodd, J., Kolb, J. M., and Nomura, M. (1991). Lack of complete cooperativity of ribosome assembly in vitro and its possible relevance to in vivo ribosome assembly and the regulation of ribosomal gene expression. Biochimie *73*, 757-767.

Dong, J., Lai, R., Jennings, J. L., Link, A. J., and Hinnebusch, A. G. (2005). The novel ATP-binding cassette protein ARB1 is a shuttling factor that stimulates 40S and 60S ribosome biogenesis. Mol. Cell. Biol *25*, 9859-9873.

Dosil, M., and Bustelo, X. R. (2004). Functional characterization of Pwp2, a WD family protein essential for the assembly of the 90 S pre-ribosomal particle. J. Biol. Chem *279*, 37385-37397.

Dragon, F., Gallagher, J. E. G., Compagnone-Post, P. A., Mitchell, B. M., Porwancher, K. A., Wehner, K. A., Wormsley, S., Settlage, R. E., Shabanowitz, J., Osheim, Y., et al. (2002). A large nucleolar U3 ribonucleoprotein required for 18S ribosomal RNA biogenesis. Nature *417*, 967-970.

Eustice, D. C., and Wilhelm, J. M. (1984). Mechanisms of action of aminoglycoside antibiotics in eucaryotic protein synthesis. Antimicrob. Agents Chemother *26*, 53-60.

Fatica, A., Cronshaw, A. D., Dlakić, M., and Tollervey, D. (2002). Ssf1p prevents premature processing of an early pre-60S ribosomal particle. Mol. Cell *9*, 341-351.

Fatica, A., and Tollervey, D. (2002). Making ribosomes. Curr. Opin. Cell Biol *14*, 313-318.

Ferreira-Cerca, S. (2008). Analysis of the in vivo functions and assembly pathway of small subunit ribosomal proteins in Saccharomyces cerevisiae. Available at: http://epub.uni-regensburg.de/10718/ [Accessed January 20, 2010].

Ferreira-Cerca, S., Pöll, G., Gleizes, P., Tschochner, H., and Milkereit, P. (2005). Roles of eukaryotic ribosomal proteins in maturation and transport of pre-18S rRNA and ribosome function. Mol. Cell *20*, 263-275.

Ferreira-Cerca, S., Pöll, G., Kühn, H., Neueder, A., Jakob, S., Tschochner, H., and Milkereit, P. (2007). Analysis of the in vivo assembly pathway of eukaryotic 40S ribosomal proteins. Mol. Cell *28*, 446-457.

Fournier, M. J., and Maxwell, E. S. (1993). The nucleolar snRNAs: catching up with the spliceosomal snRNAs. Trends Biochem. Sci *18*, 131-135.

Frank, J., Zhu, J., Penczek, P., Li, Y., Srivastava, S., Verschoor, A., Radermacher, M., Grassucci, R., Lata, R. K., and Agrawal, R. K. (1995). A model of protein synthesis based on cryo-electron microscopy of the E. coli ribosome. Nature *376*, 441-444.

Fromont-Racine, M., Senger, B., Saveanu, C., and Fasiolo, F. (2003). Ribosome assembly in eukaryotes. Gene *313*, 17-42.

Funatsu, G., and Wittmann, H. G. (1972). Ribosomal proteins. 33. Location of amino-acid replacements in protein S12 isolated from Escherichia coli mutants resistant to streptomycin. J. Mol. Biol *68*, 547-550.

Gabashvili, I. S., Agrawal, R. K., Spahn, C. M., Grassucci, R. A., Svergun, D. I., Frank, J., and Penczek, P. (2000). Solution structure of the E. coli 70S ribosome at 11.5 A resolution. Cell *100*, 537-549.

Gadal, O., Strauss, D., Braspenning, J., Hoepfner, D., Petfalski, E., Philippsen, P., Tollervey, D., and Hurt, E. (2001). A nuclear AAA-type ATPase (Rix7p) is required for biogenesis and nuclear export of 60S ribosomal subunits. EMBO J *20*, 3695-3704.

Galani, K., Nissan, T. A., Petfalski, E., Tollervey, D., and Hurt, E. (2004). Rea1, a dynein-related nuclear AAA-ATPase, is involved in late rRNA processing and nuclear export of 60 S subunits. J. Biol. Chem *279*, 55411-55418.

Gallagher, J. E. G., Dunbar, D. A., Granneman, S., Mitchell, B. M., Osheim, Y., Beyer, A. L., and Baserga, S. J. (2004). RNA polymerase I transcription and pre-rRNA processing are linked by specific SSU processome components. Genes Dev *18*, 2506-2517.

Gelperin, D., Horton, L., Beckman, J., Hensold, J., and Lemmon, S. K. (2001). Bms1p, a novel GTP-binding protein, and the related Tsr1p are required for distinct steps of 40S ribosome biogenesis in yeast. RNA *7*, 1268-1283.

Gerbasi, V. R., Weaver, C. M., Hill, S., Friedman, D. B., and Link, A. J. (2004). Yeast Asc1p and mammalian RACK1 are functionally orthologous core 40S ribosomal proteins that repress gene expression. Mol. Cell. Biol *24*, 8276-8287.

Gerbi, S. A., Borovjagin, A. V., Ezrokhi, M., and Lange, T. S. (2001). Ribosome biogenesis: role of small nucleolar RNA in maturation of eukaryotic rRNA. Cold Spring Harb. Symp. Quant. Biol *66*, 575-590.

Gérczei, T., and Correll, C. C. (2004). Imp3p and Imp4p mediate formation of essential U3-precursor rRNA (pre-rRNA) duplexes, possibly to recruit the small subunit processome to the pre-rRNA. Proc. Natl. Acad. Sci. U.S.A 101, 15301-15306.

Ghaemmaghami, S., Huh, W., Bower, K., Howson, R. W., Belle, A., Dephoure, N., O'Shea, E. K., and Weissman, J. S. (2003). Global analysis of protein expression in yeast. Nature *425*, 737-741.

Grandi, P., Rybin, V., Bassler, J., Petfalski, E., Strauss, D., Marzioch, M., Schäfer, T., Kuster, B., Tschochner, H., Tollervey, D., et al. (2002). 90S pre-ribosomes include the 35S pre-rRNA, the U3 snoRNP, and 40S subunit processing factors but predominantly lack 60S synthesis factors. Mol. Cell *10*, 105-115.

Granneman, S., and Baserga, S. J. (2004). Ribosome biogenesis: of knobs and RNA processing. Exp. Cell Res *296*, 43-50.

Granneman, S., Kudla, G., Petfalski, E., and Tollervey, D. (2009). Identification of protein binding sites on U3 snoRNA and pre-rRNA by UV cross-linking and high-throughput analysis of cDNAs. Proc. Natl. Acad. Sci. U.S.A *106*, 9613-9618.

Gu, S., Peske, F., Wieden, H., Rodnina, M. V., and Wintermeyer, W. (2003). The signal recognition particle binds to protein L23 at the peptide exit of the Escherichia coli ribosome. RNA *9*, 566-573.

Halic, M., Becker, T., Pool, M. R., Spahn, C. M. T., Grassucci, R. A., Frank, J., and Beckmann, R. (2004). Structure of the signal recognition particle interacting with the elongation-arrested ribosome. Nature *427*, 808-814.

Harnpicharnchai, P., Jakovljevic, J., Horsey, E., Miles, T., Roman, J., Rout, M., Meagher, D., Imai, B., Guo, Y., Brame, C. J., et al. (2001). Composition and functional characterization of yeast 66S ribosome assembly intermediates. Mol. Cell *8*, 505-515.

Hedges, J., West, M., and Johnson, A. W. (2005). Release of the export adapter, Nmd3p, from the 60S ribosomal subunit requires Rpl10p and the cytoplasmic GTPase Lsg1p. EMBO J *24*, 567-579.

Held, W. A., Ballou, B., Mizushima, S., and Nomura, M. (1974). Assembly mapping of 30 S ribosomal proteins from Escherichia coli. Further studies. J. Biol. Chem *249*, 3103-3111.

Hendershot, L. M., and Bulleid, N. J. (2000). Protein-specific chaperones: the role of hsp47 begins to gel. Curr. Biol *10*, R912-915.

Herold, M., and Nierhaus, K. H. (1987). Incorporation of six additional proteins to complete the assembly map of the 50 S subunit from Escherichia coli ribosomes. J. Biol. Chem *262*, 8826-8833.

Hughes, J. M. (1996). Functional base-pairing interaction between highly conserved elements of U3 small nucleolar RNA and the small ribosomal subunit RNA. J. Mol. Biol *259*, 645-654.

Inoue, K., Alsina, J., Chen, J., and Inouye, M. (2003). Suppression of defective ribosome assembly in a rbfA deletion mutant by overexpression of Era, an essential GTPase in Escherichia coli. Mol. Microbiol *48*, 1005-1016.

Inoue, K., Chen, J., Tan, Q., and Inouye, M. (2006). Era and RbfA have overlapping function in ribosome biogenesis in Escherichia coli. J. Mol. Microbiol. Biotechnol *11*, 41-52.

Ito, H., Fukuda, Y., Murata, K., and Kimura, A. (1983). Transformation of intact yeast cells treated with alkali cations. J. Bacteriol *153*, 163-168.

Jakob, S. (2006). Untersuchung der Proteinkomposition ribosomaler Assemblierungsintermediate in *Saccharomyces cerevisiae* mit Hilfe von quantitativer Massenspektrometrie. Diplomarbeit, Universität Regensburg.

Jankowsky, E., and Fairman, M. E. (2007). RNA helicases--one fold for many functions. Curr. Opin. Struct. Biol *17*, 316-324.

Karbstein, K. (2007). Role of GTPases in ribosome assembly. Biopolymers *87*, 1-11.

Kos, M., and Tollervey, D. (2005). The Putative RNA Helicase Dbp4p Is Required for Release of the U14 snoRNA from Preribosomes in Saccharomyces cerevisiae. Mol. Cell *20*, 53-64.

Kramer, G., Rauch, T., Rist, W., Vorderwülbecke, S., Patzelt, H., Schulze-Specking, A., Ban, N., Deuerling, E., and Bukau, B. (2002). L23 protein functions as a chaperone docking site on the ribosome. Nature *419*, 171-174.

Kressler, D., Roser, D., Pertschy, B., and Hurt, E. (2008). The AAA ATPase Rix7 powers progression of ribosome biogenesis by stripping Nsa1 from pre-60S particles. J. Cell Biol *181*, 935-944.

Krogan, N. J., Peng, W., Cagney, G., Robinson, M. D., Haw, R., Zhong, G., Guo, X., Zhang, X., Canadien, V., Richards, D. P., et al. (2004). High-definition macromolecular composition of yeast RNA-processing complexes. Mol. Cell *13*, 225-239.

Kühn, H., Hierlmeier, T., Merl, J., Jakob, S., Aguissa-Touré, A., Milkereit, P., and Tschochner, H. (2009). The Noc-domain containing C-terminus of Noc4p mediates both formation of the Noc4p-Nop14p submodule and its incorporation into the SSU processome. PLoS ONE *4*, e8370.

Kumar, A., and Warner, J. R. (1972). Characterization of ribosomal precursor particles from HeLa cell nucleoli. J. Mol. Biol *63*, 233-246.

Kuter, D. J., and Rodgers, A. (1976). The protein composition of HeLa ribosomal subunits and nucleolar precursor particles. Exp. Cell Res *102*, 205-212.

Laemmli, U. K. (1970). Cleavage of structural proteins during the assembly of the head of bacteriophage T4. Nature *227*, 680-685.

Lake, J. A. (1976). Ribosome structure determined by electron microscopy of Escherichia coli small subunits, large subunits and monomeric ribosomes. J. Mol. Biol *105*, 131-139.

Lavergne, J. P., Marzouki, A., Reboud, J. P., and Reboud, A. M. (1988). Reconstitution of the active rat liver 60 S ribosomal subunit from different preparations of core particles and split proteins. FEBS Lett *236*, 345-351.

Lecker, S., Lill, R., Ziegelhoffer, T., Georgopoulos, C., Bassford, P. J., Kumamoto, C. A., and Wickner, W. (1989). Three pure chaperone proteins of Escherichia coli--SecB, trigger factor and GroEL--form soluble complexes with precursor proteins in vitro. EMBO J *8*, 2703-2709.

Lee, S. J., and Baserga, S. J. (1999). Imp3p and Imp4p, two specific components of the U3 small nucleolar ribonucleoprotein that are essential for pre-18S rRNA processing. Mol. Cell. Biol *19*, 5441-5452.

Léger-Silvestre, I., Trumtel, S., Noaillac-Depeyre, J., and Gas, N. (1999). Functional compartmentalization of the nucleus in the budding yeast Saccharomyces cerevisiae. Chromosoma *108*, 103-113.

Léger-Silvestre, I., Caffrey, J. M., Dawaliby, R., Alvarez-Arias, D. A., Gas, N., Bertolone, S. J., Gleizes, P., and Ellis, S. R. (2005). Specific Role for Yeast Homologs of the Diamond Blackfan Anemia-associated Rps19 Protein in Ribosome Synthesis. J. Biol. Chem *280*, 38177-38185.

Léger-Silvestre, I., Milkereit, P., Ferreira-Cerca, S., Saveanu, C., Rousselle, J., Choesmel, V., Guinefoleau, C., Gas, N., and Gleizes, P. (2004). The ribosomal protein Rps15p is required for nuclear exit of the 40S subunit precursors in yeast. EMBO J *23*, 2336-2347.

Liang, X., and Fournier, M. J. (2006). The helicase Has1p is required for snoRNA release from pre-rRNA. Mol. Cell. Biol *26*, 7437-7450.

Liu, P. C., and Thiele, D. J. (2001). Novel stress-responsive genes EMG1 and NOP14 encode conserved, interacting proteins required for 40S ribosome biogenesis. Mol. Biol. Cell *12*, 3644-3657.

Lo, K., and Johnson, A. W. (2009). Reengineering ribosome export. Mol. Biol. Cell *20*, 1545-1554.

Loar, J. W., Seiser, R. M., Sundberg, A. E., Sagerson, H. J., Ilias, N., Zobel-Thropp, P., Craig, E. A., and Lycan, D. E. (2004). Genetic and biochemical interactions among Yar1, Ltv1 and Rps3 define novel links between environmental stress and ribosome biogenesis in Saccharomyces cerevisiae. Genetics *168*, 1877-1889.

Lövgren, J. M., Bylund, G. O., Srivastava, M. K., Lundberg, L. A. C., Persson, O. P., Wingsle, G., and Wikström, P. M. (2004). The PRC-barrel domain of the ribosome maturation protein RimM mediates binding to ribosomal protein S19 in the 30S ribosomal subunits. RNA *10*, 1798-1812.

Mangiarotti, G., and Chiaberge, S. (1997). Reconstitution of functional eukaryotic ribosomes from Dictyostelium discoideum ribosomal proteins and RNA. J. Biol. Chem *272*, 19682-19687.

Merl, J. (2009). In vivo und in vitro Charakterisierung von Proteinkomplexen eukaryotischer Ribosomenbiogenesefaktoren. Dissertation, Universität Regensburg.

Merl, J., Jakob, S., Ridinger, K., Hierlmeier, T., Deutzmann, R., Milkereit, P., and Tschochner, H. (2010). Analysis of ribosome biogenesis factor-modules in yeast cells depleted from pre-ribosomes. Nucleic Acids Res (in press).

Milkereit, P., Strauss, D., Bassler, J., Gadal, O., Kühn, H., Schütz, S., Gas, N., Lechner, J., Hurt, E., and Tschochner, H. (2003). A Noc complex specifically involved in the formation and nuclear export of ribosomal 40 S subunits. J. Biol. Chem *278*, 4072-4081.

Miller, O. L., and Beatty, B. R. (1969). Visualization of nucleolar genes. Science *164*, 955-957.

Mizushima, S., and Nomura, M. (1970). Assembly mapping of 30S ribosomal proteins from E. coli. Nature *226*, 1214.

Morita, D., Miyoshi, K., Matsui, Y., Toh-E, A., Shinkawa, H., Miyakawa, T., and Mizuta, K. (2002). Rpf2p, an evolutionarily conserved protein, interacts with ribosomal protein L11 and is essential for the processing of 27 SB Pre-rRNA to 25 S rRNA and the 60 S ribosomal subunit assembly in Saccharomyces cerevisiae. J. Biol. Chem *277*, 28780-28786.

Moy, T. I., and Silver, P. A. (1999). Nuclear export of the small ribosomal subunit requires the ran-GTPase cycle and certain nucleoporins. Genes Dev *13*, 2118-2133.

Moy, T. I., and Silver, P. A. (2002). Requirements for the nuclear export of the small ribosomal subunit. J. Cell. Sci *115*, 2985-2995.

Neumann, E., and Rosenheck, K. (1972). Permeability changes induced by electric impulses in vesicular membranes. J. Membr. Biol *10*, 279-290.

Nierhaus, K. H. (1991). The assembly of prokaryotic ribosomes. Biochimie *73*, 739-755.

Nierhaus, K. H. (1980). The assembly of the prokaryotic ribosome. BioSystems *12*, 273-282.

Nierhaus, K. H., and Dohme, F. (1974). Total reconstitution of functionally active 50S ribosomal subunits from Escherichia coli. Proc. Natl. Acad. Sci. U.S.A *71*, 4713-4717.

Nierhaus, K. H., and Wilson, D. (2004). Protein Synthesis and Ribosome Structure: Translating the Genome 1. ed. (Wiley-VCH).

Nissan, T. A., Bassler, J., Petfalski, E., Tollervey, D., and Hurt, E. (2002). 60S pre-ribosome formation viewed from assembly in the nucleolus until export to the cytoplasm. EMBO J *21*, 5539-5547.

Nissan, T. A., Galani, K., Maco, B., Tollervey, D., Aebi, U., and Hurt, E. (2004). A pre-ribosome with a tadpole-like structure functions in ATP-dependent maturation of 60S subunits. Mol. Cell *15*, 295-301.

Noller, H. F., Hoffarth, V., and Zimniak, L. (1992). Unusual resistance of peptidyl transferase to protein extraction procedures. Science *256*, 1416-1419.

Oeffinger, M., Dlakic, M., and Tollervey, D. (2004). A pre-ribosome-associated HEAT-repeat protein is required for export of both ribosomal subunits. Genes Dev *18*, 196-209.

Oeffinger, M., Wei, K. E., Rogers, R., DeGrasse, J. A., Chait, B. T., Aitchison, J. D., and Rout, M. P. (2007). Comprehensive analysis of diverse ribonucleoprotein complexes. Nat. Methods *4*, 951-956.

Ogle, J. M., Brodersen, D. E., Clemons , W. M., Tarry, M. J., Carter, A. P., and Ramakrishnan, V. (2001). Recognition of cognate transfer RNA by the 30S ribosomal subunit. Science *292*, 897-902.

Ogle, J. M., Murphy, F. V., Tarry, M. J., and Ramakrishnan, V. (2002). Selection of tRNA by the ribosome requires a transition from an open to a closed form. Cell *111*, 721-732.

Ohtake, Y., and Wickner, R. B. (1995). KRB1, a suppressor of mak7-1 (a mutant RPL4A), is RPL4B, a second ribosomal protein L4 gene, on a fragment of Saccharomyces chromosome XII. Genetics *140*, 129-137.

Orr, J. W., Hagerman, P. J., and Williamson, J. R. (1998). Protein and Mg(2+)-induced conformational changes in the S15 binding site of 16 S ribosomal RNA. J. Mol. Biol *275*, 453-464.

Osheim, Y. N., French, S. L., Keck, K. M., Champion, E. A., Spasov, K., Dragon, F., Baserga, S. J., and Beyer, A. L. (2004). Pre-18S ribosomal RNA is structurally compacted into the SSU processome prior to being cleaved from nascent transcripts in Saccharomyces cerevisiae. Mol. Cell *16*, 943-954.

Pérez-Fernández, J., Román, A., De Las Rivas, J., Bustelo, X. R., and Dosil, M. (2007). The 90S preribosome is a multimodular structure that is assembled through a hierarchical mechanism. Mol. Cell. Biol *27*, 5414-5429.

Pertschy, B., Saveanu, C., Zisser, G., Lebreton, A., Tengg, M., Jacquier, A., Liebminger, E., Nobis, B., Kappel, L., van der Klei, I., et al. (2007). Cytoplasmic recycling of 60S preribosomal factors depends on the AAA protein Drg1. Mol. Cell. Biol *27*, 6581-6592.

Planta, R. J., and Mager, W. H. (1998). The list of cytoplasmic ribosomal proteins of Saccharomyces cerevisiae. Yeast *14*, 471-477.

Pool, M. R., Stumm, J., Fulga, T. A., Sinning, I., and Dobberstein, B. (2002). Distinct modes of signal recognition particle interaction with the ribosome. Science *297*, 1345-1348.

Prestayko, A. W., Klomp, G. R., Schmoll, D. J., and Busch, H. (1974). Comparison of proteins of ribosomal subunits and nucleolar preribosomal particles from Novikoff hepatoma ascites cells by two-dimensional polyacrylamide gel electrophoresis. Biochemistry *13*, 1945-1951.

Ramakrishnan, V., and Moore, P. B. (2001). Atomic structures at last: the ribosome in 2000. Curr. Opin. Struct. Biol *11*, 144-154.

Reboud, A. M., Buisson, M., Amoros, M. J., and Reboud, J. P. (1972). Partial in vitro reconstitution of active 40S ribosomal subunits from rat liver. Biochem. Biophys. Res. Commun *46*, 2012-2018.

Recht, M. I., and Williamson, J. R. (2004). RNA tertiary structure and cooperative assembly of a large ribonucleoprotein complex. J. Mol. Biol *344*, 395-407.

Rigaut, G., Shevchenko, A., Rutz, B., Wilm, M., Mann, M., and Séraphin, B. (1999). A generic protein purification method for protein complex characterization and proteome exploration. Nat. Biotechnol *17*, 1030-1032.

Ross, P. L., Huang, Y. N., Marchese, J. N., Williamson, B., Parker, K., Hattan, S., Khainovski, N., Pillai, S., Dey, S., Daniels, S., et al. (2004). Multiplexed protein quantitation in Saccharomyces cerevisiae using amine-reactive isobaric tagging reagents. Mol. Cell Proteomics *3*, 1154-1169.

Rudra, D., Mallick, J., Zhao, Y., and Warner, J. R. (2007). Potential interface between ribosomal protein production and pre-rRNA processing. Mol. Cell. Biol *27*, 4815-4824.

Samaha, R. R., O'Brien, B., O'Brien, T. W., and Noller, H. F. (1994). Independent in vitro assembly of a ribonucleoprotein particle containing the 3' domain of 16S rRNA. Proc. Natl. Acad. Sci. U.S.A *91*, 7884-7888.

Santos, C., and Ballesta, J. P. (1994). Ribosomal protein P0, contrary to phosphoproteins P1 and P2, is required for ribosome activity and Saccharomyces cerevisiae viability. J. Biol. Chem *269*, 15689-15696.

Sasaki, T., Toh-E, A., and Kikuchi, Y. (2000). Yeast Krr1p physically and functionally interacts with a novel essential Kri1p, and both proteins are required for 40S ribosome biogenesis in the nucleolus. Mol. Cell. Biol *20*, 7971-7979.

Saveanu, C., Bienvenu, D., Namane, A., Gleizes, P. E., Gas, N., Jacquier, A., and Fromont-Racine, M. (2001). Nog2p, a putative GTPase associated with pre-60S subunits and required for late 60S maturation steps. EMBO J *20*, 6475-6484.

Schäfer, T., Maco, B., Petfalski, E., Tollervey, D., Böttcher, B., Aebi, U., and Hurt, E. (2006). Hrr25-dependent phosphorylation state regulates organization of the pre-40S subunit. Nature *441*, 651-655.

Schäfer, T., Strauss, D., Petfalski, E., Tollervey, D., and Hurt, E. (2003). The path from nucleolar 90S to cytoplasmic 40S pre-ribosomes. EMBO J *22*, 1370-1380.

Schluenzen, F., Tocilj, A., Zarivach, R., Harms, J., Gluehmann, M., Janell, D., Bashan, A., Bartels, H., Agmon, I., Franceschi, F., et al. (2000). Structure of functionally activated small ribosomal subunit at 3.3 angstroms resolution. Cell *102*, 615-623.

Schmitt, M. E., Brown, T. A., and Trumpower, B. L. (1990). A rapid and simple method for preparation of RNA from Saccharomyces cerevisiae. Nucleic Acids Res *18*, 3091-3092.

Semrad, K., Green, R., and Schroeder, R. (2004). RNA chaperone activity of large ribosomal subunit proteins from Escherichia coli. RNA *10*, 1855-1860.

Sharma, M. R., Barat, C., Wilson, D. N., Booth, T. M., Kawazoe, M., Hori-Takemoto, C., Shirouzu, M., Yokoyama, S., Fucini, P., and Agrawal, R. K. (2005). Interaction of Era with the 30S ribosomal subunit implications for 30S subunit assembly. Mol. Cell *18*, 319-329.

Siekevitz, P. (1952). Uptake of radioactive alanine in vitro into the proteins of rat liver fractions. J. Biol. Chem *195*, 549-565.

Spahn, C. M., Beckmann, R., Eswar, N., Penczek, P. A., Sali, A., Blobel, G., and Frank, J. (2001). Structure of the 80S ribosome from Saccharomyces cerevisiae--tRNA-ribosome and subunit-subunit interactions. Cell *107*, 373-386.

Spirin, A. S. (1999). Ribosomes 1. ed. (Springer, Berlin).

Stark, H., Mueller, F., Orlova, E. V., Schatz, M., Dube, P., Erdemir, T., Zemlin, F., Brimacombe, R., and van Heel, M. (1995). The 70S Escherichia coli ribosome at 23 A resolution: fitting the ribosomal RNA. Structure *3*, 815-821.

Stark, H., Rodnina, M. V., Wieden, H., Zemlin, F., Wintermeyer, W., and van Heel, M. (2002). Ribosome interactions of aminoacyl-tRNA and elongation factor Tu in the codon-recognition complex. Nat. Struct. Biol *9*, 849-854.

Stöffler, G., and Stöffler-Meilicke, M. (1984). Immunoelectron microscopy of ribosomes. Annu. Rev. Biophys. Bioeng *13*, 303-330.

Strunk, B. S., and Karbstein, K. (2009). Powering through ribosome assembly. RNA *15*, 2083-2104.

Sykes, M. T., and Williamson, J. R. (2009). A complex assembly landscape for the 30S ribosomal subunit. Annu Rev Biophys *38*, 197-215.

Synetos, D., Dabeva, M. D., and Warner, J. R. (1992). The yeast ribosomal protein S7 and its genes. J. Biol. Chem *267*, 3008-3013.

Tabb, A. L., Utsugi, T., Wooten-Kee, C. R., Sasaki, T., Edling, S. A., Gump, W., Kikuchi, Y., and Ellis, S. R. (2001). Genes encoding ribosomal proteins Rps0A/B of Saccharomyces cerevisiae interact with TOM1 mutants defective in ribosome synthesis. Genetics *157*, 1107-1116.

Tabb-Massey, A., Caffrey, J. M., Logsden, P., Taylor, S., Trent, J. O., and Ellis, S. R. (2003). Ribosomal proteins Rps0 and Rps21 of Saccharomyces cerevisiae have overlapping functions in the maturation of the 3' end of 18S rRNA. Nucleic Acids Res *31*, 6798-6805.

Talkington, M. W. T., Siuzdak, G., and Williamson, J. R. (2005). An assembly landscape for the 30S ribosomal subunit. Nature *438*, 628-632.

Tollervey, D., Lehtonen, H., Jansen, R., Kern, H., and Hurt, E. C. (1993). Temperature-sensitive mutations demonstrate roles for yeast fibrillarin in pre-rRNA processing, pre-rRNA methylation, and ribosome assembly. Cell *72*, 443-457.

Trapman, J., Retèl, J., and Planta, R. J. (1975). Ribosomal precursor particles from yeast. Exp. Cell Res *90*, 95-104.

Traub, P., and Nomura, M. (1968). Structure and function of E. coli ribosomes. V. Reconstitution of functionally active 30S ribosomal particles from RNA and proteins. Proc. Natl. Acad. Sci. U.S.A *59*, 777-784.

Traub, P., and Nomura, M. (1969). Structure and function of Escherichia coli ribosomes. VI. Mechanism of assembly of 30 s ribosomes studied in vitro. J. Mol. Biol *40*, 391-413.

Udem, S. A., and Warner, J. R. (1972). Ribosomal RNA synthesis in Saccharomyces cerevisiae. J. Mol. Biol *65*, 227-242.

Ulbrich, C., Diepholz, M., Bassler, J., Kressler, D., Pertschy, B., Galani, K., Böttcher, B., and Hurt, E. (2009). Mechanochemical removal of ribosome biogenesis factors from nascent 60S ribosomal subunits. Cell *138*, 911-922.

Urlaub, H., Hartmuth, K., Kostka, S., Grelle, G., and Lührmann, R. (2000). A general approach for identification of RNA-protein cross-linking sites within native human spliceosomal small nuclear ribonucleoproteins (snRNPs). Analysis of RNA-protein contacts in native U1 and U4/U6.U5 snRNPs. J. Biol. Chem *275*, 41458-41468.

Vioque, A., Pintor-Toro, J. A., and Palacián, E. (1982). Partial reconstitution of active eukaryotic ribosomes following dissociation with dimethylmaleic anhydride. J. Biol. Chem *257*, 6477-6480.

Wehner, K. A., Gallagher, J. E. G., and Baserga, S. J. (2002). Components of an interdependent unit within the SSU processome regulate and mediate its activity. Mol. Cell. Biol *22*, 7258-7267.

Weitzmann, C. J., Cunningham, P. R., Nurse, K., and Ofengand, J. (1993). Chemical evidence for domain assembly of the Escherichia coli 30S ribosome. FASEB J *7*, 177-180.

Wery, M., Ruidant, S., Schillewaert, S., Leporé, N., and Lafontaine, D. L. J. (2009). The nuclear poly(A) polymerase and Exosome cofactor Trf5 is recruited cotranscriptionally to nucleolar surveillance. RNA *15*, 406-419.

West, M., Hedges, J. B., Chen, A., and Johnson, A. W. (2005). Defining the order in which Nmd3p and Rpl10p load onto nascent 60S ribosomal subunits. Mol. Cell. Biol *25*, 3802-3813.

Williamson, J. R. (2000). Induced fit in RNA-protein recognition. Nat. Struct. Biol *7*, 834-837.

Wilson, D. N., and Nierhaus, K. H. (2005). Ribosomal proteins in the spotlight. Crit. Rev. Biochem. Mol. Biol *40*, 243-267.

Wimberly, B. T., Brodersen, D. E., Clemons, W. M., Morgan-Warren, R. J., Carter, A. P., Vonrhein, C., Hartsch, T., and Ramakrishnan, V. (2000). Structure of the 30S ribosomal subunit. Nature *407*, 327-339.

Xu, Z., O'Farrell, H. C., Rife, J. P., and Culver, G. M. (2008). A conserved rRNA methyltransferase regulates ribosome biogenesis. Nat. Struct. Mol. Biol *15*, 534-536.

Yan, W., and Chen, S. S. (2005). Mass spectrometry-based quantitative proteomic profiling. Brief Funct Genomic Proteomic *4*, 27-38.

Yao, W., Roser, D., Köhler, A., Bradatsch, B., Bassler, J., and Hurt, E. (2007). Nuclear export of ribosomal 60S subunits by the general mRNA export receptor Mex67-Mtr2. Mol. Cell *26*, 51-62.

Yusupov, M. M., Yusupova, G. Z., Baucom, A., Lieberman, K., Earnest, T. N., Cate, J. H., and Noller, H. F. (2001). Crystal structure of the ribosome at 5.5 A resolution. Science *292*, 883-896.

Zamecnik, P. C. (1969). An historical account of protein synthesis, with current overtones--a personalized view. Cold Spring Harb. Symp. Quant. Biol *34*, 1-16.

Zebarjadian, Y., King, T., Fournier, M. J., Clarke, L., and Carbon, J. (1999). Point mutations in yeast CBF5 can abolish in vivo pseudouridylation of rRNA. Mol. Cell. Biol *19*, 7461-7472.

Zhang, J., Harnpicharnchai, P., Jakovljevic, J., Tang, L., Guo, Y., Oeffinger, M., Rout, M. P., Hiley, S. L., Hughes, T., and Woolford, J. L. (2007). Assembly factors Rpf2 and Rrs1 recruit 5S rRNA and ribosomal proteins rpL5 and rpL11 into nascent ribosomes. Genes Dev *21*, 2580-2592.

7 PUBLICATIONS

Merl*, J., Jakob*, S., Ridinger, K., Hierlmeier, T., Deutzmann, R., Milkereit, P., and Tschochner, H. (2010). Analysis of ribosome biogenesis factor-modules in yeast cells depleted from pre-ribosomes. Nucleic Acids Res (in press). * = both authors contributed equally to this work

Kühn, H., Hierlmeier, T., Merl, J., Jakob, S., Aguissa-Touré, A., Milkereit, P., and Tschochner, H. (2009). The Noc-domain containing C-terminus of Noc4p mediates both formation of the Noc4p-Nop14p submodule and its incorporation into the SSU processome. PLoS ONE *4*, e8370.

Pöll, G., Braun, T., Jakovljevic, J., Neueder, A., Jakob, S., Woolford, J. L., Tschochner, H., and Milkereit, P. (2009). rRNA maturation in yeast cells depleted of large ribosomal subunit proteins. PLoS ONE 4, e8249.

Gerber, J., Reiter, A., Steinbauer, R., Jakob, S., Kuhn, C., Cramer, P., Griesenbeck, J., Milkereit, P., and Tschochner, H. (2008). Site specific phosphorylation of yeast RNA polymerase I. Nucleic Acids Res *36*, 793-802.

Ferreira-Cerca, S., Pöll, G., Kühn, H., Neueder, A., Jakob, S., Tschochner, H., and Milkereit, P. (2007). Analysis of the in vivo assembly pathway of eukaryotic 40S ribosomal proteins. Mol. Cell *28*, 446-457.

8 ABBREVIATIONS

Amp	ampicillin
APS	ammonium persulfate
ATP	adenosine triphosphate
bp	base pair(s)
C-terminal	carboxy-terminal
cryo-EM	cryo-electron microscopy
Da	Dalton
DNA	desoxyribonucleic acid
dNTP	2-desoxyribonucleotide 5' triphosphate
E. coli	Escherichia coli
EDTA	ethylene diamine tetra acetate
EGTA	ethylene glycol tetraacetic acid,
g	gram(s)
h	hour(s)
iTRAQ	isobaric tag for relative and absolute quantitation
k	kilo
kb	kilo base pair(s)
l	liter(s)
LB	lysogeny broth
LSU	large ribosomal subunit
mg	milligram(s)
min	minute(s)
ml	milliliter(s)
mRNA	messenger RNA
MW	molecular weight
M	molar (mol/l)
MS	mass spectrometry
MS/MS	tandem mass spectrometry
nm	nanometer(s)
OD	optical density
ORF	open reading frame
PAGE	poly acryl amide electrophoresis
PCR	polymerase chain reaction
PEG	poly ethylene glycol
pH	negative decadic logarithm of [H+]
Pol I	RNA polymerase I
Pol II	RNA polymerase II

Pol III	RNA polymerase III
rDNA	ribosomal DNA
RNA	ribonucleic acid
RNP	ribonucleoprotein
RP	ribosomal protein
rpm	rotations per minute
r-protein	ribosomal protein
rRNA	ribosomal RNA
RT	room temperature
S	sedimentation coefficient
S. cerevisiae	Saccharomyces cerevisiae
SDS	sodium dodecyl sulfate
s	second(s)
snoRNA	small nucleolar ribonucleic acid
snoRNP	small nucleolar ribonucleoprotein
SSU	small ribosomal subunit
Taq	Thermus aquaticus
TBS	Tris buffered saline
TCA	tri chloro acetic acid
TEMED	tetramethylethylenediamine
TOF	time of flight
Tris	tris(hydroxy methyl) amino methane
U	unit(s)
wt	wild-type
µ	micro
co-IP	co-immunoprecipitation
qMS	quantitative mass spectrometry

Acknowledgments

Ich bedanke mich aufrichtig bei meinem Mentor Dr. Philipp Milkereit für die professionelle Betreuung dieser Arbeit, die interessante Fragestellung und die anregenden Diskussionen.

Mein herzlicher Dank gilt Prof. Dr. Herbert Tschochner, der mir die Möglichkeit gegeben hat an seinem Lehrstuhl zu promovieren und mich dabei stets unterstütze.

Weiterhin danke ich allen Mitarbeitern des House of the Ribosome, insbesondere denen, die direkt zum Gelingen dieser Arbeit beigetragen haben. Vor allem zählt hierzu meine kleine aber feine Subgruppe. Nicht unerwähnt möchte ich den guten Musikgeschmack meiner Labormitarbeiter lassen, entgegen weniger Ausnahmen.

Mein Dank richtet sich zudem an Eduard Hochmuth und Prof. Dr. Rainer Deutzmann für die Hilfestellung bei der Massenspektrometrie und die Instandhaltung des Gerätes.

Vielen Dank auch an Dr. Max Felle, Manuel Wittner, Thomas Hierlmeier und Juliane Merl.

Meinen Freunden und Verwandten danke ich für ihre, zwar nichtfachliche aber unschätzbar wertvolle, Unterstützung in jeglicher Form. Zu guter Letzt ein Lob auf die wundervollste Nachbarin.